



# THE UNIVERSITY *of* EDINBURGH

This thesis has been submitted in fulfilment of the requirements for a postgraduate degree (e.g. PhD, MPhil, DClInPsychol) at the University of Edinburgh. Please note the following terms and conditions of use:

This work is protected by copyright and other intellectual property rights, which are retained by the thesis author, unless otherwise stated.

A copy can be downloaded for personal non-commercial research or study, without prior permission or charge.

This thesis cannot be reproduced or quoted extensively from without first obtaining permission in writing from the author.

The content must not be changed in any way or sold commercially in any format or medium without the formal permission of the author.

When referring to this work, full bibliographic details including the author, title, awarding institution and date of the thesis must be given.

# The phase structure of five-dimensional anisotropic lattice gauge theories

*Eliana Lambrou*



Doctor of Philosophy  
University of Edinburgh  
2015

# Abstract

The idea that we live in a higher-dimensional space was first introduced almost 100 years ago. In the past two decades many extra-dimensional models have been proposed in order to solve fundamental problems of nature such as the hierarchy problem. Most of them need exploration via non-perturbative approaches and Lattice Gauge Theory provides a tool for doing this.

In this thesis, we make attempts to find a non-perturbative way to localize gauge fields that arise from five-dimensional  $SU(2)$  gauge theories on 3-branes. In 1984, it was proposed that the phase diagram of anisotropic extra-dimensional lattice gauge theories inherits a new phase, called the “layered” phase, where the gauge fields behave as four-dimensional ones. This was shown for the abelian case, but the existence of this new phase for the simplest non-abelian group,  $SU(2)$ , was still in doubt. We investigated this system in large volumes using Monte Carlo simulations and we could not find a second order phase transition from a five-dimensional to a continuous four-dimensional theory when all directions were kept large. This made the model unattractive for further exploration as nothing suggests that a non-trivial fixed point could exist.

The above investigation was done in a flat background metric. We extended the previous work by putting our theory into a slice of  $AdS_5$  space, usually called the warped background. The motivation for this is that our  $SU(2)$  theory looks like the gauge-sector of the Randall-Sundrum model, which does not have a concrete solution to the problem of localization of the gauge fields on a 3-brane. We carried out our investigation using the Mean-Field Approach and we present novel results for the phase diagram and measurements of important observables.

---

In our implementation we have a finite extent of the extra dimension and one layer (or 3-brane) on each extra-dimensional coordinate. At weak coupling, we observed that each layer decouples one at a time in the transition to the fully layered phase of the system, forming a mixed phase, whereas there is a strong and sharp transition between the fully layered and the strong-coupling phase. Within the mixed phase, close to the transition into the layered phase, we found evidence that the system is four-dimensional acquiring a Yukawa mass and resembling a Higgs-like phase. The mixed phase grows as the curvature increases suggesting that for an infinite extra dimension the entire weak-coupling phase is mixed.

# Lay Summary

There are four known fundamental interactions of nature: the electromagnetic, the nuclear weak, the nuclear strong and the gravitational interactions. The Standard Model (SM) of particle physics is the theory that concerns the first three and it includes all known elementary particles, that is the fermions (quarks and leptons), the gauge bosons and the Higgs boson. Even though experiments at the Large Hadron Collider (LHC) confirmed the existence of all the SM particles, there are still some unanswered questions in nature, for example if there is a Grand Unified Theory (GUT) and why gravity is much weaker than the other forces.

Many solutions to these problems have been proposed over the years and a noticeable class of solutions is the one that involves the introduction of extra dimensions, i.e. the proposal that the universe consists of more than the usual four dimensions (time and the three spatial ones), but the extra dimensions are hidden from the observed world via different mechanisms, a procedure called dimensional reduction.

A very powerful tool to explore models when the analytical methods fail, is called the lattice, that is a space-time grid. In this thesis we explore two different five-dimensional models on a lattice using computer simulations and semi-analytical methods, one having the extra dimension in a flat space, as the one we live on, and the other having the extra dimension in a curved space.

By simulating the first model on powerful computers, we look for a four-dimensional theory arising from the five-dimensional one when the extra dimension is large, but we could not find evidence of it up to the point that the available computer resources allowed us to look at.

---

The previous studies of models with the extra dimension embedded in a curved spacetime are limited to mostly analytical calculations. In this work, we provide novel results of the model with semi-analytical methods, which open up the possibility that the presence of the curved space breaks a symmetry associated with the system and a mass is generated, a result which is unexpected and opens up the possibility of further investigation of the model especially using computer simulations.

# Declaration

I declare that this thesis was composed by myself, that the work contained herein is my own except where explicitly stated otherwise in the text, and that this work has not been submitted for any other degree or professional qualification except as specified.

*Eliana Lambrou*

August 2015

*Στους γονείς μου*

*« Όταν μας έρχονται ανάποδα όλα, τι χαρά να δοκιμάζουμε την ψυχή μας αν έχει αντοχή κι αξία! Θαρρείς κι ένας οχτρός αόρατος, παντοδύναμος - άλλοι τον λένε Θεό κι άλλοι διάολο - χιμάει να μας ρίξει, μα εμείς στέκουμε όρθιοι. Κι έτσι κάθε φορά που εσωτερικά είμαστε νικητές, όταν εξωτερικά είμαστε νικημένοι κατά κράτος, ο αληθινός άντρας νιώθει άφραστη περηφάνια και χαρά, η εξωτερική συμφορά μετουσιώνεται σε ανώτατη, δυσκολώτατη ευδαιμονία. »*

*Νίκος Καζαντζάκης*



*To my parents*

*“When everything goes wrong, what a joy to test your soul and see if it has endurance and courage! An invisible and all-powerful enemy - some call him God, others the Devil - seems to rush upon us to destroy us; but we are not destroyed! Each time that within ourselves we are the conquerors, although externally utterly defeated, we human beings feel an indescribable pride and joy. Outward calamity is transformed into a supreme and unshakable felicity.”*

*Nikos Kazantzakis*

# Acknowledgements

Foremost, I wish to express my sincere gratitude to my supervisor Prof. Richard Kenway for all his support during my PhD studies, for sharing his vast knowledge with me and for providing useful ideas, taking time out of his busy schedule. I would also like to thank my second supervisor Prof. Luigi Del Debbio for our fruitful discussions and his overall help.

Many thanks go to Dr. Enrico Rinaldi and Dr. Frank Winter for all their help during my first year. Furthermore, I would like to thank Prof. Francesco Knechtli, Prof. Nikos Irges and Dr. Philippe De Forcrand for our stimulating discussions and their useful comments on my work.

By joining this department, I have been lucky to meet great people. I want to thank especially my officemates Jack, Pol, Rafa, Samuel, Tom, Mark and Øyvind but also Sam, Vlad, Susi, Ava, Ashley and the rest of PPT group for making daily life in Edinburgh much more fun.

The last four years would have been impossible without the unconditional love and support of my parents and my sister who have been next to me during all my difficult times. I am grateful for having them in my life. Next, I would like to thank my two best friends Maria and Niki for being there for me, my Greek friends in Scotland Daphné, Nicola, Vasilis and Haris but also Myria, Tasos, Chris, Evi, Despo, Maria, Katerina, Koula and Valentina for being close even though we were miles apart. Lastly, a huge thanks goes to Savvas for our endless discussions and his vital encouragement to pursue my goals in life, *“γιατί καμιά φορά οι αλήτες βοηθούν τις Αλίκες να βρουν το φως στη χώρα των θαυμάτων”*.

# Contents

<b>Abstract</b>	<b>i</b>
<b>Lay Summary</b>	<b>iii</b>
<b>Declaration</b>	<b>v</b>
<b>Acknowledgements</b>	<b>viii</b>
<b>Contents</b>	<b>ix</b>
<b>List of figures</b>	<b>xii</b>
<b>List of tables</b>	<b>xvi</b>
<b>List of acronyms</b>	<b>xvii</b>
<b>1 Introduction</b>	<b>1</b>
1.1 Dimensional Reduction . . . . .	3
1.1.1 Kaluza-Klein compactification . . . . .	3
1.1.2 Localization - Non-compact extra dimensions . . . . .	4
1.2 Gauge Field Localization Problem . . . . .	7
1.2.1 Dvali-Shifman mechanism . . . . .	8
1.3 Well-known extra-dimensional models . . . . .	10
1.3.1 Gauge-Higgs Unification . . . . .	11
1.3.2 Arkani-Hamed-Dimopoulos-Dvali model . . . . .	12
1.3.3 Randall-Sundrum models . . . . .	14
1.4 Present Work and Thesis Outline . . . . .	17
<b>2 Lattice Gauge Theories</b>	<b>19</b>
2.1 QFT on the lattice - Lattice discretization . . . . .	20
2.1.1 Pure lattice gauge theory - The Wilson action . . . . .	23
2.1.2 Observables . . . . .	24
2.1.3 Discrete symmetries of the Wilson action . . . . .	27
2.2 Fermions on the lattice . . . . .	28

2.3	Anisotropic Lattice Gauge Theories . . . . .	32
2.4	Phase structure of LGTs . . . . .	33
2.4.1	Phases of pure LGTs . . . . .	34
2.4.2	Order parameters and their behaviour . . . . .	35
2.5	The Continuum Limit . . . . .	36
2.6	Methods for LGT exploration . . . . .	37
2.6.1	Monte Carlo simulations . . . . .	38
2.6.2	Mean-Field approach . . . . .	39
2.6.2.1	Gauge fixing . . . . .	43
2.6.2.2	First-order corrections . . . . .	45
<b>3</b>	<b>Anisotropic 5D Yang-Mills theory in flat spacetime</b>	<b>47</b>
3.1	The phase structure of the model from the Literature . . . . .	48
3.1.1	Dimensional Reduction via compactification . . . . .	48
3.1.2	Layered phase idea . . . . .	49
3.2	The set-up of five-dimensional anisotropic LGTs . . . . .	53
3.2.1	Anisotropic Action . . . . .	53
3.2.2	Observables . . . . .	54
3.3	Results from Lattice Simulations . . . . .	55
3.4	Discussion and Outlook . . . . .	62
<b>4</b>	<b>Anisotropic 5D Yang-Mills theory in a warped background</b>	<b>63</b>
4.1	Formalism using Mean-Field approach . . . . .	65
4.1.1	Saddle-point equations . . . . .	65
4.1.2	First-order corrections . . . . .	68
4.2	Observables . . . . .	70
4.2.1	Scalar mass . . . . .	71
4.2.2	Static quark-antiquark potential . . . . .	74
4.3	Implementation details . . . . .	78
4.3.1	Solutions to the saddle-point equations . . . . .	78
4.3.2	Boundary Conditions . . . . .	78
4.4	The phase diagram . . . . .	80
4.5	Various checks of our formalism . . . . .	82
4.5.1	Boundary Conditions . . . . .	82
4.5.2	Gauge dependence on observables . . . . .	84
4.5.3	Four-dimensional volume dependence . . . . .	85
4.6	Towards a physical interpretation . . . . .	86
4.6.1	Scalar Mass . . . . .	86
4.6.2	Static Potential . . . . .	89
4.7	Discussion and Outlook . . . . .	97
4.8	Theoretical set-up for future work . . . . .	99
4.8.1	Fermions in a warped background in the continuum . . . . .	99
4.8.2	Wilson fermions in a warped background . . . . .	101

---

<b>5</b>	<b>Conclusions</b>	<b>105</b>
<b>A</b>	<b>Further details for the Randall-Sundrum model</b>	<b>108</b>
A.1	Christoffel symbols . . . . .	108
A.2	Ricci tensor and Ricci scalar . . . . .	109
A.3	Einstein tensor . . . . .	110
<b>B</b>	<b>Character Expansions</b>	<b>111</b>
<b>C</b>	<b>First-order corrections to the Mean-Field approach</b>	<b>113</b>
C.1	V field contribution . . . . .	113
C.2	Auxiliary field contribution (H field) . . . . .	124
C.3	Gauge fixing contribution . . . . .	126
C.4	Faddeev-Popov Determinant . . . . .	129
<b>D</b>	<b>Derivations of expressions for observables in the Mean-Field Approach</b>	<b>133</b>
D.1	Scalar Mass . . . . .	134
D.2	Static Potential . . . . .	136
<b>E</b>	<b>Further results from the warped model</b>	<b>144</b>
E.1	Fits of the measured static potential to different functional forms	144
E.2	Fitting parameters of the potential . . . . .	146
<b>F</b>	<b>Mathematical Framework for fermions in a warped background</b>	<b>149</b>
F.1	Vielbeins . . . . .	149
F.2	Spin Connections . . . . .	150
F.2.1	Derivations of spin connections for the warped case . . . . .	151
F.3	Dirac operators in momentum space . . . . .	152
	<b>Bibliography</b>	<b>155</b>
	<b>Publications</b>	<b>161</b>

# List of Figures

- 1.1 A schematic illustration of the solution to the gauge field localization problem of  $U(1)$  with the DS mechanism. In both figures the region in the middle is the domain wall and the rest is the bulk. The black dot placed in the middle of the DW in both figures is a test electric charge and the lines are the associated electric field lines. In the left figure, the gauge field localization problem is shown where, due to the breaking of the gauge symmetry, the bulk behaves as a superconductor (Higgs phase) and due to Meissner effect the electric field lines are screened to the bulk. In the right figure the solution to this problem is shown when the DS mechanism is applied. The non-abelian nature of the gauge group causes the appearance of a confined phase and not a Higgs phase and consequently a dual-superconductor is created. Therefore, long-range electric fields lines exist and they are not screened to the bulk. . . . . 10
- 3.1 The phase diagram of the five-dimensional anisotropic  $SU(2)$  YM model when dimensional reduction is achieved via compactification of the extra dimension. The red points show the bulk phase transition in the absence of compactification and the rest are lines of second order transitions showing the dimensionally reduced phase. The figure was taken from Ref. [56] which uses results from [52] denoted as “Ejiri” and [58] denoted as “Knechtli”. . . . 50

3.2	A sketch of the phase diagram of the anisotropic SU(2) YM model. The dashed blue line denotes the isotropic case $\gamma = 1$ . The region above this line was previously investigated in [52, 55, 56] and the region below in [58, 71]. The dashed-dotted green line appears when the extra dimension is compactified [52, 56, 58]. When no compactification is involved, there is a bulk phase transition which is shown in the figure as a red solid line. It was shown to exist up to $\beta_4 = 2.50$ in [58]. In this work we extend the range of this line up to $\beta_4 = 2.60$ with no evidence that this line will not continue for larger values of $\beta_4$ . For $\beta_4 > 2.60$ the idea of the existence of the layered phase arises. . . . .	56
3.3	The susceptibility of the plaquette in the extra dimension, $\hat{P}_5$ for $V = 16^5$ keeping $\beta_4$ fixed at 2.60 and varying $\beta_5$ . The critical point is the point at which the susceptibility gains its maximum value. . . . .	57
3.4	The histograms for the plaquette in the extra dimension for $V = 20^4 \times 8$ , fixed $\beta_4 = 2.60$ and for two different values of $\beta_5$ : $\beta_5 = 0.843$ (top) and $\beta_5 = 0.8445$ (bottom) are shown on the left. We can see that the peak moves towards the right as we go to higher values of $\beta_5$ . The corresponding histograms for the temporal Polaykov loop are shown on the right. We can see that for $\beta_5 = 0.843$ it has a zero expectation value whereas for $\beta_5 = 0.8445$ it shows a two-peak structure. . . . .	58
3.5	Histograms of the average plaquette in the extra dimension, $\hat{P}_5$ starting from both cold and hot configurations for $V = 20^4 \times 8$ , $\beta_4 = 2.60$ and $\beta_5 = 0.8435$ . We can see that since this point is very close to the critical one, the plaquette fluctuates between the two vacua and thus the distribution is not Gaussian anymore. . . . .	59
3.6	Histograms of the average plaquette in the extra dimension, $\hat{P}_5$ starting from both cold and hot configurations for $V = 24^4 \times 8$ , $\beta_4 = 2.60$ and $\beta_5 = 0.8435$ . Here, we can see that the distributions, starting from either cold or hot, build up as two Gaussian distributions, one for each vacuum that the system equilibrates to. . . . .	60
3.7	Histograms of the average plaquette in the extra dimension, $\hat{P}_5$ starting from both cold and hot configurations for $V = 32^4 \times 8$ , $\beta_4 = 2.60$ and $\beta_5 = 0.844$ . It is clear that a first-order phase transition is present since starting from different configurations, the system equilibrates in different states with no tunnelling between them. . . . .	61

4.1	The schematic illustration of the first order mean-field corrections to the correlation function out of which a scalar mass is extracted. This is just a gauge boson exchange between two Polyakov loops at times $t_0$ and $t_0 + t$ . . . . .	73
4.2	The schematic illustration of the contributions to the first-order mean-field corrections to the static potential. These are associated with the terms in Eq. (4.46) that correspond to a gauge boson exchange(left), self-energy (centre) and tadpole (right). This figure was taken from Ref. [68]. . . . .	76
4.3	A schematic illustration of the Neumann Boundary Conditions along the extra dimension for a system with $N_5 = 5$ . The green lines represent four-dimensional layers embedded in the extra dimension. The extra-dimensional links (red arrows) are multiplied by the warp factor ( $e^{-k n_5 }$ ) and thus the exponential profile ( $AdS_5$ -space) along the extra dimension is created which is shown by the yellow dashed line. The system in the positive $n_5$ -direction is mirrored in the negative direction and then the whole system is repeated periodically. . . . .	79
4.4	The phase diagram obtained for each layer for fixed $k = 0.10$ using Neumann boundary conditions (NBC). We observe three phases, the confining(S), the deconfining(D) and the layered(L). However, there is a new phase that appears, the mixed phase, in which some of the layers are in the layered phase and some are in the deconfining phase. The width of the mixed phase increases with increasing $k$ . . . . .	81
4.5	The lattice scalar mass on four-dimensional layers as measured using 8 layers with DBC and NBC. It is clear that there is good agreement between the values for the middle layers, i.e. layers $n_5 = 3, 4, 5, 6$ . . . . .	83
4.6	The static quark potential on four-dimensional layers as measured using 8 layers with DBC and NBC. It is clear that there is good agreement between the values for the middle layers, i.e. layers $n_5 = 3, 4, 5, 6$ . . . . .	84
4.7	The lattice mass on four-dimensional layers for $N_5 = 8$ as measured using DBC and NBC. It is clear that there is good agreement between the values of the middle layers, i.e. layers $n_5 = 2, 3, 4, 5$ . . . . .	85
4.8	The lattice mass on four-dimensional layers for $N_5 = 8$ as measured imposing different choices of the gauge parameter, $\xi$ . It is clear that observables are independent of this choice. . . . .	86
4.9	The lattice mass on four-dimensional layers for $N_5 = 8$ as measured imposing different volumes along the ordinary four-dimensional space. The observables seem to be independent of the four-dimensional volume. . . . .	87



4.10	The static potential on four-dimensional layers for $N_5 = 8$ as measured when imposing different lattice sizes in the ordinary four-dimensional space. The volumes $T = L = 24, 32, 48$ and 100 were used and we show here the static potential for the layers at $n_5 = 1, 4, 8$ , i.e. the first layer, the last one and one in the middle. It seems that it behaves the same independently of the four-dimensional volume. . . . .	88
4.11	The lattice spacing along the four dimensions in physical units, $r_0$ , on each four-dimensional layer for $\beta = 2.30, \gamma = 0.505, k = 0.10, N_5 = 8$ . . . . .	90
4.12	The scalar mass in physical units, $r_0$ , on each four-dimensional layer for $\beta = 2.30, \gamma = 0.505, k = 0.10, N_5 = 8$ . The errors were estimated using standard error analysis techniques. . . . .	91
4.13	Fits to the mean-field points of the static potential for $\beta = 2.50, \gamma = 1.00, k = 0.10, N_5 = 8$ using different five-dimensional and four-dimensional forms of the potential. . . . .	92
4.14	Fits to the mean-field points of the static potential of the first layer $n_5 = 1$ using various potential forms for a lattice size of $T = L = 32, N_5 = 8$ and for $\beta = 2.30, \gamma = 0.505, k = 0.10$ . . . . .	93
4.15	Fits to the mean-field points of the static potential of the last layer $n_5 = 8$ using various potential forms for a lattice size of $T = L = 32, N_5 = 8$ and for $\beta = 2.30, \gamma = 0.505, k = 0.10$ . . . . .	94
4.16	The infinite-volume Yukawa mass in lattice spacing units on each four-dimensional layer for $\beta = 2.30, \gamma = 0.505, k = 0.10, N_5 = 8$ . First a mass was extracted from the fits of the measured potential to a four-dimensional Yukawa potential form for sizes $T = L = 24, 32, 48, 100$ and then finite-size scaling analysis was performed to get the infinite-volume mass. All error bars are tiny except for the last layer. . . . .	95
4.17	The infinite-volume Yukawa mass in physical units, $r_0$ , on each four-dimensional layer for $\beta = 2.30, \gamma = 0.505, k = 0.10, N_5 = 8$ . . . . .	96
4.18	The infinite-volume Yukawa mass in physical units, $r_0$ , on each four-dimensional layer for $\beta = 2.30, \gamma = 0.505, k = 0.10, N_5 = 8$ . . . . .	97
E.1	Fits to the static potential for $\beta = 2.50, \gamma = 1.00, k = 0.10$ and $N_5 = 8$ using various potential forms for $n_5 = 2$ . . . . .	144
E.2	Fits to the static potential for $\beta = 2.50, \gamma = 1.00, k = 0.10$ and $N_5 = 8$ using various potential forms for $n_5 = 4$ . . . . .	145
E.3	Fits to the static potential for $\beta = 2.50, \gamma = 1.00, k = 0.10$ and $N_5 = 8$ using various potential forms for $n_5 = 6$ . . . . .	145
E.4	Fits to the static potential for $\beta = 2.50, \gamma = 1.00, k = 0.10$ and $N_5 = 8$ using various potential forms for $n_5 = 8$ . . . . .	146

# List of Tables

3.1	Estimated compute time required on an NVIDIA Tesla C2070 Computing Processor for 100,000 measurements for a single point in the parameter space $(\beta_4, \beta_5)$ . . . . .	61
4.1	The lattice mass $a_4 m_4$ as measured directly from the fit to a plateau. The missing masses are at points where the excited state masses were contributing and not an obvious plateau could be obtained. It seems that as we go towards smaller $\beta$ and $\gamma$ values, the mass is decreasing (within error) but not by a large amount. .	89
4.2	The different functional behaviour of potentials in different phases.	91
E.1	Fitting parameters for $\beta = 2.30, \gamma = 0.505, k = 0.10$ for $T = L = 32, N_5 = 8$ . . . . .	147
E.2	Fitting parameters for $\beta = 2.30, \gamma = 0.505, k = 0.10$ for $T = L = 100, N_5 = 8$ . . . . .	148

# List of Acronyms

SM	Standard Model
GUT	Grand Unified Theory
GR	General Relativity
KK	Kaluza Klein
DW	Domain Wall
DS	Dvali-Shifman
SSB	Spontaneous Symmetry Breaking
GHU	Gauge-Higgs Unification
ADD	Arkani-Hamed-Dvali-Dimopoulos
RS	Randall-Sundrum
QCD	Quantum Chromodynamics
LGT	Lattice Gauge Theory
YM	Yang-Mills
QFT	Quantum Field Theory
NBC	Neumann Boundary Conditions
DBC	Dirichlet Boundary Conditions

# Chapter 1

## Introduction

The observed world that we live in seems to be accurately described by the Standard Model (SM). However, the aforementioned includes only the three out of the four fundamental forces in nature, failing to include gravity in its prescription. The ultimate goal in theoretical physics is to find a Grand Unified Theory (GUT) that will unify gravity with the strong and electroweak forces.

The idea of unifying gravity with the electromagnetic force ages back to the 1920s, when first Kaluza and Klein introduced a five-dimensional gauge theory out of which they tried to decouple the four-dimensional gauge fields from the extra-dimensional gauge field, that would give the electromagnetic potential [1, 2]. This was the first attempt to unify the known forces of nature at that time, that is electromagnetism and gravity.

Kaluza and Klein independently realized that the connection coefficient of general relativity (GR) and the field strength tensor of electromagnetism had a very similar form. As a consequence, Maxwell's equations and Einstein's field equations for GR have similar features. Therefore, they imposed some changes to the four-dimensional theory that was known in order to be able to have a theory that contains both GR and the electromagnetic potential. They introduced an extra dimension, changing the topology of the spacetime to  $M^4 \times S^1$ , and they extended the four-dimensional metric,  $g_{\mu\nu}$ , to a five-dimensional tensor,  $g_{MN}$ . By the specific choice of topology, the "cylinder condition" could be introduced, i.e. the derivatives of the extra dimension can be neglected. With this, the

---

connection coefficient

$$\Gamma_{\mu\nu\lambda} = g_{\mu\rho}\Gamma_{\nu\lambda}^{\rho} = \frac{1}{2}(\partial_{\lambda}g_{\mu\nu} + \partial_{\nu}g_{\mu\lambda} - \partial_{\mu}g_{\nu\lambda}) \quad (1.1)$$

can be written as

$$\Gamma_{\mu\nu 5} = \frac{1}{2}(\partial_{\nu}g_{\mu 5} - \partial_{\mu}g_{\nu 5}) \quad (1.2)$$

which gives the field strength tensor if we identify  $A_{\mu} = \frac{1}{2}\alpha g_{\mu 5}$ , where  $\alpha$  is the coupling constant between gravity and electromagnetism.

From a quantum mechanical point of view, the compactification of the extra dimension, i.e. the periodicity, could associate its momentum with the de Broglie wavelength. From the five-dimensional geodesic hypothesis we can identify the velocity, and therefore the momentum along the extra dimension, with the electric charge. For the latter, there is a maximum wavelength which was found to be of order  $\sim 10^{-32}\text{m}$ . This value enhanced their claim that the extra dimension is hidden from the four-dimensional world as it is very small. Kaluza's and Klein's idea is associated with what we call nowadays "compact extra dimensions" and we will come back to this when we talk about dimensional reduction later on.

Since then, many theorists have proposed models in which our four-dimensional world lives in a higher-dimensional spacetime. These models try to describe a GUT or at least to attack some of the problems which appear in current models that describe our world. One of these unsolved problems of nature is the gauge coupling unification, that is the issue that the gauge couplings of strong and electroweak forces do not have a single value at all scales in the current observed theory. For a successful GUT we require these coupling to have the same value at a large energy scale. Secondly, the fact that our observed subatomic physics are seen at the electroweak scale,  $m_{EW} \sim 10^3 \text{ GeV}$ , whereas gravity is strong at the Planck scale  $M_{Pl} \sim 10^{19} \text{ GeV}$  is one of the biggest problems in theoretical physics. This dispersion of the two scales, that are considered the two fundamental scales in nature, is called the hierarchy problem and we will see later in this chapter that many models were built with their main goal to give a solution to this. Lastly, more problems that are unsolved by the SM are those of the cosmological constant problem, dark matter and the strong CP (charge-parity) problem.

## 1.1 Dimensional Reduction

The elegance with which extra-dimensional models can solve the above problems contributed in their popularity. However, the observed world is four-dimensional and therefore we need to find ways to dimensionally reduce the proposed models to four-dimensional ones that describe accurately the physics that we measure at current accelerators. This is achieved by mainly two scenarios: compactification and localization. The former is related to the Kaluza-Klein idea and the latter is based on the brane-world scenario that will be explained below.

### 1.1.1 Kaluza-Klein compactification

We have explained earlier the idea of Kaluza and Klein to introduce an extra dimension to unify gravity with electromagnetism. The Kaluza-Klein picture has been extended to any number of dimensions, with the extra ones envisioned as being compact and small. As a toy model to illustrate dimensional reduction using the Kaluza-Klein method, we consider the scalar field theory in five dimensions with the usual Lagrangian

$$S = \frac{1}{2} \int d^4x \int_0^{2\pi R} dy (\partial_M \Phi(x^\mu, y) \partial^M \Phi(x^\mu, y) - m^2 \Phi(x^\mu, y)^2). \quad (1.3)$$

The scalar field can go through the standard Fourier decomposition to separate the extra dimensions from the usual four-dimensional ones (as a tower of states) and it is usually called Kaluza-Klein (KK) decomposition

$$\Phi(x^\mu, y) = \sum_{n=0}^{\infty} \omega_n(y) \phi_n(x^\mu). \quad (1.4)$$

After separating the variables, we know that for our theory to be dimensionally reduced we require the four-dimensional fields  $\phi_n$  to satisfy the four-dimensional Klein-Gordon equation

$$(\partial^\mu \partial_\mu + m_n^2) \phi_n = 0. \quad (1.5)$$

By requiring the extra dimension to live on a circle with a small radius,  $R$ , one finds that the field  $\Phi(x^\mu, y)$  can be written in the form

$$\Phi(x^\mu, y) = \frac{1}{\sqrt{2\pi R}}\phi_0 + \sum_{n=1}^{\infty} \frac{1}{\sqrt{\pi R}} \left[ \phi_n(x^\mu) \cos\left(\frac{ny}{R}\right) + \phi'_n(x^\mu) \sin\left(\frac{ny}{R}\right) \right]. \quad (1.6)$$

Going back to the action, we can perform the extra dimensional integral and this leaves us with

$$S = \frac{1}{2} \int d^4x \left[ \partial_\mu \phi_0 \partial^\mu \phi_0 - m^2 \phi_0^2 + \sum_{n=1}^{\infty} \left( \partial_\mu \phi_n \partial^\mu \phi_n - \left(m^2 + \frac{n^2}{R^2}\right) \phi_n^2 \right) + \sum_{n=1}^{\infty} \left( \partial_\mu \phi'_n \partial^\mu \phi'_n - \left(m^2 + \frac{n^2}{R^2}\right) \phi_n'^2 \right) \right]. \quad (1.7)$$

Now, it is clear that we recover the standard four-dimensional Lagrangian from the first two terms while the rest of them give a doubly degenerate spectrum, i.e. a tower of excited states, the so-called Kaluza-Klein (KK) modes, which are considered to be too heavy to be detected in experiments.

The same procedure as above can be applied to any extra dimensional theory out of which the corresponding four-dimensional action is recovered from the zero KK-mode, whereas the excited KK modes are decoupled from the theory by having masses on the compactification scale. The aforementioned does not imply necessarily that they live on a compact sphere. Other topologies are also allowed and indeed investigated especially in string theory models.

### 1.1.2 Localization - Non-compact extra dimensions

Until the 1980s, extra dimensions were used purely as a tool. This, however, changed in the early 1980s when people started building models where extra dimensions were seen as constituents of the universe. Firstly, Akama [3] and Rubakov and Shaposhnikov [4] independently, envisaged that the familiar four-dimensional world is trapped inside a topological defect, that is the SM particles can propagate freely along the three spatial directions but are confined in the extra dimensions, inside which the topological defect lives.

In particular, Akama considered a six-dimensional spacetime with a charged Higgs

field coupled to a U(1) gauge field with these fields creating a vortex, outside which fields are suppressed. He also showed that GR is valid in the dimensionally reduced spacetime.

On the other hand, Rubakov and Shaposhnikov, in their famous paper “*Do we live inside a Domain Wall?*”, considered a five-dimensional bulk with a real scalar field that was responsible for creating a Domain Wall (DW). In their toy model, they could show that ordinary four-dimensional scalar fields and fermions, could be trapped inside the wall. The mechanism for showing this is called “localization” and it is an alternative dimensional reduction process to compactification when extra dimensions are considered large or even infinite.

In general, one can show that a field can be localized following a standard procedure. First, we write the field that we want to localize as a product of a field that depends only on the usual four dimensions and a field that depends on the extra dimensions (separation of variables). Then, we look at the classical equations of motion that arise from the action and, by requiring that the field which depends on the ordinary four dimensions satisfies its Standard Model properties (four dimensional equation of motion, chirality etc.), we try to find a solution for the field that depends only on the extra dimensions. This will give a non-trivial topology which might be possible to accommodate the four dimensional fields. To elucidate this idea of localization, we present it for the fermionic field as proposed in Rubakov’s and Shaposhnikov’s paper, where the topological defect that traps the field is considered to be a Domain Wall [4]. The fermionic action is given by

$$S_{5D,\Psi} = \int d^5x \bar{\Psi} (i\Gamma^M \partial_M - h\phi_{DW}) \Psi \quad (1.8)$$

where  $M$  contains the usual four dimensions ( $\mu = 0, 1, 2, 3$ ) and the extra dimension, denoted as  $M = 5$  and the gamma matrices are the usual four-dimensional Dirac matrices given by  $\Gamma^\mu = \gamma^\mu$  and  $\Gamma^5 = i\gamma^5$ . The 5D equation of motion (Dirac equation) reads as

$$(i\Gamma^M \partial_M - h\phi_{DW}) \Psi = 0. \quad (1.9)$$



By separation of variables the fermionic field can be written as

$$\Psi(x^\mu, y) = \psi(x^\mu)\chi(y). \quad (1.10)$$

We impose the conditions that arise from the Standard Model on  $\psi(x^\mu)$ , i.e. that it satisfies the massless Dirac equation

$$i\gamma^\mu\partial_\mu\psi = 0 \quad (1.11)$$

and it is a left-handed fermionic field

$$\gamma^5\psi = \psi. \quad (1.12)$$

Solving the differential equation, one can show that the field  $\chi(y)$  has a solution given by

$$\chi(y) = \left[ \cosh\left(\sqrt{\frac{\lambda}{2}}vy\right) \right]^{-h\sqrt{\frac{2}{\lambda}}} \quad (1.13)$$

where the  $h$  is the strength of the coupling between the DW and the fermions and  $\lambda$  and  $v$  are parameters of the potential of the scalar field that creates the topological defect. This particular solution shows that the field  $\chi(y)$  has a peak in the center where the four-dimensional field can be localized.

Notwithstanding the aforementioned it should be noted, without further details, how these ideas of compactification and localization apply to superstring theory and M-theory. The ten-dimensional superstring theory was first shown to be a consistent theory by Green and Schwarz who realized that for the specific choice of Yang-Mills gauge groups  $SO(32)$  or  $E_8 \times E_8$  and for ten-dimensional supergravity, there is a full anomaly cancellation [5]. This theory has a redundant six-dimensional space that has to be hidden from the observed world. Kaluza-Klein idea is used to produce a lower-dimensional subspace and by Antoniadès's work [6], the KK excited states from the extra dimensions gained phenomenological interest as he proposed that the compact extra dimensions could be of much larger size than that of the original KK proposal. This would mean that in a collider of the order of a few TeVs we could be able to detect them.

A breakthrough discovery for extra-dimensional models and string theory was

made by Dai, Leigh and Polchinski [7]. This was the discovery of Dirichlet-branes (D-branes), which can be visualized as a string in higher dimensions. The idea behind them is that the strings that propagate in the bulk hit these D-branes losing a number of degrees of freedom keeping only those that allow them to move freely on the D-branes, i.e. they become localized on them. In their proposal, D2-branes were used, where the number two corresponds to the degrees of freedom that the brane has. For example, in this model the branes can be considered as a two-dimensional surface and this is the reason that they are usually visualised as walls, usually referred to as “fundamental” walls.

In the two aforementioned discoveries, compactification and localization are used independently. In the M-theory, discovered by Witten and Horava [8] and then investigated further by them and others [9, 10], which is a theory that inherits eleven spacetime dimensions, dimensional reduction is achieved by both compactification and localization. First, six out of the ten spatial dimensions are hidden using KK compactification and then D3-branes are used in the remaining five-dimensional spacetime to localize the familiar low-energy physics inside them, while gravity is allowed to propagate in the extra dimensions. Therefore, we recover the SM particles that live in a four-dimensional spacetime but also the known four-dimensional GR laws that are satisfied on the brane.

## 1.2 Gauge Field Localization Problem

The theories mentioned above that use localization to dimensionally reduce the system to the familiar low-energy regime are often called “*brane-world scenarios*”. The Domain-Wall approach, mentioned at the beginning of the localization section, provides a mechanism to localize scalar and fermionic fields and Witten’s M-Theory localizes gravity on the D3-branes. However, the most challenging problem is to find a mechanism to localize gauge fields, mostly inside a topological defect.

To illustrate the problem that arises, let us think of a five-dimensional U(1) gauge theory that couples to a scalar field that creates the topological defect (DW). The presence of this scalar field breaks the gauge symmetry in the bulk and thus the gauge field becomes massive outside the domain-wall. Moreover, the scalar field is

zero in the middle, where the defect is located, which means that the gauge field inside the DW is massless as the gauge symmetry is unbroken. The presence of the Higgs phase in the bulk, that is the development of a vacuum expectation value, creates a superconducting medium. For the U(1) gauge theory, we want to recover electromagnetism, therefore we are seeking a massless gauge field localized on the DW. However, this is not the case here as, due to Meissner effect, magnetic fields are excluded from the bulk but instead are confined to the defect, forcing electric fields to end in the bulk as the superconducting bulk attracts them. In other words electric charge is screened. This is the “gauge field localization problem” and, although there were a few proposals to resolve this issue, its solution is still elusive.

The localization of non-abelian gauge fields is also not possible because of violation of charge universality [11]. The problem arises when one considers four-dimensional effective interactions of the zero modes of charged particles with the gauge fields which depend on their wave functions along the extra dimensions. For example, the interactions with the fermionic zero modes will involve integrals like

$$\int dy \psi_0^\dagger(y) A(y) \psi_0(y) \quad (1.14)$$

From Section 1.1.2, we know that these wave functions depend on different parameters of the system which will result in different values of the above integral and thus the gauge charges of the four-dimensional theory will not be universal.

### 1.2.1 Dvali-Shifman mechanism

The most well-known solution to the gauge field localization problem that preserved charge universality was given by Dvali and Shifman in [12]. The basic idea behind this mechanism is that the Higgs phase that creates the superconductor in the bulk should be replaced by a confined phase, that creates a dual-superconductor. This is achieved when one considers a Lagrangian with a non-abelian gauge symmetry which inherits asymptotic freedom. Of course, other modifications should be done in the Lagrangian to reach spontaneously symmetry breaking in the desired regions.

The Lagrangian that Dvali and Shifman considered has an SU(2) gauge field coupled to fermions, the real scalar field,  $\phi$ , that is responsible for creating the DW configuration discussed in [4] and, in addition to this, another scalar field,  $\chi$ , in the adjoint representation of SU(2). The form of the Lagrangian is the following

$$\begin{aligned} \mathcal{L} = & -\frac{1}{2g^2} \text{Tr} F^{MN} F_{MN} + \bar{\Psi} \Gamma^M D_M \Psi - h\phi \bar{\Psi} \Psi \\ & + \frac{1}{2} (D^M \chi)^\dagger D_M \chi - \frac{1}{2} \lambda' (\chi^2 + \kappa^2 - v^2 + \phi^2)^2 \\ & + \frac{1}{2} \partial^M \phi \partial_M \phi - \frac{1}{2} \lambda (\phi^2 - v^2)^2 \end{aligned} \quad (1.15)$$

where  $\kappa, v, \lambda'$  and  $\lambda$  are real parameters and the condition  $\kappa^2 - v^2 < 0$  is imposed.

Using exactly the same idea as Rubakov's and Shaposhnikov's, the real scalar field acquires the values  $\phi = \pm v$  when the  $Z_2$  symmetry is spontaneously broken, and the DW profile is created. In the presence of the DW, the potential of the field  $\chi$  in the bulk is stable, that is the SU(2) symmetry is preserved and no SSB takes place. However, looking at the position of the wall where the value of the real scalar field,  $\phi$ , is close to zero,  $\chi$  becomes tachyonic leading to spontaneous SU(2) symmetry breaking down to U(1).

This modification of the starting gauge group of the theory, to be a non-abelian gauge group, solves the problem that was discussed before, that is the massless photon cannot be localized inside the DW. Using the Dvali-Shifman (DS) mechanism, this is no longer true as the bulk behaves as a dual superconductor which attracts magnetic field lines, in contrast to a superconductor. This makes possible long-range electric field lines to be present inside the DW and not be screened to the bulk as shown in Figure 1.1. Confinement in the bulk also ensures charge universality. Even though this is a very powerful mechanism for gauge field localization, since the bulk is in a confined phase, non-perturbative field theory is required to explore the physics of the gauge sector outside the DW.

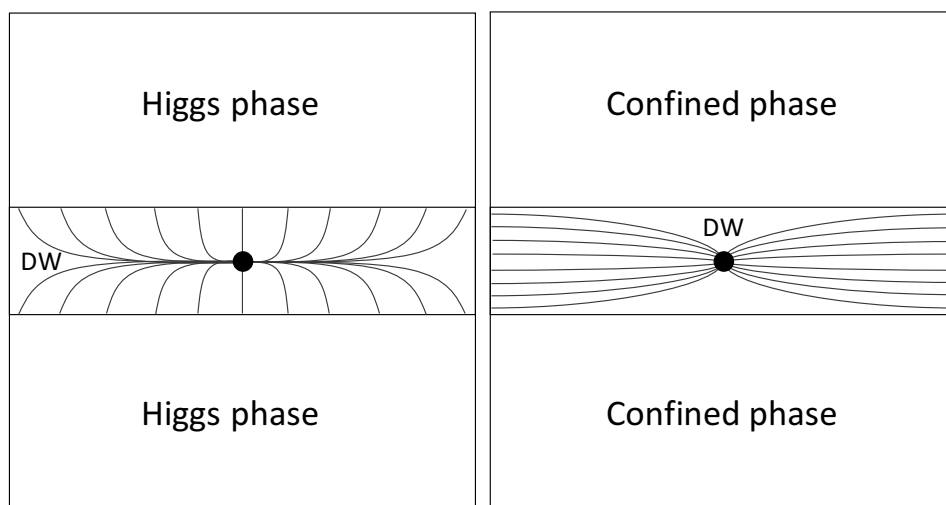


Figure 1.1: A schematic illustration of the solution to the gauge field localization problem of  $U(1)$  with the DS mechanism. In both figures the region in the middle is the domain wall and the rest is the bulk. The black dot placed in the middle of the DW in both figures is a test electric charge and the lines are the associated electric field lines. In the left figure, the gauge field localization problem is shown where, due to the breaking of the gauge symmetry, the bulk behaves as a superconductor (Higgs phase) and due to Meissner effect the electric field lines are screened to the bulk. In the right figure the solution to this problem is shown when the DS mechanism is applied. The non-abelian nature of the gauge group causes the appearance of a confined phase and not a Higgs phase and consequently a dual-superconductor is created. Therefore, long-range electric fields lines exist and they are not screened to the bulk.

### 1.3 Well-known extra-dimensional models

At the end of the 20th century there was a big boost in the formulation of new models which use extra dimensions to solve one or more of the problems that were stated above. After experimental results from the LHC and other collider experiments, and especially after the discovery of a Higgs-like particle, the number of extra-dimensional models that give possible candidates for a theory that describes our universe, has been limited and the existing ones have gained some bounds on their validity. The most important ones which are still under investigation, either in their original form or with modifications, are the the

Gauge-Higgs Unification (GHU) idea [13, 14], the Arkani-Hamed-Dimopoulos-Dvali (ADD) model [15] and the Randall-Sundrum models (RS1 and RS2) [16, 17]. Each of these will be addressed below, briefly.

### 1.3.1 Gauge-Higgs Unification

The Higgs mechanism, even if it successfully gives mass to all the SM fields, has the disadvantage that its potential is put into the SM Lagrangian arbitrarily. The idea of Gauge-Higgs Unification gives a possible solution to this, by considering the SM Lagrangian embedded in an extended spacetime instead of the ordinary four-dimensional one, without a scalar field to begin with. The gauge fields along the extra dimensions can be seen as ordinary four-dimensional scalar fields. This new idea was first proposed by [18] and [13].

Hosotani started with a theory with gauge fields and massless fermions on a manifold with topology  $M^d \times S^1$ , i.e. with an extra dimension compactified on a circle, with radius  $R$ . By making the analogy of the theory to finite temperature theories, with  $T \sim \frac{1}{R}$ , he was able to show that, due to the presence of adjoint fermions, independently of the number of fermionic flavors, the gauge symmetry is broken and the gauge field along the extra dimension is destabilized, corresponding to a scalar field in the adjoint representation, giving dynamically mass to the fermions. This mechanism is called the *Hosotani Mechanism* that introduces the dynamical electroweak spontaneous symmetry breaking.

It is obvious though, that the model that Hosotani proposed cannot be a correct extension of the SM, as the four-dimensional scalar field which is associated with the extra-dimensional gauge field belongs to the adjoint representation and not to the fundamental as the observed scalar field, the Higgs boson. What one has to do to overcome this problem is to enlarge the group of the gauge symmetry,  $G$ , and find a way to break it down to the desired  $SU(2)_L \times U(1)_Y$ .

One way of achieving this, is to replace the topology of the system from  $M^4 \times S^1$  to  $M^4 \times S^1/Z_2$ , i.e. the extra dimension is an orbifold. The Hosotani Mechanism was investigated on a  $Z_2$ -orbifold by [14], providing a realistic GHU scenario out of it. The details of the orbifold set-up are not given in this thesis, however we state the main achievements from the above work. The models under consideration were

five-dimensional SU(2) and SU(3) gauge theories coupled to fermions. As long as the inverse of the radius of the circle was close to the energies of the electroweak scale, they could show that, by assigning non-trivial  $Z_2$ -parity matrices, they could not only break the gauge symmetry spontaneously but also break the chiral symmetry. This means that the zero-mode fermions could acquire mass dynamically.

During the last decade, the GHU scenarios started being investigated using lattice techniques after the orbifold geometry was formulated on the lattice in [19]. Using the aforementioned formulation, using both Monte Carlo and mean-field calculations, SSB could be shown to occur in pure SU(2) Yang-Mills theories when the symmetry was broken at the fixed points of the orbifold, giving rise to a mass spectrum which is consistent with the SM [20–24]. From the same studies, there is evidence of localization of gauge fields on the orbifold boundaries, as the phase diagram shows a Higgs-layered phase. Non-perturbative studies for the Hosotani Mechanism using the SU(3) Yang-Mills theory, were also performed [25, 26].

### 1.3.2 Arkani-Hamed-Dimopoulos-Dvali model

In 1998, Arkani-Hamed, Dimopoulos and Dvali, proposed a new model that would solve the hierarchy problem [15]. The main idea of their model was based on the idea that everyone until that year, had been making the wrong assumption that there are two fundamental scales in nature, i.e. the electroweak scale  $m_{ew}$  and the Planck scale  $M_{pl}$ . Instead, they proposed the existence of only one fundamental scale,  $M_F$ , which is identified with the electroweak scale,  $m_{ew} \sim 1\text{TeV}$ , where gauge interactions and gravity are unified. Therefore, they abandoned the idea that gravity is unchanged from the scale that it is measured (1cm) up to the Planck Scale. To support this new idea, they extended the current manifold, in which it is believed that we live, to a  $R^{1,3} \times M^n$  manifold, where  $R^{1,3}$  is the usual pseudo-Riemannian manifold, i.e. our usual Minkowski spacetime and  $M^n$  is a compact manifold of  $n$  extra spatial dimensions with radius,  $R$ . The extra compact dimensions are responsible for weakening gravity as it propagates through them.

The main achievement of these extra compact dimensions is that gravity gets

weaker as it propagates through them. In order to find the relation between  $M_{pl}$  and the fundamental energy scale,  $M_F$ , we consider the gravitational potential that two charges feel when they are at distances much larger than the radius of the extra dimensions,  $r \gg R$ . By Gauss law, we get

$$V(r) \sim \frac{m_1 m_2}{M_F^{(2+n)}} \frac{1}{R^n r}. \quad (1.16)$$

Now, comparing it with the standard  $1/r$  potential, we can easily find the relation

$$M_{pl}^2 = M_F^{2+n} R^n \quad (1.17)$$

and considering, for example, only two extra dimensions, we can estimate the radius of the latter to be  $R \sim 0.1 - 1\text{mm}$ . The wide acceptance of this new model and the eagerness of many theorists to work on modifications and further phenomenological tests that come out of it, are mainly because of the fact that the prediction of the size of the radius of the compact extra dimensions made the latter detectable in future experiments. Even though there are still no indications of extra-dimensions from the current collider experiments, the model has not been excluded.

Even if an extra-dimensional graviton propagates in the bulk, the SM particles should be localized on a four-dimensional submanifold, that would be our observed world. In the original paper, they consider a six-dimensional  $SU(4) \times SU(2) \times SU(2)$  model with a charged  $U(1)$  scalar field which is responsible for the formation of the vortex inside which the observed low-energy physics is localized. Fermions and scalars are localized in a straight-forward way using the standard procedure described in Section 1.1.2. Localization of gauge fields, on the throat of the vortex suffers for the problem discussed in Section 1.2 and therefore they use a mechanism analogous to the DS mechanism to overcome it.

The final remark for this model is that even if it solves the original hierarchy problem, it introduces another hierarchy problem between the length scale of the fundamental scale, i.e. the electroweak scale which is of order  $10^{-16}\text{mm}$  and the radius of the extra dimensions,  $R \sim 1\text{mm}$ .



### 1.3.3 Randall-Sundrum models

In 1999, Randall and Sundrum provided an alternative solution to the Hierarchy problem using only one extra dimension by deducing an exponential relation between the weak and the Planck scales, as a consequence of a background metric that depends on the extra dimension, usually referred to as the RS1 model [16]. Using the same set-up, in a more cosmologically motivated work, they introduced the RS2 model where they could localize four-dimensional gravity to the observed universe [17].

Let us first, introduce the set-up for RS models. We start with a five-dimensional spacetime  $M^4 \times S^1/Z_2$ , that is the extra dimension,  $y$ , is of a finite extent  $2L_5$ , periodic and obeys the orbifold condition  $(x^\mu, -y) = (x^\mu, y)$ . Moreover, we consider as fundamental constituents of the theory two 3-branes located at  $y = 0$  and  $y = L_5$ . It is important to notice that these branes are not generated by the topology of the system, as in models mentioned before, but instead they are put in by hand as a starting ingredient of the model and thus it is favorable to be called 3-branes and not Domain Walls. The full action of the system will be given by the sum of the gravitational action in the bulk and the four-dimensional actions of the two branes and, following the discussion in [27], Randall and Sundrum wrote down the following terms for the five-dimensional action

$$S_{\text{bulk}} = \int d^4x \int_{-L_5}^{L_5} dy \sqrt{-G} (2M_F^3 R - \Lambda) \quad (1.18)$$

$$S_1 = \int d^4x \sqrt{-g^{(1)}} (\mathcal{L}_1 - V_1) \quad (1.19)$$

$$S_2 = \int d^4x \sqrt{-g^{(2)}} (\mathcal{L}_2 - V_2) \quad (1.20)$$

where  $R$  is the five-dimensional Ricci scalar,  $\Lambda$  a cosmological constant,  $M_F$  the five-dimensional fundamental energy scale equivalent to the Planck scale and the four-dimensional metric on the 3-branes is given by evaluating the five-dimensional one at the position of the corresponding brane, i.e.  $g_{\mu\nu}^{(1)} = G_{MN}(x^\mu, 0)$  and  $g_{\mu\nu}^{(2)} = G_{MN}(x^\mu, L_5)$ . To determine the exact form of the metric of the spacetime we use concepts of GR. In the 3-brane actions we include separate terms of the vacuum energy  $V_1, V_2$ , where the Lagrangian is kept in a general form as it contains the SM fields that should be localized on one of the 3-branes.

By making an ansatz of the background metric to be

$$ds^2 = e^{-2\sigma(y)} \eta_{\mu\nu} dx^\mu dx^\nu + dy^2 \quad (1.21)$$

the five-dimensional Einstein's equations can be solved to determine the function of the fifth dimension,  $\sigma(y)$ , to be

$$\sigma = |y| \sqrt{\frac{-\Lambda}{24M_F^3}}. \quad (1.22)$$

This leads to the conclusion that the space along the fifth dimension should be anti-de Sitter as for  $\sigma$  to make sense, a negative cosmological constant is required. More details about this are given in Appendix A.

By defining  $k^2 \equiv \frac{-\Lambda}{24M_F^3}$  the metric becomes

$$ds^2 = e^{-2k|y|} \eta_{\mu\nu} dx^\mu dx^\nu + dy^2 \quad (1.23)$$

which is sometimes referred to as the warped metric since  $e^{-2k|y|}$  is called the “warp” factor.

By considering four-dimensional fluctuations,  $h_{\mu\nu}(x)$ , about the Minkowski metric one can get an effective four-dimensional version of GR. By substituting the warped metric of Eq. (1.23) with the above fluctuations into Eq. (1.18), we get

$$\begin{aligned} S_{\text{eff},4D} &\sim \int d^4x \int_{-L_5}^{L_5} dy \sqrt{-g(x)} 2M_F^3 e^{-2k|y|} R^{(4D)} \\ &= \int d^4x \frac{2M_F^3}{k} (1 - e^{-2kL_5}) R^{(4D)} \end{aligned} \quad (1.24)$$

where  $R^{(4D)}$  is the Ricci scalar in four dimensions and in the second line we performed the integral over the fifth dimension. We can compare this effective action with the Einstein-Hilbert action for four-dimensional GR

$$S_{\text{E-H}} \sim \int d^4x \sqrt{-g} 2M_{Pl}^2 R \quad (1.25)$$

to see the effect of the warp factor on the Planck scale. This is given by

$$M_{pl}^2 = \frac{M_F^3}{k} (1 - e^{-2kL_5}). \quad (1.26)$$

It is obvious that in the limit in which  $kL_5$  is taken to be large, there is only a negligible modification to the Planck scale.

In the RS1 model, the observed four-dimensional world is considered to be the brane that is placed at  $y = L_5$ . To demonstrate how the hierarchy problem is solved we consider the Lagrangian density in Eq. (1.20) to be

$$\mathcal{L}_2 = g_{(2)}^{\mu\nu} \partial_\mu \phi^\dagger \partial_\nu \phi - \lambda (\phi^\dagger \phi - v^2)^2 \quad (1.27)$$

where  $v$  is the dimensionful parameter of the model, and here it is the Planck scale. The action then becomes

$$S_2 \sim \int d^4x e^{-4kL_5} \sqrt{-g(x)} \left( e^{2kL_5} g^{\mu\nu} \partial_\mu \phi^\dagger \partial_\nu \phi - \lambda (\phi^\dagger \phi - v^2)^2 \right). \quad (1.28)$$

In order to have a quantized theory with a spectrum, we need to have a canonical kinetic term which is achieved by rescaling the scalar fields,  $\phi = e^{kL_5} \phi'$ . Then we get

$$S_2 \sim \int d^4x \sqrt{-g(x)} \left( g^{\mu\nu} \partial_\mu \phi'^\dagger \partial_\nu \phi' - \lambda (\phi'^\dagger \phi' - (ve^{-kL_5})^2)^2 \right). \quad (1.29)$$

Now, we can see that the dimensionful parameter is exponentially suppressed from  $v$  to  $ve^{-kL_5}$ , and thus it can get the natural value of the electroweak scale,  $m_{ew} \sim \text{TeV}$ , for values of  $kL_5 \sim 35$ .

Even if RS2 focuses on the localization of gravity on a 3-brane which is not so relevant to this thesis, we give the main idea of it just for completeness of the discussion on the RS models. The whole set-up of the model is the same as above with the only difference being that the brane that is considered as the four-dimensional world is considered to be the one that is placed at  $y = 0$ . The main focus of [16] was to show that by determining the behaviour of the five-dimensional perturbations along the extra dimension in the presence of the warped metric, i.e.  $h_{MN}(x^\mu, y)$ , one can identify them as the usual four-dimensional perturbations of GR. The process of localizing gravity is similar to the one that we used

for localizing the other fields, that is one performs a KK decomposition to the perturbations,  $h_{MN}$  as

$$h_{MN}(x^\mu, y) = \sum_n h_{\mu\nu}^n(x^\mu) \chi_n(y). \quad (1.30)$$

We require four-dimensional perturbations to satisfy the wave equation i.e.

$$\partial^\sigma \partial_\sigma h_{\mu\nu}^n(x^\mu) = -m_n^2 h_{\mu\nu}^n(x^\mu) \quad (1.31)$$

and from this the extra-dimensional profile of the modes  $\chi_n$  can be determined. After some redefinitions of the modes and defining the extra-dimensional coordinate in terms of  $z$  using

$$k|z| = e^{k|y|} - 1 \quad (1.32)$$

which is consistent with a conformally flat metric, one can show, with systematic work, that the extra-dimensional perturbation modes obey a Schrödinger-like equation with potential of the form

$$V(z) = \frac{15}{4} \frac{k^2}{(1+k|z|)^2} - \frac{3k(\delta(z) - \delta(z - L_z))}{1+k|z|}. \quad (1.33)$$

The shape of this potential, which looks like a volcano, enhances the trapping of gravity at the position of the brane,  $z = 0$ . In other words, the wavefunction of the graviton zero-mode has a peak around the position of the brane on which we live on (visible brane) and therefore it is localized on it.

## 1.4 Present Work and Thesis Outline

In this thesis, we investigate five-dimensional gauge theories on the lattice, focusing in particular on the SU(2) anisotropic lattice gauge theory. The main motivation for this, is the need to find a non-perturbative way to localize gauge fields on four-dimensional branes. As the gauge field localization problem appears in both flat and warped spacetime, we implement studies for both spacetime geometries. We are particularly interested in finding a non-trivial UV fixed

point at which the five-dimensional theory can be dimensionally reduced to a four-dimensional one, in the case where the extra dimension is not compactified. Therefore, we investigate the phase structure of the five-dimensional anisotropic  $SU(2)$  Yang-Mills theory to search for such a fixed point.

This thesis is structured as following: In Chapter 2 we give details of the non-perturbative way we chose to investigate our systems, that is Lattice Gauge Theories. At the end of the Chapter we describe the two specific methods for Lattice Gauge Theories investigations that are used here. In Chapter 3 and Chapter 4 we present the details of the exploration of the phase diagram of the five-dimensional anisotropic  $SU(2)$  model in flat and warped spacetime, respectively. Finally, our conclusions and an outlook of our work are presented in Chapter 5.

## Chapter 2

# Lattice Gauge Theories

In particle physics, theories with strong dynamics, such as Quantum Chromodynamics (QCD), cannot be investigated using perturbation theory at low energy scales, as at these scales the coupling becomes strong and perturbative analysis is not possible anymore. The need to investigate these theories with strong coupling forced researchers to develop non-perturbative ways that would allow their exploration. A very powerful tool that allows their investigation is the lattice that is widely used for particle physics and condensed matter theories.

The idea behind Lattice Gauge Theories (LGTs) as a non-perturbative tool, is the discretization of spacetime. The discretization of time in the path integral formulation is well-known, in which one takes the limit of the discretization parameter of time, usually referred to as  $\epsilon$ , to zero and recovers the continuum spacetime. In contrast, in Lattice Theories, the whole spacetime is discretized and the world can be seen as a hypercubic lattice, with a lattice spacing,  $a$ . The advantage of using LGTs in the investigation of quantum field theories is twofold. Not only can one investigate a theory in its strongly coupled region but also, the Euclidean quantum field theory associated with it comes with a natural cutoff/regulator which is related to the inverse of the lattice spacing. Even though simulations of theories are allowed at strong coupling, the discretization does not come without cost as one not only has to force the lattice spacing to go to zero to recover the continuum, but also has to deal with the fact that the simulations are done in a finite volume which might have an effect on the extracted physics of the theories.

In the following chapter, we use a toy model of a scalar field theory to introduce concepts that we use to construct the pure Yang-Mills (YM) theory on the lattice and useful observables associated with it. Then we briefly present how fermions can be formulated on the lattice followed by an introduction to the anisotropic LGTs. Furthermore, we discuss the phase structure of LGTs and how one can go from the discretized version to the continuum theory that describes the observed world. Towards the end, methods of investigating these theories are discussed. This Chapter is based on the material of [28–31].

It is also worth mentioning the convention that is used from now on in this thesis. In all equations, the Greek letters run from 0 to 3 and they correspond to the usual four-dimensional spacetime coordinates, with the 0th direction identified as the temporal direction (sometimes denoted by  $T$  or  $\tau$  as well). Capital Roman letters are used to include extra dimensions as well. To say, in the case of a five-dimensional spacetime  $M, N = 0, 1, 2, 3, 5$ . Finally the small Roman letters, usually  $i, j$ , are used only for the three spatial directions.

## 2.1 QFT on the lattice - Lattice discretization

This thesis focuses on studies of gauge field theories. In order to see how gauge fields, and consequently gauge theories, can be formulated on a lattice from their Euclidean continuum formulation, we first consider a toy model of a theory with  $N$  complex scalar fields. The Euclidean scalar action reads as

$$S_E = \int d^4x [\partial_\mu \phi^\dagger(x) \partial_\mu \phi(x) + m^2 |\phi(x)|^2]. \quad (2.1)$$

The integral on a lattice grid can be replaced by a sum over all lattice points as

$$\int d^4x \rightarrow a^4 \sum_n \quad (2.2)$$

and the partial derivatives by the discretized forward derivative,  $\Delta_\mu^{(f)}$  (or any other discretized form of a derivative)

$$\Delta_\mu^{(f)}\phi(n) = \frac{\phi(n + a\hat{\mu}) - \phi(n)}{a}. \quad (2.3)$$

Using the above, Eq.(2.1) takes the following discretized form

$$\begin{aligned} S_{\text{latt}}^{(\phi)} &= 8a^2 \sum_n \phi^\dagger(n)\phi(n) - 2a^2 \sum_{\mu;n} \phi^\dagger(n + a\hat{\mu})\phi(n) + a^4 \sum_n m^2 |\phi(n)|^2 \\ &= 8a^2 \sum_n \phi^\dagger(n)\phi(n) - 2a^2 \sum_{\langle n'n \rangle} \phi^\dagger(n')\phi(n) + a^4 \sum_n m^2 |\phi(n)|^2 \end{aligned} \quad (2.4)$$

where  $\langle n'n \rangle$  denotes the sum of nearest-neighbouring sites.

It is known that the path integral in Euclidean quantum field theory can be seen as a partition function with Boltzmann weight factor  $e^{-S_E^{(\phi)}}$  which relates the quantum field theory to statistical systems. However, in the case of Euclidean path integrals one deals with divergent integrals as they are integrals over an infinite number of field configurations. The discretization of the spacetime provides a regulator for free and thus the functional integral of the theory on a four-dimensional lattice becomes a well-defined integral; a multiple integral over all values of the field at all lattice points given by

$$Z = \int_{-\infty}^{+\infty} \prod_n d\text{Re}\phi(n)d\text{Im}\phi(n)e^{-S_{\text{latt}}^{(\phi)}}. \quad (2.5)$$

where  $d\text{Re}\phi(n)d\text{Im}\phi(n)$  is the measure of the functional integral.

Before discussing further how one deals with a discretized action to compute observables and relate them back to continuum physics, let us look at the symmetries of the kinetic term of the latticized scalar action. If we consider global gauge transformations,  $\phi \rightarrow \phi'(n) = \Omega\phi(n)$ , it is trivial to see that the action is invariant as the transformation matrix  $\Omega$  has no coordinate dependence. However, it is easily seen that it loses its gauge symmetry under local transformations,  $\phi \rightarrow \phi'(n) = \Omega(n)\phi(n)$ , as the second term transforms as

$$\phi^\dagger(n')\phi(n) \rightarrow \phi^\dagger(n')\Omega^\dagger(n')\Omega(n)\phi(n). \quad (2.6)$$



and  $\Omega^\dagger(n')\Omega(n)$  is not equal to  $\mathbb{1}$  anymore.

Inspired by GR, we can introduce an analogue to the parallel transporter, i.e. a matrix  $U \in \text{SU}(N)$  that maps a field from a vector space  $V_x$  to a vector space  $V_y$  where  $x$  and  $y$  are two spacetime points connected by a continuous curve  $\mathcal{C}_{yx}$ . Under local gauge transformations, the parallel transporter satisfies the following relation

$$U'(\mathcal{C}_{yx}) = \Omega(y)U(\mathcal{C}_{yx})\Omega^\dagger(x). \quad (2.7)$$

Having Eq.(2.7) in mind, we can see that if we introduce a matrix  $U(n', n)$  in our discretized version of the scalar field action, with the curve being the smallest possible distance between point  $n$  and  $n'$  on the lattice, which is the lattice spacing,  $a$ , we can recover local gauge invariance as the second part of the kinetic term transforms as

$$\phi^\dagger(n')U(n', n)\phi(n) \rightarrow \phi^\dagger(n')\Omega^\dagger(n')\Omega(n')U(n, n')\Omega^\dagger(n)\Omega(n)\phi(n). \quad (2.8)$$

This parallel transporter on the lattice is called the *link variable* and satisfies all the properties of the parallel transporter with  $U(n', n) = U^\dagger(n, n')$ , being the most important. Also, it is useful to note that the link variable is usually called  $U_\mu(n)$  which corresponds to the oriented link that connects the site at position  $n$  to the one at  $n + a\hat{\mu}$  and thus  $U_\mu^\dagger(n)$  will correspond to the opposite orientation.

Requiring the fields to have a local gauge symmetry, the newly introduced link variables have to be included in the action. However, in the naive continuum limit, the continuous action of Eq. (2.1) is not recovered anymore, but instead an action in which scalar fields are coupled to gauge fields can be obtained. In other words, we promote the partial derivatives of the action to the covariant ones. We define the lattice covariant derivative to be

$$D_\mu\phi(n) = \frac{U_\mu^\dagger(n)\phi(n + a\hat{\mu}) - \phi(n)}{a} \quad (2.9)$$

so the action can be written as

$$S_{\text{latt}}^{(\phi)} = a^4 \sum_{n;\mu} (D_\mu\phi(n))^\dagger (D_\mu\phi(n)) + a^4 \sum_n m^2 |\phi(n)|^2. \quad (2.10)$$

The link variables are matrices of  $SU(N)$ , therefore they can be related to the gauge fields  $A_\mu(x)$ . From standard Group theory we know that an element of a special unitary group can be written as

$$U = \exp(i\omega^a T_a) \quad (2.11)$$

where  $\omega^a$  are real variables and  $T_a$  are the generators of the Lie algebra of the group. We also know that a gauge field associated with an  $SU(N)$  group can be written as

$$A_\mu(x) = -igA_\mu^a(x)T_a \quad (2.12)$$

therefore we can write the link variables in terms of the gauge fields, i.e.

$$U_\mu(n) = \exp(-igaA_\mu^b(n)T_b). \quad (2.13)$$

With this connection between the link variables and the gauge fields, one can easily check that the lattice covariant derivative becomes the usual covariant derivative that we use in the continuum.

### 2.1.1 Pure lattice gauge theory - The Wilson action

Starting from a toy model of a scalar field theory, the link variables associated with the gauge fields were introduced. Wilson in 1974 [32], formulated an  $SU(N)$  lattice action which leads to the pure Yang-Mills action in the naive continuum limit. He first introduced the smallest closed loop that one can define on a lattice out of the link variables, that is the plaquette given by

$$U_{\mu\nu}(n) = U_\mu(n)U_\nu(n + a\hat{\mu})U_\mu^\dagger(n + a\hat{\nu})U_\nu^\dagger(n) \quad (2.14)$$

and then defined the pure lattice gauge action on the lattice, the so-called Wilson action, to be

$$S_W[U] = \sum_n \sum_{1 \leq \mu < \nu \leq 4} \beta \left[ 1 - \frac{1}{2\text{Tr}\mathbb{1}} (\text{Tr}U_{\mu\nu}(n) + \text{Tr}U_{\mu\nu}^\dagger(n)) \right] \quad (2.15)$$

and specifically for  $SU(N)$  groups to be

$$S_W[U] = \sum_n \sum_{1 \leq \mu < \nu \leq 4} \beta \left[ 1 - \frac{1}{N} \text{ReTr} U_{\mu\nu}(n) \right]. \quad (2.16)$$

Using Eq.(2.13) one can easily show that

$$U_{\mu\nu}(n) = \exp(-iga^2 F_{\mu\nu}(n) + \mathcal{O}(a^3)). \quad (2.17)$$

Plugging it back into Eq.(2.16) one shows that, due to asymmetry of  $F_{\mu\nu}(n)$  and since we cannot have gauge invariant operators of  $\mathcal{O}(a^5)$ , the action up to order  $\mathcal{O}(a^6)$  becomes

$$S_W[U] = \beta \sum_n \sum_{\mu, \nu} \left[ \frac{g^2 a^4}{4N} \text{Tr}(F_{\mu\nu}(n)^2) + \mathcal{O}(a^6) \right] \quad (2.18)$$

which is identified with the pure Yang-Mills action if one defines

$$\beta = \frac{2N}{g^2}. \quad (2.19)$$

## 2.1.2 Observables

Out of the ingredients of a LGT, we can construct gauge invariant observables. Here we present the most commonly used in the exploration of pure LGTs.

- **The plaquette**

It was mentioned above that the trace of the plaquette is gauge invariant. Therefore, an observable that is measured is the internal energy of the plaquette, given by the mean value of its trace. This is analogous to the statistical systems, with  $\beta \sim 1/T$ .

$$U \sim \frac{\partial(\ln Z(\beta))}{\partial\beta}. \quad (2.20)$$

So, varying the lattice coupling,  $\beta$ , is analogous to thermal changes of the system and the behaviour of the internal energy close to phase transitions give signals of either first-order transition, if there is a discontinuity, or a

continuous one.

- **Wilson loop - Static quark potential**

The Wilson loop is a closed loop made out of link variables. It can be formed along only two directions or along more than two and they are distinguished into planar or non-planar, respectively. In the following discussion we consider only planar-rectangular Wilson loops, along a spatial and a temporal direction. We define the Wilson line along direction  $\mu$  to be

$$l_\mu^{(r)}(n) = \prod_{k=0}^{r-1} U_\mu(n + ka\hat{\mu}) \quad (2.21)$$

where  $r$  is the length of the line and  $n$  is the starting point of the line. A Wilson loop is then given by

$$W_{\mathcal{L}} = \text{Tr} \left[ l_j^{(r)}(n_0) l_0^{(t)}(n_0 + ra\hat{\mu}) l_j^{\dagger(r)}(n_0 + ta\hat{0}) l_0^{\dagger(t)}(n_0) \right] \quad (2.22)$$

where,  $j$ , denotes one of the spatial directions and 0 the temporal direction. If we consider a two-dimensional lattice with  $t_0$  and  $r_0$  the temporal and spatial starting positions respectively we can define the Wilson lines as

$$l_S^{(r)}(t_0, r_0) = \prod_{k=0}^{r-1} U_s(t_0, r_0 + ak) \quad (2.23)$$

$$l_T^{(n_t)}(t_0, r_0) = \prod_{k=0}^{n_t-1} U_t(t_0 + ak, r_0) \quad (2.24)$$

and the last equation is also called the temporal transporter. Then the Wilson loop is given by

$$W_{\mathcal{L}} = \text{Tr} \left[ l_S^{(r)}(t_0, r_0) l_T^{(n_t)}(t_0, r_0 + r) l_S^{\dagger(r)}(t_0 + n_t, r_0) l_T^{\dagger(n_t)}(t_0, r_0) \right]. \quad (2.25)$$

where  $t_0 + n_t$  is less than the whole lattice extent along the temporal direction,  $N_T$  and similar for  $r_0 + r$ .

The expectation value of the Wilson loop is related to the static potential of a quark-antiquark pair,  $V(r)$ . To show exactly how this relation holds, one has to go to the axial gauge, i.e. set  $U_T = \mathbb{1}$ . Then Eq.(2.25), starting

from  $t_0 = 0$  reads as

$$W_{\mathcal{L}} = \text{Tr} \left[ l_S^{(r)}(0, r_0) l_S^{\dagger(r)}(n_t, r_0) \right]. \quad (2.26)$$

This expectation value is nothing else but the Euclidean correlator of two Wilson lines located at different timeslices. From Euclidean field theory it is well-known that

$$\lim_{T \rightarrow \infty} \langle O_2(t) O_1(0) \rangle_T = \sum_n \langle 0 | \hat{l}_S^{(r)}(r_0) | n \rangle \langle n | \hat{l}_S^{\dagger(r)}(r_0) | 0 \rangle e^{-tE_n}. \quad (2.27)$$

where  $E_n$  is the energy state relative to the ground state. The lowest energy state,  $E_1$ , corresponds to the static quark-antiquark pair potential,  $V(r)$  so we conclude

$$\langle W_{\mathcal{L}} \rangle \sim e^{-tV(r)} = e^{-an_t V(r)}. \quad (2.28)$$

At short distances ( $r \rightarrow 0$ ), the QCD quark-anti-quark potential is analogous to the QED potential and using perturbative calculations one can show that it appears to be Coulomb-like, proportional to  $\alpha_s$ , i.e. the QCD running coupling as shown in Eq. (2.29).

$$V(r) = -\frac{4}{3} \frac{\alpha_s}{r} + c. \quad (2.29)$$

In the limit  $r \rightarrow \infty$ , QCD is considered to be a string model. Analogous to the electric field lines between two electric charges, one can think that the color field lines hold together a quark- anti-quark pair. The strong self-interaction of the gluons pulls the line together to form a string. In this limit the potential, due to confinement, must increase indefinitely and thus it rises linearly with the distance. Lüscher et al. in [33] showed that quantum fluctuations of the string give rise to an attractive effective Coulomb potential, which is a universal term in four dimensions. Thus, the potential form at  $r \rightarrow \infty$  reads as

$$V(r) = \sigma r - \frac{\pi}{12r} + c \quad (2.30)$$

where  $\sigma$  is the string tension and the second term is called the Lüscher term.

- **Polyakov Loop**

Another gauge-invariant quantity of pure LGTs is the Polyakov loop which is defined as a Wilson line covering all lattice points in that direction. In the temporal direction one can define it as

$$P_T(\vec{n}) = \text{Tr} \left[ \prod_{j=0}^{N_T-1} U_0(j, \vec{n}) \right]. \quad (2.31)$$

In spite of the fact that the expectation value of the Polyakov loop itself is an important observable when exploring the phase diagram of a theory, the expectation value of two Polyakov loops located at two different spatial points of a distance,  $r = a|\vec{m} - \vec{n}|$ , can also give an estimate of the potential as the Wilson loop

$$\langle P_T(\vec{m}) P_T^\dagger(\vec{n}) \rangle \sim e^{-a N_T V(r)}. \quad (2.32)$$

### 2.1.3 Discrete symmetries of the Wilson action

After the discretization of spacetime, the known continuous spacetime symmetries like translational and rotational symmetries are broken. However, one can define discrete symmetries that are used in order to construct useful quantities for investigations of systems on the lattice.

The first symmetry to discuss is the *charge conjugation*, usually denoted as  $\mathcal{C}$ . Charge conjugation, is responsible for changing the sign of the quantum properties of a particle in order to transform it to its anti-particle. The charge conjugation on the link variables acts as

$$U_\mu(n)^{\mathcal{C}} = U_\mu(n)^* = (U_\mu(n)^\dagger)^T. \quad (2.33)$$

We can easily check that this means that a gauge field  $A_\mu(n)$  will become  $-A_\mu(n)^T$ , i.e. the gauge coupling changes sign, as one would expect for the antiparticle.

The next symmetry to consider is *parity*, denoted by  $\mathcal{P}$ . Parity transformation is the one under which the sign of a spatial coordinate is flipped. On the gauge

links this is given by

$$U_j(n_0, \vec{n})^{\mathcal{P}} = U_j(n_0, -\vec{n} - \hat{j})^\dagger \quad \text{for } j = 1, 2, 3 \quad (2.34)$$

$$U_0(n_0, \vec{n})^{\mathcal{P}} = U_0(n_0, -\vec{n}). \quad (2.35)$$

In the usual Minkowski spacetime, we know that a fundamental symmetry in nature is the so-called  $\mathcal{CPT}$ -symmetry.  $\mathcal{T}$  denotes the time-reversal transformation, i.e. a reflection in the temporal coordinate. On the lattice this is realized as the product of three Euclidean reflections, i.e.  $\mathcal{E}_1\mathcal{E}_2\mathcal{E}_3$  where we define

$$U_\mu(n)^{\mathcal{E}_\mu} = U_\mu(R_\mu(n)) \quad (2.36)$$

$$U_\nu(n)^{\mathcal{E}_\mu} = U_\nu(R_\mu(n) - \hat{\nu})^\dagger \quad (2.37)$$

where  $R_\mu(n)$  is the four-vector  $n$  with all components reflected except in the direction  $\mu$ .

## 2.2 Fermions on the lattice

Fermions are fundamental constituents of the SM and their investigation is of high importance. The fact that QCD is a strongly coupled theory involving fermions and gauge fields highlights the importance of finding methods to investigate fermionic fields on the lattice. As a starting point we discretize the Euclidean action of the aforementioned fields given by

$$S_E^{(f)} = \int d^4x \bar{\psi}(x) (\gamma_\mu \partial_\mu + m) \psi(x). \quad (2.38)$$

Using the central discretized derivative the action for free fermions on the lattice reads as

$$S_{\text{lat}}^{(f)} = a^4 \sum_n \bar{\psi}(n) \left[ \sum_\mu \gamma_\mu \frac{\psi(n + \hat{\mu}) - \psi(n - \hat{\mu})}{2a} + m\psi(n) \right]. \quad (2.39)$$

If we want this fermionic action to be invariant under local gauge transformations, similar arguments as in the scalar field theory in Section 2.1 apply and we can see that the fermionic action corresponding to the continuum action of QCD, in

which the fermionic fields are coupled to gauge fields via the covariant derivative, is given by

$$S_{\text{lat}}^{(f)}[\bar{\psi}, \psi, U] = a^4 \sum_n \bar{\psi}(n) \left[ \sum_{\mu} \gamma_{\mu} \frac{U_{\mu}(n)\psi(n + \hat{\mu}) - U_{\mu}^{\dagger}(n - \hat{\mu})\psi(n - \hat{\mu})}{2a} + m\psi(n) \right]. \quad (2.40)$$

The above action can be written as

$$S_{\text{lat}}^{(f)}[\bar{\psi}, \psi, U] = a^4 \sum_{n,m} \bar{\psi}(n) D(n, m) \psi(m) \quad (2.41)$$

where the Dirac operator is given by

$$D(n, m) = \sum_{\mu} \gamma_{\mu} \frac{U_{\mu}(n)\delta_{n+\hat{\mu},m} - U_{\mu}^{\dagger}(n - \hat{\mu})\delta_{n-\hat{\mu},m}}{2a} + m\delta_{n,m}. \quad (2.42)$$

The path integral of QCD, which is the desired calculable quantity to extract physics, is given by

$$\begin{aligned} Z_{QCD} &= \int \mathcal{D}U \int \mathcal{D}\bar{\psi} \mathcal{D}\psi e^{-S_{QCD}} \\ &= \int \prod_l dU_l \int \prod_i d\bar{\psi}_i d\psi_i e^{-S_W[U] - S_{\text{lat}}^{(f)}} \\ &= \int \prod_l dU_l e^{-S_W[U]} \det(-D[U]) \end{aligned} \quad (2.43)$$

where going from the second line to the third we have performed a Gaussian integral over Grassmann variables.

An interesting quantity that we want to measure is the fermion propagator. This is given by the inverse of the Dirac operator given in Eq. (2.42). In order to invert



it we go into momentum space as shown in Eq.(2.44).

$$\begin{aligned}
 \tilde{D}(p, q) &= \frac{1}{N^4} \sum_{n, m} e^{-ip \cdot na} e^{iq \cdot ma} \left( \sum_{\mu} \gamma_{\mu} \frac{U_{\mu}(n) \delta_{n+\hat{\mu}, m} - U_{\mu}^{\dagger}(n - \hat{\mu}) \delta_{n-\hat{\mu}, m}}{2a} + m \delta_{n, m} \right) \\
 &= \frac{1}{N^4} \sum_n e^{-ip \cdot na} \left( \sum_{\mu} \gamma_{\mu} \frac{U_{\mu}(n) e^{iq \cdot (n+\hat{\mu})a} - U_{\mu}^{\dagger}(n - \hat{\mu}) e^{iq \cdot (n-\hat{\mu})a}}{2a} + m e^{iq \cdot na} \right) \\
 &= \frac{1}{N^4} \sum_n e^{-i(p-q) \cdot na} \left( \sum_{\mu} \gamma_{\mu} \frac{U_{\mu}(n) e^{iq_{\hat{\mu}} a} - U_{\mu}^{\dagger}(n - \hat{\mu}) e^{-iq_{\hat{\mu}} a}}{2a} + m \mathbb{1} \right). \quad (2.44)
 \end{aligned}$$

Imposing the trivial gauge, i.e. setting all gauge fields to  $\mathbb{1}$ , the Dirac operator in momentum space is

$$\begin{aligned}
 \tilde{D}(p, q) &= \frac{1}{N^4} \sum_n e^{-i(p-q) \cdot na} \left( \sum_{\mu} \gamma_{\mu} \frac{e^{iq_{\hat{\mu}} a} - e^{-iq_{\hat{\mu}} a}}{2a} + m \mathbb{1} \right) \\
 &= \delta_{p, q} \left( m \mathbb{1} + \frac{i}{a} \sum_{\mu} \gamma_{\mu} \sin(p_{\mu} a) \right) \\
 &\equiv \delta_{p, q} \tilde{D}(p). \quad (2.45)
 \end{aligned}$$

To get the fermion propagator, the only thing that is left is to invert it to get

$$\tilde{D}(p)^{-1} = \frac{m \mathbb{1} - \frac{i}{a} \sum_{\mu} \gamma_{\mu} \sin(p_{\mu} a)}{m^2 + \sum_{\mu} \frac{\sin(p_{\mu} a)^2}{a^2}}. \quad (2.46)$$

In the naive continuum limit this recovers the free fermion propagator in Euclidean spacetime which is given by

$$G(p)^{-1} = \frac{m - i \not{p}}{p^2 + m^2}. \quad (2.47)$$

For simplicity we consider the free massless propagator which in the continuum has a pole at  $p = 0$ . In Lattice Gauge theories, the momentum space is restricted to the first Brillouin zone with periodic boundary conditions, i.e.  $p_{\mu} \in (-\pi/a, \pi/a]$ . Therefore in addition to the physical  $p = (0, 0, 0, 0)$  pole, 15 more values of  $p$  that involve zeroes and  $\pi/a$  give rise to unphysical poles that need to be removed. This is known as the doubling problem. Of course one can show the existence of the unphysical poles for the massive propagator using

complex analysis by illustrating that the energy is equal to the mass not only at the rest frame but at other points as well that can be visualized as corners of the Brillouin zone in the four-dimensional plane.

A solution to this problem was proposed by Wilson, who introduced a new term in the Dirac operator that could be considered as an effective mass that vanishes in the naive continuum limit as in Eq. (2.48)

$$\tilde{D}(p) = m\mathbb{1} + \frac{i}{a} \sum_{\mu} \gamma_{\mu} \sin(p_{\mu}a) + \mathbb{1} \frac{1}{a} \sum_{\mu} (1 - \cos(p_{\mu}a)) \quad (2.48)$$

so that the inverse reads as

$$\tilde{D}(p)^{-1} = \frac{\left(m + \frac{1}{a} \sum_{\mu} (1 - \cos(p_{\mu}a))\right) \mathbb{1} - \frac{i}{a} \sum_{\mu} \gamma_{\mu} \sin(p_{\mu}a)}{\left(m + \frac{1}{a} \sum_{\mu} (1 - \cos(p_{\mu}a))\right)^2 + \sum_{\mu} \frac{\sin(p_{\mu}a)^2}{a^2}}. \quad (2.49)$$

With this modification, the unwanted poles become heavy, as the extra term gives an “effective” contribution to the mass proportional to  $1/a$ . Lastly, one wants to go back to the coordinate space, where the Wilson-Dirac operator is given by

$$D_W(n, m) = \left(m + \frac{4}{a}\right) \delta_{n,m} - \frac{1}{2a} \sum_{\mu=\pm 1}^{\pm 4} (\mathbb{1} - \gamma_{\mu}) U_{\mu}(n) \delta_{n+\hat{\mu},m} \quad (2.50)$$

where the definition  $\gamma_{-\mu} \equiv -\gamma_{\mu}$  is used.

In 1981, Nielsen and Ninomiya [34–36] proved a no-go theorem according to which it is impossible to construct a lattice fermion action that inherits all the following simultaneously:

- it is local
- it has the correct continuum limit
- it is free from doublers
- it implements chiral symmetry, i.e.  $\{D, \gamma_5\} = 0$

This is consistent with Wilson fermions, as in order to remove the doublers one has to give up chirality.

This thesis mostly focuses on pure  $SU(2)$  gauge theory on the lattice. However,

Wilson fermions appear in a formalism that we give at the end of Chapter 4. Therefore, we do not mention other types of fermions that are formulated on the lattice as they are irrelevant to this thesis.

## 2.3 Anisotropic Lattice Gauge Theories

The investigation of QCD at non-zero temperature was the major force driving the development of anisotropic LGTs. The main reason is that the temperature,  $T$ , is related to the lattice spacing and the extent of the temporal direction as  $T = 1/(N_\tau a)$ , which means that the maximum temperature that can be reached is given by the inverse lattice spacing with only one lattice point along the temporal direction. Introducing an asymmetry between the spatial and the temporal lattice spacings,  $a_s$  and  $a_\tau$  respectively given by the asymmetry parameter

$$\xi = \frac{a_s}{a_\tau} \quad (2.51)$$

one can have a smaller  $a_\tau$  or more lattice points giving a higher temperature.

For the formulation of the anisotropic action, we consider two lattice couplings, one for the spatial and one for the temporal plaquettes,  $\beta_s$  and  $\beta_\tau$  respectively, such that the anisotropic Wilson action is read as

$$S_G[U_s, U_\tau] = \beta_s \sum_n \sum_{1 \leq i < j \leq 3} \left[ 1 - \frac{1}{N} \text{ReTr} U_{ij} \right] + \beta_\tau \sum_n \sum_i \left[ 1 - \frac{1}{N} \text{ReTr} U_{0i} \right] \quad (2.52)$$

or by introducing the anisotropy parameter,  $\gamma$ , we can write it as

$$S_G[U_s, U_\tau] = \frac{\beta}{\gamma} \sum_n \sum_{1 \leq i < j \leq 3} \left[ 1 - \frac{1}{N} \text{ReTr} U_{ij} \right] + \beta \gamma \sum_n \sum_i \left[ 1 - \frac{1}{N} \text{ReTr} U_{0i} \right] \quad (2.53)$$

with

$$\beta = \sqrt{\beta_s \beta_\tau} \quad \gamma = \sqrt{\frac{\beta_\tau}{\beta_s}}. \quad (2.54)$$

In order to go back to the naive continuum action, one can use the connection between the plaquettes and the field strength tensors as in Eq.(2.17), which read

as

$$U_{ij}(n) = \exp(-ig_0 a_s^2 F_{ij}(n)) \quad U_{0i}(n) = \exp(-ig_0 a_s a_\tau F_{0i}(n)) \quad (2.55)$$

where  $g_0$  is the bare gauge coupling of the starting theory. Then the continuum action can be related to the lattice version of it by identifying

$$\beta_s = \frac{2N}{g_0^2} \frac{1}{\xi} \quad \beta_\tau = \frac{2N}{g_0^2} \xi. \quad (2.56)$$

However, the dynamics of the system are expected to change the coupling along the temporal and the spatial direction and thus the true definitions of the lattice couplings are given by

$$\beta_s = \frac{2N}{g_s^2(g_0, \xi)} \frac{1}{\xi} \quad \beta_\tau = \frac{2N}{g_\tau^2(g_0, \xi)} \xi \quad (2.57)$$

where  $g_s^2 = g_\tau^2 = g_0^2$  for  $\xi = 1$ , as proposed in [37, 38]. In other words, the lattice spacing in temporal and spatial directions changes dynamically. In [38], it was illustrated how one can relate  $\beta_s$  and  $\beta_\tau$  to the parameters  $\beta$  (or  $g_0^2$ ) and the asymmetry parameter  $\xi$  as

$$\begin{aligned} \xi \beta_s &= \frac{2N}{g_0^2} + 2N c_s(\xi) + \mathcal{O}(g_0^2) \\ \frac{1}{\xi} \beta_\tau &= \frac{2N}{g_0^2} + 2N c_\tau(\xi) + \mathcal{O}(g_0^2) \end{aligned}$$

where the functions  $c_\tau$  and  $c_s$  should be determined using non-perturbative approaches. More about anisotropic lattice gauge theories will be discussed in Chapter 3, in the context of extra-dimensional models.

## 2.4 Phase structure of LGTs

Putting QFT on a lattice can be seen as investigating the theory in an analogous way to a statistical system. In particular, one expects to be able to investigate the phase structure of a specific LGT. This investigation can be done by measuring order parameters of the system at different values of the relevant couplings. These are observables that show a different behaviour in different phases, so one can determine the nature of the system in the various regions of the parameter

space.

In the determination of phase transitions, a very important issue is the order of the aforementioned. The discretization of spacetime sometimes shows a phase transition which is not physically continuous but a lattice artefact instead, forbidding us from taking the continuum limit. These phase transitions are called bulk or first-order phase transitions. Higher-order phase transitions, usually of second order, allow us to take the continuum limit since they are characterized by a divergent correlation length and universal behaviour.

### 2.4.1 Phases of pure LGTs

The phase structure of Abelian and non-Abelian gauge theories have been explored extensively over the past years. The usual phases that appear in the phase diagrams are three. First, there is the *confining phase*, or strong-coupling phase that appears at small values of  $\beta$ , i.e. large values of the gauge coupling. This is the phase that is blind to perturbation theory as it occurs at strong coupling. For large values of  $\beta$ , and consequently small values of the gauge coupling, the *deconfining phase* exists. This phase is also called weak-coupling phase or Coulombic, as one expects a Coulombic behaviour in the static quark-antiquark potential. The last phase that exists in gauge theories is the *Higgs phase*, which usually appears if there is spontaneous gauge symmetry breaking. Most of the times this phase is implemented on the lattice by coupling the gauge fields to scalars by hand.

When one deals with an anisotropic gauge theory in a higher-dimensional spacetime, a new phase appears, which is called the *layered phase*, first proposed by Fu and Nielsen [39]. In this phase, the usual four-dimensional spacetime is in a deconfining phase, whereas the extra dimensions exhibit confinement. This takes us to the idea of branes or layers, as in this phase the ordinary four-dimensional world can be seen to exist on a layer embedded in extra dimensions but being blind to it. Hunting this new phase in five-dimensional non-abelian gauge theories is one of the main purposes of this thesis, and we leave the details of it to Chapter 3.

### 2.4.2 Order parameters and their behaviour

The order parameters of pure LGTs are given by the observables that were defined in Sect. 2.1.2. Let us take a closer look at each of them and their behaviour in different phases.

Firstly, we consider the plaquette. As it was already mentioned before, the expectation value of it is related to the thermodynamic quantity of the specific internal energy of a statistical system. If it inherits a discontinuity, then it signals a first-order phase transition. On the other hand, if it is continuous but its first derivative is discontinuous at the critical point, then it signals a second, or a higher-order, phase transition and the lattice theory possesses a continuum limit.

Furthermore, the Polyakov loop plays an important role in the investigation of phase structures. We have mentioned above that the correlator of two temporal Polyakov loops at spatial coordinates  $\vec{n}$  and  $\vec{m}$  is related to the static quark-antiquark potential (Eq. (2.32)). Here, we define the correlator in terms of the free energy and the lattice coupling  $\beta$ .

$$\langle P_T(\vec{m})P_T^\dagger(\vec{n}) \rangle \sim e^{-\beta F_{q\bar{q}}}. \quad (2.58)$$

If the distance between the two point charges tends to infinity the correlator can be considered as

$$\langle P_T(\vec{m})P_T^\dagger(\vec{n}) \rangle = |\langle P_T \rangle|^2. \quad (2.59)$$

So, one can see that if  $\langle P_T \rangle = 0$ , at very large spatial separation, the free energy increases and therefore the system is in a confining phase. On the other hand if  $\langle P_T \rangle \neq 0$ , at large distances the free energy approaches a constant value which signals deconfinement.

Lastly, the Wilson loop serves as a good order parameter as well. We have already seen that it is related to the static quark-antiquark potential which gives a hint that from it, and therefore from the potential, one can see if the system is in a strong-coupling or a weak-coupling phase. In particular, if the potential rises linearly with the distance, there is a strong indication of confinement, whereas if it behaves as  $1/r$  in four dimensions it gives a signal of Coulombic behaviour.

Directly from the Wilson loop one can say that the system is in the confined phase if it exhibits the area law, i.e.

$$\lim_{L,R \rightarrow \infty} \langle W_{\mathcal{L}} \rangle \sim c e^{-\sigma' RT} \quad (2.60)$$

and in the deconfined phase if it exhibits the perimeter law, i.e.

$$\lim_{L,R \rightarrow \infty} \langle W_{\mathcal{L}} \rangle \sim c e^{-\rho(R+T)}. \quad (2.61)$$

## 2.5 The Continuum Limit

In everything that has been mentioned so far, we referred to the naive continuum limit, that is by requiring  $a \rightarrow 0$  the discretized version of an action reveals a corresponding classical action in the continuum. This is the equivalent of removing the cut-off of a theory in standard QFT. However, taking the true continuum limit is much more complicated than that.

The most crucial thing when taking the continuum limit is to be able to identify a continuous phase transition in our system. For this, a divergent correlation length at a critical point or region is essential. As in statistical systems, a critical point, and thus a continuum field theory, can be found only when the correlation length goes to infinity. The latter is defined as the inverse of a scalar mass. On the lattice this mass is measured in lattice units, i.e. as  $am$ , so when taking  $a \rightarrow 0$  the mass is finite. Equivalently, the lattice correlation length is defined as  $\xi a^{-1}$  which diverges in the  $a \rightarrow 0$  limit.

The correlation length depends on the bare parameters of a statistical system. Considering the pure lattice gauge action, the only bare parameter is the lattice coupling,  $\beta$ . Therefore, we can say that a critical point exists at  $\beta_{\text{cr}}$  and for a continuum limit to exist we require

$$\xi_{\text{lat}}(\beta_{\text{cr}}) \rightarrow \infty \quad (2.62)$$

So far the limit  $a \rightarrow 0$  was mentioned. However, before taking this limit, we need to consider the infinite volume limit or the so-called thermodynamic limit.

Everything is simulated in a finite box of volume  $V = L^4 = a^4 N^4$ . If one attempts to take the lattice spacing to zero then the volume also goes to zero unless  $N$  is taken to infinity. In actual calculations, one can overcome the issue of infinite volume limit by requiring the physical system to remain constant over measurements of an observable. That is if the number of sites,  $N$ , is increased then the lattice spacing should be decreased to ensure that  $V$  remains constant and large compared to the physical scale of interest. By taking measurements at different values of  $N$ , one can extrapolate to  $N \rightarrow \infty$  to reach the thermodynamic limit.

Changing  $N$  in numerical simulations is straightforward, however changing the lattice spacing is more involved. One desires to take the continuum limit in the context of measuring observables on the lattice that will be able to give the value of a physical quantity. Observables on the lattice depend on the bare parameters of the system, which for the pure Wilson action is only the lattice coupling  $\beta$  (or  $g_0$ ). Moreover, the bare parameters have an explicit dependence on the lattice spacing. As soon as one determines the relation between the two, observables at different bare parameter values can be measured on a lattice of a constant physical volume, as now the lattice spacing can be determined from the parameters of the system. Then scaling analysis can be performed, that is to extrapolate to  $a \rightarrow 0$  to determine the physical value of the desired quantity.

## 2.6 Methods for LGT exploration

As mentioned above, LGTs are Euclidean quantum field theories which have an exact matching with statistical systems. This allows quantum field theories to be investigated using methods that are used in statistical-spin systems. Some of these methods are the strong-coupling expansion, the Mean-Field approach and Monte Carlo numerical simulations. The latter two are the methods used in this thesis so more details about them are given below.



### 2.6.1 Monte Carlo simulations

With the development of new supercomputers and the increase in computing resources in particle physics, Monte Carlo algorithms are the main way to generate configurations that are used to measure useful quantities since they are more trustworthy as they are mostly blind to the value of the coupling of a gauge theory. This applies when the system has a well-defined path integral, which is not hindered by the sign problem, analogous to the partition function of a statistical system with a Boltzmann distribution function

$$P(s) = e^{-\beta\mathcal{H}[s]}. \quad (2.63)$$

Different Monte Carlo algorithms have been developed for LGTs over the years but they all inherit some fundamental properties that we describe briefly below. The project presented in Chapter 3 has been implemented using a specific Monte Carlo algorithm, called the Kennedy-Pendleton Heat-Bath algorithm [40].

The desired quantities that one wants to evaluate are usually expectation values of observables that involve the path integral, which, for large lattices, corresponds to a huge sum of configurations that is impossible to be performed analytically. However, one can compute such an integral approximately with the average over a finite number of points in a probability distribution function, which for LGTs is the analogous Boltzmann distribution function. For example, the expectation value of an observable  $\mathcal{O}$  is evaluated using

$$\langle \mathcal{O} \rangle = \lim_{N \rightarrow \infty} \frac{1}{N} \sum_{n=1}^N \mathcal{O}[U_n] \quad (2.64)$$

where the gauge field configurations are generated such that they have the largest contribution to the path integral, i.e. with probability distribution density

$$\rho(U) = \frac{\prod_l dU_l e^{-S[U]}}{\int \prod_l dU_l e^{-S[U]}}. \quad (2.65)$$

This process is called *importance sampling*. One is restricted to the finite number of configurations that the available computing resources can give and this leads to statistical errors in the measurements.

In order to sample these configurations, one starts either from a unit or a random one, and then builds a Markov chain, that is a sequence of configurations that each depends on the previous one. Each of these configurations occurs with a probability weight of  $e^{-S[U]}$ . The probability to go from a configuration  $U$  to a configuration  $U'$  is given by the transition probability  $w(U'|U)$  that satisfies

$$\sum_{U'} w(U'|U) = 1 \quad (2.66)$$

$$0 \leq w(U'|U) \leq 1 \quad (2.67)$$

which ensures that all configurations can be reached and one can say that the algorithm is *ergodic*. In order to have a system being in equilibrium, we desire a fixed probability distribution, that is to satisfy

$$\sum_U w(U'|U)e^{-S[U]} = e^{-S[U']}. \quad (2.68)$$

This arises from the idea that once equilibrium is reached, one expects that probabilities of reaching to or leaving from one configuration must be the same, that is

$$\sum_U w(U'|U)e^{-S[U]} = \sum_U w(U|U')e^{-S[U']}. \quad (2.69)$$

The above condition is necessary for our algorithm to obtain correct results. A solution to the above is called the *detailed balance* condition and is given by

$$e^{-S[U]}w(U'|U) = e^{-S[U']}w(U|U'). \quad (2.70)$$

So, once this condition is satisfied it is ensured that the configurations are sampled with the correct weight in the Markov chain.

## 2.6.2 Mean-Field approach

The Mean-Field approximation is well known in statistical-spin systems for evaluating the partition function and it has been adapted such that it can be used for LGTs. A very powerful way to investigate a system using the Mean Field approach is the so-called saddle-point method, which can be thought of as

an expansion of the integrand of the partition function around a point, which corresponds to the mean field. The idea behind it is to add a random external field, that can absorb constraints on the measure of the integrand such that the final expression of the partition function will be a regular integral over unconstrained variables. The approximation of the integral at the mean-field values is seen as the classical solution and one can obtain corrections to it by considering fluctuations of the mean field. Below, we show how this works for LGTs based on a detailed analysis of this method in [41] and [42].

In a pure LGT, the path integral that one wants to evaluate is given by

$$Z = \int \mathcal{D}U e^{-S_W[U]} \quad (2.71)$$

where the link-variables are  $SU(N)$  matrices, therefore the integral is constrained on group elements. In order to go into a flat measure, we use an identity to replace the constrained matrices  $U$  with the unconstrained  $N \times N$  complex matrices  $V$  by inserting the integral of a delta function in Eq. (2.71). Then, the delta function is written in its exponential representation and we get

$$\begin{aligned} Z &= \int \mathcal{D}U e^{-S_W[U]} \\ &= \int \mathcal{D}U \mathcal{D}V \delta(V - U) e^{-S_W[V]} \\ &= \int \mathcal{D}U \int \mathcal{D}V \int \mathcal{D}H e^{\frac{1}{N} \text{ReTr}(H(U-V))} e^{-S_W[V]} \\ &= \int \mathcal{D}V \int \mathcal{D}H e^{-S_{\text{eff}}[V, H]} \end{aligned} \quad (2.72)$$

where the integral in the last line involves flat measures and regular integrand. The effective action is given by

$$S_{\text{eff}}[V, H] = S_W[V] + \sum_l u(H_l) + \sum_l \frac{1}{N} \text{Re}(H_l V_l). \quad (2.73)$$

where the function  $u(H)$  can be thought of as the test free energy per gauge field given by

$$e^{-u(H)} = \int \mathcal{D}U e^{\frac{1}{N} \text{ReTr}(UH)} \quad (2.74)$$

and it is the only term in the effective action that has a dependence on the gauge group of the theory.

The idea of the saddle-point method is to find the points where this effective action has saddle points which behave as minima, and are called mean-field values or background values. These are considered to be uniform in all directions and are assumed to be proportional to the identity matrix, i.e:

$$V \rightarrow \bar{V}\mathbb{1}_N \quad H \rightarrow \bar{H}\mathbb{1}_N. \quad (2.75)$$

To find saddle-point equations we take derivatives of  $S_{\text{eff}}$  and we evaluate them at  $\bar{H}\mathbb{1}_N$  and  $\bar{V}\mathbb{1}_N$ . So at zero'th order approximation we get

$$\left. \frac{\partial S_{\text{eff}}}{\partial V} \right|_{\bar{V}, \bar{H}} = 0 \Rightarrow \bar{H} = - \left. \frac{\partial S_W[V]}{\partial V} \right|_{\bar{V}} \quad (2.76)$$

and

$$\left. \frac{\partial S_{\text{eff}}}{\partial H} \right|_{\bar{V}, \bar{H}} = 0 \Rightarrow \bar{V} = - \left. \frac{\partial u(H)}{\partial H} \right|_{\bar{V}, \bar{H}}. \quad (2.77)$$

Finally, the free energy at zero'th order can be written as

$$F^{(0)} = -\frac{1}{\mathcal{N}} \ln Z^{(0)} = -\frac{1}{\mathcal{N}} \ln Z[\bar{V}, \bar{H}] = \frac{S_{\text{eff}}[\bar{V}, \bar{H}]}{\mathcal{N}} \quad (2.78)$$

where  $\mathcal{N}$  denotes the total number of lattice points, i.e.  $L_T \times L_S^3$  for a four-dimensional space.

This thesis focuses on investigations of the SU(2) gauge group so it is worth showing the approximation of the path integral for the gauge action for this specific group using the Mean-Field approach. First we parametrize the SU(2) gauge links as

$$U_\mu(n) = u_{\alpha_\mu}(n)\sigma^\alpha = u_{0_\mu}(n)\mathbb{1} + iu_{A_\mu}(n)\sigma^A \quad (2.79)$$

where  $\sigma^A$  ( $A = 1, 2, 3$ ) are the Pauli matrices and Einstein summation is assumed. The group properties imply that  $u_{\alpha_\mu}$  are real numbers and they satisfy  $u_{\alpha_\mu}u_{\alpha_\mu} = \mathbb{1}$ . As in the general SU( $N$ ) case, the path integral is approximated at tree level with integrals over unconstrained  $2 \times 2$  complex matrices  $V$  and  $H$

that can be parametrized as

$$\begin{aligned} V_\mu(n) &= v_{0_\mu}(n)\mathbb{1} + i \sum_A v_{A_\mu}(n)\sigma^A, \quad v_\alpha \in \mathbb{C} \\ H_\mu(n) &= h_{0_\mu}(n)\mathbb{1} - i \sum_A h_{A_\mu}(n)\sigma^A, \quad h_\alpha \in \mathbb{C}. \end{aligned} \quad (2.80)$$

With this parametrization we repeat the procedure of the general case  $SU(N)$  to get the effective action. The identity inserted in the path integral in Eq. (2.72) is now equivalent to

$$\begin{aligned} \mathbb{1} &= \prod_n \prod_\mu \prod_\alpha \int d\text{Re}v_\alpha d\text{Im}v_\alpha \delta[(\text{Re}v_\alpha) - u_\alpha] \delta(\text{Im}v_\alpha) \\ &= \prod_{n;\mu;\alpha} \int_{-i\infty}^{+i\infty} \frac{d\text{Re}h_\alpha d\text{Im}h_\alpha}{(2\pi i)^2} d\text{Re}v_\alpha d\text{Im}v_\alpha \exp[-(\text{Re}h_\alpha)(u_\alpha - \text{Re}v_\alpha) - \text{Im}h_\alpha \text{Im}v_\alpha] \end{aligned} \quad (2.81)$$

Thus, the effective action can be read as

$$S_{\text{eff}} = -\frac{\beta}{2} \sum_n \sum_{\mu < \nu} \text{ReTr} V_{\mu\nu}(n) + \sum_n \sum_\mu (u(h_\mu(n))) + \sum_\alpha h_{\alpha_\mu}(n) v_{\alpha_\mu}(n) \quad (2.82)$$

where  $V_{\mu\nu}(n)$  is the unconstrained equivalent to the plaquette and both  $h_\alpha$  and  $v_\alpha$  are real.

The final step to determine the saddle-point equations and their solutions is to evaluate the only group integral that appears in the second term of Eq. (2.82). To do this we use character expansions as given in Appendix B and we find that

$$u(h_{\alpha_\mu}) = -\ln \left[ \frac{2}{\rho_\mu} I_1(\rho_\mu) \right] \quad (2.83)$$

where

$$\rho_\mu = \sqrt{(\text{Re}h_0)^2 + (\text{Re}h_A)^2}. \quad (2.84)$$

and  $I_1$  is the modified Bessel function of the first kind of order 1.

Considering again the matrices to be set to a constant value proportional to the

identity, the field values that minimize the action are given by

$$\begin{aligned}
 \left. \frac{\partial S_{eff}}{\partial v_\alpha} \right|_{\bar{v}_0, \bar{h}_0} &= -2 \frac{\beta}{2} \sum_n \sum_{\mu < \nu} 4 \bar{v}_0^3 + \sum_n \sum_\mu \bar{h}_0 = 0 \\
 \Rightarrow \beta \frac{d(d-1)}{2} 4 \bar{v}_0^3 &= d \bar{h}_0 \\
 \Rightarrow \bar{h}_0 &= 2\beta(d-1) \bar{v}_0^3
 \end{aligned} \tag{2.85}$$

and

$$\begin{aligned}
 \left. \frac{\partial S_{eff}}{\partial h_\alpha} \right|_{\bar{v}_0, \bar{h}_0} &= \sum_n \sum_\mu \left. \frac{\partial u(h_{\alpha_\mu})}{\partial h_\alpha} \right|_{\bar{h}_0} + \sum_n \sum_\mu \bar{v}_0 = 0 \\
 \Rightarrow \bar{v}_0 &= \frac{I_2(\bar{h}_0)}{I_1(\bar{h}_0)}.
 \end{aligned} \tag{2.86}$$

Generally, from these equations one can determine the phase diagram of the SU(2) gauge theory. The separation of phases is given by determining whether the above equations inherit a trivial solution ( $v_0 = h_0 = 0$ ) or whether they have a non-trivial solution. The trivial solution occurs in the strong-coupling phase in contrast to the non-trivial one that occurs in the weak-coupling phase.

### 2.6.2.1 Gauge fixing

As this method gives an approximation to the path integral, by considering corrections to the solutions of the saddle-point equations, one can estimate the next-to-leading order action. Consequently, first-order corrections can be added to the free energy and its investigation can give a more accurate idea of the phase diagram and whether the mean values for the fields determined are the true minima of the system or not. Before proceeding into the discussion of the first-order corrections of the free energy we need to discuss gauge fixing.

When one uses numerical methods to estimate the path integral of a LGT, gauge fixing is not necessary but it is not forbidden either and Creutz was the first one to propose a choice of the gauge called the maximal tree [43]. Using this choice one is able to set some of the link variables to the identity leaving them out of the integration of the gauge fields, as long as they do not form a closed loop. This

gauge choice has no equivalent in the continuum.

On the other hand, in the Mean-Field approach, which is an analytical method, it is essential to fix the gauge otherwise we face infinities caused by the local gauge transformations of the mean-field values obtained when trying to compute corrections to the path integral. Over the years, higher-order corrections in the Mean-Field approach were computed [44–46] and different choices of the gauge were proposed depending on the model investigated. Here, we only mention two cases that are more relevant to our work.

Very often, the gauge is fixed using the axial gauge in which one sets all the links along the temporal direction to  $\mathbb{1}$ . This is analogous to the temporal gauge in the continuum, where we set  $A_4(x) = 0$ . Even though, usually, axial gauge corresponds to fixing the temporal direction, there is also the possibility of setting the link variables along any other direction to unity. This is the most well-known way to fix the gauge in U(1) models.

Furthermore, any other choice of gauge that is used in the continuum can be used on the lattice as long as one finds the corresponding discretized expressions. In this thesis the gauge fixing procedure that is followed is based on the Faddeev-Popov method used in the continuum [47], in which a generalized Lorenz gauge condition is used

$$G(A) = \partial_\mu A_\mu^a(x) - \omega^a(x) \quad (2.87)$$

where  $\omega^a$  accounts for a Gaussian weight over which we perform the Gaussian integral. Using this trick, we get an extra term in our Euclidean Lagrangian that reads as

$$\mathcal{L}_{\text{gf}} = \frac{(\partial_\mu A_\mu)^2}{2\xi} \quad (2.88)$$

where  $\xi$  is a real number that arises from the Gaussian integral. Usually it is set to 1 and this is called the Feynman gauge. For the non-abelian gauge theories, the Faddeev-Popov method gives rise to a determinant in the path integral that can be written as an integral over ghosts, i.e.

$$\det(\partial_\mu D_\mu) = \int \mathcal{D}c\mathcal{D}\bar{c} e^{\int d^4x \bar{c}(\partial_\mu D_\mu)c}. \quad (2.89)$$

The Wilson action now will have an extra contribution from the gauge fixing term

and it will be given by

$$S_G[U]' = S_G[U] + S_{\text{gf}}[U] \quad (2.90)$$

where

$$S_{\text{gf}}[U] = \frac{1}{2\xi} \sum_{\mu} \sum_n \text{Tr} \left[ U_{\mu}(n) - U_{\mu}(n - \hat{\mu}) \right]^2. \quad (2.91)$$

### 2.6.2.2 First-order corrections

First-order corrections to the approximation of the path integral, and consequently to the Free Energy, can be found by evaluating second-order derivatives of the action, that is its Gaussian fluctuations around the mean-field values. To achieve this we add corrections to each mean-field value and, in particular, for SU(2) we get

$$\begin{aligned} V_{\mu}(n) &= \bar{v} + v_{\mu}(n) \quad ; \quad v_{\mu}(n) = v_{\mu_0}(n)\mathbb{1} + iv_{\mu_A}(n)\sigma^A \\ H_{\mu}(n) &= \bar{h} + h_{\mu}(n) \quad ; \quad h_{\mu}(n) = h_{\mu_0}(n)\mathbb{1} + ih_{\mu_A}(n, n_5)\sigma^A \end{aligned} \quad (2.92)$$

From the usual Taylor expansion we get

$$\begin{aligned} S_{\text{eff}} &= S_{\text{eff}}^{(0)} \Big|_{\bar{v}, \bar{h}} + \frac{1}{2} \left( \frac{\partial^2 S_{\text{eff}}}{\partial V^2} \Big|_{\bar{v}, \bar{h}} v^2 + 2 \frac{\partial^2 S_{\text{eff}}}{\partial H \partial V} \Big|_{\bar{v}, \bar{h}} hv + \frac{\partial^2 S_{\text{eff}}}{\partial H^2} \Big|_{\bar{v}, \bar{h}} h^2 \right) \\ &\equiv S_{\text{eff}}^{(0)}[\bar{v}, \bar{h}] + S^{(2)}[v, h]. \end{aligned} \quad (2.93)$$

The second derivatives can be seen as propagators between the corresponding fields and we write them as

$$\begin{aligned} \frac{\partial^2 S_{\text{eff}}}{\partial H^2} \Big|_{\bar{v}, \bar{h}} &\equiv \Delta^{(hh)} \\ \frac{\partial^2 S_{\text{eff}}}{\partial H \partial V} \Big|_{\bar{v}, \bar{h}} &\equiv \Delta^{(hv)} \\ \frac{\partial^2 S_{\text{eff}}}{\partial V^2} \Big|_{\bar{v}, \bar{h}} &\equiv \Delta^{(vv)} + \Delta^{(gf)} \end{aligned} \quad (2.94)$$

where  $\Delta^{(gf)}$  arises from the gauge fixing term which is taken into account in the effective action as discussed in the previous section.



To approximate the path integral to first order, we rewrite it as

$$Z^{(1)} = e^{-S_{\text{eff}}^{(0)}[\bar{v}, \bar{h}]} \int \mathcal{D}v \mathcal{D}h e^{-S^2[v, h]} \quad (2.95)$$

and performing the Gaussian integral one finds it to be

$$\begin{aligned} Z^{(1)} &= e^{-S_{\text{eff}}^{(0)}[\bar{v}, \bar{h}]} \left[ \prod_{\alpha} \det \left( \Delta^{(hh)} \left( (\Delta^{(vv)} + \Delta^{(gf)}) - \Delta^{(vh)} \Delta^{(hh)^{(-1)}} \Delta^{(hv)} \right) \right) \right]^{-1/2} \\ &\equiv e^{-S_{\text{eff}}^{(0)}[\bar{v}, \bar{h}]} \left[ \prod_{\alpha} \det (\Delta^{(hh)} \mathcal{K}) \right]^{-1/2}. \end{aligned} \quad (2.96)$$

As a final remark we say that one has to include the Faddeev-Popov determinant,  $D_{FP}$ , as well and thus the partition function defined above is modified to be

$$\begin{aligned} Z^{(1)} &= e^{-S_{\text{eff}}^{(0)}[\bar{v}, \bar{h}]} \left[ \det (\Delta^{(hh)} \mathcal{K}) \right]^{-1/2} D_{FP} \\ &\equiv e^{-S_{\text{eff}}^{(0)}[\bar{v}, \bar{h}]} \cdot \mathcal{Z}. \end{aligned} \quad (2.97)$$

Having all the above, it is trivial to show that the free energy to first order can be expressed as

$$F^{(1)} = F^{(0)} + \frac{1}{2\mathcal{N}} \ln \left[ \prod_{\alpha} \det (\Delta^{(hh)} \mathcal{K}) D_{FP}^{-2} \right]. \quad (2.98)$$

More on the determination of first-order corrections will be addressed in Chapter 4 and Appendix C.

## Chapter 3

# Anisotropic 5D Yang-Mills theory in flat spacetime

Most of the LGTs studies are performed in the observed four dimensions as the main motivation is a better understanding of the strong-coupling region of the SM (QCD) or to look for signals for beyond the Standard Model physics. However, extra-dimensional model building enhanced the application of LGTs to explorations of models with more than four dimensions.

It is known that higher-dimensional non-abelian theories are perturbatively non-renormalizable, therefore one has to impose a cutoff,  $\Lambda$ , to define an effective theory out of which low-energy physics can be extracted. As mentioned in Chapter 2, on the lattice this comes for free, as the inverse of the lattice spacing serves as the cutoff, allowing extra-dimensional models to be investigated. In this thesis the theory of interest is the one that involves the simplest non-abelian gauge group with one extra dimension, i.e. the five-dimensional  $SU(2)$  gauge theory. In this Chapter we will present a brief summary of what was the status of the phase diagram of the aforementioned model before our study, the set-up of the model with some details of the implementation and the results that lead to the current phase diagram. The details of the study presented here have been published in a refereed journal paper [48] and a conference proceeding [49].

## 3.1 The phase structure of the model from the Literature

### 3.1.1 Dimensional Reduction via compactification

The first study of the phase diagram of the five-dimensional SU(2) YM model was done by Creutz in 1979, who found that there is a bulk phase transition between the strong-coupling and the five-dimensional Coulombic phase, which was not a very exciting result as the theory does not have a continuum limit and the transition is just a lattice artefact [50]. In later years, the same model was investigated with some modifications in the action that might have revealed the existence of a non-trivial fixed point. In particular, in 1992 Kawai et al. explored the phase diagram of the five-dimensional pure SU(2) gauge theory using a mixed fundamental-adjoint action [51]. Unfortunately, they also showed no evidence of the existence of a continuum limit.

In 2001, Ejiri et al. made a new modification in the model to look for the existence of a continuum limit in the theory: they imposed an anisotropy between the lattice couplings in the four dimensions and the fifth dimension [52]. Everything that is discussed in Section 2.3 can be applied in this modified model by making the appropriate changes such that the temporal direction is replaced by the fifth one. More details on the set-up of the model will be given in Section 3.2.

The five-dimensional anisotropic SU(2) gauge theory when all directions are kept large shows a bulk phase transition. However, the idea in [52] is to compactify the extra dimension on a circle, which, by the arguments in [53, 54] one expects to see a dimensionally reduced phase, which is always present at least in the region where  $a_5 < a_4$ . The presence of a continuous transition in the aforementioned study was the driving force for further studies on the phase structure of this model when the extra dimension is compactified on  $S^1$ , in the region where the lattice coupling along the extra dimension is larger than that along the four dimensions, i.e.  $\gamma > 1$  [55, 56]. By further exploration at various anisotropy values and different sizes of the extra dimension and by finite-size scaling studies, it became clear that the five-dimensional YM theory can be reduced to a four-dimensional YM

theory via compactification. According to the Svetitsky-Yaffe conjecture a  $(d+1)$ -dimensional  $SU(N)$  gauge theory (with  $\mathbb{Z}_N$  the centre symmetry of the group) with a continuous deconfinement transition and a  $d$ -dimensional spin model with a  $\mathbb{Z}_N$  symmetry belong to the same universality class [57]. From the above statement it is clear that by matching the critical exponents of the gauge theory in the dimensionally reduced phase with those of a four-dimensional Ising model one can conclude that the compact phase describes a four-dimensional YM theory.

Lastly, a study was presented in [58] in which a dimensionally reduced phase is shown to exist in the region  $\gamma < 1$ , i.e. for  $a_5 > a_4$ . In this region, the investigation was performed when the temporal or the extra dimension was compactified and scaling analysis showed a clear signal that the model becomes a four-dimensional YM theory as in the case of  $\gamma > 1$ . However, in this region there are some upper and lower bounds on the size of each direction for each value of  $\gamma$  in order for this compact phase to appear. The first upper bound appears in the case where the four-dimensional theory is present as the result of the compactification of the temporal direction. In this case the extent of the latter should be less than an extent in the other directions,  $L_5^{\min}(\gamma)$ . The second bound is given for the case where the dimensionally reduced phase is the result of the compactification of the fifth direction. For this, it is essential to have  $L_5 < L_5^{\min}(\gamma)$  but also all the other directions should have an extent larger than  $L_5^{\min}(\gamma)$ . Finally, the signal of the bulk phase transition, which is present when no “proper” compactification is imposed in any of the directions, can only be clearly seen if the size of all directions exceeds a minimum value which increases as  $\gamma$  gets lower.

The phase diagram of the five-dimensional anisotropic  $SU(2)$  gauge theory when dimensionally reduced phases are sought via a compactification mechanism is shown in Figure 3.1 as taken from Ref. [56].

### 3.1.2 Layered phase idea

Dimensional reduction in the above discussion is achieved by compactification. In Chapter 1 we have introduced another mechanism via which theories can be dimensionally reduced: localization. However, the failure of having a viable mechanism for the localization of gauge fields in extra-dimensional models

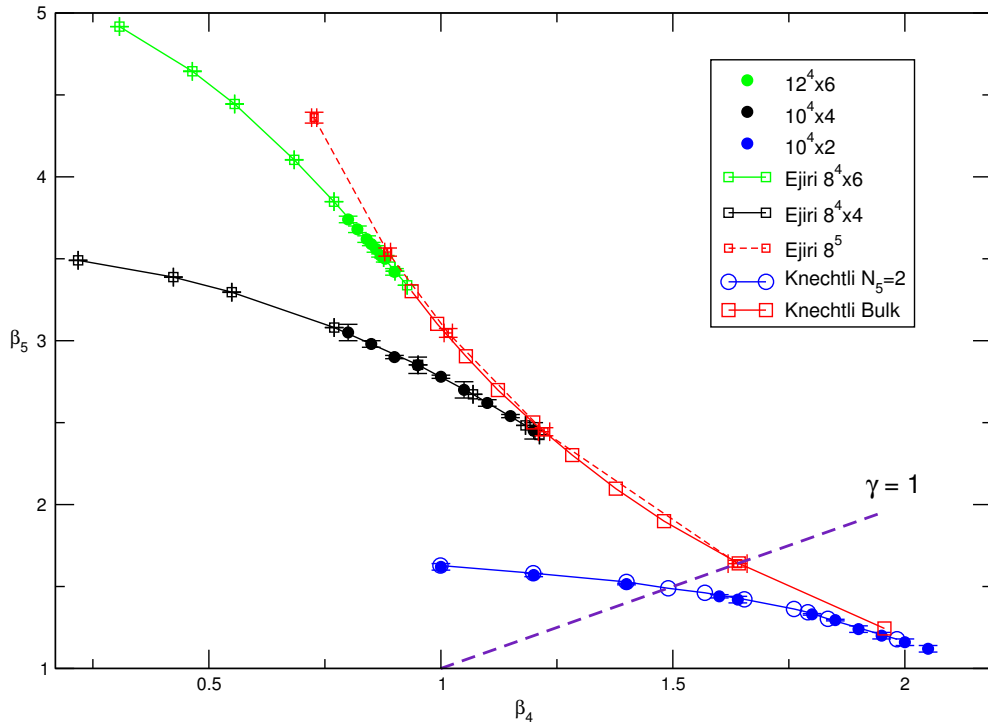


Figure 3.1: The phase diagram of the five-dimensional anisotropic  $SU(2)$  YM model when dimensional reduction is achieved via compactification of the extra dimension. The red points show the bulk phase transition in the absence of compactification and the rest are lines of second order transitions showing the dimensionally reduced phase. The figure was taken from Ref. [56] which uses results from [52] denoted as “Ejiri” and [58] denoted as “Knechtli”.

suggests the need of a non-perturbative way for accomplishing this. The first study to attain this came from Fu and Nielsen [39]. They proposed that when there is a  $D$ -dimensional lattice, a  $d$ -dimensional layered phase ( $D = n + d$ ) can be formed if the nearest-neighbour gauge couplings of the  $d$ -dimensional sublattice are different from those in the other  $n$  dimensions. Then, particles and gauge fields can travel within the  $d$ -dimensional layer phase, but they exhibit a kind of confinement when they try to propagate in any of the  $n$  extra dimensions. Their study was done using the Mean-Field approach for the abelian group  $U(1)$  and they showed the existence of a layered phase in  $(4+1)$  dimensions. It is important to notice that the new phase still holds even after computing first-order corrections to the mean-field solutions. Fu and Nielsen calculated further quantities to study the properties of this layered phase and it seems that it behaves as a four-dimensional one [59].

In 1992, Kaplan in [60] starting from a five-dimensional theory with a topological defect serving as a domain wall, was able to construct fermions which live in four dimensions that possess exact chiral symmetry, the so-called DW fermions. This new formulation for lattice fermions was very promising as it would allow us to escape from the notorious Nielsen-Ninomiya no-go theorem. Despite the fact that the fifth dimension is just a mathematical trick in Kaplan's formalism, people started being suspicious for the connection between Kaplan's localization of fermions and the layered phase proposed by Fu and Nielsen: it might have been possible that the extra dimension is not just a tool but instead it gains a physical interpretation.

Studies were carried out to confirm the findings of [39] using both analytical and numerical non-perturbative methods [61–63]. It was shown that the five-dimensional  $U(1)$  theory undergoes dimensional reduction via localization admitting a continuum limit. The pure gauge-theory was also coupled to Wilson fermions and they could show that in the layered phase the usual four-dimensional Wilson propagator is recovered and thus it loses its chirality. This is in contrast to the result that in the weak-coupling phase a chiral zero-mode can be localized. Another important outcome of these studies was that the presence of fermions does not change the order of the transitions. All the above suggest that for a chiral layer to exist, one should not just set the extra-dimensional coupling to zero but instead choose it to be close to a transition point [64]. As in this thesis all results are presented in the absence of fermions, we do not discuss these issues further.

This new point of view for the significance of the existence of a layered phase motivated further explorations of the phase diagram of the five-dimensional compact  $U(1)$  model. Measurements of more observables and studies of the scaling properties at larger volumes provide strong evidence that the transition from the Coulombic phase to the layered phase is of second order allowing a continuum limit to be taken [65–67]. More specific, measurements of the potential in the layered phase suggest that it behaves inversely proportional to the distance, that is it has a four-dimensional Coulombic behaviour.

The success of defining a layered phase for  $U(1)$  intrigued people to investigate whether this new phase appears for non-abelian gauge groups as well, and in

particular for the simplest non-abelian group  $SU(2)$ . The idea of a dimensionally reduced phase for  $SU(2)$  was investigated using the Mean-Field approach [68]. In this study, the claim is the existence of this new phase, at which the static-quark potential has exactly a four-dimensional behaviour which means that the planes transverse to the extra dimension are decoupled from each other. Studies of the finite-size scaling properties of the system show that there is a second order phase transition, however it is not clear if this is true as the Mean-Field approximation can hide the correct order of the transition, so Monte Carlo simulations had to be performed.

Actually, the first Monte Carlo study appeared soon after Fu and Nielsen's proposal, providing evidence of the existence of this phase in six dimensions but not in five dimensions [69]. However, the lattice volumes used were too small. More recent studies using Monte Carlo techniques suggest the existence of a non-trivial fixed point at which one can define a four-dimensional gauge theory arising from the dimensional reduction of a five-dimensional  $SU(2)$  YM theory [70, 71]. Specifically, in [71] they claim that there is an end point of the first-order phase transition, which separates the confining from the weak-coupling phase and it is shown in Figure 3.1 with red points, at which the transition becomes second order. The drawback of this study is the use of small lattices that might hide true physics if finite-size effects are dominant. In this region of the weak-coupling phase, one would expect to have a new phase, the layered phase, where the five-dimensional theory can be visualized as four-dimensional layers embedded in the extra dimension on which the ordinary SM matter is recovered. If a five-dimensional  $SU(2)$  gauge theory reduces to four dimensions, it results to a four-dimensional  $SU(2)$  gauge theory with a Higgs in the adjoint representation, that is the Georgi-Glashow model. The phase diagram of this model consists of a confined and a Higgs-Coulomb phase. One expects that the static potential will show characteristics of these phases. In [68], in the deconfined phase approaching the transition into the layered phase they observe a four-dimensional Coulombic behaviour in the static quark-antiquark potential instead of a five-dimensional one that is observed in the weak-coupling regime. In addition, as in this model a Higgs mechanism is not in action, one expects that at large distances the potential will rise linearly with distance, i.e. it will have a non-vanishing string tension.

In the study presented here, we extend the work of [71] to larger lattices to

see if we can still find hints that the theory might possess a continuum limit. The motivation for this came mostly from [58] in which they set some lower bounds on the size of each direction in order for the bulk phase transition to be seen, which indicates that the lattice volumes used in the previous Monte Carlo simulations [71], were too small to show the correct order of the phase transition.

## 3.2 The set-up of five-dimensional anisotropic LGTs

### 3.2.1 Anisotropic Action

The theory of interest is the anisotropic SU(2) YM gauge theory in five dimensions, whose action in the continuum is given by

$$S_E = \int d^4x \int dy \frac{1}{2g_5^2} \text{Tr} F_{MN}^2 \quad (3.1)$$

where  $M, N = 1 \dots 5$  and  $F_{MN} = \partial_M A_N - \partial_N A_M + i[A_M, A_N]$  with  $A_M = g_5 A_M^a T^a$ . The discretized version of this action when one imposes an anisotropy between the extra-dimensional plaquette and the ordinary four-dimensional plaquettes becomes

$$S = \beta_4 \sum_n \sum_{1 \leq \mu < \nu \leq 4} \left( 1 - \frac{1}{2} \text{Tr} U_{\mu\nu}(n) \right) + \beta_5 \sum_n \sum_{1 \leq \mu \leq 4} \left( 1 - \frac{1}{2} \text{Tr} U_{\mu 5}(n) \right) \quad \mu, \nu = 1 \dots 4 \quad (3.2)$$

where  $U_{\mu\nu}(n)$  represents the oriented plaquette along spacetime directions given by

$$U_{\mu\nu}(n) = U_\mu(n) U_\nu(n + \hat{\mu}a_4) U_\mu^\dagger(n + \hat{\nu}a_4) U_\nu^\dagger(n) \quad (3.3)$$

and  $U_{\mu 5}(n)$  represents the plaquette formed when one of the directions is the extra-dimensional one, given by

$$U_{\mu 5}(n) = U_\mu(x) U_5(n + \hat{\mu}a_4) U_\mu^\dagger(n + \hat{5}a_5) U_5^\dagger(x). \quad (3.4)$$



where  $U_\mu(n) = \exp(ig_5 a_4 A_\mu(n))$  and  $U_5(n) = \exp(ig_5 a_5 A_5(n))$  are the gauge links,  $a_4$  is the lattice spacing in the usual spacetime directions and  $a_5$  is the lattice spacing in the extra direction. The sums are performed over all the lattice points, i.e.  $n = (n_0, \vec{n}, n_5)$  and  $x = an$ . This is analogous to the anisotropic action defined in Section 2.3 with the difference that now the temporal direction is indistinguishable from the spatial directions and the extra dimension takes the place of the temporal direction in the anisotropic action. The anisotropy parameter on the lattice is characterized by  $\gamma$  which is defined as

$$\gamma = \sqrt{\frac{\beta_5}{\beta_4}} \quad (3.5)$$

and at tree level this is given by

$$\gamma = \frac{a_4}{a_5}. \quad (3.6)$$

Another useful quantity that we define in terms of the two lattice couplings is  $\beta$  given by

$$\beta = \sqrt{\beta_4 \beta_5}. \quad (3.7)$$

Recovering naively the continuum limit we get

$$\beta_4 = \frac{4a_5}{g_5^2} \quad \text{and} \quad \beta_5 = \frac{4a_4^2}{a_5 g_5^2}. \quad (3.8)$$

### 3.2.2 Observables

In order to investigate the phase diagram of the model we use the following observables:

- Average Plaquette along the extra dimension,  $\hat{P}_5$

$$\langle \hat{P}_5 \rangle = \left\langle \frac{1}{4VN_c} \sum_n \sum_\mu \text{Tr}(U_{\mu 5}(n)) \right\rangle \quad (3.9)$$

and its susceptibility

$$\chi_{\hat{P}_5} = V \left( \langle \hat{P}_5^2 \rangle - \langle \hat{P}_5 \rangle^2 \right) \quad (3.10)$$

where  $V$  is the lattice volume given by  $V = L_T \times L_S^3 \times L_5$ , with  $L_T$ ,  $L_S$  and  $L_5$  the size of the temporal, spatial and extra dimension respectively.

- Temporal Polyakov Loop. This can be measured on the whole lattice given by

$$\text{Poly}_T = \frac{L_T}{N_c V} \left| \sum_{\vec{n}, n_5} \text{Tr} \prod_{n_0=0}^{(L_T-1)} U_T(n) \right|. \quad (3.11)$$

Since in the layered phase each layer is uncorrelated, the Polyakov loop may be measured in one layer and so we also compute

$$\text{Poly}_T(n_5) = \frac{1}{N_c L_S^3} \left| \sum_{\vec{n}} \text{Tr} \prod_{n_0=0}^{(L_T-1)} U_T(n)|_{n_5} \right|. \quad (3.12)$$

We define the Polyakov loop susceptibilities as

$$\chi_{\text{Poly}_T} = \frac{V}{L_T} \left\langle (\text{Poly}_T^2 - \langle \text{Poly}_T \rangle^2) \right\rangle \quad (3.13)$$

$$\chi_{\text{Poly}_T}(n_5) = L_S^3 \left\langle (\text{Poly}_T(n_5)^2 - \langle \text{Poly}_T(n_5) \rangle^2) \right\rangle. \quad (3.14)$$

The expected behaviour of the plaquette for a first-order phase transition is to show hysteresis in the expectation value and a divergence in the susceptibility at the critical point. The temporal Polyakov loop is expected to have a zero expectation value in the strong-coupling phase, i.e. to fluctuate around zero and a non-zero expectation value in the five-dimensional Coulombic phase, i.e. to show a two-peak structure.

### 3.3 Results from Lattice Simulations

Our model was implemented on the lattice, using the Kennedy-Pendleton Heat-Bath algorithm [40] combined with overrelaxation updates [72]. Specifically, we took one heat-bath measurement every  $L_S/2$  overrelaxation steps. The autocorrelation that arises was taken into account in our analysis. The number of measurements varied between 100,000 and 200,000 at each set of points in our parameter space  $(\beta_4, \beta_5)$  that were investigated. Measurements were taken

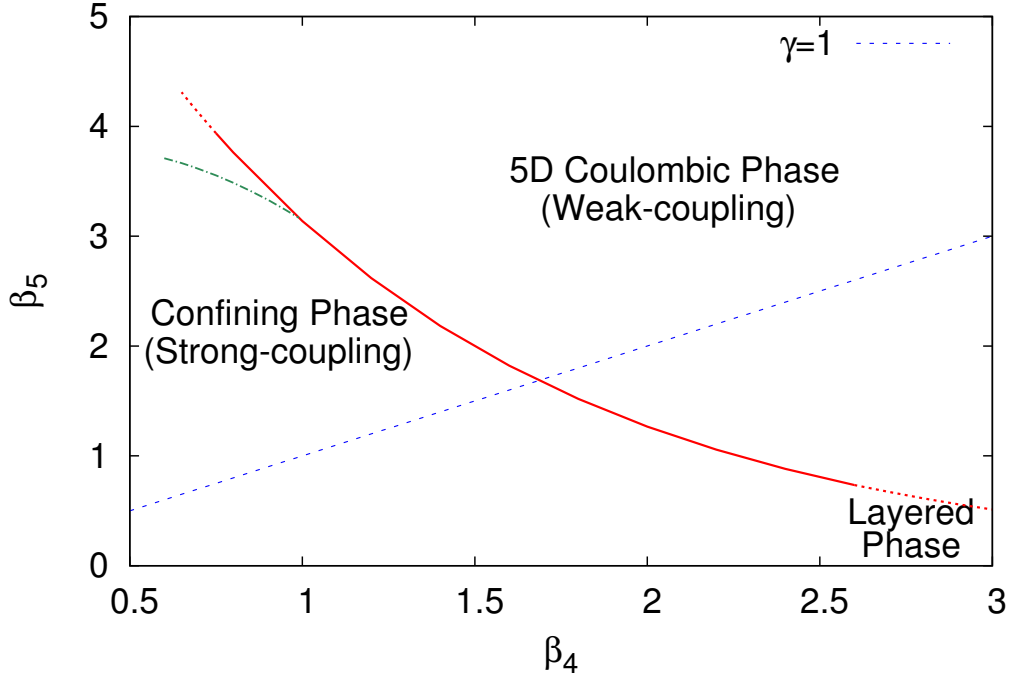


Figure 3.2: A sketch of the phase diagram of the anisotropic SU(2) YM model. The dashed blue line denotes the isotropic case  $\gamma = 1$ . The region above this line was previously investigated in [52, 55, 56] and the region below in [58, 71]. The dashed-dotted green line appears when the extra dimension is compactified [52, 56, 58]. When no compactification is involved, there is a bulk phase transition which is shown in the figure as a red solid line. It was shown to exist up to  $\beta_4 = 2.50$  in [58]. In this work we extend the range of this line up to  $\beta_4 = 2.60$  with no evidence that this line will not continue for larger values of  $\beta_4$ . For  $\beta_4 > 2.60$  the idea of the existence of the layered phase arises.

starting from either random SU(2) matrices (hot configurations) or by setting all the SU(2) matrices to the identity matrix (cold configurations). Simulations were carried out at the lattice volumes of  $16^5$ ,  $20^4 \times 8$  and  $24^4 \times 8$ . The former was the largest investigated by Farakos and Vrentzos [71] and was included in our study to provide a check of our code. The bigger volumes were used to investigate the order of the transition, since, as already mentioned, [58] showed that there is a minimum size of the spatial/temporal and the extra direction in order to see a clear first-order phase transition. We reduced the size of the extra dimension to  $L_5 = 8$  to save compute time, but since the lattice spacing in the extra dimension is much larger for high  $\beta_4$  values than the lattice spacing in the other directions

(as shown in [58]), the system remains five dimensional and no compactification is imposed.

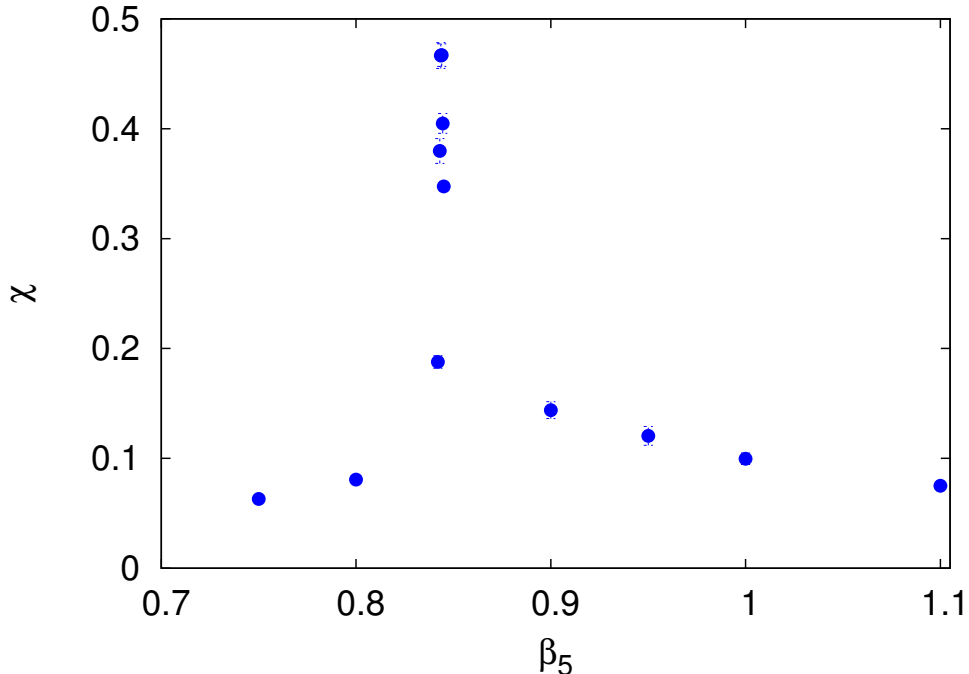


Figure 3.3: The susceptibility of the plaquette in the extra dimension,  $\hat{P}_5$  for  $V = 16^5$  keeping  $\beta_4$  fixed at 2.60 and varying  $\beta_5$ . The critical point is the point at which the susceptibility gains its maximum value.

First, we did a scan in the parameter space  $(\beta_4, \beta_5)$  using small lattices to identify the first-order phase transition that was shown in previous work up to  $\beta_5 = 2.50$ . The phase diagram of the model is shown schematically in Fig. 3.2. The layered phase was previously claimed to exist at large  $\beta_4$  and small  $\beta_5$ , as shown. Our point of interest is  $\beta_4 = 2.60$  on the line of transition, which was claimed to be the critical point at which the transition changes from first to second order in [71]. The critical point in  $\beta_5$  was found by implementing the model on a lattice of volume  $16^5$ . At this volume we were able to do a wide scan by investigating a sufficient number of different  $\beta_5$  to identify the critical point. Even though it does not show any clear evidence of first-order phase transition in terms of a two-state signal, by looking at the susceptibility it looks like it has a divergence at the critical point (Fig. 3.3). The critical  $\beta_5$  point was found to be  $\beta_5 = 0.8437(5)$  which agrees within error with the value found in [71].

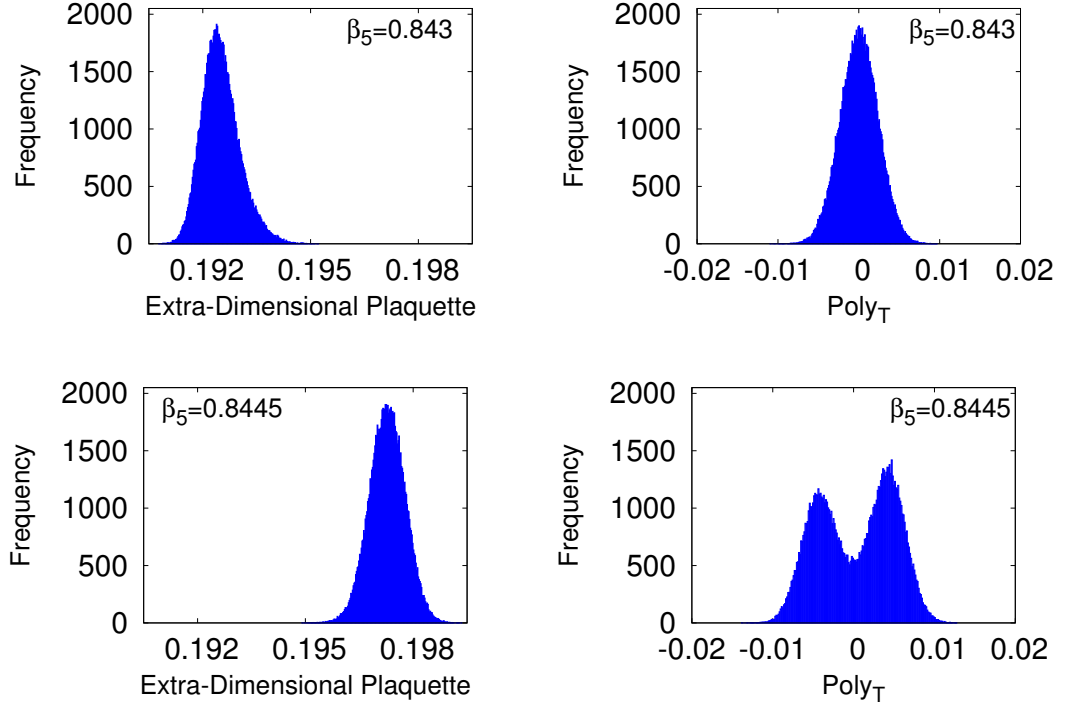


Figure 3.4: The histograms for the plaquette in the extra dimension for  $V = 20^4 \times 8$ , fixed  $\beta_4 = 2.60$  and for two different values of  $\beta_5$ :  $\beta_5 = 0.843$ (top) and  $\beta_5 = 0.8445$ (bottom) are shown on the left. We can see that the peak moves towards the right as we go to higher values of  $\beta_5$ . The corresponding histograms for the temporal Polyakov loop are shown on the right. We can see that for  $\beta_5 = 0.843$  it has a zero expectation value whereas for  $\beta_5 = 0.8445$  it shows a two-peak structure.

For the investigation of the phase transition on the larger lattices we focused on the critical region which was estimated to be between  $\beta_5 = 0.843$  and  $\beta_5 = 0.8445$ , based on the critical value found for the  $16^5$  lattice. As it can be seen from Fig. 3.4, the plaquette moves to the right as we go to higher values of  $\beta_5$  and the temporal Polyakov loop is zero for the point  $\beta_5 = 0.843$ , which is in the confining phase and has a two-peak structure for the point  $\beta_5 = 0.8445$ , which is in the deconfining phase, as expected. We also checked how the temporal Polyakov loop is distributed when all the  $n_5$ -slices are considered independently (Eq. 3.12) and we could see that each fluctuates around zero. Also, we confirmed that the critical point was included in this region by observing that, for one point that lies in between these values, either a clear two-state signal or large fluctuations between two values in the average value of the plaquette were present, as can be

seen in Fig. 3.5 and 3.6.

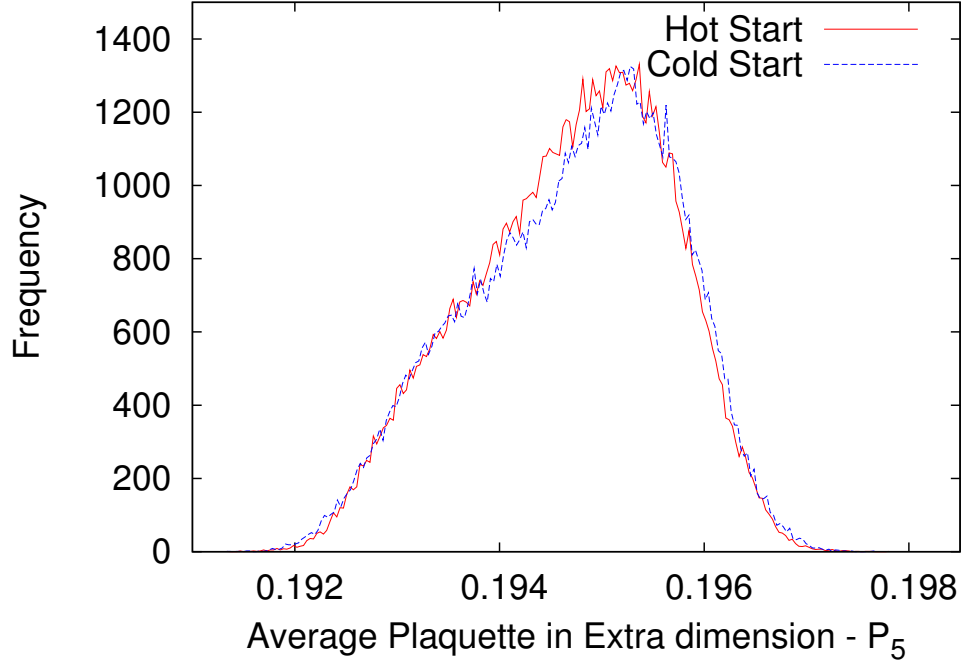


Figure 3.5: Histograms of the average plaquette in the extra dimension,  $\hat{P}_5$  starting from both cold and hot configurations for  $V = 20^4 \times 8$ ,  $\beta_4 = 2.60$  and  $\beta_5 = 0.8435$ . We can see that since this point is very close to the critical one, the plaquette fluctuates between the two vacua and thus the distribution is not Gaussian anymore.

The points that were investigated are  $\beta_5 = 0.843, 0.8435, 0.844, 0.8445$ . For the lattice volume of  $20^4 \times 8$ , we cannot distinguish the two states, since by starting either from hot or cold configurations, the expectation of the plaquette is the same. However, as shown in Fig. 3.5, the distribution is not Gaussian. This is the first hint of the existence of a first-order phase transition. The larger volume of  $24^4 \times 8$  shows an apparent two-state signal as can be seen from the histogram in Fig. 3.6. The overlap that appears between the histograms starting from hot or cold configurations is due to the fact that the two vacua of the potential energy are not so deep and thus the system fluctuates between them. For a check, we implemented one single point ( $\beta_5 = 0.844$ ) on a  $32^4 \times 8$  lattice and we can see in Fig. 3.7 that the two states are now separated by a wide gap, and there is no evidence of tunnelling from one to the other, i.e. it stays in the phase in

which it first equilibrated, depending on the initial configuration. This is also an indication that the extrapolation to the thermodynamic limit must be based on sufficiently large lattices.

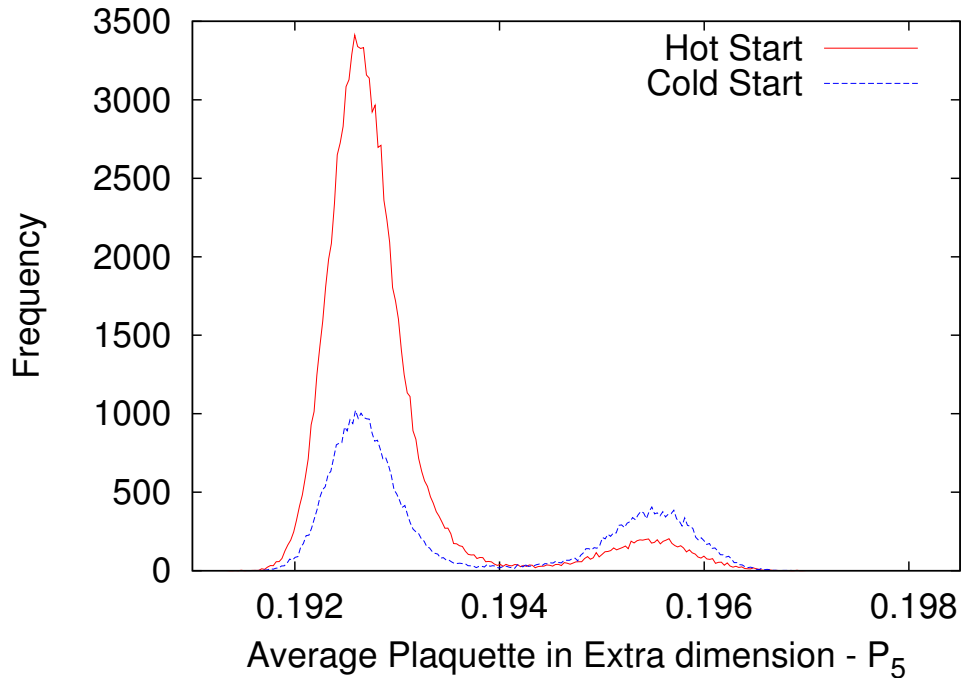


Figure 3.6: Histograms of the average plaquette in the extra dimension,  $\hat{P}_5$  starting from both cold and hot configurations for  $V = 24^4 \times 8$ ,  $\beta_4 = 2.60$  and  $\beta_5 = 0.8435$ . Here, we can see that the distributions, starting from either cold or hot, build up as two Gaussian distributions, one for each vacuum that the system equilibrates to.

We note that the pseudo-critical point was not estimated precisely, because reweighting techniques were not trustworthy for the large volumes and ensemble sizes that were used in this work due to limited statistics.

The code was written using QDP++ [73] and run on GPUs using QDP-JIT [74]. An estimate of the compute time required for the investigation of a single point on an NVIDIA Tesla C2070 Computing Processor (GPU) for the volumes used in this work for a set of 100,000 measurements with  $L_S/2$  overrelaxation steps and a heatbath update each time is shown in Table 3.1. The single point of  $V = 32^4 \times 8$  would have taken two months on GPUs and so it was simulated

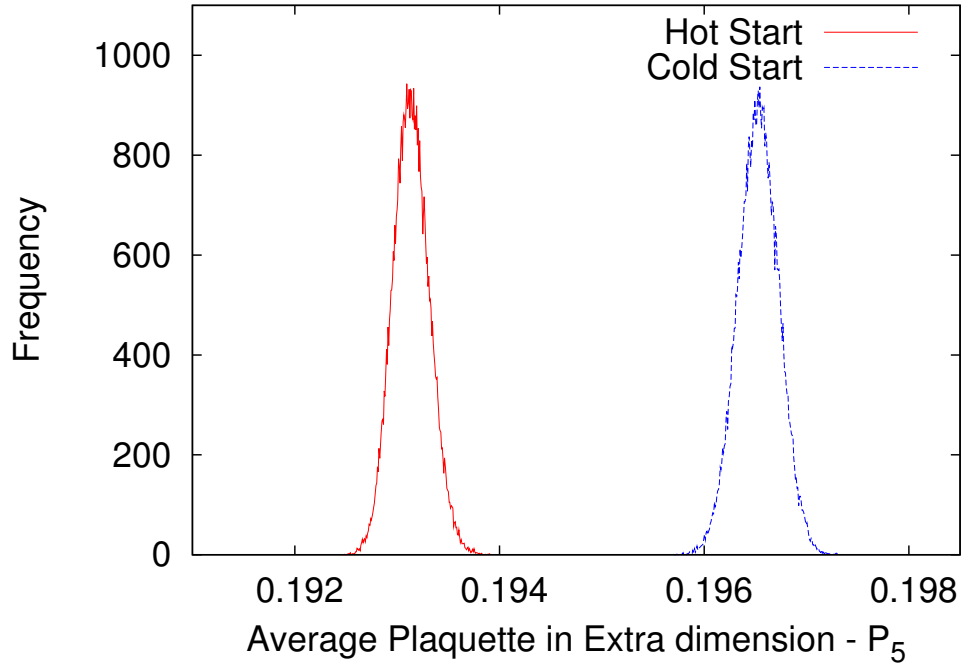


Figure 3.7: Histograms of the average plaquette in the extra dimension,  $\hat{P}_5$  starting from both cold and hot configurations for  $V = 32^4 \times 8$ ,  $\beta_4 = 2.60$  and  $\beta_5 = 0.844$ . It is clear that a first-order phase transition is present since starting from different configurations, the system equilibrates in different states with no tunnelling between them.

using IBM BlueGene/Q in Edinburgh.

Lattice Volume	Compute time (hours)
$16 \times 16 \times 16 \times 16 \times 16$	190
$20 \times 20 \times 20 \times 20 \times 8$	250
$24 \times 24 \times 24 \times 24 \times 8$	620

Table 3.1: Estimated compute time required on an NVIDIA Tesla C2070 Computing Processor for 100,000 measurements for a single point in the parameter space  $(\beta_4, \beta_5)$ .



## 3.4 Discussion and Outlook

In this work, we extended the Monte Carlo investigation of the phase diagram of the anisotropic SU(2) Yang-Mills model in five dimensions when the lattice spacing in the extra dimension is larger than that in the four other dimensions ( $\gamma < 1$ ). We showed that, up to  $\beta_4 = 2.60$ , there is no evidence of a second-order phase transition, whereas a clear two-state signal in the average plaquette favours a first-order phase transition. Based on this result, we can claim that the bulk first-order phase transition between the confining and the deconfining phase continues at least up to  $\beta_4 = 2.60$  and up to this point the continuum limit cannot be taken. Therefore, the possibility of the existence of a UV fixed point and a dimensionally reduced five-dimensional effective field theory remains open. Even though, based on this work, we cannot exclude a second-order transition at higher  $\beta_4$ , nothing in our study suggests that continuing this investigation on even bigger lattices would be worthwhile.

As a final remark for this project, it is worth mentioning that no measurements of any other observables were performed in the region where the proposed layered phase would exist. From the Mean-Field approximation results in [68], it was suggested that the static quark potential in a region very close to the layered phase becomes four-dimensional. Despite that we are not very optimistic for the existence of a non-trivial fixed point that would define a continuum four-dimensional field theory at the transition from the Coulombic to the layered phase, nothing in our study excludes the existence of a dimensionally reduced phase in the relevant region as an effective theory.

## Chapter 4

# Anisotropic 5D Yang-Mills theory in a warped background

As we have seen in Chapter 3, the phase diagram of non-abelian extra-dimensional gauge theories has been extensively explored in a flat background. One, though, can change the metric of the theory to be dependent on the extra dimensions. The driving force that leads to this modification is that in five dimensions this is the gauge-sector of the Randall-Sundrum model that has previously been introduced in Section 1.3.3 the action of which is

$$S_{AdS_5} = \int d^4x \int dy \left[ \frac{1}{4g_5^2} F_{\mu\nu}^2 + \frac{1}{2g_5^2} f(y) F_{\mu 5}^2 \right] \quad (4.1)$$

where the only difference from Eq. (3.1) is the warp factor  $f(y)$  that appears in front of the field strength tensor that involves the extra dimension. This warp factor is given by  $f(y) = e^{-2k|y|}$  as defined in the metric in Eq. 1.23. We call this action  $S_{AdS_5}$  as the extra dimension is in a slice of the  $AdS_5$  spacetime and its discretized version imposing an anisotropy is given by

$$S_{AdS_5} = \beta_4 \sum_{4D} \left( 1 - \frac{1}{2} \text{ReTr} U_{\mu\nu}(n, n_5) \right) + \beta_5 \sum_{5D} \left( 1 - \frac{1}{2} \text{ReTr} f(n_5) U_{\mu 5}(n, n_5) \right) \quad (4.2)$$

---

or

$$S_{AdS_5} = \frac{\beta}{\gamma} \sum_{4D} \left( 1 - \frac{1}{2} \text{ReTr} U_{\mu\nu}(n, n_5) \right) + \beta\gamma \sum_{5D} \left( 1 - \frac{1}{2} \text{ReTr} f(n_5) U_{\mu 5}(n, n_5) \right) \quad (4.3)$$

using the relations of  $\beta_4$  and  $\beta_5$  with  $\beta$  and  $\gamma$  as defined in Chapter 3.

This idea is not new. A previous study attempted to investigate the abelian gauge-sector of the RS model in connection with the layered phase that appears in higher-dimensional anisotropic gauge theories with the anisotropy arising from the warp factor [65]. As mentioned in the previous Chapter, the main idea behind it is to find a way to localize gauge fields on 3-branes, which might arise non-perturbatively by the presence of the layered phase in the phase diagram of the anisotropic gauge theory. For the case of non-abelian gauge theories with extra-dimensional dependent coupling, an effort to localize massless and massive modes was made in [75] but only for (2+1)-dimensional systems and in the specific work the idea of the layered phase has not been used at all.

Our work focuses on the investigation of the phase structure of the anisotropic five-dimensional SU(2) theory with an extra-dimensional dependent lattice coupling along the plaquettes that involve the extra dimensions. This warp factor in our lattice action though, is anticipated to have an effect on the lattice spacing leading to large finite-size effects. This suggests that the correct investigation of the system using Monte Carlo simulations will be computationally expensive, and as we have no previous studies to guide us to specific regions of our parameter space, the first exploration was decided to be undertaken using the Mean-Field approach. One of course might doubt the validity of the results of this method as in four dimensions it does not produce the correct results of the phase transition. The Mean-Field approximation produces a first order phase transition [41] whereas Monte Carlo simulations show a crossover [50]. However, as the former can be seen as an  $1/d$  expansion, it is expected to be more accurate for higher-dimensional systems. The decision to approach our problem using Mean-Field techniques was inspired by recent work of Irges, Knechtli and collaborators [23, 68], who developed further this way of approximating path integrals in LGTs which have been well established and discussed in [41, 42]. This opened up a new path in the investigation of non-abelian extra-dimensional

models on the lattice, as their results show that for higher-dimensional systems the method provides qualitatively correct results.

## 4.1 Formalism using Mean-Field approach

### 4.1.1 Saddle-point equations

To approximate the path integral of the current action we repeat the procedure that we have followed in Section 2.6.2 to find the saddle-point equations with a few modifications. First, as we are looking for this new phase in the phase diagram, the layered phase, we consider the link variables along the ordinary four dimensions and along the extra dimension to have a different value that minimizes the action (mean-field value). Furthermore, the lattice coupling along the extra-dimensional plaquettes will need to be multiplied by the warp factor, which we keep as a general function of  $n_5$  called  $f(n_5)$ .

Following the lines of Fu and Nielsen [39], who derived the saddle-point equations for a flat anisotropic U(1) theory, one can easily apply a similar method for the flat anisotropic SU(2) theory in five dimensions, the effective action of which reads as

$$S_{\text{eff}} = S_G[V_\mu, V_5] + \sum_n \left[ \sum_\mu u[H_\mu(n)] + u_5[H_5(n)] + \sum_\alpha h_{\alpha\mu}(n)v_{\alpha\mu}(n) + \sum_\alpha h_5(n)v_5(n) \right] \quad (4.4)$$

where  $n$  runs over all coordinates in five dimensions. Then the saddle point equations are given by

$$\begin{aligned} \bar{v}_4 &= -u(\bar{h}_4)' \\ \bar{v}_5 &= -u(\bar{h}_5)' \\ \bar{h}_4 &= 6\frac{\beta}{\gamma}\bar{v}_4^3 + 2\beta\gamma\bar{v}_4\bar{v}_5^2 \\ \bar{h}_5 &= 8\beta\gamma\bar{v}_4^2\bar{v}_5 \end{aligned} \quad (4.5)$$

In the above we explicitly separated the coordinates in the usual four dimensions from those in the extra dimension. The Mean-Field approach procedure for the curved-space case is exactly the same as the one described above. So applying it to this system we find the effective action to be

$$S_{\text{eff}} = S_{AdS_5}[V_\mu, V_5] + \sum_{n, n_5} \left[ \sum_{\mu} u[H_\mu(n, n_5)] + u_5[H_5(n, n_5)] + \sum_{\alpha} h_{\alpha\mu}(n, n_5)v_{\alpha\mu}(n, n_5) + \sum_{\alpha} h_{\alpha 5}(n, n_5)v_{\alpha 5}(n, n_5) \right]. \quad (4.6)$$

In order to make this to look like  $S_G[V_\mu, V_5]$  we do a scale transformation of the fields that involve the extra dimension, whereas the fields in the usual four dimensions remain the same.

$$\begin{aligned} U_\mu(n, n_5) &= U'_\mu(n, n_5) \Rightarrow U_{\mu\nu}(n, n_5) = U'_{\mu\nu}(n, n_5) \\ U_\mu(n, n_5) &= \sqrt{f(n_5)}U'_\mu(n, n_5) \Rightarrow U_{\mu 5}(n, n_5) = f(n_5)U'_{\mu 5}(n, n_5) \end{aligned} \quad (4.7)$$

such that

$$S_{AdS_5}[V'_\mu, V'_5] = S_G[V_\mu, V_5] \quad (4.8)$$

where the four-dimensional plaquette and the plaquette extended in the extra dimension are given by

$$V'_{\mu\nu}(n, n_5) = V'_\mu(n, n_5)V'_\nu(n + \hat{\mu}, n_5)V'_\mu(n + \hat{\nu}, n_5)V'_\nu(n, n_5) \quad (4.9)$$

$$V'_{\mu 5}(n, n_5) = V'_\mu(n, n_5)V'_5(n + \hat{\mu}, n_5)V'_\mu(n, n_5 + a_5)V'_5(n, n_5). \quad (4.10)$$

Looking at the effective action in Eq. (4.6) we see that we also need to rescale  $H_5$  as

$$H_5(n, n_5) = \frac{1}{\sqrt{f(n_5)}}H'_5(n, n_5) \quad (4.11)$$

so that we get

$$h_{\alpha 5}(n, n_5)v_{\alpha 5}(n, n_5) = h'_{\alpha 5}(n, n_5)v'_{\alpha 5}(n, n_5). \quad (4.12)$$

Rescaling the external field in the fifth dimension though, changes slightly the term  $u_5[H_5(n, n_5)]$  that becomes

$$e^{-u_5[H'_5(n, n_5)]} = \int_{\text{SU}(2)} \mathcal{D}U e^{\frac{1}{2}\text{ReTr}(UH'_5)}$$

$$= \int_{\text{SU}(2)} \mathcal{D}U e^{\frac{1}{2} \sqrt{f(n_5)} \text{ReTr}(UH_5)}. \quad (4.13)$$

The extra factor that involves the warp factor does not affect the nature of the group integral so it can be evaluated as usual using character expansions with the only difference that now the result will depend on the extra dimension.

$$u_5(H'_5) = -\ln \left( \frac{2}{\rho_5(n_5) \sqrt{f(n_5)}} I_1(\rho_5(n_5) \sqrt{f(n_5)}) \right) \quad (4.14)$$

where

$$\rho_5(n_5) = \sqrt{[\text{Re}(h_{5_0}(n_5))]^2 + \sum_A [\text{Re}(h_{5_A}(n_5))]^2}. \quad (4.15)$$

Next the saddle-point solutions are determined by setting the fields to a background value which, in contrast to the flat case, has an extra-dimensional dependence, i.e.

$$\begin{aligned} V_\mu(n, n_5) &= \bar{v}_4(n_5) \mathbb{1} & H_\mu(n, n_5) &= \bar{h}_4(n_5) \mathbb{1} \\ V_5(n, n_5) &= \bar{v}_5(n_5) \mathbb{1} & H_5(n, n_5) &= \bar{h}_5(n_5) \mathbb{1} \end{aligned} \quad (4.16)$$

This leads to the saddle-point equations given by

$$\begin{aligned} \bar{v}_4(n_5) &= u_4(\bar{h}_4(n_5), n_5)' = \frac{I_2(\bar{h}_4(n_5))}{I_1(\bar{h}_4(n_5))} \\ \bar{v}_5(n_5) &= u_5(\bar{h}_5(n_5), n_5)' = \frac{I_2(\sqrt{f(n_5)} \bar{h}_5(n_5))}{I_1(\sqrt{f(n_5)} \bar{h}_5(n_5))} \\ \bar{h}_4(n_5) &= 6 \frac{\beta}{\gamma} \bar{v}_4^3(n_5) + \beta \gamma \bar{v}_5^2(n_5) \bar{v}_4(n_5 + a_5) + \beta \gamma \bar{v}_5^2(n_5 - a_5) \bar{v}_4(n_5 - a_5) \\ \bar{h}_5(n_5) &= 8 \beta \gamma \bar{v}_5(n_5) \bar{v}_4(n_5) \bar{v}_4(n_5 + a_5) \end{aligned} \quad (4.17)$$

and the free energy at zero'th order which can be written as

$$\begin{aligned} F^{(0)} &= \frac{S_{\text{eff}}[\bar{V}, \bar{H}]}{\mathcal{N}_{(4)}} = \sum_{n_5} \left[ -6 \frac{\beta}{\gamma} \bar{v}_4(n_5)^4 - 4 \beta \gamma \bar{v}_4(n_5) \bar{v}_5^2(n_5) \bar{v}_4(n_5 + a_5) \right. \\ &\quad \left. + 4 u_4(\bar{h}_4(n_5), n_5) + u_5(\bar{h}_5(n_5), n_5) + 4 \bar{h}_4(n_5) \bar{v}_4(n_5) + \bar{h}_5(n_5) \bar{v}_5(n_5) \right] \end{aligned} \quad (4.18)$$

where  $\mathcal{N}_{(4)}$  is the volume in the four-dimensional space given by  $TL^3$ , where  $T$  and  $L$  are the lattice sizes along the temporal and spatial directions, respectively. From now on, when 1 is added or subtracted from  $n_5$ , it will mean that we add/subtract one lattice unit in the extra dimension and we do not write  $a_5$  explicitly.

### 4.1.2 First-order corrections

As already mentioned in Section 2.6.2, the solutions to the saddle-point equations should be checked to see if the point is stable or not. This can only be achieved by computing first-order corrections to the free energy following the method described in Section 2.6.2.2. The necessary modifications in our case is to define the fluctuations of the background values to be

$$\begin{aligned}
 V_\mu(n, n_5) &= \bar{v}_4(n_5) + v_\mu(n, n_5) & ; & & v_\mu(n, n_5) &= v_{\mu_0}(n, n_5) + iv_{\mu_A}(n, n_5)\sigma^A \\
 V_5(n, n_5) &= \bar{v}_5(n_5) + v_5(n, n_5) & ; & & v_5(n, n_5) &= v_{5_0}(n, n_5) + iv_{5_A}(n, n_5)\sigma^A \\
 H_\mu(n, n_5) &= \bar{h}_4(n_5) + h_\mu(n, n_5) & ; & & h_\mu(n, n_5) &= h_{\mu_0}(n, n_5) - ih_{\mu_A}(n, n_5)\sigma^A \\
 H_5(n, n_5) &= \bar{h}_5(n_5) + h_5(n, n_5) & ; & & h_5(n, n_5) &= h_{5_0}(n, n_5) - ih_{5_A}(n, n_5)\sigma^A
 \end{aligned} \tag{4.19}$$

and the effective action can now be written as

$$\begin{aligned}
 S_{\text{eff}} &= S_{\text{eff}}^{(0)} \Big|_{\bar{V}, \bar{H}} + \frac{1}{2} \left( \frac{\partial^2 S_{\text{eff}}}{\partial V_4^2} \Big|_{\bar{V}, \bar{H}} v_4^2 + \frac{\partial^2 S_{\text{eff}}}{\partial V_5^2} \Big|_{\bar{V}, \bar{H}} v_5^2 + \frac{\partial^2 S_{\text{eff}}}{\partial H_4^2} \Big|_{\bar{V}, \bar{H}} h_4^2 + \frac{\partial^2 S_{\text{eff}}}{\partial H_5^2} \Big|_{\bar{V}, \bar{H}} h_5^2 \right. \\
 &+ \left. \frac{\partial^2 S_{\text{eff}}}{\partial V_4 \partial V_5} \Big|_{\bar{V}, \bar{H}} v_4 v_5 + \frac{\partial^2 S_{\text{eff}}}{\partial V_5 \partial V_4} \Big|_{\bar{V}, \bar{H}} v_5 v_4 + 2 \frac{\partial^2 S_{\text{eff}}}{\partial H_4 \partial V_4} \Big|_{\bar{V}, \bar{H}} h_4 v_4 + 2 \frac{\partial^2 S_{\text{eff}}}{\partial H_5 \partial V_5} \Big|_{\bar{V}, \bar{H}} h_5 v_5 \right)
 \end{aligned} \tag{4.20}$$

where by the subscript “4” and “5” we imply derivatives along only the four-dimensional space and along the extra dimension respectively, by  $\bar{V}, \bar{H}$  we mean that the partial derivatives are evaluated at the background values  $(\bar{v}_4(n_5), \bar{v}_5(n_5), \bar{h}_4(n_5), \bar{h}_5(n_5))$  and the missing terms in the expansion give zero contribution, thus they were omitted. Also, we again denote the corrections to the action as  $S^{(2)}[v, h]$ .

In this case we define the propagators to be

$$\begin{aligned}
 \left. \frac{\partial^2 S_{\text{eff}}}{\partial V_4^2} \right|_{\bar{V}, \bar{H}} &\equiv \Delta_{44}^{(vv)} + \Delta_{44}^{(gf)} & \left. \frac{\partial^2 S_{\text{eff}}}{\partial V_5^2} \right|_{\bar{V}, \bar{H}} &\equiv \Delta_{55}^{(vv)} + \Delta_{55}^{(gf)} \\
 \left. \frac{\partial^2 S_{\text{eff}}}{\partial V_4 \partial V_5} \right|_{\bar{V}, \bar{H}} &\equiv \Delta_{45}^{(vv)} + \Delta_{45}^{(gf)} & \left. \frac{\partial^2 S_{\text{eff}}}{\partial V_5 \partial V_4} \right|_{\bar{V}, \bar{H}} &\equiv \Delta_{54}^{(vv)} + \Delta_{54}^{(gf)} \\
 \left. \frac{\partial^2 S_{\text{eff}}}{\partial H_4^2} \right|_{\bar{V}, \bar{H}} &\equiv \Delta_{44}^{(hh)} & \left. \frac{\partial^2 S_{\text{eff}}}{\partial H_5^2} \right|_{\bar{V}, \bar{H}} &\equiv \Delta_{55}^{(hh)} \\
 \left. \frac{\partial^2 S_{\text{eff}}}{\partial H_4 \partial V_4} \right|_{\bar{V}, \bar{H}} &\equiv \Delta_{44}^{(hv)} & \left. \frac{\partial^2 S_{\text{eff}}}{\partial H_5 \partial V_5} \right|_{\bar{V}, \bar{H}} &\equiv \Delta_{55}^{(hv)}
 \end{aligned} \tag{4.21}$$

where  $\Delta^{(gf)}$  arises from the gauge fixing term. In the particular case we choose to use the Lorenz gauge and taking into account the anisotropy we define the discretized version of the gauge-fixing action to be

$$S_{gf} = \frac{1}{2\xi} \sum_n \sum_{n_5} \sum_A \left[ \sum_{\mu} f_{\mu A}(n, n_5) + \gamma f_{5A}(n, n_5) \right]^2 \tag{4.22}$$

where

$$f_{\mu A}(n, n_5) = v_{\mu A}(n, n_5) - v_{\mu A}(n - \hat{\mu}, n_5) \tag{4.23}$$

and

$$f_{5A}(n, n_5) = v_{5A}(n, n_5) - v_{5A}(n, n_5 - 1). \tag{4.24}$$

It is important to notice that gauge fixing is imposed only to the directions  $\alpha = A = 1, 2, 3$  as the local gauge transformations evaluated at the background for  $\alpha = 0$  result to zero, and therefore no zero modes arise in that direction which means that no gauge fixing is required (see Eq. (C.48)). As discussed in Section 2.6.2.2 a Faddeev-Popov determinant arises in our formulation when we fix the gauge and the free energy at first order is given by Eq. (2.98) where in this case, the propagators are the ones defined above. It is also worth mentioning that the propagators can be seen as two large matrices given by

$$\Delta^{(vv)} + \Delta^{(gf)} = \sum_{p', p''} \sum_{n'_5, n''_5} \begin{pmatrix} \Delta_{44}^{(vv)} + \Delta_{44}^{(gf)} & \Delta_{45}^{(vv)} + \Delta_{45}^{(gf)} \\ \Delta_{54}^{(vv)} + \Delta_{54}^{(gf)} & \Delta_{55}^{(vv)} + \Delta_{55}^{(gf)} \end{pmatrix}$$



and

$$\Delta^{(hh)} = \sum_{p', p''} \sum_{n'_5, n''_5} \begin{pmatrix} \Delta_{44}^{(hh)} & 0 \\ 0 & \Delta_{55}^{(hh)} \end{pmatrix}$$

$\Delta_{44}^{(hv)}$  and  $\Delta_{55}^{(hv)}$  are found to be equal to the identity.

We derive the expressions for the above two matrices, following closely the discussion in [23], as the rescaling of the fields done in Eq. (4.7) and Eq. (4.11) allow us to match up to some factors our derivations with those presented in the aforementioned work. The full derivations and final expressions are given in Appendix C.

Finally, even though we have fixed the gauge, there is an extra zero mode in the propagators that arises from global gauge transformations when  $p = 0$ , called the toron. This arises due to the toroidal geometry of the system and it causes problems when trying to invert it. However, in the free energy, there is also a zero mode that arises when all momenta are set to zero from the Faddeev-Popov determinant. Therefore, one can regularize this term in the free energy, or anywhere else that there is this zero over zero contribution due to torons, to get a finite part. As the toron appears due to the geometry of the lattice, it is a finite-size effect and thus the extracted finite part is negligible in the infinite-volume limit. Hence, one can simply drop the  $p = 0$  contribution [76, 77].

## 4.2 Observables

To investigate the physics of the system we define some observables on the layers. We focus on a scalar mass and the static quark potential. These observables were motivated by the studies presented in [68] and [23]. To derive the expressions we follow closely the guidelines given in the aforementioned papers.

In standard QFT we know that the expectation value of an operator is given by

$$\langle O \rangle = \frac{1}{Z} \int \mathcal{D}U O[U] \exp^{-S_G[U]}. \quad (4.25)$$

In the Mean-Field approximation as discussed above we will get

$$\langle O \rangle = \frac{1}{Z} \int \mathcal{D}V \int \mathcal{D}H O[V] \exp^{-S_{\text{eff}}[V,H]} \quad (4.26)$$

In this approximation any observable can be written as a Taylor expansion about the mean-field value given by

$$O[V] = O[\bar{V}] + \left. \frac{\delta O}{\delta V} \right|_{\bar{V}} v + \frac{1}{2} \left. \frac{\delta^2 O}{\delta V^2} \right|_{\bar{V}} v^2 + \dots \quad (4.27)$$

Combining the above we get

$$\langle O \rangle = \frac{1}{Z} \int \mathcal{D}V \int \mathcal{D}H \left( O[\bar{V}] + \left. \frac{\delta O}{\delta V} \right|_{\bar{V}} v + \frac{1}{2} \left. \frac{\delta^2 O}{\delta V^2} \right|_{\bar{V}} v^2 \right) e^{-S_{\text{eff}}[\bar{V},\bar{H}]} e^{-S^{(2)}[v,h]} \quad (4.28)$$

where  $e^{-S^{(2)}[v,h]}$  inherits the first-order corrections to the action as described in Section 4.1.2. Using the definition of  $z$  as in Eq. (2.97) the correlation function becomes

$$\begin{aligned} \langle O \rangle &= O[\bar{V}] + \frac{1}{2} \left. \frac{\delta^2 O}{\delta v_j \delta v_i} \right|_{\bar{V}} \frac{1}{z} \int \mathcal{D}V \int \mathcal{D}H v_i v_j e^{-S^{(2)}[v,h]} \\ &= O[\bar{V}] + \frac{1}{2} \left. \frac{\delta^2 O}{\delta v_j \delta v_i} \right|_{\bar{V}} \Delta_{ij}^{-1} \\ &= O[\bar{V}] + \frac{1}{2} \text{Tr} \left( \left. \frac{\delta^2 O}{\delta V^2} \right|_{\bar{V}} \Delta^{-1} \right) \end{aligned} \quad (4.29)$$

where  $\Delta = -\mathbb{1} + \Delta^{(hh)}(\Delta^{(vv)} + \Delta^{(gf)})$ . So any observable can be measured by adding its tree-level value (evaluated at the mean-field values) to corrections that arise from the Gaussian fluctuations around this background.

### 4.2.1 Scalar mass

To extract masses the two-point function is used which is given by

$$\begin{aligned} C(t) &= \langle O(t_0 + t) O(t_0) \rangle - \langle O(t_0 + t) \rangle \langle O(t_0) \rangle \\ &= C^{(0)}(t) + C^{(1)}(t) + \dots \end{aligned} \quad (4.30)$$

where  $C^{(0)}(t)$  and  $C^{(1)}(t)$  denotes the zeroth order and first order corrections to the two point-function. It is known that the two-point function can be written as a sum over the energy eigenvalues of the states i.e.

$$C(t) = \sum_{\lambda} c_{\lambda} e^{-E_{\lambda} t}. \quad (4.31)$$

This means that in the large  $t$  behaviour the energy state that dominates is the ground state which gives the mass ( $E_0 = m$ ). By this, it is easily seen that we can measure the mass using

$$m = \lim_{t \rightarrow \infty} \ln \frac{C(t-1)}{C(t)}. \quad (4.32)$$

The two-point function at first order, denoted by  $C^{(1)}(t)$ , can be found by applying Eq. (4.29) in Eq. (4.30) and it is given by

$$\begin{aligned} C^{(1)}(t) &= O(t_0+t)[\bar{V}]O(t_0)[\bar{V}] + \frac{1}{2} \text{Tr} \left( \frac{\delta^2(O(t_0+t)O(t_0))}{\delta V^2} \Big|_{\bar{V}} \Delta^{-1} \right) \\ &\quad - \left[ O(t_0+t)[\bar{V}] + \frac{1}{2} \text{Tr} \left( \frac{\delta^2 O(t_0+t)}{\delta V^2} \Big|_{\bar{V}} \Delta^{-1} \right) \right] \left[ O(t_0)[\bar{V}] + \frac{1}{2} \text{Tr} \left( \frac{\delta^2 O(t_0)}{\delta V^2} \Big|_{\bar{V}} \Delta^{-1} \right) \right] \\ &= O(t_0+t)[\bar{V}]O(t_0)[\bar{V}] + \frac{1}{2} \text{Tr} \left[ \frac{\delta}{\delta V} \left( O(t_0+t) \frac{\delta O(t_0)}{\delta V} + O(t_0) \frac{\delta O(t_0+t)}{\delta V} \right) \Big|_{\bar{V}} \Delta^{-1} \right] \\ &\quad - O(t_0+t)[\bar{V}]O(t_0)[\bar{V}] - \frac{1}{2} \text{Tr} \left( O(t_0+t) \frac{\delta^2 O(t_0)}{\delta V^2} \Big|_{\bar{V}} \Delta^{-1} \right) \\ &\quad - \frac{1}{2} \text{Tr} \left( O(t_0) \frac{\delta^2 O(t_0+t)}{\delta V^2} \Big|_{\bar{V}} \Delta^{-1} \right) \\ &= \frac{1}{2} \text{Tr} \left[ \left( \frac{\delta O(t_0+t)}{\delta V} \frac{\delta O(t_0)}{\delta V} \Big|_{\bar{V}} + \frac{\delta O(t_0)}{\delta V} \frac{\delta O(t_0+t)}{\delta V} \Big|_{\bar{V}} \right) \Delta^{-1} \right]. \end{aligned} \quad (4.33)$$

The observable to extract a scalar mass on each layer will be the Polyakov loop along one of the spatial directions and by taking its trace it becomes gauge invariant as required. It should be noted that this mass is a torelon, i.e. a topological excitation winding around the toroidal lattice in the spatial direction and not the Higgs mass that appears in the Gauge-Higgs Unification models. The latter is extracted using the Polyakov loop along the extra dimension and not a

spatial one. For the torelon the observable is given by

$$\begin{aligned}
 O(t, \vec{m}, m_5) &= \text{Tr}\{P_1(t, \vec{m}, m_5)\} \\
 &= \text{Tr}\left\{\prod_{m_1=0}^{L-1} V_\mu(t, \vec{m}, m_5)\right\} \\
 &= \text{Tr}\left\{\prod_{m_1=0}^{L-1} [\bar{v}_4(m_5)\mathbb{1} + v_{1\alpha}(t, \vec{m}, m_5)\sigma^\alpha]\right\}. \quad (4.34)
 \end{aligned}$$

The first order corrections to the correlation function as given in Eq. (4.33) is shown diagrammatically in Figure 4.1 which is nothing else but a single gauge boson exchange.

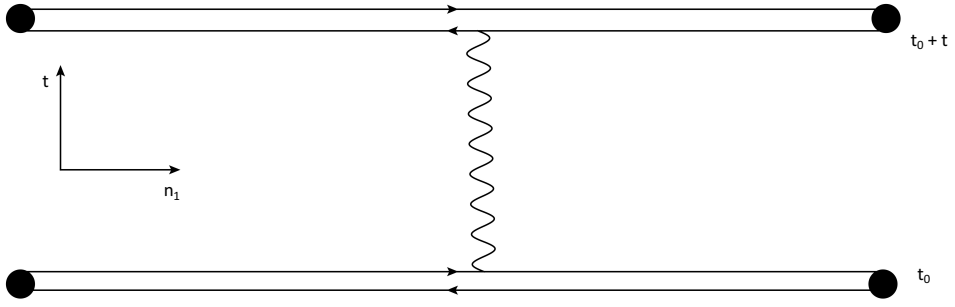


Figure 4.1: The schematic illustration of the first order mean-field corrections to the correlation function out of which a scalar mass is extracted. This is just a gauge boson exchange between two Polyakov loops at times  $t_0$  and  $t_0 + t$ .

To find  $C^{(1)}(t)$  we use the averaged version of the observable in the two-point function, i.e.

$$O_4(t; m_5) = \frac{1}{T} \sum_{t_0} \frac{1}{L^4} \sum_{\vec{m}'_{23}, \vec{m}''_{23}} O(t_0, \vec{m}', m_5) O(t_0 + t, \vec{m}'', m_5) \quad (4.35)$$

where  $\vec{m}_{23} = (m_2, m_3)$  and we get

$$\begin{aligned}
 C^{(1)}(t; m_5) &= \frac{1}{2} \text{Tr}\left\{4 \frac{(P_1^{(0)})^2}{v_4(m_5)^2} D^{(L)}(n'_1) D^{(L)}(n''_1) \delta_{M',1} \delta_{M'',1} \delta_{a',0} \delta_{a'',0} \delta_{n'_5, m_5} \delta_{n''_5, m_5}\right. \\
 &\quad \left. \frac{1}{T} \sum_{t_0} \frac{1}{L^4} \sum_{\vec{m}'_{23}, \vec{m}''_{23}} \left( \delta_{n'_0, t_0+t} \delta_{n''_0, t_0} \delta_{\vec{n}'_{23}, \vec{m}'_{23}} \delta_{\vec{n}''_{23}, \vec{m}''_{23}} \right)\right.
 \end{aligned}$$

$$+ \delta_{n'_0, t_0} \delta_{n''_0, t_0+t} \delta_{\vec{n}'_{23}, \vec{m}'_{23}} \delta_{\vec{n}''_{23}, \vec{m}''_{23}} \Big) \Delta^{-1} \Big\} \quad (4.36)$$

where we have used the definitions

$$P_1^{(0)} = \bar{v}_4(m_5)^L \quad (4.37)$$

and

$$D^{(L)}(n_1) = \sum_{m_1=0}^{L-1} \delta_{n_1, m_1}. \quad (4.38)$$

This expression in momentum space is given by

$$C^{(1)}(t; m_5) = \frac{4}{\mathcal{N}_{(4)}} \frac{(P_1^{(0)})^2}{\bar{v}_4(m_5)^2} \sum_{p'_0} \cos(p'_0 t) \sum_{p'_1} |\tilde{D}^{(L)}(p'_1)|^2 \tilde{\Delta}^{-1}((p'_0, p'_1, \vec{0}_{23}, m_5), 1, 0; (p'_0, p'_1, \vec{0}_{23}, m_5), 1, 0) \quad (4.39)$$

where

$$\tilde{D}^{(L)}(p'_1) = \sum_{m_1=0}^{L-1} e^{ip'_1 m_1}. \quad (4.40)$$

and  $\mathcal{N}_{(4)}$  is the volume of the four-dimensional subspace, i.e.  $TL^3$ . The full derivation of the expression for the correlation function from which the scalar mass can be extracted is given in Appendix D.1. From this correlation function the scalar mass on each layer  $n_5$  can be found.

### 4.2.2 Static quark-antiquark potential

The second quantity that we want to extract from our mean-field solutions is the static potential on each four-dimensional layer, i.e. layers at a fixed  $m_5$ . To get this we will make use of the Wilson loop that extends only in the usual four-dimensional space. For a planar Wilson loop along the temporal direction  $n_0$  and spatial direction  $n_1$  we use the following definition

$$O_W^{(t-r)}(t_0, \vec{m}, m_5) \equiv O_W^{(t-r)}(t_0, m_1, \vec{m}_{23}, m_5) = \text{Tr} \{ l^{(t)}(t_0, 0, \vec{m}_{23}, m_5) l^{(r)}(t_0 + t, \vec{m}_{23}, m_5) l^{(t)\dagger}(t_0, r, \vec{m}_{23}, m_5) l^{(r)\dagger}(t_0, \vec{m}_{23}, m_5) \} \quad (4.41)$$

where

$$l^{(t)}(t_0, m_1, \vec{m}_{23}, m_5) = \prod_{m_0=t_0}^{t_0+t-1} [\bar{v}_4(m_5)\mathbb{1} + v_{0_\alpha}(m_0, m_1, \vec{m}_{23}, m_5)\sigma^\alpha] \quad (4.42)$$

and

$$l^{(r)}(m_0, \vec{m}_{23}, m_5) = \prod_{m_1=0}^{r-1} [\bar{v}_4(m_5)\mathbb{1} + v_{1_\alpha}(m_0, m_1, \vec{m}_{23}, m_5)\sigma^\alpha] \quad (4.43)$$

with  $\vec{m}_{23} = (m_2, m_3)$ . As the spatial directions are indistinguishable one needs to notice that the definition applies for all spatial directions by interchanging  $n_1$  with  $n_2$  or  $n_3$  and using  $n_1$  here is just a choice.

As a matter of fact the observable that is used is the Wilson loop averaged over spacetime directions which leads to the expression

$$\begin{aligned} & \langle O_W^{(t-r)}(t_0, m_1, \vec{m}_{23}, m_5) \rangle \\ &= \bar{O}_W^{(0)}(m_5) + \frac{1}{2} \frac{1}{T} \sum_{t_0} \frac{1}{L^2} \sum_{\vec{m}_{23}} \sum_{\substack{(n', M', \alpha') \\ (n'', M'', \alpha'')}} \left( \frac{\delta^2 O_W^{(t-r)}(t_0, m_1, \vec{m}_{23}, m_5)}{\delta v_{M''_\alpha''}(n'') \delta v_{M'_\alpha'}(n')} \right) \Delta_{1;2}^{-1} \end{aligned} \quad (4.44)$$

that needs to be evaluated.

The expectation value of this observable at zero'th order is

$$\bar{O}_W^{(0)}(m_5) = 2\bar{v}_4(m_5)^{2(t+r)}. \quad (4.45)$$

According to Eq.(4.29), we want to compute

$$\begin{aligned} & \left. \frac{\delta^2 O_W}{\delta v^2} \right|_{\bar{V}} = \left. \frac{\delta^2 O_W^{(t-r)}(t_0, m_1, \vec{m}_{23}, m_5)}{\delta v_{M''_\alpha''}(n'') \delta v_{M'_\alpha'}(n')} \right|_{\bar{V}} \\ &= \text{Tr} \left\{ \frac{\delta l^{(t)}(t_0, 0, \vec{m}_{23}, m_5)}{\delta v_{M'_\alpha'}(n')} l^{(r)}(t_0 + t, \vec{m}_{23}, m_5) \frac{\delta l^{(t)\dagger}(t_0, r, \vec{m}_{23}, m_5)}{\delta v_{M''_\alpha''}(n'')} l^{(r)\dagger}(t_0, \vec{m}_{23}, m_5) \right\} \Big|_{\bar{V}} \\ &+ \text{Tr} \left\{ \frac{\delta l^{(t)}(t_0, 0, \vec{m}_{23}, m_5)}{\delta v_{M''_\alpha''}(n'')} l^{(r)}(t_0 + t, \vec{m}_{23}, m_5) \frac{\delta l^{(t)\dagger}(t_0, r, \vec{m}_{23}, m_5)}{\delta v_{M'_\alpha'}(n')} l^{(r)\dagger}(t_0, \vec{m}_{23}, m_5) \right\} \Big|_{\bar{V}} \\ &+ \text{Tr} \left\{ \frac{\delta^2 l^{(t)}(t_0, 0, \vec{m}_{23}, m_5)}{\delta v_{M''_\alpha''}(n'') \delta v_{M'_\alpha'}(n')} l^{(r)}(t_0 + t, \vec{m}_{23}, m_5) l^{(t)\dagger}(t_0, r, \vec{m}_{23}, m_5) l^{(r)\dagger}(t_0, \vec{m}_{23}, m_5) \right\} \Big|_{\bar{V}} \end{aligned}$$

$$+\text{Tr} \left\{ l^{(t)}(t_0, 0, \vec{m}_{23}, m_5) l^{(r)}(t_0 + t, \vec{m}_{23}, m_5) \frac{\delta^2 l^{(t)\dagger}(t_0, r, \vec{m}_{23}, m_5)}{\delta v_{M''_{\alpha''}}(n'') \delta v_{M'_{\alpha'}}(n')} l^{(r)\dagger}(t_0, \vec{m}_{23}, m_5) \right\} \Big|_{\bar{v}} \quad (4.46)$$

Diagrammatically, the first-order corrections are shown in Figure 4.2. The first two terms in Eq. (4.46) correspond to the left diagram, i.e. to a gauge boson exchange and the last two terms correspond to the centre and right diagrams, i.e. the self-energy and tadpole contributions.

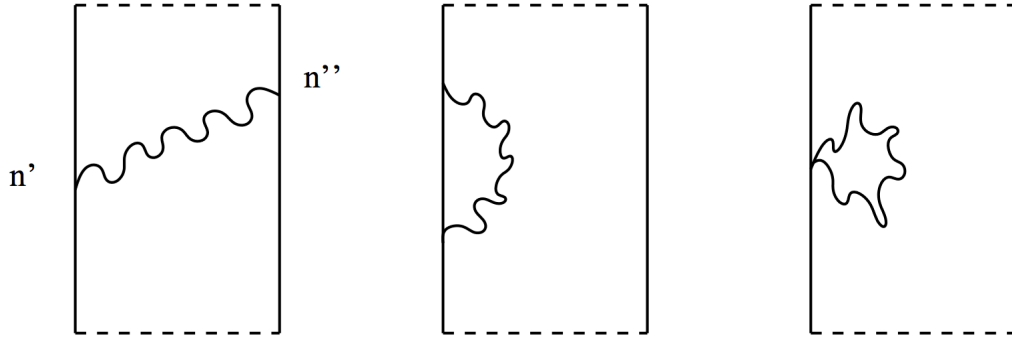


Figure 4.2: The schematic illustration of the contributions to the first-order mean-field corrections to the static potential. These are associated with the terms in Eq. (4.46) that correspond to a gauge boson exchange(left), self-energy (centre) and tadpole (right). This figure was taken from Ref. [68].

After each term of Eq. (4.46) is evaluated, the first-order corrections to the Wilson loop in coordinate space read as

$$O_W^{(1)} = \frac{1}{2} \frac{1}{T} \sum_{t_0} \frac{1}{L^2} \sum_{\vec{m}_{23}} \text{Tr} \left\{ 2\bar{v}_4(m_5)^{2(t+r)-2} \delta_{M',0} \delta_{M'',0} \delta_{\vec{n}_{23},\vec{m}_{23}} \delta_{\vec{n}'_{23},\vec{m}_{23}} \delta_{n'_5,m_5} \delta_{n''_5,m_5} \right. \\ \left[ (\delta_{\alpha',0} \delta_{\alpha'',0} + \delta_{\alpha',A} \delta_{\alpha'',A}) (\delta_{n'_1,0} \delta_{n''_1,r} + \delta_{n'_1,r} \delta_{n''_1,0}) \right. \\ (\delta_{n'_0,t_0} + \delta_{n'_0,t_0+1} + \dots + \delta_{n'_0,t_0+t-1}) (\delta_{n''_0,t_0} + \delta_{n''_0,t_0+1} + \dots + \delta_{n''_0,t_0+t-1}) \\ + (\delta_{\alpha',0} \delta_{\alpha'',0} - \delta_{\alpha',A} \delta_{\alpha'',A}) (\delta_{n'_1,0} \delta_{n''_1,0} + \delta_{n'_1,r} \delta_{n''_1,r}) \\ (\delta_{n'_0,t_0} (\delta_{n''_0,t_0+1} + \delta_{n''_0,t_0+2} + \dots + \delta_{n''_0,t_0+t-1}) \\ + \delta_{n'_0,t_0+1} (\delta_{n''_0,t_0} + \delta_{n''_0,t_0+2} + \dots + \delta_{n''_0,t_0+t-1}) + \dots \\ \left. \left. + \delta_{n'_0,t_0+t-1} (\delta_{n''_0,t_0} + \delta_{n''_0,t_0+1} + \dots + \delta_{n''_0,t_0+t-2}) \right) \right] \Delta^{-1} \Big\}. \quad (4.47)$$

In momentum space this is given by

$$\begin{aligned}
 O_W^{(1)} &= \frac{\bar{v}_4(m_5)^{2(t+r)-2}}{\mathcal{N}_{(4)}} t^2 \sum_{p'_1, p'_2, p'_3} \delta_{p'_0, 0} \\
 &\left[ (2 \cos(p'_1 r) + 2) \tilde{\Delta}^{-1} \left( (0, p'_1, \vec{p}_{23}, m_5), 0, 0; (0, p'_1, \vec{p}_{23}, m_5), 0, 0 \right) \right. \\
 &\quad \left. + 3(2 \cos(p'_1 r) - 2) \tilde{\Delta}^{-1} \left( (0, p'_1, \vec{p}_{23}, m_5), 0, 1; (0, p'_1, \vec{p}_{23}, m_5), 0, 1 \right) \right].
 \end{aligned} \tag{4.48}$$

The desired calculable quantity is the potential which is given by

$$\begin{aligned}
 \langle O_W \rangle &= \lim_{t \rightarrow \infty} e^{-tV(r)} \\
 \Rightarrow V(r) &= - \lim_{t \rightarrow \infty} \frac{1}{t} \ln \langle O_W \rangle.
 \end{aligned} \tag{4.49}$$

Using Eq. (4.44) to write the expectation of the Wilson loop as its value at tree level plus first-order corrections, we can derive an expression for the static potential at a specific layer located at  $m_5$  as following

$$\begin{aligned}
 V(r; m_5) &= - \lim_{t \rightarrow \infty} \frac{1}{t} \ln \left[ \bar{O}_W^{(0)}(m_5) + \text{corrections} \right] \\
 &= - \lim_{t \rightarrow \infty} \frac{1}{t} \ln \left[ \bar{O}_W^{(0)}(m_5) \left( 1 + \frac{\text{corrections}}{\bar{O}_W^{(0)}(m_5)} \right) \right] \\
 &= - \lim_{t \rightarrow \infty} \frac{1}{t} \ln (2\bar{v}_4(m_5)^{2(t+r)}) - \lim_{t \rightarrow \infty} \frac{1}{t} \ln \left( 1 + \frac{\text{corrections}}{\bar{O}_W^{(0)}(m_5)} \right) \\
 &= -2 \ln \bar{v}_4(m_5) - \lim_{t \rightarrow \infty} \frac{1}{t} \left( \frac{\text{corrections}}{\bar{O}_W^{(0)}(m_5)} \right).
 \end{aligned} \tag{4.50}$$

Using the expression for the corrections given in Eq. (4.48) we can show that the potential on four-dimensional layers can be expressed as

$$\begin{aligned}
 V(r; m_5) &= -2 \ln \bar{v}_4(m_5) - \frac{1}{L^3} \frac{1}{\bar{v}_4(m_5)^2} \sum_{p'_1, p'_2, p'_3} \delta_{p'_0, 0} \\
 &\left[ (2 \cos(p'_1 r) + 2) \tilde{\Delta}^{-1} \left( (0, p'_1, \vec{p}_{23}, m_5), 0, 0; (0, p'_1, \vec{p}_{23}, m_5), 0, 0 \right) \right. \\
 &\quad \left. + 3(2 \cos(p'_1 r) - 2) \tilde{\Delta}^{-1} \left( (0, p'_1, \vec{p}_{23}, m_5), 0, 1; (0, p'_1, \vec{p}_{23}, m_5), 0, 1 \right) \right]
 \end{aligned} \tag{4.51}$$



where we have used the fact that  $t$  must always be smaller than  $T$  in a finite extent, thus as  $t \rightarrow \infty$ ,  $T \rightarrow \infty$  as well.

The details of the whole derivation are given in Appendix D.2

## 4.3 Implementation details

### 4.3.1 Solutions to the saddle-point equations

As the saddle point equations are a set of non-linear coupled equations, the solutions to them were found numerically using a multi-dimensional version of the secant method, called the Broyden's Method [78]. As this is a method that depends highly on the initial guesses of the solution, we ran the method 5000-10000 times for each set of parameter values to make sure that we were getting a correct solution. Sometimes we faced more than one solution to our equations and thus we had to choose the true minimum of the system. To do this we estimated the first-order corrections to the free energy to choose the stable solution. The free energy was also used in the case where only one solution was present to check that it was indeed the minimum. This procedure was followed in [68]. However, in our case we have a large number of coupled non-linear equations and visualizing the free energy is hard. What we did was to investigate how it was affected when one of the fields was changed when the rest were kept fixed at the values of the minimum and repeat the process for all fields. Our strong evidence that actually the values of the mean fields obtained are true minima was found by indirect searches from measurements of the observables: when unstable points are used, the observables do not have a consistent well-defined behaviour and this was observed in two different cases.

### 4.3.2 Boundary Conditions

As in every finite system, one has to impose some boundary conditions on the system. We choose to have periodic boundary conditions along the usual four dimensions. For the fifth direction which has a limited finite extent,  $N_5$ , we implement the system using two different kinds of boundary conditions. First,

we use Neumann Boundary Conditions, that we call NBC. By this, we mean that we mirror all the fields from  $n_5 = 0$  to  $n_5 = N_5 - 1$  to the negative  $n_5$  side and we identify the fields  $v(-N_5 + 1) = v(N_5 - 1)$  and this is repeated periodically. The schematic illustration of these boundary conditions is given in Figure 4.3. This way of setting the boundary conditions seems more natural if one wants to identify the system to the RS model as the latter is embedded in an orbifold.

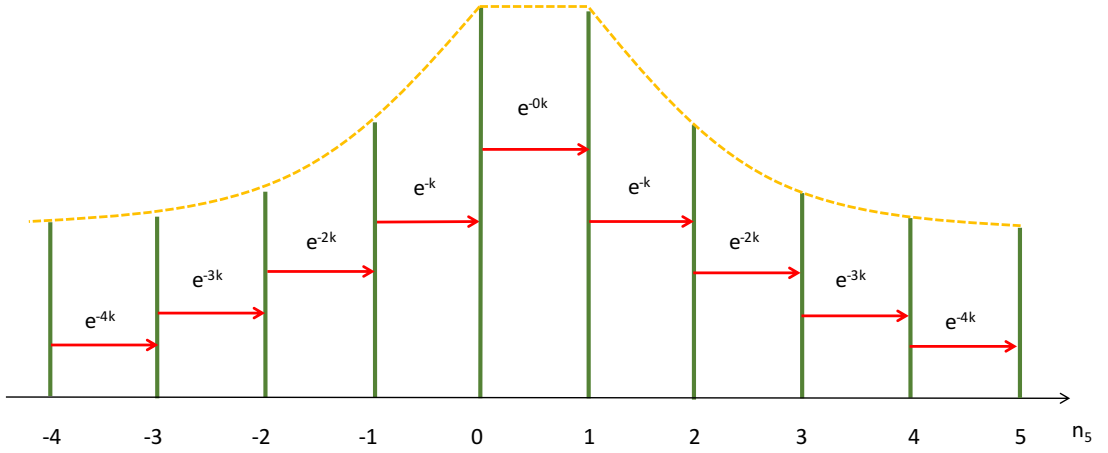


Figure 4.3: A schematic illustration of the Neumann Boundary Conditions along the extra dimension for a system with  $N_5 = 5$ . The green lines represent four-dimensional layers embedded in the extra dimension. The extra-dimensional links (red arrows) are multiplied by the warp factor ( $e^{-k|n_5|}$ ) and thus the exponential profile ( $AdS_5$ -space) along the extra dimension is created which is shown by the yellow dashed line. The system in the positive  $n_5$ -direction is mirrored in the negative direction and then the whole system is repeated periodically.

Another way of imposing boundary conditions in the extra direction is to have some sort of Dirichlet Boundary Conditions, i.e. fixed boundary conditions that we call DBC. We set the links to a constant value at the boundaries and we choose this to be 1. We expect the layers at the boundaries to lose their physical validity, however the physics in the middle should be independent of the chosen boundary conditions.

Neither choice of the boundary conditions suggests that we explicitly break the symmetry of the  $SU(2)$  group, which was the case in previous studies for the

orbifold case [23]. In [19] it was shown that one can have an orbifold projection  $\Gamma = \mathcal{T}_g \mathcal{R}$  which satisfies

$$\Gamma U_M(n, n_5) = U_M(n, n_5) \quad (4.52)$$

with the reflection property on the extra-dimensional link variables given by

$$\mathcal{R}U_5(n, n_5) = U_5^\dagger(n, -n_5 - 1) \quad (4.53)$$

and the transformation property under group conjugation by

$$\mathcal{T}_g U_M(n, n_5) = g U_M(n, n_5) g^{-1} \quad (4.54)$$

By explicitly setting  $g = -i\sigma^3$  the gauge symmetry can be broken to a U(1) symmetry at the boundaries.

## 4.4 The phase diagram

By finding the solutions to the saddle-point equations, a phase diagram of the system could be obtained. As the parameter space of our system consists of four parameters  $\beta, \gamma, k, N_5$ , we decided to keep  $k$  fixed and get the  $(\beta, \gamma)$  phase diagram for each layer. In Fig. 4.4, we present the phase diagram for fixed  $k = 0.10$  for 8 layers.

The phase diagram was obtained by finding the solutions to saddle point equations given in Eq. (4.17) for different values of  $(\beta, \gamma)$ . The ‘‘critical’’ points were determined by observing where there was a change in the behaviour of the solutions. The phases were characterized as following:

- $v_4(n_5) = 0, v_5(n_5) = 0$  Strong-coupling phase (S)
- $v_4(n_5) \neq 0, v_5(n_5) \neq 0$  Deconfining phase (D)
- $v_4(n_5) \neq 0, v_5(n_5) = 0$  Layered phase (L)

As we have already mentioned above, the free energy at first order was used to check the stability of the critical points and, as far as we could check, we believe that those presented in this phase diagram are stable.

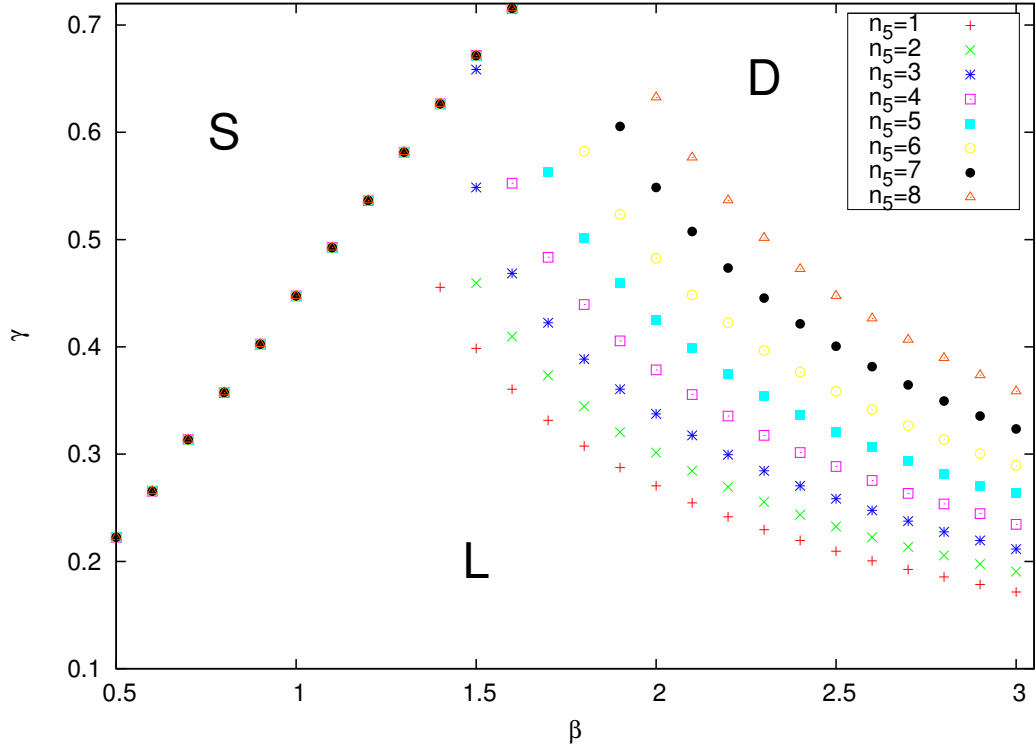


Figure 4.4: The phase diagram obtained for each layer for fixed  $k = 0.10$  using Neumann boundary conditions (NBC). We observe three phases, the confining(S), the deconfining(D) and the layered(L). However, there is a new phase that appears, the mixed phase, in which some of the layers are in the layered phase and some are in the deconfining phase. The width of the mixed phase increases with increasing  $k$ .

It is clear that in our phase diagram the three phases described above are present for all layers. Even though the transition to the confining phase seems to happen at the same point for all layers, we observe that each layer goes from a weak-coupling phase to the layered phase at different values of  $(\beta, \gamma)$ . Therefore, we observe an extra phase, a mixed phase, where some layers are in the weak-coupling phase and some in the layered one, and this can be seen in Fig. 4.4 as the phase between the orange and the red points. The last layer,  $n_5 = 8$ , is the first one to decouple and the first layer,  $n_5 = 1$ , the last one.

In the flat case, there were also three different phases in the phase diagram which were characterized as confining, five-dimensional Coulombic and layered. In order to determine if the same phases with same characteristics are those that

appear in the phase diagram of Fig. 4.4, further investigation is required for each phase.

As a final remark, it is annotated that even though we chose to keep the value of  $k$  constant for all our results, we performed a few tests to see the effect of  $k$  on the phase diagram. We noticed, as expected, that the width of this mixed phase depends highly on the value of  $k$ : the larger the curvature, the wider the mixed phase.

## 4.5 Various checks of our formalism

### 4.5.1 Boundary Conditions

The first check is done on the observables of the static potential and the scalar mass on each layer given by Eq. (4.51) and Eq. (4.32) respectively, for the two different choices of the boundary conditions described in Section 4.3.2. We choose three different points of the parameter space.

First we chose two points close to the phase transition, that is the transition from the region where all layers are in the weak-coupling phase and the region where one layer enters the layered phase. We first investigated the point  $\beta = 2.30$ ,  $\gamma = 0.505$ ,  $k = 0.10$  for  $N_5 = 8$  which means 8 layers using DBC and 14 layers in NBC, that actually means that we get 8 unique layers in this case. The way our system is implemented matches the layers  $n_5 = 0$  with  $n_5 = 1$ ,  $n_5 = -1$  with  $n_5 = 2$  and so on. We plotted the scalar mass and the static potential on each layer to see the effect of the boundary conditions as shown in Fig. 4.5 and Fig. 4.6 respectively. It is clear that the observables have the same behaviour for the middle layers, that is the layers at  $n_5 = 3, 4, 5, 6$ , whereas the behaviour is different close to the boundaries, as expected. The scalar mass was obtained by fitting a horizontal line to a plateau obtained when plotting Eq. (4.32) for different values of  $t$ . The error is the one extracted from the fit.

The next point close to the transition was chosen to be  $\beta = 2.30$ ,  $\gamma = 0.50$ ,  $k = 0.10$  with  $N_5 = 7$  unique layers (i.e. 12 layers using NBC). The measurements of the scalar mass and the static potential at this point suggest that the agreement

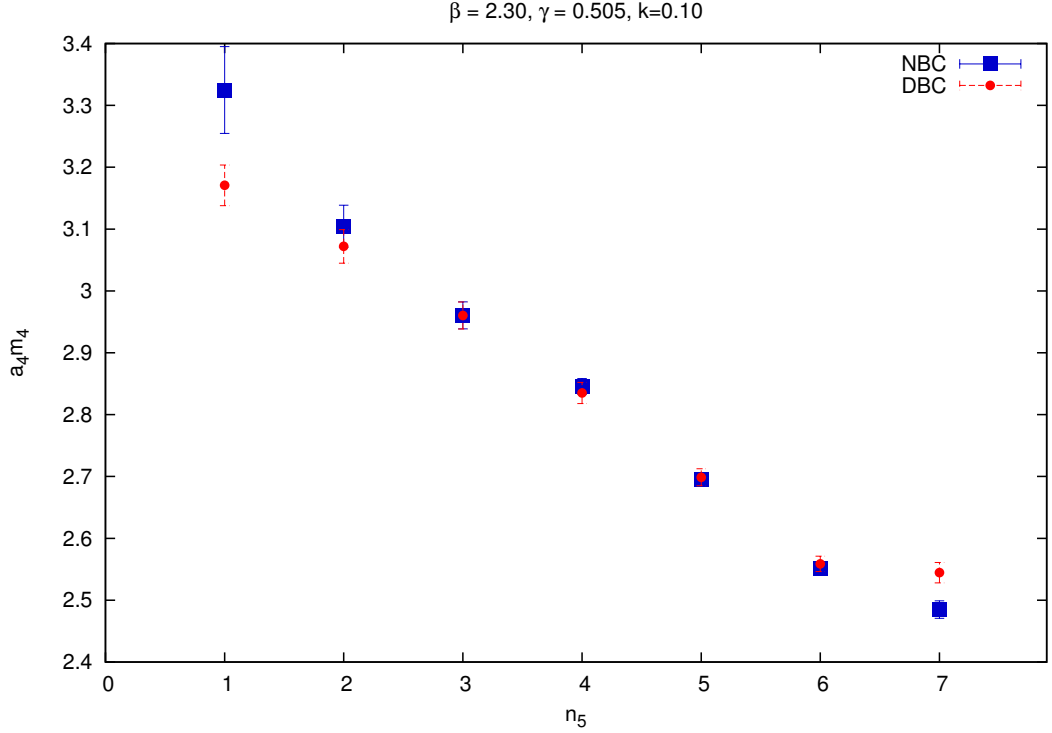


Figure 4.5: The lattice scalar mass on four-dimensional layers as measured using 8 layers with DBC and NBC. It is clear that there is good agreement between the values for the middle layers, i.e. layers  $n_5 = 3, 4, 5, 6$ .

holds when we discard two layers from the beginning and two from the end. This is similar to the previous case. Unfortunately, we could not go to more layers to do the matching using the NBC as our numerical recipe did not converge to a solution.

Finally, we need to ensure that the same applies when we go to a point deep in the deconfining phase. We chose the point  $\beta = 2.50, \gamma = 1.00, k = 0.10$  for  $N_5 = 8$  to repeat the process and the scalar mass comparison is shown in Fig. 4.7. For this point, the results suggest that the matching holds for the layers at  $n_5 = 2, 3, 4, 5$ , i.e. the bulk is not affected from the boundary conditions which is the conclusion obtained from the points discussed previously.

Neumann Boundary conditions (NBC) will be assumed to be used in the rest of this Chapter unless otherwise stated. Also  $N_5$  will denote the number of the unique layers only.

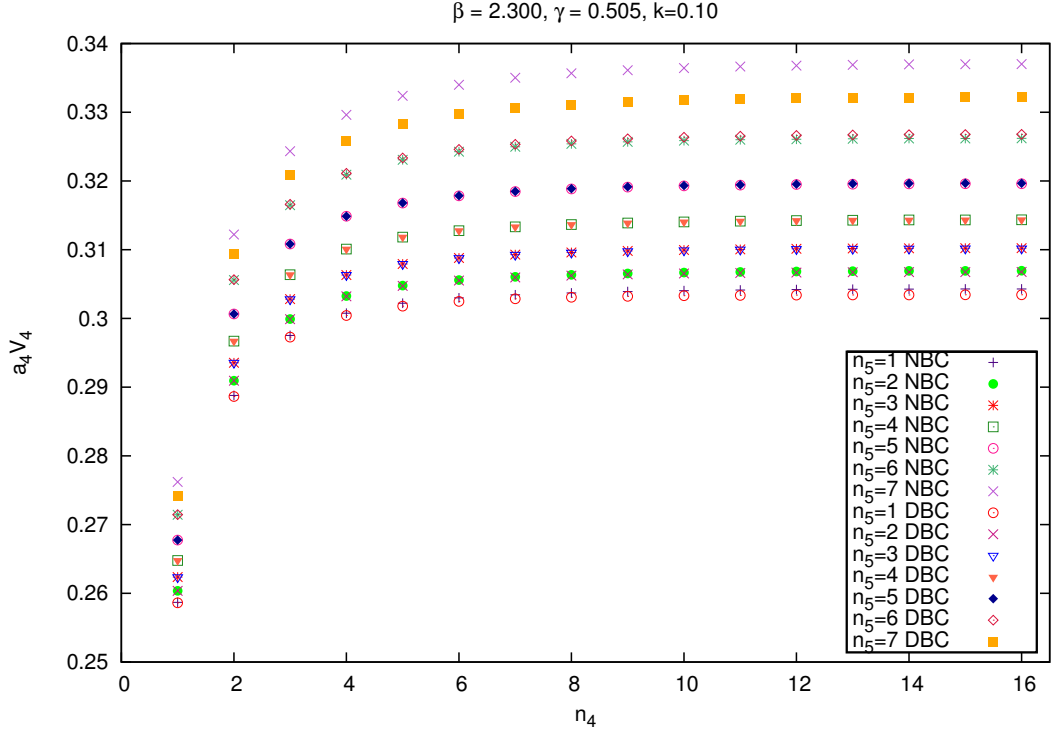


Figure 4.6: The static quark potential on four-dimensional layers as measured using 8 layers with DBC and NBC. It is clear that there is good agreement between the values for the middle layers, i.e. layers  $n_5 = 3, 4, 5, 6$ .

### 4.5.2 Gauge dependence on observables

Next, we checked the gauge fixing effect on the observables. For the Faddeev-Popov gauge fixing that we have used in our calculations, we chose three different values of the  $\xi$  gauge fixing parameter,  $\xi = 1, 10, 100$ , keeping the rest of the bare parameters constant to  $\beta = 2.30, \gamma = 0.505, k = 0.10, N_5 = 8$ . We performed this on both the static potential and the scalar mass and it turns out that they are gauge independent as one can see from the results of the latter in Fig. 4.8. From now on we stick to the Feynman gauge,  $\xi = 1$  for all calculations.

It is important to notice here that even though our results seem to be independent of the choice of the gauge, the free energy is still highly dependent on  $\xi$ .

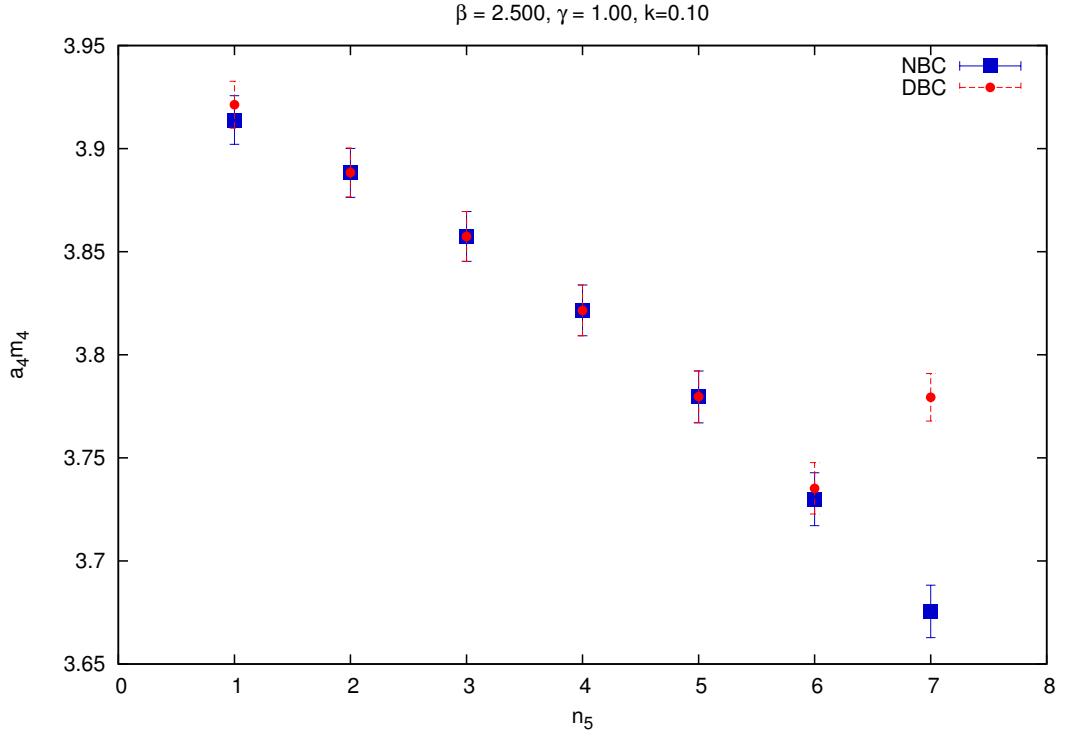


Figure 4.7: The lattice mass on four-dimensional layers for  $N_5 = 8$  as measured using DBC and NBC. It is clear that there is good agreement between the values of the middle layers, i.e. layers  $n_5 = 2, 3, 4, 5$ .

### 4.5.3 Four-dimensional volume dependence

The ultimate goal is to achieve measurements of our observables in their infinite-volume limit. However, as we deal with a finite lattice, we measured the observables for different four-dimensional volumes to see the effect of the volume on our measurements. This was performed on lattices of sizes  $T = L = 64, 100, 200$  and as one can see from Fig. 4.9, it seems that the scalar mass is unaffected by the lattice size so we can say that from the measurements we get its infinite-volume mass and for the rest of the measurements we stick to a lattice extent of  $T = L = 64$ . The static potential shows a similar behaviour, however as we can only match a certain amount of points for each volume, as shown in Fig. 4.10, we need to be careful when considering it to be independent of the four-dimensional volume. More on this issue will be discussed later in this Chapter.



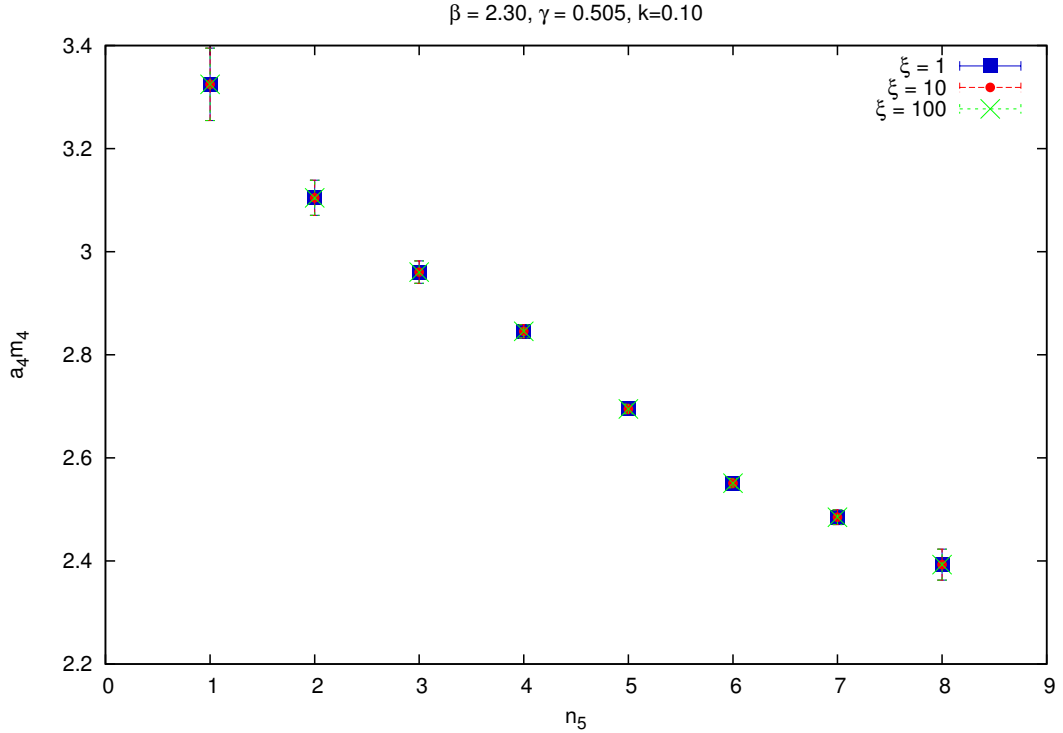


Figure 4.8: The lattice mass on four-dimensional layers for  $N_5 = 8$  as measured imposing different choices of the gauge parameter,  $\xi$ . It is clear that observables are independent of this choice.

## 4.6 Towards a physical interpretation

Having checked all the above, we focus on the physical interpretation of the phase diagram obtained. To do this we make use of the scalar mass and the static potential for each layer.

### 4.6.1 Scalar Mass

First, we chose a point close to the phase transition at which the last layer  $n_5 = 8$  goes from the deconfining to the layered phase. This point was chosen to be  $\beta = 2.30, \gamma = 0.505, k = 0.10$ . The lattice scalar mass with its error was estimated as described in the previous section. The values obtained are actually shown in Fig. 4.9. It seems that as we move towards larger values of  $n_5$  the lattice

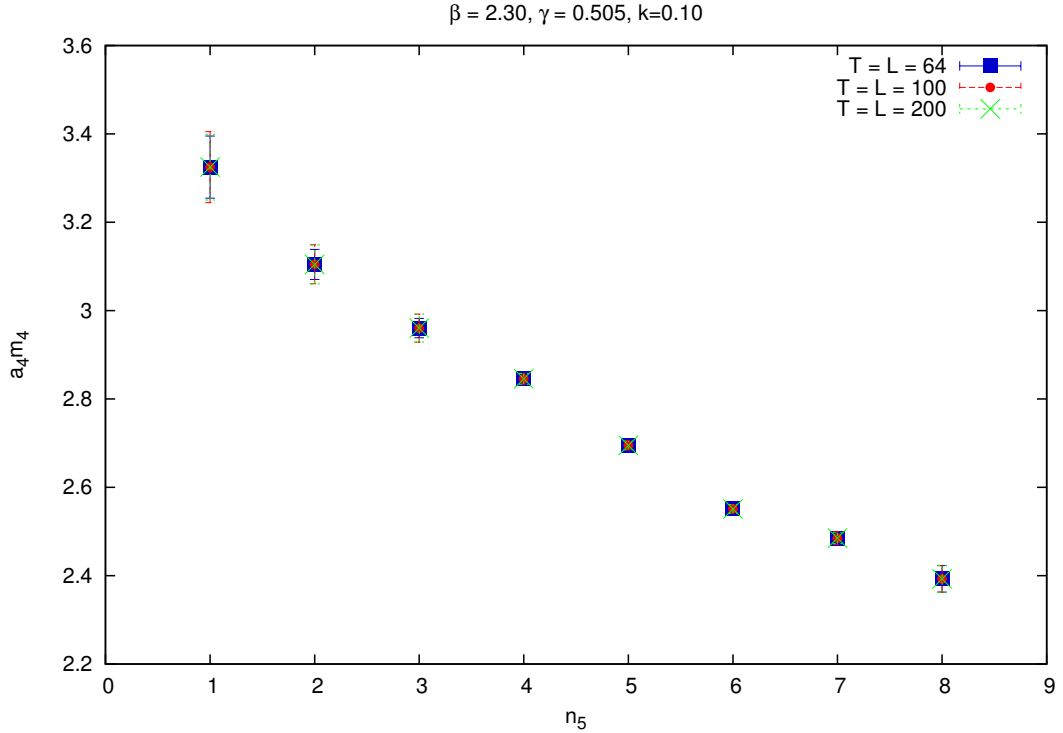


Figure 4.9: The lattice mass on four-dimensional layers for  $N_5 = 8$  as measured imposing different volumes along the ordinary four-dimensional space. The observables seem to be independent of the four-dimensional volume.

mass decreases. As this mass can be thought of as the inverse correlation length, the fact that the mass remains large, even for the last layer, suggests there is a first-order phase transition. However, this large mass might be a mean-field effect that arises due to our formalism and the other layers contribute to the value of the last layer that undergoes the phase transition. We cannot make a concrete conclusion on this and further studies should be done. It is noted here that we believe the point chosen is a stable point. Also, in the four-dimensional isotropic case the transition point that the Mean-Field approach predicts is located at  $\beta_c \simeq 2.235$  and thus we are beyond this point in our case.

The way to approach lines of constant physics is still unknown in the system investigated here, so we tried “trivial” cases, at least to make sure that the lattice mass is reduced as we approach the transition line. Indeed this is the general case, within error, as it can be seen from Table 4.1.

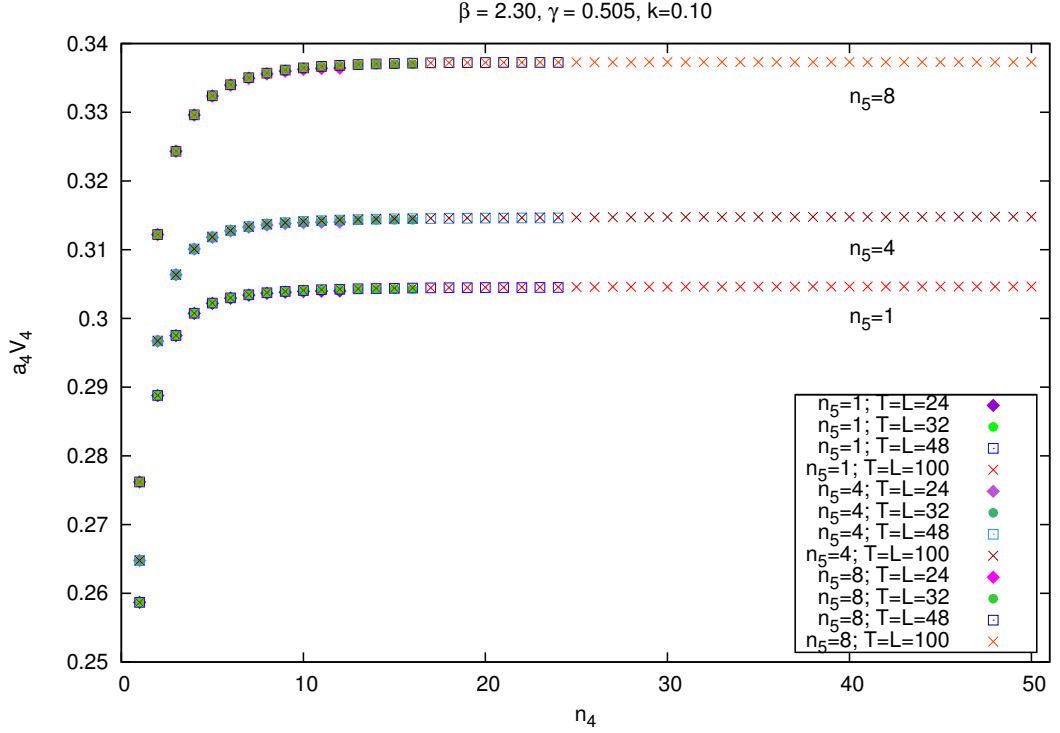


Figure 4.10: The static potential on four-dimensional layers for  $N_5 = 8$  as measured when imposing different lattice sizes in the ordinary four-dimensional space. The volumes  $T = L = 24, 32, 48$  and  $100$  were used and we show here the static potential for the layers at  $n_5 = 1, 4, 8$ , i.e. the first layer, the last one and one in the middle. It seems that it behaves the same independently of the four-dimensional volume.

Furthermore, in order to estimate this scalar mass in physical units we followed a procedure similar to the method defined in [79]. By taking the derivative of the potential, we can obtain the physical dimensionless force which is given by

$$\bar{r}^2 F(\bar{r}) = \bar{r}^2 \frac{V(r) - V(r - a_4)}{a_4}, \quad \bar{r} = r - \frac{a_4}{2}. \quad (4.55)$$

Then we fix the value obtained to  $r_0^2 F(r_0) = 0.025$ . This  $r_0$  is taken to be our physical length. As we do not have a physical system out of which we can get the value of  $r_0$  in any units of length, we keep calling it  $r_0$ , i.e. a fixed scale. What we did was to look at the plot of the force, extracted from the potential using Eq. (4.55) for each layer, and find the value of  $r/a$  at which  $r^2 F(r) = 0.025$ . This

$\beta$	$\gamma$	1	2	3	4	5	6	7	8
2.40	0.515	—	3.39(4)	3.27(4)	3.11(9)	2.92(6)	2.75(9)	2.62(5)	2.59(3)
2.40	0.510	3.48(4)	3.26(4)	3.21(8)	3.10(6)	2.89(4)	2.73(2)	2.59(3)	2.57(2)
2.40	0.505	3.35(8)	3.21(5)	3.19(8)	3.04(2)	2.85(8)	2.70(1)	2.57(2)	2.55(9)
2.35	0.515	3.34(5)	3.22(4)	3.29(6)	3.00(6)	2.82(6)	2.68(1)	2.55(4)	2.51(5)
2.35	0.510	3.36(9)	3.34(3)	3.22(7)	2.95(4)	2.80(7)	2.65(4)	2.51(3)	2.49(2)
2.35	0.505	3.33(8)	3.17(4)	3.026(4)	2.931(5)	2.77(4)	2.62(1)	2.51(3)	2.48(4)
2.30	0.515	3.30(4)	3.15(4)	3.08(7)	2.90(5)	2.74(7)	2.60(2)	2.49(3)	2.46(3)
2.30	0.510	3.29(5)	3.13(8)	2.98(4)	2.86(6)	2.72(2)	2.56(3)	2.48(4)	2.45(1)
2.30	0.505	3.32(6)	3.10(5)	2.96(9)	2.84(3)	2.69(3)	2.55(3)	2.47(4)	2.39(3)

Table 4.1: The lattice mass  $a_4 m_4$  as measured directly from the fit to a plateau. The missing masses are at points where the excited state masses were contributing and not an obvious plateau could be obtained. It seems that as we go towards smaller  $\beta$  and  $\gamma$  values, the mass is decreasing (within error) but not by a large amount.

gives a determination of the lattice spacing along the ordinary four dimensions in terms of a physical length,  $r_0$  for each layer as shown in Fig. 4.11. This is also a check that the warped model works non-perturbatively as this is the behaviour that was expected. As both the lattice scalar mass and the lattice spacing,  $a_4$ , decrease as we go to higher  $n_5$ , if there is a continuum limit that can be taken in the  $n_5$  direction, the scalar mass in physical units should remain constant. This is not the case though, as the physical mass increases as we go further into  $n_5$  as shown in Fig. 4.12. This behaviour of the physical mass was also observed for all the points given in Table 4.1. Unfortunately, we cannot really conclude any physical interpretation for the scalar mass as it stands.

## 4.6.2 Static Potential

In the previous section, we have used the static potential in order to find the dimensionless force and set a scale for our system. This procedure was independent of the form of the potential. As previous explorations using the Mean-Field approach showed that the order of the transition predicted by it might be wrong, even though the above results suggest a first-order phase transition, it is worth taking a closer look at the static potential to see if there is a change in the behaviour of it at different points of the phase diagram.

The confining phase is blind to the Mean-Field approach so we focus on the other two phases. In the flat case, as already mentioned, there was a phase close to

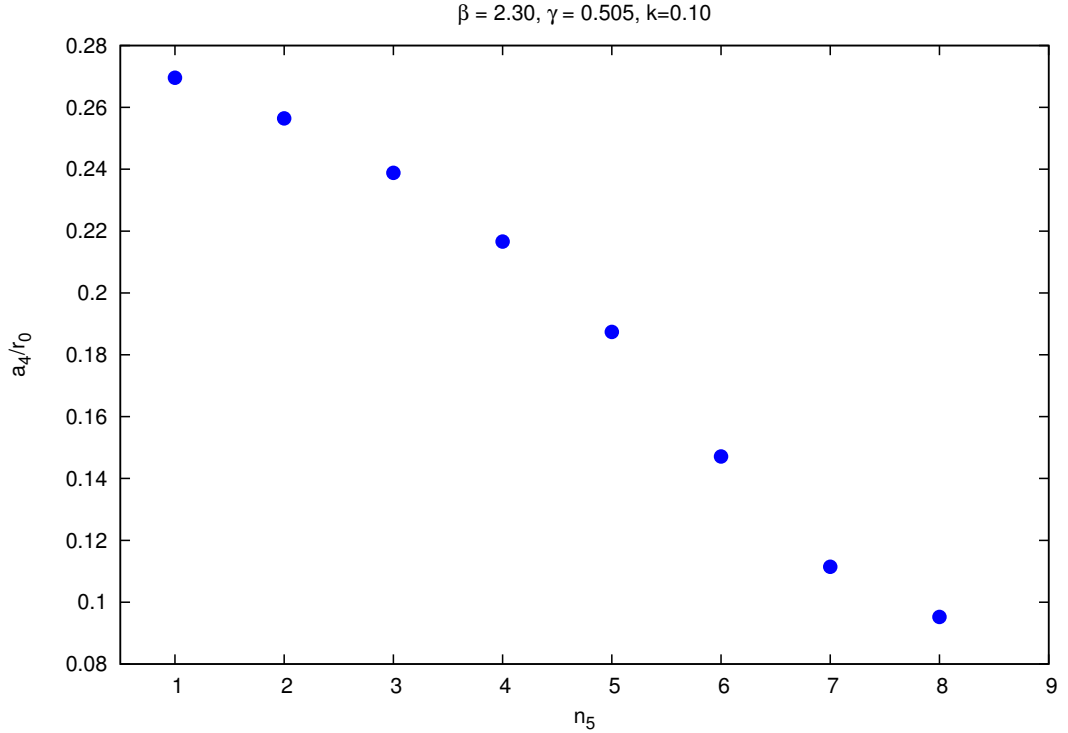


Figure 4.11: The lattice spacing along the four dimensions in physical units,  $r_0$ , on each four-dimensional layer for  $\beta = 2.30, \gamma = 0.505, k = 0.10, N_5 = 8$ .

the transition going from five-dimensional Coulombic to layered where the system seemed to be dimensionally reduced to a four-dimensional one. The indication for this was that the static potential measured fitted perfectly to a four-dimensional Coulombic one. In the warped case, the goal is to see if this behaviour still holds and if at least one of the layers behaves as a four-dimensional one.

Before proceeding to our results, we list in Table 4.2 the expected behaviour of the static potential in different phases. The derivation for the form of the Yukawa potential in five dimensions can be found in [21].

We first looked at the point  $\beta = 2.50, \gamma = 1.00, k = 0.10$  which, by looking at the phase diagram in Fig. 4.4, it is believed that it is deep into the pure deconfining phase. We measured and fitted the potential on each layer to four-dimensional and five-dimensional potentials and we looked at the degrees-of-freedom adjusted goodness of fit,  $R^2$ , for which values closer to 1 indicate a better fit (Appendix E.2). The lattice sizes used were  $T = L = 32$  and  $N_5 = 8$ .

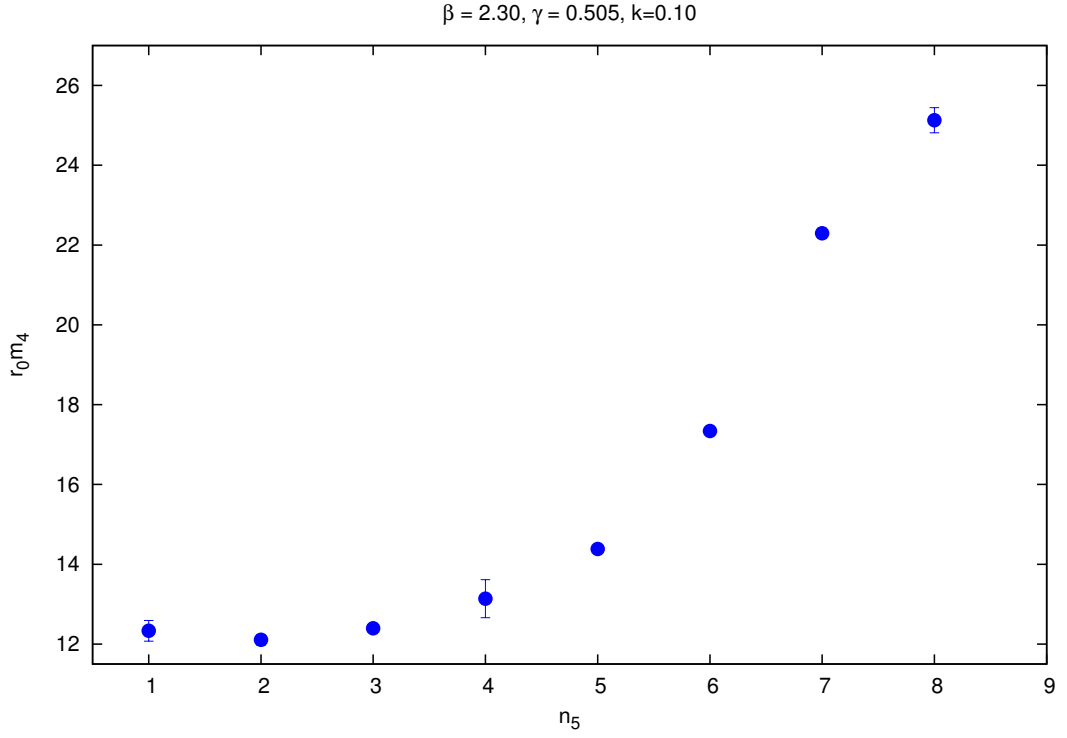


Figure 4.12: The scalar mass in physical units,  $r_0$ , on each four-dimensional layer for  $\beta = 2.30, \gamma = 0.505, k = 0.10, N_5 = 8$ . The errors were estimated using standard error analysis techniques.

Type of potential	Functional Behaviour	Phase
4D Coulombic	$a - \frac{b}{r}$	4D Coulombic
4D Yukawa	$a - \frac{be^{-m_Y r}}{r}$	4D Higgs-like
5D Coulombic	$a - \frac{b}{r^2}$	5D Coulombic
5D Yukawa	$a - \frac{bK_1(m_Y^{(5)} r)}{r}$	5D Higgs-like
Confining Potential	$a + br$	Strong-coupling

Table 4.2: The different functional behaviour of potentials in different phases.

For all layers a four-dimensional Coulombic potential can be excluded, but we could not really see a big difference between the other three forms of the potential. The adjusted  $R^2$  is most of the times a value very close to 1 for all three different fits. We cannot really distinguish in which phase the system lives so we cannot really conclude if it is in a five-dimensional phase or in a four-dimensional phase where a Yukawa mass is observed, i.e. a four-dimensional Higgs-like phase. In Fig. 4.13, the measured potential on the first layer with the four different fits can be seen. A similar behaviour is observed for all the other layers and a choice of them is shown in Appendix E in Fig. E.1-E.4.

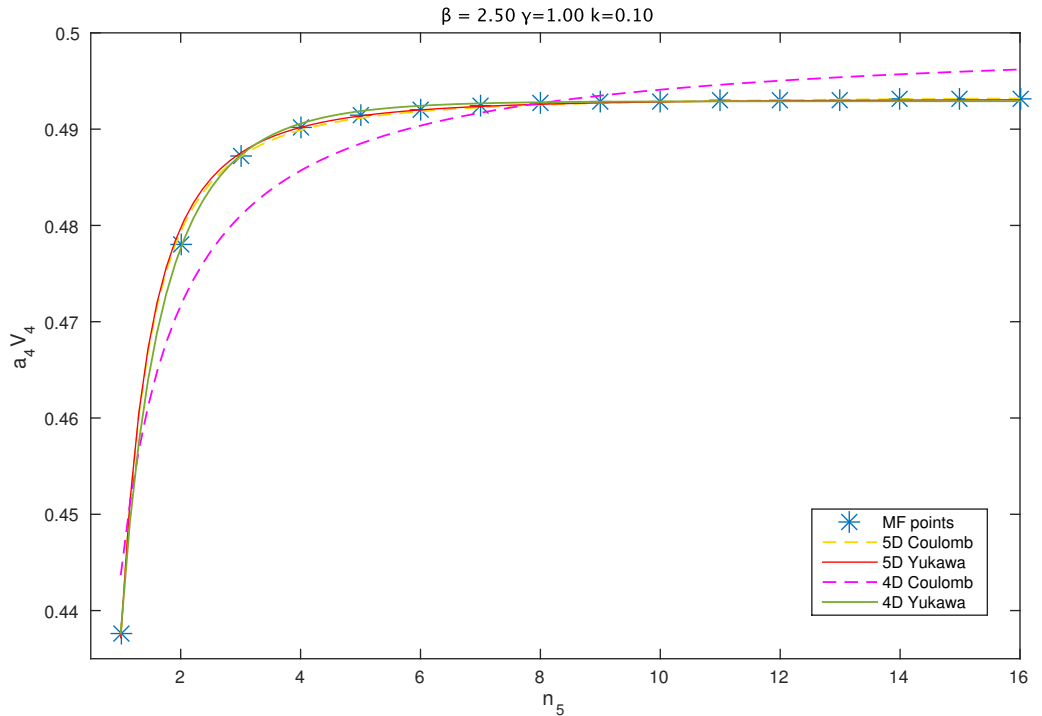


Figure 4.13: Fits to the mean-field points of the static potential for  $\beta = 2.50$ ,  $\gamma = 1.00$ ,  $k = 0.10$ ,  $N_5 = 8$  using different five-dimensional and four-dimensional forms of the potential.

It is worth mentioning that we have checked the behaviour of the potential for the same values of  $\beta$  and  $\gamma$  in the flat case and it is in a very good agreement with a five-dimensional Coulombic potential.

Furthermore, we looked at the potential at a point close to the transition line. This point was chosen to be  $\beta = 2.30$ ,  $\gamma = 0.505$ ,  $k = 0.10$  with an initial lattice

size of  $T = L = 32, N_5 = 8$ . It looks like the potential behaves as a four-dimensional Yukawa one for all layers. Also, it can be noticed that starting from the first layer,  $n_5 = 1$  the five-dimensional Yukawa and Coulombic potentials could also be fitted quite well. Going to larger values of  $n_5$  the fits to the two aforementioned forms loose their goodness so, at least for the last layers, we tend to believe that the potential behaves as a four-dimensional Yukawa one. The MF calculated points with the four different potential-form fits are shown in Figures 4.14 and 4.15 for the first and last layer respectively. The fitting parameters for all layers can be found in Table E.1.

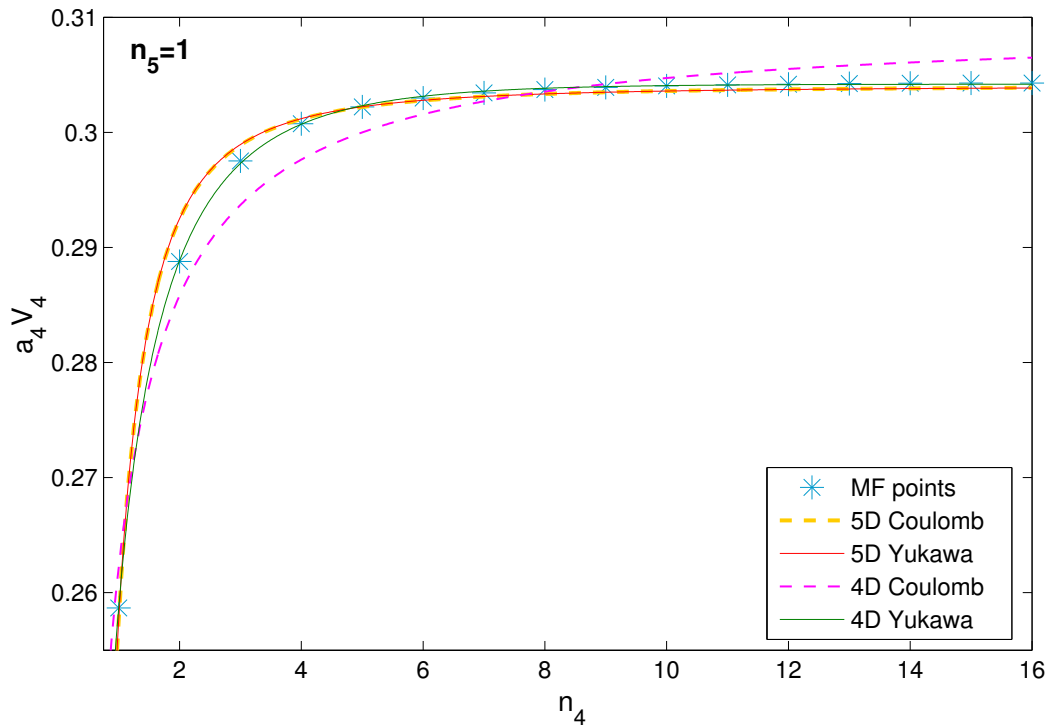


Figure 4.14: Fits to the mean-field points of the static potential of the first layer  $n_5 = 1$  using various potential forms for a lattice size of  $T = L = 32, N_5 = 8$  and for  $\beta = 2.30, \gamma = 0.505, k = 0.10$ .

All the above provide preliminary evidence that, as a Yukawa mass can be obtained, the system close to the transition line is in a four-dimensional Higgs-like phase and not in a Coulombic phase. We also observed that the extracted mass for this point decreases for larger  $n_5$ . Although this mass could, in principle, be found by taking derivatives of the force, as done in [23], limitation of time restricted us



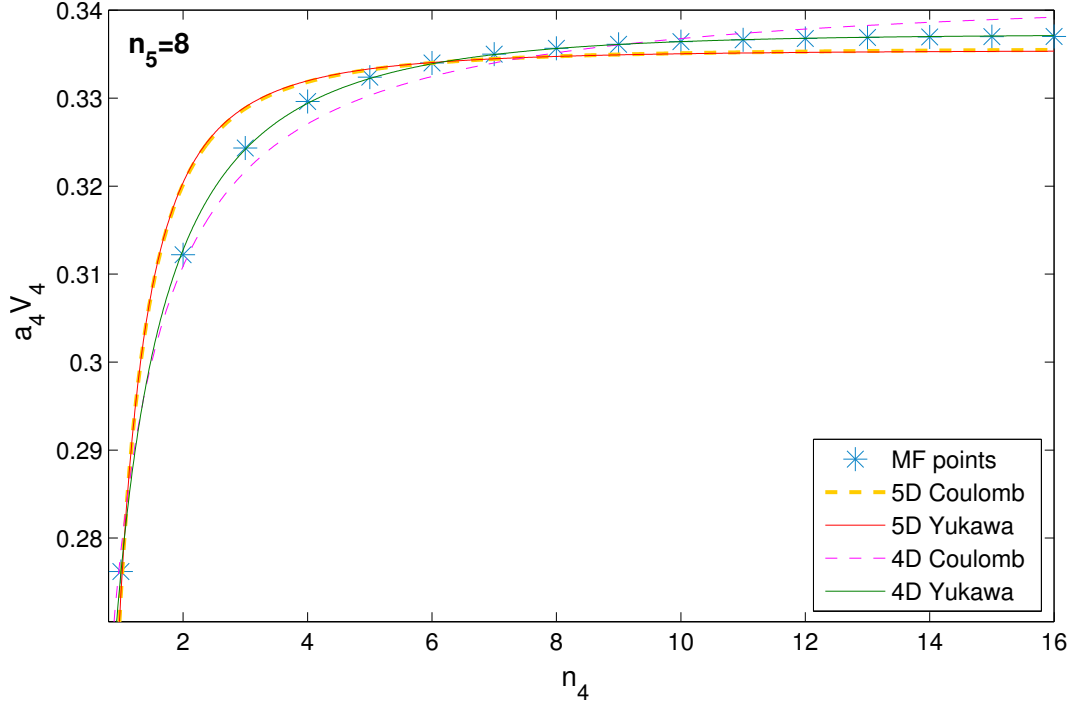


Figure 4.15: Fits to the mean-field points of the static potential of the last layer  $n_5 = 8$  using various potential forms for a lattice size of  $T = L = 32$ ,  $N_5 = 8$  and for  $\beta = 2.30$ ,  $\gamma = 0.505$ ,  $k = 0.10$ .

to small volumes which did not allow us to get a good value out of it and thus the mass was only recorded as the relevant fitting parameter of the four-dimensional Yukawa potential. The same conclusions on the behaviour of the potential were observed for other lattice sizes as well ( $T = L = 24, 48, 100$ ,  $N_5 = 8$ ). All fitting parameters for all layers for  $T = L = 32$  and  $T = L = 100$  are given in Table E.1 and Table E.2 respectively. As a remark we state that we fitted the MF points to the four-dimensional Yukawa potential excluding the first and second points and the Yukawa mass agreed within error with the value extracted when all points were included in the fit.

To ensure that the Yukawa mass is not the result of the finite extent of our system and it will remain non-zero in the infinite-volume limit, we performed finite-size scaling on the Yukawa mass by fitting it to

$$m_Y(L) = m_Y^{(\text{inf})} + \frac{c}{L}. \quad (4.56)$$

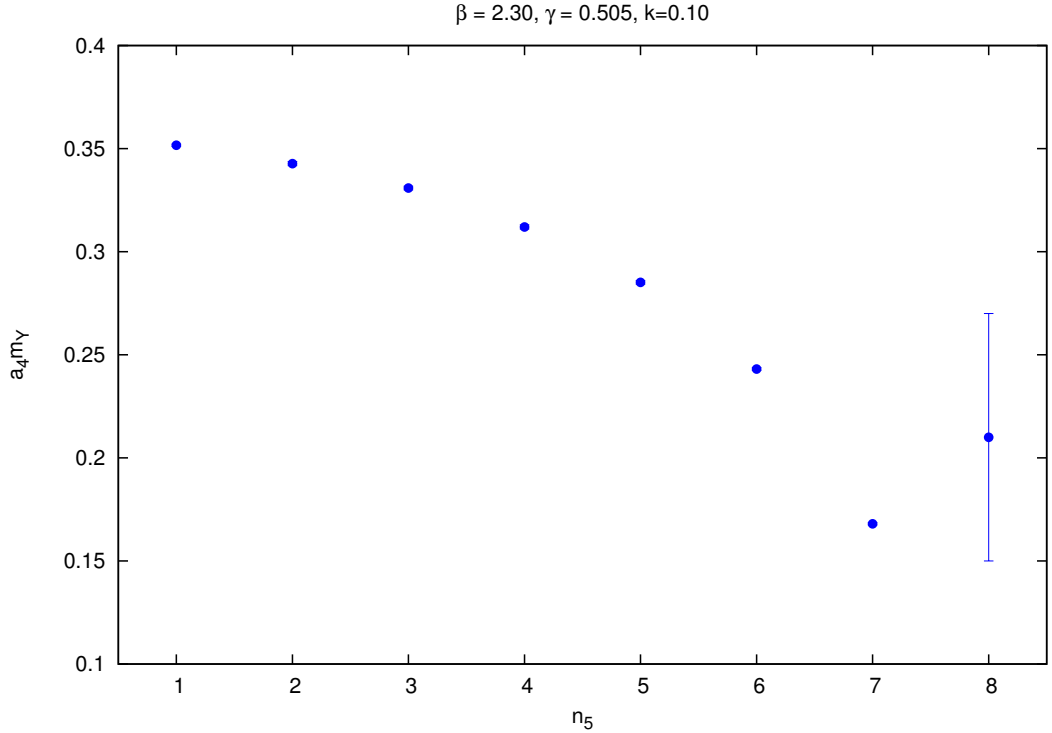


Figure 4.16: The infinite-volume Yukawa mass in lattice spacing units on each four-dimensional layer for  $\beta = 2.30$ ,  $\gamma = 0.505$ ,  $k = 0.10$ ,  $N_5 = 8$ . First a mass was extracted from the fits of the measured potential to a four-dimensional Yukawa potential form for sizes  $T = L = 24, 32, 48, 100$  and then finite-size scaling analysis was performed to get the infinite-volume mass. All error bars are tiny except for the last layer.

Indeed we could get a finite value for the infinite-volume Yukawa mass,  $m_Y^{(\text{inf})}$  on each layer as shown in Fig. 4.16. This suggests that the suspicion that we had from the fits that the system is in a Higgs-like phase and not in a Coulombic phase is valid and not just a finite-size effect. The value of the Yukawa mass on the last layer seemed to remain roughly constant for all volumes and hence there is a large error bar when trying to do finite-size scaling to it. This might be due to the boundary conditions and therefore we do not reach any conclusions considering the last layer. As a further check, we set the curvature to zero and we measured the potential at a point close to the phase transition ( $\beta = 2.30$ ,  $\gamma = 0.2298$ ) for lattice sizes of  $T = L = 32, 48, 100, 200$ . Then by extracting the mass and doing a finite-size scaling as above, we got the infinite-volume Yukawa mass to be a very small number that can be considered to be zero which is what was expected in

the flat case.

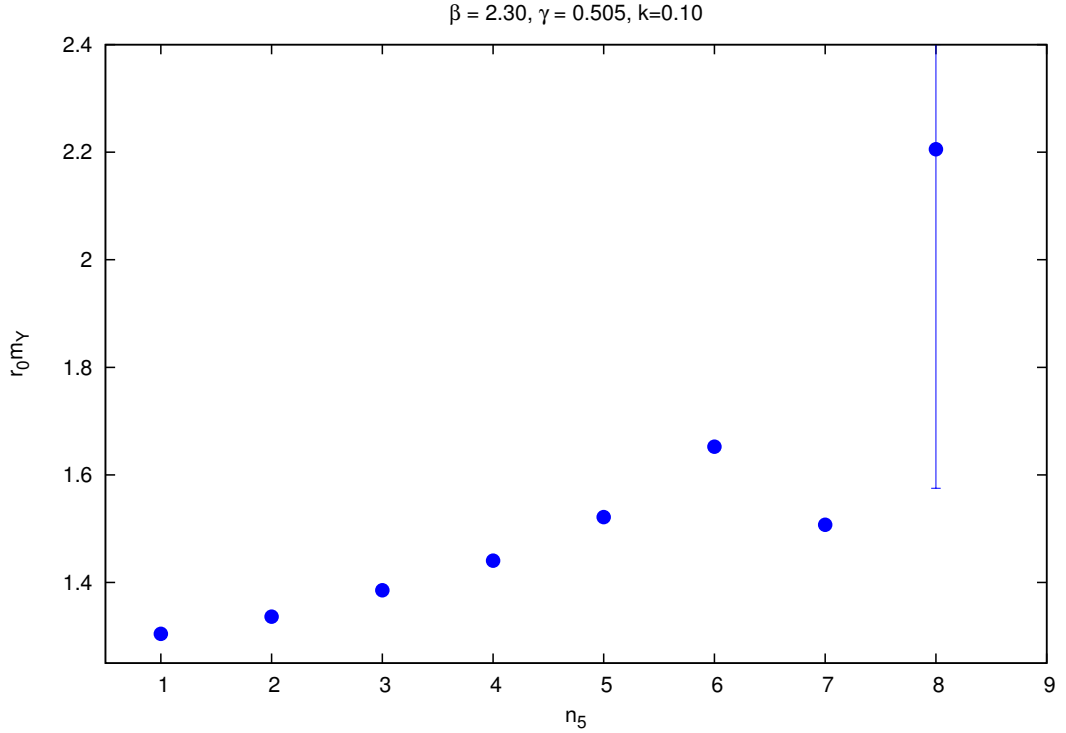


Figure 4.17: The infinite-volume Yukawa mass in physical units,  $r_0$ , on each four-dimensional layer for  $\beta = 2.30, \gamma = 0.505, k = 0.10, N_5 = 8$ .

In lattice units the Yukawa mass seems to decrease with  $n_5$  as can be seen from Fig. 4.16. To see its behaviour in physical units, we employ the unit of length  $r_0$  defined in the previous section as shown in Fig. 4.17. It seems that for the first four layers it increases, very slowly though, but then it decreases for  $n_5 = 7$ . This might be just an artefact and it has no physical meaning, or it might be the case that actually for larger  $n_5$  the physical Yukawa mass will either decrease or go to zero. Studies with more layers should be done in order to clarify the situation.

In addition, the ratio of the infinite-volume Yukawa mass over the scalar mass for each layer was taken as it can be seen in Fig. 4.18. It seems that the first four layers might have a constant value, but then the ratio drops, suggesting that it might go to zero for large  $n_5$ .

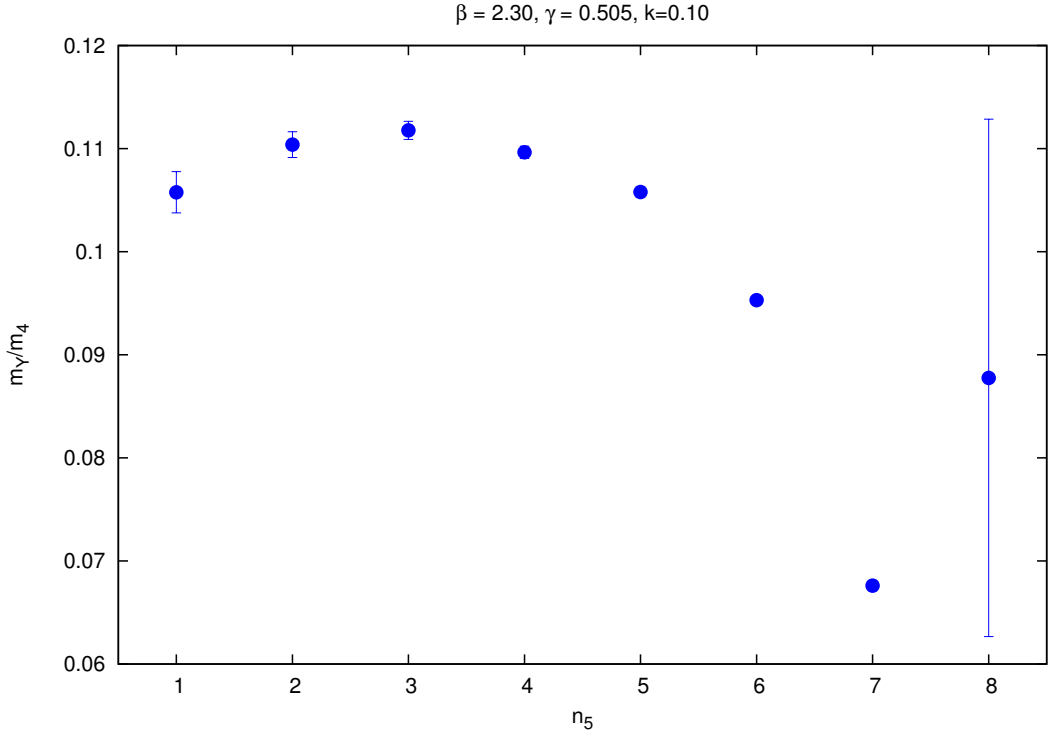


Figure 4.18: The infinite-volume Yukawa mass in physical units,  $r_0$ , on each four-dimensional layer for  $\beta = 2.30, \gamma = 0.505, k = 0.10, N_5 = 8$ .

## 4.7 Discussion and Outlook

As already mentioned in the previous section, the existence of a Yukawa mass suggests the presence of a four-dimensional Higgs-like phase close to the line of transition in the phase diagram. This phase suggests that some symmetry breaking may be happening. In our case (with NBC) we have not explicitly broken the gauge symmetry by our boundary conditions, as done in previous investigations where a Higgs-like phase is the result of imposing certain boundary conditions [23, 24]. To ensure the validity of the argument that the boundary conditions do not affect the gauge symmetry of the model (which we checked for DBC), further studies should be done with different choices of boundary conditions, with and without explicit breaking of the symmetry to compare the two cases. The only modification that we have done here from the flat case, where we do not observe a Yukawa potential, is the introduction of the curvature.

In this case, we expect that the warping breaks the symmetry everywhere in the “deconfining phase” on our phase diagram, therefore a Higgs-like phase should be present there. This was not clear from the form of the potential away from the transition line but was not excluded either. So further studies are necessary in order to clarify the nature of the phase in the weak-coupling regime. A possibility is to study the behaviour of the Yukawa mass for different volumes and see if a value in the infinite-volume limit can be extracted or not.

It is noteworthy that along the extra dimension we have a small extent of lattice points which restricts the region of the “mixed” phase to a small width. One though, could think of the pure deconfining phase as a finite-size effect of the fifth direction. This would suggest that the system is actually in a four-dimensional Higgs-like phase everywhere in the weak-coupling regime and the pure deconfining phase is just a result of truncating the extra dimension. This also relates to the observation that the mixed phase grows with curvature,  $k$ .

Going back to the question that motivated this project, i.e. if we can see a dimensionally reduced phase close to the “layered” phase, we can claim that the existence of a Yukawa mass close to this transition suggests the presence of a four-dimensional Higgs-like phase. Of course, if there is a five-dimensional Higgs-like phase away from the transition line, then we see dimensional reduction. If not, then the system, by its formalism, due to the warping behaves as a four-dimensional one everywhere outside the strong-coupling phase.

The fact that the Yukawa mass decreases as we go to larger  $n_5$  leaves open the possibility that it can go to zero for very large  $n_5$ . This would mean that the system for large  $n_5$  will have a four-dimensional Coulombic behaviour as in the flat case, which is expected from our formalism. Looking though, at the behaviour of the Yukawa mass in physical units using both  $r_0$  and  $1/m_4$  as the length scales, it seems that the first four layers might be considered to have a constant value of  $m_Y$  but, beyond the fourth layer, the data is messier and no definite conclusions can be reached. Further explorations with more layers should be performed in order to be able to say something concrete about it.

Another big question is whether this Higgs-like phase is physical, a lattice artefact or a fake result of the Mean-Field approximation. Limitation of time for this project did not allow additional studies but there are many possibilities to explore

this model further. Doubts about the physical existence of this phase arise as a consequence of Elitzur's theorem [80], which excludes spontaneous breaking of local gauge symmetries. However, we have no evidence of spontaneous symmetry breaking but only of the existence of a Yukawa potential and it is not clear whether Elitzur's theorem applies to the warped geometry.

Also, nothing can be said for the layered phase at the moment. Studies using Monte Carlo simulations are expected to show the true behaviour of the system in this phase which might be four-dimensional Higgs-like or Coulombic. All in all, the unforeseen result of this study, that is the existence of a four-dimensional Higgs-like phase, opens up a wide range of different tests and explorations that can be done, especially with numerical simulations to clarify the picture.

## 4.8 Theoretical set-up for future work

The investigation of the warp model on the lattice is still at its beginning. From everything that was discussed above, it seems that there is a variety of different studies that can be done in the pure gauge model. However, we live in a world with fermions and a more realistic picture can be drawn when fermions are coupled to the gauge fields. In this section we give a preliminary construction of Wilson fermions on the lattice in a warped background.

### 4.8.1 Fermions in a warped background in the continuum

As we deal with a curved background, we need to find relations between the gamma matrices in the coordinate basis and in a non-coordinate one, but also the modified covariant derivative that includes the spin connection,  $\nabla_M$  that accounts for the curvature of the system. To do this, we use the mathematical framework given in Appendix F where vielbeins and spin connections are introduced.

In the RS models, presented in Section 1.3.3, we defined the warped metric as in Eq. (1.21). In this section we use  $f(y) \equiv e^{-2\sigma(y)}$ . The fermionic sector of the

action in warped models can be expressed as

$$S_F = \int d^4x dy \sqrt{-g} \bar{\Psi} (i\Gamma^M \nabla_M - m) \Psi \quad (4.57)$$

where  $\Gamma^M$  are the gamma matrices in the coordinate basis.

We first notice that the gamma matrices can be expressed in a non-coordinate basis via

$$\Gamma^M = e^M_a \Gamma^a. \quad (4.58)$$

Then the action in Eq. (4.57) can also be written as

$$\begin{aligned} S_F &= \int d^4x dy \sqrt{-g} \bar{\Psi}(x, y) (i\Gamma^a e^M_a \nabla_M - m) \Psi(x, y) \\ &= \int d^4x dy \sqrt{-g} \bar{\Psi}(x, y) (i\Gamma^a e^\mu_a \nabla_\mu + i\Gamma^a e^5_a \nabla_5 - m) \Psi(x, y). \end{aligned} \quad (4.59)$$

Using Eq. (F.6), we can express the vielbeins as

$$e^M_a = g^{MN} \eta_{ab} e_M^b \quad \text{and} \quad e_M^a = g_{MN} \eta^{ab} e^N_b \quad (4.60)$$

which lead to the following

$$\begin{aligned} e^\mu_a &= \sqrt{f(y)} \delta_\mu^a & e^5_a &= \frac{1}{\sqrt{f(y)}} \delta_a^\mu \\ e_5^a &= \delta_5^a & e^5_a &= \delta_a^5 \end{aligned} \quad (4.61)$$

Using these, the gamma matrices in the coordinate space can be written in terms of the local gamma matrices as

$$\begin{aligned} \Gamma^\mu &= e^\mu_a \Gamma^a = \frac{1}{\sqrt{f(y)}} \delta_a^\mu \Gamma^a = \frac{1}{\sqrt{f(y)}} \gamma^\mu \\ \Gamma^5 &= e^5_a \Gamma^a = \delta_a^5 \Gamma^a = \gamma^5 \end{aligned} \quad (4.62)$$

where  $\gamma^\mu$  and  $\gamma^5$  are the usual local Dirac matrices satisfying the Clifford algebra, i.e.

$$\{\gamma^M, \gamma^N\} = 2\eta^{MN} \mathbb{1} \quad (4.63)$$

where we use the convention  $\eta^{MN} = \text{diag}(-1, 1, 1, 1, 1)$ .

Next, we derive the spin connection that contributes to the covariant derivative, the two different components of which are given by

$$\nabla_\mu = \partial_\mu + \frac{1}{2}\Omega_\mu^{ab}\sigma_{ab} \quad \nabla_5 = \partial_5 + \frac{1}{2}\Omega_5^{ab}\sigma_{ab} \quad (4.64)$$

where  $\sigma_{ab}$  are the generators of the Lorentz transformations in the spinor representation given by  $\sigma_{ab} = \frac{1}{4}[\gamma_a, \gamma_b]$ . After they are evaluated (Appendix F.2) we find

$$\begin{aligned} \Omega_\mu &= \frac{1}{4} \frac{f(y)'}{\sqrt{f(y)}} \gamma_\mu \gamma^5 \\ \Omega_5 &= 0. \end{aligned} \quad (4.65)$$

If we want to couple fermions to gauge fields, we must replace the partial derivatives,  $\partial_M$  with the standard covariant ones and in curved spacetime we get

$$D_M = \partial_M + igA_M + \Omega_M \quad (4.66)$$

so in the fermionic action (Eq. (4.59)) we replace  $\nabla_M$  with  $D_M$ .

## 4.8.2 Wilson fermions in a warped background

To construct this fermionic action on the lattice, we first need to go to Euclidean spacetime and use the Euclidean Dirac matrices as in the standard four-dimensional flat fermionic case. Vielbeins are unchanged under Wick rotation, hence the action reads as

$$S_E^{(f)} = \int d^4x dy \sqrt{g} \bar{\Psi}(x, y) \left( \Gamma^a e^\mu{}_a D_\mu + \Gamma^a e^5{}_a D_5 + m \right) \Psi(x, y). \quad (4.67)$$

Examining further the kernel we can express it as

$$D = f(y)^2 \left( \frac{\gamma^\mu}{\sqrt{f(y)}} \left( \partial_\mu + igA_\mu + \frac{1}{4} \frac{f(y)'}{\sqrt{f(y)}} \gamma_\mu \gamma^5 \right) + \gamma^5 (\partial_5 + igA_5) + m \right). \quad (4.68)$$

The discretized version of this action, when a Wilson term is included as described



in Section 2.2, can be expressed as

$$S_{\text{latt}}^{(f)} = \sum_{\substack{n, n_5 \\ m, m_5}} \Psi(n, n_5) \mathcal{M}_{n;m}(U) \Psi(m, m_5) \quad (4.69)$$

where

$$\begin{aligned} \mathcal{M}_{n;m}(U) = & -f(n_5)^2 \left[ \sum_{\mu} \frac{\gamma_{\mu}}{\sqrt{f(n_5)}} \frac{1}{2} \left( U_{\mu}(n, n_5) \delta_{n+\hat{\mu}, m} \delta_{n_5, m_5} - U_{\mu}^{\dagger}(n - \hat{\mu}, n_5) \delta_{n-\hat{\mu}, m} \delta_{n_5, m_5} \right) \right. \\ & - \frac{\gamma_5}{2} \left( U_5(n, n_5) \delta_{n, m} \delta_{n_5+1, m_5} - U_5^{\dagger}(n, n_5 - 1) \delta_{n, m} \delta_{n_5-1, m_5} \right) \\ & + \left( \frac{f(n_5)'}{f(n_5)} \gamma_5 + m \right) \delta_{n, m} \delta_{n_5, m_5} \\ & + \sum_{\mu} \frac{1}{\sqrt{f(n_5)}} \frac{1}{2} \left( U_{\mu}(n, n_5) \delta_{n+\hat{\mu}, m} \delta_{n_5, m_5} - 2\delta_{n, m} \delta_{n_5, m_5} \right. \\ & \quad \left. + U_{\mu}^{\dagger}(n - \hat{\mu}, n_5) \delta_{n-\hat{\mu}, m} \delta_{n_5, m_5} \right) \\ & \left. + \frac{1}{2} \left( U_5(n, n_5) \delta_{n, m} \delta_{n_5+1, m_5} - 2\delta_{n, m} \delta_{n_5, m_5} + U_5^{\dagger}(n, n_5 - 1) \delta_{n, m} \delta_{n_5-1, m_5} \right) \right]. \end{aligned} \quad (4.70)$$

The partition function of fermions coupled to gauge fields, and consequently to link variables on the lattice, can be expressed as Eq. (2.43) which can also be expressed as

$$\begin{aligned} Z &= \int \prod_l \mathcal{D}U_l \det(\mathcal{M}_{n;m}(U)) \\ &= \int \prod_l \mathcal{D}U_l e^{\text{Tr} \ln \mathcal{M}_{n;m}(U)}. \end{aligned} \quad (4.71)$$

In the full system the action is given by

$$S = S_W + S_{\text{latt}}^{(f)} = S_W - \text{Tr} \ln \mathcal{M}_{n;m}(U). \quad (4.72)$$

Inspired by the work of [62] where fermions were coupled to the flat anisotropic U(1) model and the investigation was carried out using the Mean-Field approach, we try to demonstrate how this method works in our case in connection with the formalism given in Section 4.1.

Firstly, we realise that the procedure to find the saddle points is exactly the same as before. The only modification is that we replace  $S_{AdS}[U_\mu, U_5]$  with

$$S' = S_{AdS}[U_\mu, U_5] - \text{Tr} \ln \mathcal{M}_{n;m}(U) \quad (4.73)$$

and the rest of Eq. (4.6) remains the same. The rescaling of the fields can be done exactly in the same way as before and the new saddle-point equations become

$$\begin{aligned} \bar{v}_4(n_5) &= u_4(\bar{h}_4(n_5), n_5)' = \frac{I_2(\bar{h}_4(n_5))}{I_1(\bar{h}_4(n_5))} \\ \bar{v}_5(n_5) &= u_5(\bar{h}_5(n_5), n_5)' = \frac{I_2(\sqrt{f(n_5)}\bar{h}_5(n_5))}{I_1(\sqrt{f(n_5)}\bar{h}_5(n_5))} \\ \bar{h}_4(n_5) &= 6\frac{\beta}{\gamma}\bar{v}_4^3(n_5) + \beta\gamma\bar{v}_5^2(n_5)\bar{v}_4(n_5 + a_5) + \beta\gamma\bar{v}_5^2(n_5 - a_5)\bar{v}_4(n_5 - a_5) + j_\mu(\bar{v}_4, \bar{v}_5) \\ \bar{h}_5(n_5) &= 8\beta\gamma\bar{v}_5(n_5)\bar{v}_4(n_5)\bar{v}_4(n_5 + a_5) + j_5(\bar{v}_4, \bar{v}_5) \end{aligned} \quad (4.74)$$

where  $j_\mu$  and  $j_5$  are the currents given by

$$j_\mu(\bar{v}_4, \bar{v}_5) = \left. \frac{\partial}{\partial v_\mu} \text{Tr} \ln \mathcal{M}_{n;m}(U) \right|_{\bar{v}} \quad (4.75)$$

$$j_5(\bar{v}_4, \bar{v}_5) = \left. \frac{\partial}{\partial v_5} \text{Tr} \ln \mathcal{M}_{n;m}(U) \right|_{\bar{v}} \quad (4.76)$$

To evaluate these, we need the modified Wilson-Dirac operator after the rescaling of the fields which is given by

$$\begin{aligned} \mathcal{M}_{n;m}(U) &= -f(n_5)^2 \left[ \sum_\mu \frac{\gamma_\mu}{\sqrt{f(n_5)}} \frac{1}{2} \left( U_\mu(n, n_5) \delta_{n+\hat{\mu}, m} \delta_{n_5, m_5} - U_\mu^\dagger(n - \hat{\mu}, n_5) \delta_{n-\hat{\mu}, m} \delta_{n_5, m_5} \right) \right. \\ &\quad - \frac{\gamma_5}{2} \left( \frac{U_5(n, n_5)}{\sqrt{f(n_5)}} \delta_{n, m} \delta_{n_5+1, m_5} - \frac{U_5^\dagger(n, n_5 - 1)}{\sqrt{f(n_5 - 1)}} \delta_{n, m} \delta_{n_5-1, m_5} \right) \\ &\quad + \left( \frac{f(n_5)'}{f(n_5)} \gamma_5 + m \right) \delta_{n, m} \delta_{n_5, m_5} \\ &\quad + \sum_\mu \frac{1}{\sqrt{f(n_5)}} \frac{1}{2} \left( U_\mu(n, n_5) \delta_{n+\hat{\mu}, m} \delta_{n_5, m_5} - 2\delta_{n, m} \delta_{n_5, m_5} \right. \\ &\quad \left. + U_\mu^\dagger(n - \hat{\mu}, n_5) \delta_{n-\hat{\mu}, m} \delta_{n_5, m_5} \right) \end{aligned}$$

$$+ \frac{1}{2} \left( \frac{U_5(n, n_5)}{\sqrt{f(n_5)}} \delta_{n,m} \delta_{n_5+1, m_5} - 2\delta_{n,m} \delta_{n_5, m_5} + \frac{U_5^\dagger(n, n_5 - 1)}{\sqrt{f(n_5 - 1)}} \delta_{n,m} \delta_{n_5-1, m_5} \right) \Big]. \quad (4.77)$$

Let us first look at  $j_\mu$ . We need to find the derivative of  $\mathcal{M}$  with respect to  $v_\mu$ . This can be found to be

$$\begin{aligned} \frac{\partial \mathcal{M}_{n, n_5; m, m_5}}{\partial v_\mu(n', n'_5)} &= \frac{1}{2} f(n_5)^{3/2} (1 - \gamma_\mu) \delta_{n', n} \delta_{n+\hat{\mu}, m} \delta_{n'_5, n_5} \delta_{n_5, m_5} \\ &+ \frac{1}{2} f(n_5)^{3/2} (1 + \gamma_\mu) \delta_{n', n-\hat{\mu}} \delta_{n-\hat{\mu}, m} \delta_{n'_5, n_5} \delta_{n_5, m_5}. \end{aligned} \quad (4.78)$$

Then using Eq. (4.75) we get

$$\begin{aligned} j_\mu(\bar{v}_4(n_5), \bar{v}_5(n_5)) &= \text{Tr} \left[ \frac{1}{2} f(n_5)^{3/2} (1 - \gamma_\mu) \bar{\mathcal{M}}_{n, n_5; n+\hat{\mu}, n_5}^{-1} \right] \\ &+ \text{Tr} \left[ \frac{1}{2} f(n_5)^{3/2} (1 + \gamma_\mu) \bar{\mathcal{M}}_{n+\hat{\mu}, n_5; n, n_5}^{-1} \right]. \end{aligned} \quad (4.79)$$

Employing a similar method and using Eq. (4.76) we get

$$\begin{aligned} j_5(\bar{v}_4(n_5), \bar{v}_5(n_5)) &= \text{Tr} \left[ \frac{1}{2} f(n_5)^{3/2} (1 - \gamma_5) \bar{\mathcal{M}}_{n, n_5; n, n_5+1}^{-1} \right] \\ &+ \text{Tr} \left[ \frac{1}{2} \frac{f(n_5)^2}{\sqrt{f(n_5 - 1)}} (1 + \gamma_5) \bar{\mathcal{M}}_{n, n_5+1; n, n_5}^{-1} \right]. \end{aligned} \quad (4.80)$$

To evaluate these currents, we can find expressions for the Wilson-Dirac operators in momentum space. For this we go into momentum space in the usual four dimensions but we keep the extra dimension in coordinate space as we have done when computing first order corrections to the path integral approximation earlier in this Chapter. The derivations of these can be found in Appendix F.3. Then one has to invert them and evaluate the currents restricting the momenta to the first Brillouin zone.

The effect of fermions on our mean-field values for the warped model investigated in this Chapter is unknown. Here we have provided a starting point for their implementation to see if and how the presence of fermions modifies the phase diagram. We conclude with the remark that these calculations have not been tested and thus numerical tests would be a potential direction for extending the exploration of the phase structure of the SU(2) warped model.

# Chapter 5

## Conclusions

The aim of this thesis has been to explore the phase structure of five-dimensional anisotropic SU(2) Yang-Mills theory on the lattice in two different cases. Firstly, the model was embedded in a flat background and Monte-Carlo numerical simulations were carried out to extend the phase diagram in the case where all directions were kept large in size. In this case, the main motivation was to find if there is an end-point to the first-order phase transition that separates the five-dimensional Coulombic phase from the confining phase, as previously claimed by others. If this point exists then one can define a continuum four-dimensional Yang-Mills theory at this point, an SU(2) gauge-Higgs model with the Higgs being in the adjoint representation, and it can provide a way of localizing gauge fields on four-dimensional layers. This would happen in the region where the lattice coupling along the extra dimension is smaller than that in the usual four-dimensional subspace. From our work, there is strong evidence that, up to the point  $\beta_4 = 2.60$ , a first-order transition exists between the strong-coupling and the five-dimensional Coulombic phase and nothing suggests that an end-point exists, giving rise to a four-dimensional continuum field theory. As finite-size effects were proven to be dominant in the average plaquette, large volumes are required to see a clear two-peak structure in it. So going to even larger values of  $\beta_4$ , to look for an end-point, would be computationally expensive and it was decided not to explore the model further.

Next, the five-dimensional anisotropic SU(2) Yang-Mills theory was embedded in a warped background, giving the gauge sector of the Randall-Sundrum models.

---

The motivation for this was the need to find a way of localizing gauge fields in these models and the so-called layered phase might provide a solution to this. In this thesis, we presented a novel investigation of this model using the Mean-Field approach. From the solutions to the saddle-point equations for a finite extra dimension, a phase diagram could be obtained that has a strong-coupling phase, a pure deconfining, a layered phase and a mixed phase where some layers are in the deconfining phase and some in the layered one. From measurements of the static potential on each layer, we have evidence that close to the transition line between the deconfining and the mixed phase the system acquires a Yukawa mass, signalling a four-dimensional Higgs-like phase. As we have not explicitly broken the symmetry by any means, it seems that the appearance of this phase arises from the warped geometry of our model. Away from the transition line and deep into the weak-coupling phase, we could not reach definite conclusions on the nature of the potential and further studies are needed to be performed.

In the region where a four-dimensional Yukawa potential was observed, the extracted lattice Yukawa mass seems to be going to zero for larger  $n_5$ . This suggests that if a continuum limit can be taken in the extra-dimension, the mass will go to zero, resulting to a four-dimensional Coulomb phase. The static potential was measured only at relatively short distances and as discussed in Chapter 3 further studies, especially at long distances, might show a non-vanishing string tension as expected. The Yukawa mass in physical units, seems to be almost constant for the first four layers, but for larger  $n_5$  our results do not show a clear behaviour. Further exploration should be done with a larger extent of the lattice along the extra dimension to clarify the situation.

There is a number of open questions requiring additional investigation to allow concrete conclusions, but also to open up the possibility of extracting physics that matches the observed world. These questions suggest a variety of research directions that need to be pursued.

One such direction is, as already mentioned, to investigate the system at larger extent of the lattice in the extra dimension, but also for different points in the parameter space to see if its behaviour remains the same and how it is affected at larger  $n_5$ . The observation that the width of the mixed phase grows with the curvature  $k$  suggests that for infinite extra dimension, the pure deconfining phase

---

is absent.

Another possibility would be to perform Monte Carlo numerical simulations so that the nature of all phases will be clarified and the order of the transitions will be shown clearly. The unexpected Higgs-like phase that appears in the Mean-Field approximation, suggests that actually Monte Carlo studies will be worthwhile, although large lattices will be needed to avoid finite-size effects when the extra dimension is large.

Furthermore, we have provided a framework for constructing fermions on the lattice in a warped background. A very interesting potential direction would be to couple the gauge fields to fermions to investigate their effect on the phase diagram. Also, the possibility to find chiral four-dimensional layers makes this extension of the work attractive.

Finally, one can explicitly break the symmetry by formulating the theory in an orbifold geometry and compare the two cases. As a matter of fact this last extension of our work might be the most appealing as the original Randall-Sundrum model was formulated in the  $S^1/Z_2$  space. Therefore, more phenomenological implications might arise from the latter set-up.

# Appendix A

## Further details for the Randal-Sundrum model

In this appendix, we derive the Einstein tensor,  $G_{MN}$  associated with the RS metric given by

$$ds^2 = e^{-2\sigma(y)}\eta_{\mu\nu}dx^\mu dx^\nu + dy^2. \quad (\text{A.1})$$

The first and second derivatives with respect to the extra dimension are denoted by ' and '' respectively. To find  $G_{MN}$  we first derive the Christoffel symbols, the Ricci tensor and the Ricci scalar

### A.1 Christoffel symbols

The Christoffel symbols are given by

$$\Gamma_{MN}^P = \frac{1}{2}g^{PR}(\partial_M g_{NR} + \partial_N g_{RM} - \partial_R g_{MN}) \quad (\text{A.2})$$

The only non-vanishing derivative terms are those that involve derivatives along the extra dimension when acting on  $g_{\mu\nu}$ , i.e.  $\partial_5 g_{\mu\nu}$ . Therefore, the only non-vanishing Christoffel symbols are the following:

$$\Gamma_{\mu 5}^\nu = \frac{1}{2}g^{\nu R}(\partial_5 g_{R\mu})$$

$$\begin{aligned}
&= \frac{1}{2}e^{2\sigma}\eta^{\nu\rho}(-2\sigma'e^{-2\sigma}\eta_{\rho\mu}) \\
&= -\sigma'\delta_\mu^\nu
\end{aligned} \tag{A.3}$$

and

$$\begin{aligned}
\Gamma_{\mu\nu}^5 &= \frac{1}{2}g^{5R}(-\partial_R g_{\mu\nu}) \\
&= \frac{1}{2}g^{55}(-\partial_5 g_{\mu\nu}) \\
&= \frac{1}{2}2\sigma'e^{-2\sigma}\eta_{\mu\nu} \\
&= \sigma'e^{-2\sigma}\eta_{\mu\nu}.
\end{aligned} \tag{A.4}$$

## A.2 Ricci tensor and Ricci scalar

The Ricci tensor is given by

$$R_{MN} = \partial_P \Gamma_{MN}^P - \partial_N \Gamma_{MP}^P + \Gamma_{PQ}^P \Gamma_{MN}^Q - \Gamma_{NQ}^P \Gamma_{MP}^Q. \tag{A.5}$$

For the three different cases of  $MN$  we find

- $$\begin{aligned}
R_{\mu\nu} &= \partial_5 \Gamma_{\mu\nu}^5 + \Gamma_{\sigma 5}^\sigma \Gamma_{\mu\nu}^5 - \Gamma_{\nu 5}^\sigma \Gamma_{\mu\sigma}^5 - \Gamma_{\nu\sigma}^5 \Gamma_{\mu 5}^\sigma \\
&= (\sigma'' - 2\sigma'^2)e^{-2\sigma}\eta_{\mu\nu} - 4\sigma'^2 e^{-2\sigma}\eta_{\mu\nu} + \sigma'^2 e^{-2\sigma}\eta_{\mu\nu} + \sigma'^2 e^{-2\sigma}\eta_{\mu\nu} \\
&= (\sigma'' - 4\sigma'^2)g_{\mu\nu}
\end{aligned} \tag{A.6}$$

- $$\begin{aligned}
R_{55} &= -\partial_5 \Gamma_{5\sigma}^\sigma - \Gamma_{5\rho}^\sigma \Gamma_{5\sigma}^\rho \\
&= 4\sigma'' - 4\sigma'^2
\end{aligned} \tag{A.7}$$

- $$R_{\mu 5} = 0 \tag{A.8}$$

Then, the Ricci scalar is found to be

$$\begin{aligned}
R &= g^{MN} R_{MN} \\
&= g^{\mu\nu} R_{\mu\nu} + g^{55} R_{55} \\
&= 4(\sigma'' - 4\sigma'^2) + 4\sigma'' - 4\sigma'^2 \\
&= 8\sigma'' - 20\sigma'^2
\end{aligned} \tag{A.9}$$



### A.3 Einstein tensor

Combining all the above we find

$$\begin{aligned} G_{\mu\nu} &= R_{\mu\nu} - \frac{1}{2}g_{\mu\nu}R \\ &= (6\sigma'^2 - 3\sigma'')g_{\mu\nu} \end{aligned} \tag{A.10}$$

$$\begin{aligned} G_{55} &= R_{55} - \frac{1}{2}g_{55}R \\ &= 6\sigma'^2 \end{aligned} \tag{A.11}$$

The equations of motion (Einstein Equations) of an action

$$S_{E-H} + S_M = \int d^4x dy \sqrt{-G} (2M_F^3 R - \Lambda) \tag{A.12}$$

are given by

$$G_{MN} = \frac{1}{4M_F^3} T_{MN} \tag{A.13}$$

where one defines

$$T_{MN} = \frac{-2}{\sqrt{-G}} \frac{\delta S_M}{\delta g^{MN}} \tag{A.14}$$

and thus

$$T_{MN} = -\Lambda g_{MN}. \tag{A.15}$$

Then from the fifth component of the Einstein equation we get

$$\begin{aligned} G_{55} &= 6\sigma'^2 = \frac{-\Lambda}{4M_F^3} \\ \Rightarrow \sigma'^2 &= \frac{-\Lambda}{24M_F^3} \end{aligned} \tag{A.16}$$

which implies that a negative cosmological constant is needed for  $\sigma$  to be real. The argument in Section 1.3.3 is that as the cosmological constant,  $\Lambda$ , is negative the space along the extra direction should be anti-de Sitter. This statement arises from the case of a conformally flat metric in any dimensions ( $AdS_D$  metric), where one can show that the cosmological constant is necessarily negative.

# Appendix B

## Character Expansions

By character expansion we can express  $u(H)$ , given by Eq. (2.74), in terms of Bessel functions. This is done as following

We define

$$u_2(H) = e^{u(H)} = \int \mathcal{D}U e^{(1/2)\text{ReTr}(HU)}. \quad (\text{B.1})$$

For  $SU(2)$ , we can parametrize the matrices  $H$  and  $U$  using the standard way of doing this for complex  $2 \times 2$  matrices and we can write  $\text{ReTr}(HU)$  as

$$\begin{aligned} \text{ReTr}(HU) &= 2[(\text{Re}h_0)u_0 + (\text{Re}h_A)u_A] \\ &= \text{ReTr}(U[\text{Re}h_0 + i\vec{\sigma} \cdot (\text{Re}\vec{h})]). \end{aligned} \quad (\text{B.2})$$

Now define a  $W \in SU(2)$  as

$$\begin{aligned} W &= [\text{Re}h_0 + i\vec{\sigma} \cdot (\text{Re}\vec{h})] / \sqrt{(\text{Re}h_0)^2 + (\text{Re}h_A)^2} \\ &= [\text{Re}h_0 + i\vec{\sigma} \cdot (\text{Re}\vec{h})] / \rho. \end{aligned} \quad (\text{B.3})$$

Then

$$\begin{aligned} \text{ReTr}(HU) &= \rho \text{ReTr}(UW) \\ \Rightarrow u_2(H) &= \int \mathcal{D}U e^{(1/2)\text{ReTr}(HU)} = \int_{SU(2)} \mathcal{D}U e^{(\rho/2)\text{ReTr}(UW)} \end{aligned}$$

---


$$= \int_{SU(2)} \mathcal{D}U e^{(\rho/2)\text{ReTr}(U)} \quad (\text{B.4})$$

due to the invariance of the Haar measure. Then we use character expansion to write

$$e^{\frac{\rho}{2}\text{ReTr}(U)} = \frac{2}{\rho} \sum_{\nu} (2\nu + 1) I_{2\nu+1}(\rho) \chi^{\nu}(U) \quad (\text{B.5})$$

where  $I_{2\nu+1}(\rho)$  is the modified Bessel function of the first kind of order  $2\nu + 1$  with argument  $\rho$ .

Knowing that

$$\chi_{\nu_{SU(2)}} = \frac{\sin((\nu + 1)\theta)}{\sin \theta} \quad (\text{B.6})$$

and using the orthonormality of characters we get

$$u_2(H) = \frac{2}{\rho} I_1(\rho). \quad (\text{B.7})$$

# Appendix C

## First-order corrections to the Mean-Field approach

In the following subsections, we derive the expressions for the propagators in momentum space. In addition to these propagators, we also include a gauge fixing term. To do this we use the following definition of the Fourier transformation for the propagator  $\Delta(n', n'_5, M', \alpha'; n'', n''_5, M'', \alpha'')$

$$\tilde{\Delta} = \frac{1}{TL^3} \sum_{n', n''} e^{ip'n'} e^{-ip''n''} e^{i\frac{p'_5}{2}(1-\delta_{M',5})} e^{-i\frac{p''_5}{2}(1-\delta_{M'',5})} (-i)^{\delta_{M',5}} i^{\delta_{M'',5}} \frac{\partial^2 S}{\partial v'_{M'_{\alpha'}} \partial v''_{M''_{\alpha''}}} \quad (\text{C.1})$$

where we make use of the four-vector notation  $n = (n_0, \vec{n})$  and similarly for  $p$ . We also use the standard notation  $\hat{p}_\mu = 2 \sin(p_\mu/2)$ . The extra factors of  $i$  were added to the Fourier transformation for the direction that remains in the coordinate space in order to ensure that the propagators remain real as proposed in [81].

### C.1 V field contribution

$$\Delta^{(vv)} = \frac{\partial^2}{\partial v_{\alpha'}(n', n'_5) \partial v_{\alpha''}(n'', n''_5)} \left[ \sum_{n, n_5} S_W[V_4, V_5] \right] \Big|_{\bar{v}_4, \bar{v}_5} \quad (\text{C.2})$$

The partial differentiation is performed by replacing  $v_\alpha$ 's with  $v_{\mu_\alpha}$  and  $v_{5_\alpha}$  and thus we get four terms. By replacing the links with their parametrization according to Eq. (4.19) the plaquette along the four dimensions becomes

$$V_{\mu\nu}(n, n_5) = (\bar{v}_4(n_5) + v_\mu(n, n_5))(\bar{v}_4(n_5) + v_\nu(n + \hat{\mu}, n_5)) \\ (\bar{v}_4^\dagger(n_5) + v_\mu^\dagger(n + \nu, n_5))(\bar{v}_4^\dagger(n_5) + v_\nu^\dagger(n, n_5)) \quad (C.3)$$

and the plaquette along the extra dimension

$$V_{\mu 5}(n, n_5) = (\bar{v}_4(n_5) + v_\mu(n, n_5))(\bar{v}_5(n_5) + v_5(n + \hat{\mu}, n_5)) \\ (\bar{v}_4^\dagger(n_5) + v_\mu^\dagger(n, n_5 + 1))(\bar{v}_5^\dagger(n_5) + v_5^\dagger(n, n_5)). \quad (C.4)$$

As we stated in the introduction of first-order corrections, we are about to take second derivatives of our action terms. The constant term of each link will vanish when we differentiate it, so we are left with the second part. Also, in the Mean-Field approach we decoupled the imaginary parts of  $v_\alpha$  and  $h_\alpha$ , so we consider them here as real numbers, i.e.  $V_\mu(n, n_5) = v_{\mu 0}(n, n_5)\mathbb{1} + iv_{\mu A}\sigma^A$  and  $V_\mu^\dagger(n, n_5) = v_{\mu 0}(n, n_5)\mathbb{1} - iv_{\mu A}\sigma^A$  where  $v_{\mu 0}(n, n_5)$  and  $v_{\mu A}(n, n_5)$  are real and similar arguments hold for the links along the fifth direction. The action that contributes after taking the derivatives is given by

$$S_W = -\frac{\beta}{2\gamma} \sum_{\mu, \nu; n; n_5} \text{Tr} \left( (v_{\mu 0}(n, n_5)\mathbb{1} + iv_{\mu A}(n, n_5)\sigma^A) \right. \\ \left. (v_{\nu 0}(n + \hat{\mu}, n_5)\mathbb{1} + iv_{\nu B}(n + \hat{\mu}, n_5)\sigma^B) (v_{\mu 0}(n + \hat{\nu}, n_5)\mathbb{1} - iv_{\mu C}(n + \hat{\nu}, n_5)\sigma^C) \right. \\ \left. (v_{\nu 0}(n, n_5)\mathbb{1} - iv_{\nu D}(n, n_5)\sigma^D) \right) (1 - \delta_{\mu\nu}) \\ - \frac{\beta\gamma}{2} \sum_{\mu, 5; n; n_5} \text{Tr} \left( (v_{\mu 0}(n, n_5)\mathbb{1} + iv_{\mu A}(n, n_5)\sigma^A) \right. \\ \left. (v_{5_0}(n + \hat{\mu}, n_5)\mathbb{1} + iv_{5_B}(n + \hat{\mu}, n_5)\sigma^B) (v_{\mu 0}(n, n_5 + 1)\mathbb{1} - iv_{\mu C}(n, n_5 + 1)\sigma^C) \right. \\ \left. (v_{5_0}(n, n_5)\mathbb{1} - iv_{5_D}(n, n_5)\sigma^D) \right) + \dots \quad (C.5)$$

Taking the trace of the above expression, there are only certain non-vanishing

terms that contribute to the first order corrections which read as

$$\begin{aligned}
 S_W = & -\frac{\beta}{\gamma} \sum_{\mu, \nu; n; n_5} \left( \frac{(1 - \delta_{\mu, \nu})}{2} (v_{\mu_0}(n, n_5) v_{\mu_0}(n + \hat{\nu}, n_5) v_{\nu_0}(n + \hat{\mu}, n_5) v_{\nu_0}(n, n_5) \right. \\
 & - v_{\mu_0}(n, n_5) v_{\nu_0}(n + \hat{\mu}, n_5) v_{\mu_A}(n + \hat{\nu}, n_5) v_{\nu_A}(n, n_5) \\
 & + v_{\mu_0}(n, n_5) v_{\mu_0}(n + \hat{\nu}, n_5) v_{\nu_A}(n + \hat{\mu}, n_5) v_{\nu_A}(n, n_5) \\
 & + v_{\mu_0}(n, n_5) v_{\nu_0}(n, n_5) v_{\nu_A}(n + \hat{\mu}, n_5) v_{\mu_A}(n + \hat{\nu}, n_5) \\
 & + v_{\mu_0}(n + \hat{\nu}, n_5) v_{\nu_0}(n + \hat{\mu}, n_5) v_{\mu_A}(n, n_5) v_{\nu_A}(n, n_5) \\
 & + v_{\nu_0}(n, n_5) v_{\nu_0}(n + \hat{\mu}, n_5) v_{\mu_A}(n, n_5) v_{\mu_A}(n + \hat{\nu}, n_5) \\
 & \left. - v_{\mu_0}(n + \hat{\nu}, n_5) v_{\nu_0}(n, n_5) v_{\mu_A}(n, n_5) v_{\nu_A}(n + \hat{\mu}, n_5) + \dots \right) \\
 & - \beta \gamma \sum_{\mu; n; n_5} \left( v_{\mu_0}(n, n_5) v_{5_0}(n + \hat{\mu}, n_5) v_{\mu_0}(n, n_5 + 1) v_{5_0}(n, n_5) \right. \\
 & - v_{\mu_0}(n, n_5) v_{5_0}(n + \hat{\mu}, n_5) v_{\mu_A}(n, n_5 + 1) v_{5_A}(n, n_5) \\
 & + v_{\mu_0}(n, n_5) v_{5_0}(n, n_5) v_{\mu_A}(n, n_5 + 1) v_{5_A}(n + \hat{\mu}, n_5) \\
 & + v_{\mu_0}(n, n_5) v_{5_A}(n + \hat{\mu}, n_5) v_{\mu_0}(n, n_5 + 1) v_{5_A}(n, n_5) \\
 & + v_{\mu_A}(n, n_5) v_{5_0}(n + \hat{\mu}, n_5) v_{\mu_A}(n, n_5 + 1) v_{5_0}(n, n_5) \\
 & + v_{\mu_A}(n, n_5) v_{5_0}(n + \hat{\mu}, n_5) v_{\mu_0}(n, n_5 + 1) v_{5_A}(n, n_5) \\
 & \left. - v_{\mu_A}(n, n_5) v_{5_A}(n + \hat{\mu}, n_5) v_{\mu_0}(n, n_5 + 1) v_{5_0}(n, n_5) + \dots \right). \tag{C.6}
 \end{aligned}$$

Now, we use these terms of the action to find the V-field contribution to the propagator. The derivations are shown for all  $\Delta_{44}^{(vv)}$ ,  $\Delta_{45}^{(vv)}$ ,  $\Delta_{54}^{(vv)}$  and  $\Delta_{55}^{(vv)}$ . For each of these we present final expressions for the cases of  $\alpha' = \alpha'' = 0$  and  $\alpha' = A', \alpha'' = A'$  separately.

### B.1.1 $\Delta_{44}^{(vv)}$

We first consider the case  $\alpha' = 0, \alpha'' = 0$

$$\begin{aligned}
 & \frac{\partial^2 S_W}{\partial v_{\sigma_0}(n', n'_5) \partial v_{\rho_0}(n'', n''_5)} \\
 = & \frac{\partial}{\partial v_{\sigma_0}(n', n'_5)} \left[ \frac{\beta}{\gamma} \sum_{n, n_5; \mu, \nu} \frac{(1 - \delta_{\mu, \nu})}{2} (v_{\mu_0}(n + \hat{\nu}, n_5) v_{\nu_0}(n + \hat{\mu}, n_5) v_{\nu_0}(n, n_5) \delta_{n'', n} \delta_{n''_5, n_5} \delta_{\rho, \mu} \right. \\
 & \left. + v_{\mu_0}(n, n_5) v_{\nu_0}(n + \hat{\mu}, n_5) v_{\nu_0}(n, n_5) \delta_{n'', n + \hat{\nu}} \delta_{n''_5, n_5} \delta_{\rho, \mu} \right.
 \end{aligned}$$

$$\begin{aligned}
 & + v_{\mu_0}(n, n_5)v_{\mu_0}(n + \hat{\nu}, n_5)v_{\nu_0}(n, n_5)\delta_{n'', n+\hat{\mu}}\delta_{n_5'', n_5}\delta_{\rho, \nu} \\
 & + v_{\mu_0}(n, n_5)v_{\mu_0}(n + \hat{\nu}, n_5)v_{\nu_0}(n + \hat{\mu}, n_5)\delta_{n'', n}\delta_{n_5'', n_5}\delta_{\rho, \nu} \Big) \\
 & - \beta\gamma \sum_{n, n_5; \mu} v_{5_0}(n + \hat{\mu}, n_5)v_{5_0}(n, n_5)\delta_{\rho, \mu} \left( v_{\mu_0}(n, n_5 + 1)\delta_{n'', n}\delta_{n_5'', n_5} + v_{\mu_0}(n, n_5)\delta_{n'', n}\delta_{n_5'', n_5+1} \right) \Big] \\
 & = -\frac{\beta}{2\gamma} \sum_{n, n_5; \mu, \nu} (1 - \delta_{\mu, \nu}) \left[ v_{\nu_0}(n + \hat{\mu}, n_5)v_{\nu_0}(n, n_5)\delta_{n'', n}\delta_{n_5'', n_5}\delta_{n', n+\hat{\nu}}\delta_{n_5', n_5}\delta_{\rho, \mu}\delta_{\sigma, \mu} \right. \\
 & + v_{\mu_0}(n + \hat{\nu}, n_5)v_{\nu_0}(n, n_5)\delta_{n'', n}\delta_{n_5'', n_5}\delta_{n', n+\hat{\mu}}\delta_{n_5', n_5}\delta_{\rho, \mu}\delta_{\sigma, \nu} \\
 & + v_{\mu_0}(n + \hat{\nu}, n_5)v_{\nu_0}(n + \hat{\mu}, n_5)\delta_{n'', n}\delta_{n_5'', n_5}\delta_{n', n}\delta_{n_5', n_5}\delta_{\rho, \mu}\delta_{\sigma, \nu} \\
 & + v_{\nu_0}(n + \hat{\mu}, n_5)v_{\nu_0}(n, n_5)\delta_{n'', n+\hat{\nu}}\delta_{n_5'', n_5}\delta_{n', n}\delta_{n_5', n_5}\delta_{\rho, \mu}\delta_{\sigma, \mu} \\
 & + v_{\mu_0}(n, n_5)v_{\nu_0}(n, n_5)\delta_{n'', n+\hat{\nu}}\delta_{n_5'', n_5}\delta_{n', n+\hat{\mu}}\delta_{n_5', n_5}\delta_{\rho, \mu}\delta_{\sigma, \nu} \\
 & + v_{\mu_0}(n, n_5)v_{\nu_0}(n + \hat{\mu}, n_5)\delta_{n'', n+\hat{\nu}}\delta_{n_5'', n_5}\delta_{n', n}\delta_{n_5', n_5}\delta_{\rho, \mu}\delta_{\sigma, \nu} \\
 & + v_{\mu_0}(n + \hat{\nu}, n_5)v_{\nu_0}(n, n_5)\delta_{n'', n+\hat{\mu}}\delta_{n_5'', n_5}\delta_{n', n}\delta_{n_5', n_5}\delta_{\rho, \nu}\delta_{\sigma, \mu} \\
 & + v_{\mu_0}(n, n_5)v_{\nu_0}(n, n_5)\delta_{n'', n+\hat{\nu}}\delta_{n_5'', n_5}\delta_{n', n+\hat{\mu}}\delta_{n_5', n_5}\delta_{\rho, \nu}\delta_{\sigma, \mu} \\
 & + v_{\mu_0}(n, n_5)v_{\mu_0}(n + \hat{\nu}, n_5)\delta_{n'', n+\hat{\mu}}\delta_{n_5'', n_5}\delta_{n', n}\delta_{n_5', n_5}\delta_{\rho, \nu}\delta_{\sigma, \nu} \\
 & + v_{\mu_0}(n + \hat{\nu}, n_5)v_{\mu_0}(n + \hat{\mu}, n_5)\delta_{n'', n}\delta_{n_5'', n_5}\delta_{n', n}\delta_{n_5', n_5}\delta_{\rho, \nu}\delta_{\sigma, \mu} \\
 & + v_{\mu_0}(n, n_5)v_{\nu_0}(n + \hat{\mu}, n_5)\delta_{n'', n}\delta_{n_5'', n_5}\delta_{n', n+\hat{\nu}}\delta_{n_5', n_5}\delta_{\rho, \nu}\delta_{\sigma, \mu} \\
 & + v_{\mu_0}(n, n_5)v_{\mu_0}(n + \hat{\nu}, n_5)\delta_{n'', n}\delta_{n_5'', n_5}\delta_{n', n+\hat{\mu}}\delta_{n_5', n_5}\delta_{\rho, \nu}\delta_{\sigma, \nu} \Big] \\
 & - \beta\gamma \sum_{n, n_5; \mu} v_{5_0}(n + \hat{\mu}, n_5)v_{5_0}(n, n_5)\delta_{\rho, \mu}\delta_{\sigma, \mu} \left( \delta_{n'', n}\delta_{n_5'', n_5}\delta_{n', n}\delta_{n_5', n_5+1} + \delta_{n'', n}\delta_{n_5'', n_5+1}\delta_{n', n}\delta_{n_5', n_5} \right) \\
 & = -\frac{\beta}{\gamma} \sum_{n, n_5; \mu} \left[ (1 - \delta_{\rho, \mu})\delta_{\rho\sigma} \left( v_{\mu_0}(n + \hat{\rho}, n_5)v_{\mu_0}(n, n_5)\delta_{n'', n}\delta_{n_5'', n_5}\delta_{n', n+\hat{\mu}}\delta_{n_5', n_5} \right. \right. \\
 & + v_{\mu_0}(n + \hat{\rho}, n_5)v_{\mu_0}(n, n_5)\delta_{n'', n+\hat{\mu}}\delta_{n_5'', n_5}\delta_{n', n}\delta_{n_5', n_5} \Big) \\
 & + (1 - \delta_{\rho, \sigma}) \left( v_{\rho_0}(n + \hat{\sigma}, n_5)v_{\sigma_0}(n, n_5)\delta_{n'', n}\delta_{n_5'', n_5}\delta_{n', n+\hat{\rho}}\delta_{n_5', n_5} \right. \\
 & + v_{\rho_0}(n + \hat{\sigma}, n_5)v_{\sigma_0}(n + \hat{\rho}, n_5)\delta_{n'', n}\delta_{n_5'', n_5}\delta_{n', n}\delta_{n_5', n_5} \\
 & + v_{\rho_0}(n, n_5)v_{\sigma_0}(n, n_5)\delta_{n'', n+\hat{\sigma}}\delta_{n_5'', n_5}\delta_{n', n+\hat{\rho}}\delta_{n_5', n_5} \\
 & + v_{\rho_0}(n, n_5)v_{\sigma_0}(n + \hat{\rho}, n_5)\delta_{n'', n+\hat{\sigma}}\delta_{n_5'', n_5}\delta_{n', n}\delta_{n_5', n_5} \Big) \Big] \\
 & - \beta\gamma \sum_{n, n_5} v_{5_0}(n + \hat{\rho}, n_5)v_{5_0}(n, n_5)\delta_{\rho, \sigma} \left( \delta_{n'', n}\delta_{n_5'', n_5}\delta_{n', n}\delta_{n_5', n_5+1} + \delta_{n'', n}\delta_{n_5'', n_5+1}\delta_{n', n}\delta_{n_5', n_5} \right).
 \end{aligned} \tag{C.7}$$

In momentum space we write this as

$$\begin{aligned}
 \tilde{\Delta}_{44}^{(vv)-0} &= -\frac{\beta}{\gamma} \frac{1}{TL^3} \sum_{n', n''} \sum_{n, n_5} e^{ip'n'} e^{-ip''n''} e^{ip'_\sigma/2} e^{-ip''_\sigma/2} \delta_{n'_5, n_5} \delta_{n''_5, n_5} (\bar{v}_4(n_5))^2 \\
 &\quad \left[ \sum_{\mu \neq \rho} \left[ (\delta_{n'', n} \delta_{n', n+\hat{\mu}} + \delta_{n'', n+\hat{\mu}} \delta_{n', n}) \delta_{\rho, \sigma} \right] \right. \\
 &\quad \left. + (1 - \delta_{\rho, \sigma}) (\delta_{n'', n} \delta_{n', n+\hat{\rho}} + \delta_{n'', n} \delta_{n', n} + \delta_{n''+\hat{\sigma}, n} \delta_{n', n+\hat{\rho}} + \delta_{n''+\hat{\sigma}, n} \delta_{n', n}) \right] \\
 &\quad - \beta \gamma \frac{1}{TL^3} \sum_{n', n''} \sum_{n, n_5} e^{ip'n'} e^{-ip''n''} e^{ip'_\sigma/2} e^{-ip''_\sigma/2} \\
 &\quad \left[ (\bar{v}_5(n_5))^2 \delta_{\rho, \sigma} \delta_{n'', n} \delta_{n', n} (\delta_{n'_5, n_5} \delta_{n'_5, n_5+1} + \delta_{n''_5, n_5+1} \delta_{n''_5, n_5}) \right] \\
 &= -\frac{\beta}{\gamma} \delta_{p', p''}^{(4)} \delta_{n'_5, n''_5} (\bar{v}_4(n'_5))^2 \left[ \sum_{\mu \neq \rho} \delta_{\rho, \sigma} (e^{ip'_\mu} + e^{-ip''_\mu}) \right. \\
 &\quad \left. + (1 - \delta_{\rho, \sigma}) (e^{ip'_\sigma/2} e^{ip''_\sigma/2} + e^{ip'_\sigma/2} e^{-ip''_\sigma/2} + e^{-ip'_\sigma/2} e^{ip''_\sigma/2} + e^{-ip'_\sigma/2} e^{-ip''_\sigma/2}) \right] \\
 &\quad - \beta \gamma \delta_{p', p''}^{(4)} \delta_{\rho, \sigma} \left[ (\bar{v}_5(n'_5 - 1))^2 \delta_{n'_5, n'_5-1} + (\bar{v}_5(n'_5))^2 \delta_{n'_5, n'_5+1} \right] \\
 &= -\frac{\beta}{\gamma} \delta_{p', p''}^{(4)} \delta_{n'_5, n''_5} (\bar{v}_4(n'_5))^2 \left[ \sum_{\mu \neq \rho} \delta_{\rho, \sigma} (2 \cos(p'_\mu)) \right. \\
 &\quad \left. + 4(1 - \delta_{\rho, \sigma}) \cos(p'_\rho/2) \cos(p''_\rho/2) \right] \\
 &\quad - \beta \gamma \delta_{p', p''}^{(4)} \delta_{\rho, \sigma} \left[ (\bar{v}_5(n'_5 - 1))^2 \delta_{n'_5, n'_5-1} + (\bar{v}_5(n'_5))^2 \delta_{n'_5, n'_5+1} \right]. \tag{C.8}
 \end{aligned}$$

We then look at the case  $\alpha' = A'$ ;  $\alpha'' = A''$

$$\begin{aligned}
 \frac{\partial^2 S_W}{\partial v_{\sigma A'}(n', n'_5) \partial v_{\rho A''}(n'', n''_5)} &= \frac{\partial}{\partial v_{\sigma A'}(n', n'_5)} \left[ -\frac{\beta}{\gamma} \sum_{n, n_5; \mu, \nu; A} \frac{(1 - \delta_{\mu, \nu})}{2} \delta_{A'', A} \right. \\
 &\quad \left( -v_{\mu_0}(n, n_5) v_{\nu_0}(n + \hat{\mu}, n_5) v_{\mu A}(n + \hat{\nu}, n_5) \delta_{n'', n} \delta_{n'_5, n_5} \delta_{\rho, \nu} \right. \\
 &\quad - v_{\mu_0}(n, n_5) v_{\nu_0}(n + \hat{\mu}, n_5) v_{\nu A}(n, n_5) \delta_{n'', n+\hat{\nu}} \delta_{n'_5, n_5} \delta_{\rho, \mu} \\
 &\quad + v_{\mu_0}(n, n_5) v_{\mu_0}(n + \hat{\nu}, n_5) v_{\nu A}(n, n_5) \delta_{n'', n+\hat{\mu}} \delta_{n'_5, n_5} \delta_{\rho, \nu} \\
 &\quad + v_{\mu_0}(n, n_5) v_{\mu_0}(n + \hat{\nu}, n_5) v_{\nu A}(n + \hat{\mu}, n_5) \delta_{n'', n} \delta_{n'_5, n_5} \delta_{\rho, \nu} \\
 &\quad + v_{\mu_0}(n, n_5) v_{\nu_0}(n, n_5) v_{\mu A}(n + \hat{\nu}, n_5) \delta_{n'', n+\hat{\mu}} \delta_{n'_5, n_5} \delta_{\rho, \nu} \\
 &\quad + v_{\mu_0}(n, n_5) v_{\nu_0}(n, n_5) v_{\nu A}(n + \hat{\mu}, n_5) \delta_{n'', n+\hat{\nu}} \delta_{n'_5, n_5} \delta_{\rho, \mu} \\
 &\quad \left. \left. + v_{\mu_0}(n + \hat{\nu}, n_5) v_{\nu_0}(n + \hat{\mu}, n_5) v_{\mu A}(n, n_5) \delta_{n'', n} \delta_{n'_5, n_5} \delta_{\rho, \nu} \right) \right]
 \end{aligned}$$



$$\begin{aligned}
 & + v_{\mu_0}(n + \hat{\nu}, n_5)v_{\nu_0}(n + \hat{\mu}, n_5)v_{\nu_A}(n, n_5)\delta_{n'',n}\delta_{n_5'',n_5}\delta_{\rho,\mu} \\
 & + v_{\nu_0}(n, n_5)v_{\nu_0}(n + \hat{\mu}, n_5)v_{\mu_A}(n, n_5)\delta_{n'',n+\hat{\nu}}\delta_{n_5'',n_5}\delta_{\rho,\mu} \\
 & + v_{\nu_0}(n, n_5)v_{\nu_0}(n + \hat{\mu}, n_5)v_{\mu_A}(n + \hat{\nu}, n_5)\delta_{n'',n}\delta_{n_5'',n_5}\delta_{\rho,\mu} \\
 & - v_{\mu_0}(n + \hat{\nu}, n_5)v_{\nu_0}(n, n_5)v_{\mu_A}(n, n_5)\delta_{n'',n+\hat{\mu}}\delta_{n_5'',n_5}\delta_{\rho,\nu} \\
 & - v_{\mu_0}(n + \hat{\nu}, n_5)v_{\nu_0}(n, n_5)v_{\nu_A}(n + \hat{\mu}, n_5)\delta_{n'',n}\delta_{n_5'',n_5}\delta_{\rho,\mu} \Big) \\
 & - \beta\gamma \sum_{n,n_5;\mu;A} \delta_{A'',A}\delta_{\rho,\mu} v_{5_0}(n + \hat{\mu}, n_5)v_{5_0}(n, n_5) \\
 & \quad \left( v_{\mu_A}(n, n_5)\delta_{n'',n}\delta_{n_5'',n_5+1} + v_{\mu_A}(n, n_5 + 1)\delta_{n'',n}\delta_{n_5'',n_5} \right) \Big] \\
 & = -\frac{\beta}{2\gamma} \sum_{n,n_5;\mu,\nu;A} (1 - \delta_{\mu,\nu})\delta_{A',A}\delta_{A'',A} \Big[ \\
 & \quad - v_{\nu_0}(n + \hat{\mu}, n_5)v_{\mu_0}(n, n_5)\delta_{n'',n}\delta_{n_5'',n_5}\delta_{n',n+\hat{\nu}}\delta_{n_5',n_5}\delta_{\rho,\nu}\delta_{\sigma,\mu} \\
 & \quad - v_{\nu_0}(n + \hat{\mu}, n_5)v_{\mu_0}(n, n_5)\delta_{n'',n+\hat{\nu}}\delta_{n_5'',n_5}\delta_{n',n}\delta_{n_5',n_5}\delta_{\rho,\mu}\delta_{\sigma,\nu} \\
 & \quad + v_{\mu_0}(n, n_5)v_{\mu_0}(n + \hat{\nu}, n_5)\delta_{n'',n+\hat{\mu}}\delta_{n_5'',n_5}\delta_{n',n}\delta_{n_5',n_5}\delta_{\rho,\nu}\delta_{\sigma,\nu} \\
 & \quad + v_{\mu_0}(n, n_5)v_{\mu_0}(n + \hat{\nu}, n_5)\delta_{n'',n}\delta_{n_5'',n_5}\delta_{n',n+\hat{\mu}}\delta_{n_5',n_5}\delta_{\rho,\nu}\delta_{\sigma,\nu} \\
 & \quad + v_{\mu_0}(n, n_5)v_{\nu_0}(n, n_5)\delta_{n'',n+\hat{\mu}}\delta_{n_5'',n_5}\delta_{n',n+\hat{\nu}}\delta_{n_5',n_5}\delta_{\rho,\nu}\delta_{\sigma,\mu} \\
 & \quad + v_{\mu_0}(n, n_5)v_{\nu_0}(n, n_5)\delta_{n'',n+\hat{\nu}}\delta_{n_5'',n_5}\delta_{n',n+\hat{\mu}}\delta_{n_5',n_5}\delta_{\rho,\mu}\delta_{\sigma,\nu} \\
 & \quad + v_{\mu_0}(n + \hat{\nu}, n_5)v_{\nu_0}(n + \hat{\mu}, n_5)\delta_{n'',n}\delta_{n_5'',n_5}\delta_{n',n}\delta_{n_5',n_5}\delta_{\rho,\nu}\delta_{\sigma,\mu} \\
 & \quad + v_{\mu_0}(n + \hat{\nu}, n_5)v_{\nu_0}(n + \hat{\mu}, n_5)\delta_{n'',n}\delta_{n_5'',n_5}\delta_{n',n}\delta_{n_5',n_5}\delta_{\rho,\mu}\delta_{\sigma,\nu} \\
 & \quad + v_{\nu_0}(n, n_5)v_{\nu_0}(n + \hat{\mu}, n_5)\delta_{n'',n+\hat{\nu}}\delta_{n_5'',n_5}\delta_{n',n}\delta_{n_5',n_5}\delta_{\rho,\mu}\delta_{\sigma,\mu} \\
 & \quad + v_{\nu_0}(n, n_5)v_{\nu_0}(n + \hat{\mu}, n_5)\delta_{n'',n}\delta_{n_5'',n_5}\delta_{n',n+\hat{\nu}}\delta_{n_5',n_5}\delta_{\rho,\mu}\delta_{\sigma,\mu} \\
 & \quad - v_{\mu_0}(n + \hat{\nu}, n_5)v_{\nu_0}(n, n_5)\delta_{n'',n+\hat{\mu}}\delta_{n_5'',n_5}\delta_{n',n}\delta_{n_5',n_5}\delta_{\rho,\nu}\delta_{\sigma,\mu} \\
 & \quad - v_{\mu_0}(n + \hat{\nu}, n_5)v_{\nu_0}(n, n_5)\delta_{n'',n}\delta_{n_5'',n_5}\delta_{n',n+\hat{\mu}}\delta_{n_5',n_5}\delta_{\rho,\mu}\delta_{\sigma,\nu} \Big] \\
 & - \beta\gamma \sum_{n,n_5;\mu;A} \delta_{A',A}\delta_{A'',A'}v_{5_0}(n + \hat{\mu}, n_5)v_{5_0}(n, n_5)\delta_{\rho,\mu}\delta_{\sigma,\mu} \\
 & \quad \left( \delta_{n'',n}\delta_{n_5'',n_5}\delta_{n',n}\delta_{n_5',n_5+1} + \delta_{n'',n}\delta_{n_5'',n_5+1}\delta_{n',n}\delta_{n_5',n_5} \right) \\
 & = -\frac{\beta}{\gamma}\delta_{A',A''} \sum_{n,n_5} (\bar{v}_4(n_5))^2 \delta_{n_5',n_5}\delta_{n_5'',n_5} \left[ \sum_{\mu} \left[ (1 - \delta_{\rho,\mu})\delta_{\rho,\sigma} (\delta_{n'',n+\hat{\mu}}\delta_{n',n} + \delta_{n'',n}\delta_{n',n+\hat{\mu}}) \right] \right. \\
 & \quad \left. + (1 - \delta_{\rho,\sigma}) \left( -\delta_{n'',n+\hat{\sigma}}\delta_{n',n} + \delta_{n'',n+\hat{\sigma}}\delta_{n',n+\hat{\rho}} + \delta_{n'',n}\delta_{n',n} - \delta_{n'',n}\delta_{n',n+\hat{\rho}} \right) \right] \\
 & - \beta\gamma\delta_{A',A''} \sum_{n,n_5} \delta_{\rho,\sigma} (\bar{v}_5(n_5))^2 \delta_{n',n}\delta_{n'',n} (\delta_{n_5'',n_5}\delta_{n_5',n_5+1} + \delta_{n_5'',n_5+1}\delta_{n_5',n_5}) \quad (C.9)
 \end{aligned}$$

where in the last step we evaluated the expression at the mean-field values. In momentum space it can be written as

$$\begin{aligned}
 \tilde{\Delta}_{44}^{(vv)-A} &= -\frac{\beta}{\gamma} \frac{1}{TL^3} \delta_{A',A''} \sum_{n',n''} \sum_{n,n_5} e^{ip'n'} e^{-ip''n''} e^{ip'_\sigma/2} e^{-ip''_\sigma/2} \delta_{n'_5,n_5} \delta_{n''_5,n_5} (\bar{v}_4(n_5))^2 \\
 &\quad \left[ \sum_{\mu \neq \rho} \left[ (\delta_{n'',n} \delta_{n',n+\hat{\mu}} + \delta_{n'',n+\hat{\mu}} \delta_{n',n}) \delta_{\rho,\sigma} \right] \right. \\
 &\quad \left. + (1 - \delta_{\rho,\sigma}) \left( -\delta_{n''+\hat{\sigma},n} \delta_{n',n} + \delta_{n''+\hat{\sigma},n} \delta_{n',n+\hat{\rho}} + \delta_{n'',n} \delta_{n',n} - \delta_{n'',n} \delta_{n',n+\hat{\rho}} \right) \right] \\
 &\quad - \beta \gamma \frac{1}{TL^3} \sum_{n',n''} \sum_{n,n_5} e^{ip'n'} e^{-ip''n''} e^{ip'_\sigma/2} e^{-ip''_\sigma/2} \\
 &\quad \left[ (\bar{v}_5(n_5))^2 \delta_{\rho,\sigma} \delta_{n'',n} \delta_{n',n} (\delta_{n''_5,n_5} \delta_{n'_5,n_5+1} + \delta_{n''_5,n_5+1} \delta_{n'_5,n_5}) \right] \\
 &= -\frac{\beta}{\gamma} \delta_{p',p''}^{(4)} \delta_{n'_5,n''_5} (\bar{v}_4(n'_5))^2 \left[ \sum_{\mu \neq \rho} \delta_{\rho,\sigma} (e^{ip'_\mu} + e^{-ip'_\mu}) \right. \\
 &\quad \left. + (1 - \delta_{\rho,\sigma}) \left( -e^{-ip'_\sigma/2} e^{-ip'_\rho/2} + e^{-ip'_\sigma/2} e^{ip'_\rho/2} + e^{ip'_\sigma/2} e^{-ip'_\rho/2} - e^{ip'_\sigma/2} e^{ip'_\rho/2} \right) \right] \\
 &\quad - \beta \gamma \delta_{p',p''}^{(4)} \delta_{\rho,\sigma} \left[ (\bar{v}_5(n'_5 - 1))^2 \delta_{n''_5,n'_5-1} + (\bar{v}_5(n'_5))^2 \delta_{n''_5,n'_5+1} \right] \\
 &= -\frac{\beta}{\gamma} \delta_{p',p''}^{(4)} \delta_{n'_5,n''_5} (\bar{v}_4(n'_5))^2 \left[ \sum_{\mu \neq \rho} \delta_{\rho,\sigma} (2 \cos(p'_\mu)) \right. \\
 &\quad \left. + 4(1 - \delta_{\rho,\sigma}) \sin(p'_\rho/2) \sin(p'_\sigma/2) \right] \\
 &\quad - \beta \gamma \delta_{p',p''}^{(4)} \delta_{\rho,\sigma} \left[ (\bar{v}_5(n'_5 - 1))^2 \delta_{n''_5,n'_5-1} + (\bar{v}_5(n'_5))^2 \delta_{n''_5,n'_5+1} \right]. \tag{C.10}
 \end{aligned}$$

### B.1.2 $\Delta_{45}^{(vv)}$

We first consider the contribution from  $\alpha' = 0, \alpha'' = 0$

$$\begin{aligned}
 &\frac{\partial^2 S_W}{\partial v_{\rho_0}(n', n'_5) \partial v_{\bar{5}_0}(n'', n''_5)} \\
 &= \frac{\partial}{\partial v_{\rho_0}(n', n'_5)} \left[ -\beta \gamma \sum_{n,n_5;\mu} \delta_{\rho,\mu} \left( v_{\mu_0}(n, n_5) v_{\mu_0}(n, n_5 + 1) v_{\bar{5}_0}(n, n_5) \delta_{n'',n+\hat{\mu}} \delta_{n''_5,n_5} \right. \right. \\
 &\quad \left. \left. + v_{\mu_0}(n, n_5) v_{\mu_0}(n, n_5 + 1) v_{\bar{5}_0}(n + \hat{\mu}, n_5) \delta_{n'',n} \delta_{n''_5,n_5} \right) \right] \\
 &= -\beta \gamma \sum_{n,n_5;\mu} \delta_{\rho,\mu} \left[ v_{\mu_0}(n, n_5 + 1) v_{\bar{5}_0}(n, n_5) \delta_{n'',n+\hat{\mu}} \delta_{n''_5,n_5} \delta_{n',n} \delta_{n'_5,n_5} \right. \\
 &\quad \left. + v_{\mu_0}(n, n_5) v_{\bar{5}_0}(n + \hat{\mu}, n_5) \delta_{n'',n} \delta_{n''_5,n_5} \delta_{n',n} \delta_{n'_5,n_5} \right]
 \end{aligned}$$

$$\begin{aligned}
 & + v_{\mu_0}(n, n_5)v_{5_0}(n, n_5)\delta_{n'', n+\hat{\mu}}\delta_{n_5'', n_5}\delta_{n', n}\delta_{n_5', n_5+1} \\
 & + v_{\mu_0}(n, n_5+1)v_{5_0}(n+\hat{\mu}, n_5)\delta_{n'', n}\delta_{n_5'', n_5}\delta_{n', n}\delta_{n_5', n_5} \\
 & + v_{\mu_0}(n, n_5)v_{5_0}(n+\hat{\mu}, n_5)\delta_{n'', n}\delta_{n_5'', n_5}\delta_{n', n}\delta_{n_5', n_5+1} \Big]. \tag{C.11}
 \end{aligned}$$

In momentum space this is given by

$$\begin{aligned}
 \tilde{\Delta}_{45}^{(vv)-0} &= -i\beta\gamma \frac{1}{TL^3} \sum_{n, n_5} e^{i(p'-p'')n} e^{ip'_\rho/2} \sum_{\mu} \delta_{\rho, \mu} \Big[ \\
 & \bar{v}_4(n_5+1)\bar{v}_5(n_5)e^{-ip'_\mu}\delta_{n_5', n_5}\delta_{n_5'', n_5} + \bar{v}_4(n_5)\bar{v}_5(n_5)e^{-ip''_\mu}\delta_{n_5', n_5+1}\delta_{n_5'', n_5} \\
 & + \bar{v}_4(n_5+1)\bar{v}_5(n_5)\delta_{n_5', n_5}\delta_{n_5'', n_5} + \bar{v}_4(n_5)\bar{v}_5(n_5)\delta_{n_5', n_5+1}\delta_{n_5'', n_5} \Big] \\
 &= -i\beta\gamma\delta_{p'', p'}^{(4)} \Big[ \bar{v}_4(n_5'+1)\bar{v}_5(n_5')\delta_{n_5'', n_5'}e^{-ip'_\rho/2} + \bar{v}_4(n_5'-1)\bar{v}_5(n_5'-1)\delta_{n_5'', n_5'-1}e^{-ip'_\rho/2} \\
 & + \bar{v}_4(n_5'+1)\bar{v}_5(n_5')\delta_{n_5'', n_5'}e^{ip'_\rho/2} + \bar{v}_4(n_5'-1)\bar{v}_5(n_5'-1)\delta_{n_5'', n_5'-1}e^{ip'_\rho/2} \Big] \\
 &= -i\beta\gamma\delta_{p'', p'}^{(4)} \Big[ (\bar{v}_4(n_5'+1)\bar{v}_5(n_5')\delta_{n_5'', n_5'} + \bar{v}_4(n_5'-1)\bar{v}_5(n_5'-1)\delta_{n_5'', n_5'-1}) \\
 & \quad (e^{ip'_\rho/2} + e^{-ip'_\rho/2}) \Big] \\
 &= -2i\beta\gamma\delta_{p'', p'}^{(4)} \cos(p'_\rho/2) \Big[ \delta_{n_5'', n_5'}\bar{v}_4(n_5'+1)\bar{v}_5(n_5') + \delta_{n_5'', n_5'-1}\bar{v}_4(n_5'-1)\bar{v}_5(n_5'-1) \Big]. \tag{C.12}
 \end{aligned}$$

For the case  $\alpha' = A', \alpha'' = A''$  we have

$$\begin{aligned}
 & \frac{\partial^2 S_W}{\partial v_{\rho A'}(n', n'_5)\partial v_{5 A''}(n'', n''_5)} \\
 &= \frac{\partial}{\partial v_{\rho A'}(n', n'_5)} \Big[ -\beta\gamma \sum_{n, n_5; \mu; A} \left( -v_{\mu_0}(n, n_5)v_{5_0}(n+\hat{\mu}, n_5)v_{\mu_A}(n, n_5+1)\delta_{n'', n}\delta_{n_5'', n_5}\delta_{A'', A} \right. \\
 & \quad + v_{\mu_0}(n, n_5)v_{5_0}(n, n_5)v_{\mu_A}(n, n_5+1)\delta_{n'', n+\hat{\mu}}\delta_{n_5'', n_5}\delta_{A'', A} \\
 & \quad + v_{\mu_0}(n, n_5+1)v_{5_0}(n+\hat{\mu}, n_5)v_{\mu_A}(n, n_5)\delta_{n'', n}\delta_{n_5'', n_5}\delta_{A'', A} \\
 & \quad \left. - v_{\mu_0}(n, n_5+1)v_{5_0}(n, n_5)v_{\mu_A}(n, n_5)\delta_{n'', n+\hat{\mu}}\delta_{n_5'', n_5}\delta_{A'', A} \right) \Big] \\
 &= -\beta\gamma \sum_{n, n_5; \mu; A} \delta_{A'', A}\delta_{A', A}\delta_{\rho, \mu} \Big[ -v_{\mu_0}(n, n_5)v_{5_0}(n+\hat{\mu}, n_5)\delta_{n'', n}\delta_{n_5'', n_5}\delta_{n', n}\delta_{n_5', n_5+1} \\
 & \quad + v_{\mu_0}(n, n_5)v_{5_0}(n, n_5)\delta_{n'', n+\hat{\mu}}\delta_{n_5'', n_5}\delta_{n', n}\delta_{n_5', n_5+1} \\
 & \quad + v_{\mu_0}(n, n_5+1)v_{5_0}(n+\hat{\mu}, n_5)\delta_{n'', n}\delta_{n_5'', n_5}\delta_{n', n}\delta_{n_5', n_5} \\
 & \quad \left. - v_{\mu_0}(n, n_5+1)v_{5_0}(n, n_5)\delta_{n'', n+\hat{\mu}}\delta_{n_5'', n_5}\delta_{n', n}\delta_{n_5', n_5} \right]. \tag{C.13}
 \end{aligned}$$

In momentum space this is written as

$$\begin{aligned}
 \tilde{\Delta}_{45}^{(vv)-A} &= -i\beta\gamma\delta_{A',A''}\frac{1}{TL^3}\sum_{n,n_5}e^{i(p'-p'')n}e^{ip'_\rho/2}\sum_{\mu}\delta_{\rho,\mu}\left[ \right. \\
 &\quad -\bar{v}_4(n_5+1)\bar{v}_5(n_5)e^{-ip''_\mu}\delta_{n'_5,n_5}\delta_{n''_5,n_5}+\bar{v}_4(n_5)\bar{v}_5(n_5)e^{-ip''_\mu}\delta_{n'_5,n_5+1}\delta_{n''_5,n_5} \\
 &\quad \left. +\bar{v}_4(n_5+1)\bar{v}_5(n_5)\delta_{n'_5,n_5}\delta_{n''_5,n_5}-\bar{v}_4(n_5)\bar{v}_5(n_5)\delta_{n'_5,n_5+1}\delta_{n''_5,n_5}\right] \\
 &= -i\beta\gamma\delta_{p'',p'}^{(4)}\delta_{A',A''}\left[-\bar{v}_4(n'_5+1)\bar{v}_5(n'_5)\delta_{n''_5,n'_5}e^{-ip'_\rho/2} \right. \\
 &\quad +\bar{v}_4(n'_5-1)\bar{v}_5(n'_5-1)\delta_{n''_5,n'_5-1}e^{-ip'_\rho/2}+\bar{v}_4(n'_5+1)\bar{v}_5(n'_5)\delta_{n''_5,n'_5}e^{ip'_\rho/2} \\
 &\quad \left. -\bar{v}_4(n'_5-1)\bar{v}_5(n'_5-1)\delta_{n''_5,n'_5-1}e^{ip'_\rho/2}\right] \\
 &= -i\beta\gamma\delta_{p'',p'}^{(4)}\delta_{A',A''}\left[\left(e^{ip'_\rho/2}-e^{-ip'_\rho/2}\right) \right. \\
 &\quad \left.\left(\bar{v}_4(n'_5+1)\bar{v}_5(n'_5)\delta_{n''_5,n'_5}-\bar{v}_4(n'_5-1)\bar{v}_5(n'_5-1)\delta_{n''_5,n'_5-1}\right)\right] \\
 &= 2\beta\gamma\delta_{p'',p'}^{(4)}\delta_{A',A''}\sin(p'_\rho/2)\left[\delta_{n''_5,n'_5}\bar{v}_4(n'_5+1)\bar{v}_5(n'_5)-\delta_{n''_5,n'_5-1}\bar{v}_4(n'_5-1)\bar{v}_5(n'_5-1)\right].
 \end{aligned} \tag{C.14}$$

### B.1.3 $\Delta_{54}^{(vv)}$

As before we look first at  $\alpha' = \alpha'' = 0$  contribution

$$\begin{aligned}
 &\frac{\partial^2 S_W}{\partial v_{50}(n',n'_5)\partial v_{\rho_0}(n'',n''_5)} \\
 &= \frac{\partial}{\partial v_{50}(n',n'_5)}\left[-\beta\gamma\sum_{n,n_5;\mu}\left(v_{50}(n+\hat{\mu},n_5)v_{50}(n,n_5)v_{\mu_0}(n,n_5+1)\delta_{n'',n}\delta_{n''_5,n_5}\delta_{\rho,\mu} \right. \right. \\
 &\quad \left. \left. +v_{\mu_0}(n,n_5)v_{50}(n+\hat{\mu},n_5)v_{50}(n,n_5)\delta_{n'',n}\delta_{n''_5,n_5+1}\delta_{\rho,\mu}\right)\right] \\
 &= -\beta\gamma\sum_{n,n_5;\mu}\delta_{\rho,\mu}\left[v_{\mu_0}(n,n_5+1)v_{50}(n+\hat{\mu},n_5)\delta_{n'',n}\delta_{n''_5,n_5}\delta_{n',n}\delta_{n'_5,n_5} \right. \\
 &\quad +v_{\mu_0}(n,n_5+1)v_{50}(n,n_5)\delta_{n'',n}\delta_{n''_5,n_5}\delta_{n',n+\hat{\mu}}\delta_{n'_5,n_5} \\
 &\quad +v_{\mu_0}(n,n_5)\left(v_{50}(n+\hat{\mu},n_5)\delta_{n'',n}\delta_{n''_5,n_5+1}\delta_{n',n}\delta_{n'_5,n_5} \right. \\
 &\quad \left. \left. +v_{50}(n,n_5)\delta_{n'',n}\delta_{n''_5,n_5+1}\delta_{n',n+\hat{\mu}}\delta_{n'_5,n_5}\right)\right].
 \end{aligned} \tag{C.15}$$

In momentum space we get

$$\begin{aligned}
 \tilde{\Delta}_{54}^{(vv)-0} &= i\beta\gamma \frac{1}{TL^3} \sum_{n, n_5} e^{i(p'-p'')n} e^{-ip''/2} \sum_{n_5; \mu} \delta_{\rho, \mu} \left[ \right. \\
 &\quad \bar{v}_4(n_5 + 1) \bar{v}_5(n_5) \delta_{n_5'', n_5} \delta_{n_5', n_5} + \bar{v}_4(n_5 + 1) \bar{v}_5(n_5) \delta_{n_5'', n_5} \delta_{n_5', n_5} e^{ip'_\mu/2} \\
 &\quad \left. + \bar{v}_4(n_5) \bar{v}_5(n_5) \delta_{n_5'', n_5+1} \delta_{n_5', n_5} + \bar{v}_4(n_5) \bar{v}_5(n_5) \delta_{n_5'', n_5+1} \delta_{n_5', n_5} e^{ip'_\mu/2} \right] \\
 &= i\beta\gamma \delta_{p'', p'}^{(4)} \left( \bar{v}_4(n_5' + 1) \bar{v}_5(n_5') \delta_{n_5'', n_5'} + \bar{v}_4(n_5') \bar{v}_5(n_5') \delta_{n_5'', n_5'+1} \right) \left( e^{-ip'_\rho/2} + e^{ip'_\rho/2} \right) \\
 &= 2i\beta\gamma \cos(p'_\rho/2) \left( \bar{v}_4(n_5' + 1) \bar{v}_5(n_5') \delta_{n_5'', n_5'} + \bar{v}_4(n_5') \bar{v}_5(n_5') \delta_{n_5'', n_5'+1} \right). \quad (C.16)
 \end{aligned}$$

For  $\alpha' = A', \alpha'' = A''$  we find

$$\begin{aligned}
 &\frac{\partial^2 S_W}{\partial v_{5A'}(n', n_5') \partial v_{\rho A''}(n'', n_5'')} \\
 &= \frac{\partial}{\partial v_{5A'}(n', n_5')} \left[ -\beta\gamma \sum_{n; n_5; \mu; A} \delta_{A'', A} \delta_{\rho, \mu} \right. \\
 &\quad \left( -v_{5_0}(n + \hat{\mu}, n_5) v_{\mu_0}(n, n_5) v_{5_A}(n, n_5) \delta_{n'', n} \delta_{n_5'', n_5+1} \right. \\
 &\quad + v_{\mu_0}(n, n_5) v_{5_0}(n, n_5) v_{5_A}(n + \hat{\mu}, n_5) \delta_{n'', n} \delta_{n_5'', n_5+1} \\
 &\quad + v_{5_0}(n + \hat{\mu}, n_5) v_{\mu_0}(n, n_5 + 1) v_{5_A}(n, n_5) \delta_{n'', n} \delta_{n_5'', n_5} \\
 &\quad \left. \left. - v_{5_A}(n + \hat{\mu}, n_5) v_{\mu_0}(n, n_5 + 1) v_{5_0}(n, n_5) \delta_{n'', n} \delta_{n_5'', n_5} \right) \right] \\
 &= -\beta\gamma \sum_{n; n_5; \mu' A} \delta_{\rho, \mu} \delta_{A'', A} \delta_{A', A} \left[ -v_{\mu_0}(n, n_5) v_{5_0}(n + \hat{\mu}, n_5) \delta_{n'', n} \delta_{n_5'', n_5+1} \delta_{n', n} \delta_{n_5', n_5} \right. \\
 &\quad + v_{\mu_0}(n, n_5) v_{5_0}(n, n_5) \delta_{n'', n} \delta_{n_5'', n_5+1} \delta_{n', n+\hat{\mu}} \delta_{n_5', n_5} \\
 &\quad + v_{\mu_0}(n, n_5 + 1) v_{5_0}(n + \hat{\mu}, n_5) \delta_{n'', n} \delta_{n_5'', n_5} \delta_{n', n} \delta_{n_5', n_5} \\
 &\quad \left. - v_{\mu_0}(n, n_5 + 1) v_{5_0}(n, n_5) \delta_{n'', n} \delta_{n_5'', n_5} \delta_{n', n+\hat{\mu}} \delta_{n_5', n_5} \right]. \quad (C.17)
 \end{aligned}$$

In momentum space this is given by

$$\begin{aligned}
 \tilde{\Delta}_{54}^{(vv)-A} &= i\beta\gamma \frac{1}{TL^3} \sum_{n, n_5} e^{i(p'-p'')n} e^{-ip''/2} \delta_{A'', A'} \sum_{n_5; \mu} \delta_{\rho, \mu} \left[ \right. \\
 &\quad \bar{v}_4(n_5 + 1) \bar{v}_5(n_5) \delta_{n_5'', n_5} \delta_{n_5', n_5} - \bar{v}_4(n_5 + 1) \bar{v}_5(n_5) \delta_{n_5'', n_5} \delta_{n_5', n_5} e^{ip'_\mu/2} \\
 &\quad \left. - \bar{v}_4(n_5) \bar{v}_5(n_5) \delta_{n_5'', n_5+1} \delta_{n_5', n_5} + \bar{v}_4(n_5) \bar{v}_5(n_5) \delta_{n_5'', n_5+1} \delta_{n_5', n_5} e^{ip'_\mu/2} \right] \\
 &= i\beta\gamma \delta_{p'', p'}^{(4)} \delta_{A'', A'} \left[ \bar{v}_4(n_5' + 1) \bar{v}_5(n_5') \delta_{n_5'', n_5'} \left( e^{-ip'_\rho/2} - e^{ip'_\rho/2} \right) \right.
 \end{aligned}$$

$$\begin{aligned}
 & + \bar{v}_4(n'_5) \bar{v}_5(n'_5) \delta_{n''_5, n'_5+1} (e^{ip'_\rho/2} - e^{-ip'_\rho/2}) \\
 & = 2\beta\gamma \delta_{p''_5, p'_5}^{(4)} \delta_{A'', A'} \sin(p'_\rho/2) \left( \bar{v}_4(n'_5 + 1) \bar{v}_5(n'_5) \delta_{n''_5, n'_5} - \bar{v}_4(n'_5) \bar{v}_5(n'_5) \delta_{n''_5, n'_5+1} \right).
 \end{aligned} \tag{C.18}$$

### B.1.4 $\Delta_{55}^{(vv)}$

For  $\alpha' = 0, \alpha'' = 0$  we find

$$\begin{aligned}
 & \frac{\partial^2 S_W}{\partial v_{50}(n', n'_5) \partial v_{50}(n'', n''_5)} \\
 & = \frac{\partial}{\partial v_{50}(n', n'_5)} \left[ -\beta\gamma \sum_{n; n_5; \mu} \left( v_{\mu_0}(n, n_5) v_{\mu_0}(n, n_5 + 1) v_{50}(n + \hat{\mu}, n_5) \delta_{n'', n} \delta_{n''_5, n_5} \right. \right. \\
 & \quad \left. \left. + v_{\mu_0}(n, n_5) v_{\mu_0}(n, n_5 + 1) v_{50}(n, n_5) \delta_{n'', n+\hat{\mu}} \delta_{n''_5, n_5} \right) \right] \\
 & = -\beta\gamma \sum_{n; n_5; \mu} \left[ v_{\mu_0}(n, n_5) v_{\mu_0}(n, n_5 + 1) \delta_{n'', n} \delta_{n''_5, n_5} \delta_{n', n+\hat{\mu}} \delta_{n'_5, n_5} \right. \\
 & \quad \left. + v_{\mu_0}(n, n_5) v_{\mu_0}(n, n_5 + 1) \delta_{n'', n+\hat{\mu}} \delta_{n''_5, n_5} \delta_{n', n} \delta_{n'_5, n_5} \right].
 \end{aligned} \tag{C.19}$$

In momentum space this becomes

$$\begin{aligned}
 \tilde{\Delta}_{55}^{(vv)-0} & = -\beta\gamma \delta_{p''_5, p'_5}^{(4)} \sum_{\mu} \left[ \bar{v}_4(n'_5) \bar{v}_4(n'_5 + 1) \left( e^{ip'_\mu} \delta_{n''_5, n'_5} + e^{-ip'_\mu} \delta_{n''_5, n'_5} \right) \right] \\
 & = -2\beta\gamma \bar{v}_4(n'_5) \bar{v}_4(n'_5 + 1) \delta_{n''_5, n'_5} \sum_{\mu} \cos(p'_\mu).
 \end{aligned} \tag{C.20}$$

Finally, the contribution when  $\alpha' = A', \alpha'' = A''$  is found to be

$$\begin{aligned}
 & \frac{\partial^2 S_W}{\partial v_{5A'}(n', n'_5) \partial v_{5A''}(n'', n''_5)} \\
 & = \frac{\partial}{\partial v_{5A'}(n', n'_5)} \left[ -\beta\gamma \sum_{n, n_5; \mu; A} \left( v_{\mu_0}(n, n_5) v_{\mu_0}(n, n_5 + 1) v_{5A}(n + \hat{\mu}, n_5) \delta_{n'', n} \delta_{n''_5, n_5} \delta_{A'', A} \right. \right. \\
 & \quad \left. \left. + v_{\mu_0}(n, n_5) v_{\mu_0}(n, n_5 + 1) v_{5A}(n, n_5) \delta_{n'', n+\hat{\mu}} \delta_{n''_5, n_5} \delta_{A'', A'} \right) \right] \\
 & = -\beta\gamma \sum_{n, n_5; \mu; A} \delta_{A'', A'} \delta_{A', A} \left[ v_{\mu_0}(n, n_5) v_{\mu_0}(n, n_5 + 1) \delta_{n'', n} \delta_{n''_5, n_5} \delta_{n', n+\hat{\mu}} \delta_{n'_5, n_5} \right. \\
 & \quad \left. + v_{\mu_0}(n, n_5) v_{\mu_0}(n, n_5 + 1) \delta_{n'', n+\hat{\mu}} \delta_{n''_5, n_5} \delta_{n', n} \delta_{n'_5, n_5} \right].
 \end{aligned} \tag{C.21}$$

In momentum space this becomes

$$\begin{aligned}\tilde{\Delta}_{55}^{(vv)-A} &= -\beta\gamma\delta_{p'',p'}^{(4)}\delta_{A'',A'}\sum_{\mu}\left[\bar{v}_4(n'_5)\bar{v}_4(n'_5+1)\left(e^{ip'_\mu}\delta_{n''_5,n'_5}+e^{-ip''_\mu}\delta_{n''_5,n'_5}\right)\right] \\ &= -2\beta\gamma\delta_{A'',A'}\bar{v}_4(n'_5)\bar{v}_4(n'_5+1)\delta_{n''_5,n'_5}\sum_{\mu}\cos(p'_\mu).\end{aligned}\quad (\text{C.22})$$

## C.2 Auxiliary field contribution (H field)

Here we show the derivations of  $\Delta_{44}^{(hh)}$  and  $\Delta_{55}^{(hh)}$ . As for the case of  $\Delta^{(vv)}$  we derive final expressions for the cases of  $\alpha' = \alpha'' = 0$  and  $\alpha' = A', \alpha'' = A''$  separately for each term.

### B.2.1 $\Delta_{44}^{(hh)}$ considering $M' = M'' = \mu$

The contribution to this kernel comes from equation

$$u_4(H_\mu(n, n_5)) = -\ln\left(\frac{2}{\rho_\mu(n, n_5)}I_1(\rho_\mu(n, n_5))\right)\quad (\text{C.23})$$

where  $I_1$  is the modified bessel function of the first kind and  $\rho_\mu$  is given by

$$\rho_\mu(n, n_5) = \sqrt{[\text{Re}(h_{\mu_0}(n, n_5))]^2 + \sum_A [\text{Re}(h_{\mu_A}(n, n_5))]^2}.\quad (\text{C.24})$$

Then we evaluate the second derivative as following

$$\begin{aligned}&\frac{\partial^2 S}{\partial h_{\mu'_{\alpha'}}(n', n'_5)\partial h_{\mu''_{\alpha''}}(n'', n''_5)} \\ &= \frac{\partial}{\partial h_{\mu'_{\alpha'}}(n', n'_5)}\left[\sum_{n, n_5}\delta_{n, n''}\delta_{n_5, n''_5}\delta_{\alpha, \alpha''}\delta_{\mu', \mu''}(u_4(\rho_\mu(n, n_5))' + v_\alpha)\right] \\ &= \sum_n\delta_{n', n''}\delta_{n', n}\delta_{\mu', \mu''}\sum_{n_5}\delta_{n_5, n''_5}\delta_{n_5, n'_5}\delta_{\alpha', \alpha''}\left[\delta_{\alpha', 0}\frac{(u_4(\rho_\mu(n, n_5))')}{\rho_\mu(n, n_5)}\right. \\ &\quad \left.+ (1 - \delta_{\alpha', 0})\left[\frac{u_4(\rho_\mu(n, n_5))'}{\rho_\mu(n, n_5)} + \rho_\mu(n, n_5)\left(\frac{u_4(\rho_\mu(n, n_5))'}{\rho_\mu(n, n_5)}\right)'\right]\right]\end{aligned}\quad (\text{C.25})$$

and in momentum space we get

$$\begin{aligned} \tilde{\Delta}_{44}^{(hh)} &= \delta_{p,p'}^{(4)} \delta_{\mu',\mu''} \delta_{n'_5,n''_5} \delta_{\alpha',\alpha''} \left[ (1 - \delta_{\alpha',0}) \frac{(u_4(\rho_\mu(n'_5)))'}{\rho_\mu(n_5)} \right. \\ &\quad \left. + \delta_{\alpha',0} \left[ \frac{u_4(\rho_\mu(n'_5))'}{\rho_\mu(n'_5)} + \rho_\mu(n'_5) \left( \frac{u_4(\rho_\mu(n'_5))'}{\rho_\mu(n'_5)} \right)' \right] \right] \Big|_{\rho_4(n'_5)=\bar{h}_4(n'_5)}. \end{aligned} \quad (\text{C.26})$$

For  $\alpha' = 0$  and  $\alpha'' = 0$

$$\tilde{\Delta}_{44}^{(hh)-0} = \delta_{p',p''}^{(4)} \delta_{n'_5,n''_5} \left[ -\frac{2}{(\bar{h}_4(n'_5))^2} - 1 - \frac{1}{\bar{h}_4(n'_5)} \frac{I_0(\bar{h}_4(n'_5))}{I_1(\bar{h}_4(n'_5))} + \left( \frac{I_0(\bar{h}_4(n'_5))}{I_1(\bar{h}_4(n'_5))} \right)^2 \right]. \quad (\text{C.27})$$

For  $\alpha' = A'$  and  $\alpha'' = A''$

$$\tilde{\Delta}_{44}^{(hh)-A} = \delta_{p',p''}^{(4)} \delta_{n'_5,n''_5} \left[ \frac{2}{(\bar{h}_4(n'_5))^2} - \frac{1}{\bar{h}_4(n'_5)} \frac{I_0(\bar{h}_4(n'_5))}{I_1(\bar{h}_4(n'_5))} \right]. \quad (\text{C.28})$$

### B.2.2 $\Delta_{55}^{(hh)}$ considering $M' = M'' = 5$

In this case we consider derivatives in the fifth direction. We recall that the relevant part of the action contains the function  $u_5$  which is given in Eq. (4.14) and we find  $\Delta_{55}^{(hh)}$  to be

$$\begin{aligned} &\frac{\partial^2 S}{\partial h_{5\alpha'}(n', n'_5) \partial h_{5\alpha''}(n'', n''_5)} \Big|_{\rho_5(n_5)=\bar{h}_5(n_5)} \\ &= \frac{\partial}{\partial h_{5\alpha'}(n', n'_5)} \left[ \sum_n \delta_{n,n''} \sum_{n_5} \delta_{n_5,n''_5} \delta_{\alpha,\alpha''} [u_5(\rho_5(n, n_5) \sqrt{f(n_5)})' + v_{5\alpha}] \right] \\ &= \sum_n \delta_{n',n} \delta_{n',n''} \sum_{n_5} \delta_{n_5,n''_5} \delta_{\alpha',\alpha''} \left[ (1 - \delta_{\alpha',0}) \frac{(u_5(\rho_5(n_5) \sqrt{f(n_5)})')}{\rho_5(n_5) \sqrt{f(n_5)}} \right. \\ &\quad \left. + \delta_{\alpha',0} \left[ \frac{(u_5(\rho_5(n_5)))'}{\rho_5(n_5) \sqrt{f(n_5)}} + \rho_5 \left( \frac{(u_5(\rho_5(n_5)))'}{\rho_5(n_5) \sqrt{f(n_5)}} \right)' \right] \right] \Big|_{\rho_5(n_5)=\bar{h}_5(n_5)}. \end{aligned} \quad (\text{C.29})$$



In momentum space this is given by

$$\begin{aligned} \tilde{\Delta}_{55}^{(hh)} &= \delta_{p,p'}^{(4)} \delta_{n'_5, n''_5} \delta_{\alpha', \alpha''} \left[ (1 - \delta_{\alpha', 0}) \frac{(u_5(\rho_5(n'_5)) \sqrt{f(n'_5)})')}{\rho_5(n'_5) \sqrt{f(n'_5)}} \right. \\ &\quad \left. + \delta_{\alpha', 0} \left[ \frac{u_5(\rho_5(n'_5)) \sqrt{f(n'_5)})'}{\rho_5(n'_5) \sqrt{f(n'_5)}} + \rho_5 \sqrt{f(n'_5)} \left( \frac{u_5(\rho_5(n'_5)) \sqrt{f(n'_5)})'}{\rho_5(n'_5) \sqrt{f(n'_5)}} \right)' \right] \right] \Big|_{\rho_5(n'_5) = \bar{h}_5(n'_5)}. \end{aligned} \quad (C.30)$$

By explicitly evaluating the derivatives of  $u_5$  we find the following expressions considering separately the cases of  $\alpha' = \alpha'' = 0$  and  $\alpha' = A; \alpha = A''$ .

For  $\alpha' = 0$  and  $\alpha'' = 0$  we have

$$\begin{aligned} \tilde{\Delta}_{55}^{(hh)-0} &= \delta_{p', p''}^{(4)} \delta_{n'_5, n''_5} \left[ - \frac{2}{(\bar{h}_{50}(n'_5))^2} - \frac{\sqrt{f(n'_5)} I_0(\bar{h}_{50}(n'_5)) \sqrt{f(n'_5)}}{\bar{h}_{50}(n'_5) I_1(\bar{h}_{50}(n'_5)) \sqrt{f(n'_5)}} \right. \\ &\quad \left. - f(n'_5) + f(n'_5) \left( \frac{I_0(\bar{h}_{50}(n'_5)) \sqrt{f(n'_5)}}{I_1(\bar{h}_{50}(n'_5)) \sqrt{f(n'_5)}} \right)^2 \right]. \end{aligned} \quad (C.31)$$

For  $\alpha' = A'$  and  $\alpha'' = A''$  we get

$$\tilde{\Delta}_{55}^{(hh)-A} = \delta_{p', p''}^{(4)} \delta_{n'_5, n''_5} \left[ \frac{2}{(\bar{h}_{50}(n'_5))^2} - \frac{\sqrt{f(n'_5)} I_0(\bar{h}_{50}(n'_5)) \sqrt{f(n'_5)}}{\bar{h}_{50}(n'_5) I_1(\bar{h}_{50}(n'_5)) \sqrt{f(n'_5)}} \right]. \quad (C.32)$$

## C.3 Gauge fixing contribution

We recall that the gauge-fixing action is given by Eq. (4.22). Depending on the direction we have four different contributions in this kernel which are found to be as following

### B.3.1 $\Delta_{44}^{(gf)}$ considering $M' = \sigma, M'' = \rho$

$$\Delta_{44}^{(gf)} = \frac{\partial^2 S_{gf}}{\partial v_{\sigma A'}(n', n'_5) \partial v_{\rho A''}(n'', n''_5)}$$

$$\begin{aligned}
 &= \frac{\partial}{\partial v_{\sigma A'}(n'', n''_5)} \sum_{n, n_5; \mu} \delta_{\rho, \mu} \left[ \frac{1}{\xi} \sum_A \delta_{A'', A} (\delta_{n'', n} \delta_{n''_5, n_5} - \delta_{n'', n-\hat{\mu}} \delta_{n''_5, n_5}) \right. \\
 &\quad \left. \left[ \sum_{\mu} f_{\mu A}(n, n_5) + \gamma f_{5A}(n, n_5) \right] \right] \\
 &= \frac{1}{\xi} \delta_{A', A''} \sum_{n, n_5} \left( \delta_{n'', n} \delta_{n''_5, n_5} - \delta_{n'', n-\hat{\rho}} \delta_{n''_5, n_5} \right) \left( \delta_{n', n} \delta_{n'_5, n_5} - \delta_{n', n-\hat{\sigma}} \delta_{n'_5, n_5} \right).
 \end{aligned} \tag{C.33}$$

Thus,

$$\begin{aligned}
 \tilde{\Delta}_{44}^{(gf)} &= \frac{1}{\xi} \delta_{p', p''}^{(4)} \delta_{A', A''} e^{ip'_\sigma/2} e^{-ip'_\rho/2} \left[ 1 - e^{-ip'_\sigma} - e^{ip'_\rho} + e^{-ip'_\sigma} e^{ip'_\rho} \right] \delta_{n''_5, n'_5} \\
 &= \frac{1}{\xi} \delta_{p', p''}^{(4)} \delta_{A', A''} \left[ - (2i \sin(p'_\rho/2)) (2i \sin(p'_\sigma/2)) \right] \delta_{n''_5, n'_5} \\
 &= \frac{1}{\xi} \hat{p}'_\rho \hat{p}'_\sigma \delta_{p', p''}^{(4)} \delta_{A', A''} \delta_{n''_5, n'_5}.
 \end{aligned} \tag{C.34}$$

### B.3.2 $\Delta_{45}^{(gf)}$ considering $M' = \rho, M'' = 5$

$$\begin{aligned}
 \Delta_{45}^{(gf)} &= \frac{\partial^2 S_{gf}}{\partial v_{\rho A'}(n', n'_5) \partial v_{5 A''}(n'', n''_5)} \\
 &= \frac{\partial}{\partial v_{\rho A'}(n', n'_5)} \sum_{n, n_5; \mu} \left[ \frac{\gamma}{\xi} \sum_A \delta_{A, A''} (\delta_{n'', n} \delta_{n''_5, n_5} - \delta_{n'', n} \delta_{n''_5, n_5-1}) \right. \\
 &\quad \left. \left[ \sum_{\mu} f_{\mu A}(n, n_5) + \gamma f_{5A}(n, n_5) \right] \right] \\
 &= \frac{\gamma}{\xi} \delta_{A', A''} \sum_{n, n_5} \delta_{\rho, \mu} \left( \delta_{n'', n} \delta_{n''_5, n_5} - \delta_{n'', n} \delta_{n''_5, n_5-1} \right) \left( \delta_{n', n} \delta_{n'_5, n_5} - \delta_{n', n-\hat{\mu}} \delta_{n'_5, n_5} \right).
 \end{aligned} \tag{C.35}$$

Therefore,

$$\begin{aligned}
 \tilde{\Delta}_{45}^{(gf)} &= \frac{i\gamma}{\xi} \delta_{p', p''}^{(4)} \delta_{A', A''} e^{ip'_\rho/2} \left( 1 - e^{-ip'_\rho} \right) \sum_{n_5} \left[ \delta_{n'_5, n''_5} \delta_{n'_5, n_5} - \delta_{n'_5, n_5-1} \delta_{n''_5, n_5+1} \right] \\
 &= \frac{-\gamma}{\xi} \delta_{p', p''}^{(4)} \hat{p}'_\rho \delta_{A', A''} \sum_{n_5} \left[ \delta_{n'_5, n''_5} \delta_{n'_5, n_5} - \delta_{n'_5, n_5-1} \delta_{n''_5, n_5+1} \right].
 \end{aligned} \tag{C.36}$$

**B.3.3**  $\Delta_{54}^{(gf)}$  considering  $M' = 5, M'' = \rho$ 

$$\begin{aligned}
 \Delta_{54}^{(gf)} &= \frac{\partial^2 S_{gf}}{\partial v_{5A'}(n', n'_5) \partial v_{\rho A''}(n'', n''_5)} \\
 &= \frac{\partial}{\partial v_{5A'}(n', n'_5)} \sum_{n, n_5; \mu} \delta_{\rho, \mu} \left[ \frac{1}{\xi} \sum_A \delta_{A, A''} \left( \delta_{n'', n} \delta_{n''_5, n_5} - \delta_{n'', n-\hat{\mu}} \delta_{n''_5, n_5} \right) \right. \\
 &\quad \left. \left[ \sum_{\mu} f_{\mu A}(n, n_5) + \gamma f_{5A}(n, n_5) \right] \right] \\
 &= \frac{\gamma}{\xi} \delta_{A', A''} \sum_{n, n_5} \left( \delta_{n'', n} \delta_{n''_5, n_5} - \delta_{n'', n-\hat{\rho}} \delta_{n''_5, n_5} \right) \left( \delta_{n', n} \delta_{n'_5, n_5} - \delta_{n', n} \delta_{n'_5, n_5-1} \right).
 \end{aligned} \tag{C.37}$$

Thus,

$$\begin{aligned}
 \tilde{\Delta}_{54}^{(gf)} &= \frac{(-i)\gamma}{\xi} \delta_{p', p''}^{(4)} \delta_{A', A''} e^{-ip'_\rho/2} \left( 1 - e^{ip'_\rho} \right) \sum_{n_5} \left( \delta_{n'_5, n_5} \delta_{n'_5, n_5} - \delta_{n'_5, n_5-1} \delta_{n'_5, n_5} \right) \\
 &= \frac{-\gamma}{\xi} \delta_{p', p''}^{(4)} \hat{p}'_\rho \delta_{A', A''} \sum_{n_5} \left( \delta_{n'_5, n_5} \delta_{n'_5, n_5} - \delta_{n'_5, n_5-1} \delta_{n'_5, n'_5+1} \right).
 \end{aligned} \tag{C.38}$$

**B.3.4**  $\Delta_{55}^{(gf)}$  considering  $M' = M'' = 5$ 

$$\begin{aligned}
 \Delta_{55}^{(gf)} &= \frac{\partial^2 S_{gf}}{\partial v_{5A'}(n', n'_5) \partial v_{5A''}(n'', n''_5)} \\
 &= \frac{\partial}{\partial v_{5A'}(n', n'_5)} \left[ \frac{\gamma}{\xi} \sum_n \delta_{n, n''} \sum_{n_5} \sum_A \delta_{A, A''} \left( \delta_{n_5, n''_5} - \delta_{n_5-1, n''_5} \right) \right. \\
 &\quad \left. \left[ \sum_{\mu} f_{\mu A}(n, n_5) + \gamma f_{5A}(n, n_5) \right] \right] \\
 &= \frac{\gamma^2}{\xi} \sum_n \delta_{n, n''} \delta_{n, n'} \delta_{A'', A'} \sum_{n_5} \left( \delta_{n_5, n''_5} - \delta_{n_5-1, n''_5} \right) \left( \delta_{n_5, n'_5} - \delta_{n_5-1, n'_5} \right).
 \end{aligned} \tag{C.39}$$

Thus,

$$\tilde{\Delta}_{55}^{(gf)} = \frac{\gamma^2}{\xi} \delta_{p',p''}^{(4)} \delta_{A',A''} \sum_{n_5} \left( \delta_{n_5',n_5''} \delta_{n_5,n_5'} + \delta_{n_5',n_5''} \delta_{n_5-1,n_5'} - \delta_{n_5'+1,n_5''} \delta_{n_5-1,n_5'} - \delta_{n_5'-1,n_5''} \delta_{n_5,n_5'} \right). \quad (\text{C.40})$$

## C.4 Faddeev-Popov Determinant

For the free energy it is necessary to find the Faddeev-Popov determinant. We know that the ghost action is given by

$$S_{FP} = \sum_{A',A''} \sum_{n',n''} \sum_{n_5',n_5''} \bar{c}^{A'}(n', n_5') \mathcal{M}_{A',n',n_5';A'',n'',n_5''} c^{A''}(n'', n_5'') \quad (\text{C.41})$$

where the ghost kernel is obtained summing over all directions

$$\mathcal{M}_{A',n',n_5';A'',n'',n_5''} = \sum_{\mu} \mathcal{M}_{A',n',n_5';A'',n'',n_5''}^{(\mu)} + \gamma \mathcal{M}_{A',n',n_5';A'',n'',n_5''}^{(5)}. \quad (\text{C.42})$$

To determine this ghost kernel, and therefore the Faddeev-Popov determinant, we need to find the infinitesimal gauge transformations on the gauge fixing functions given in Eq. (4.23) and Eq. (4.24) since

$$\delta f_{M_{A'}}(n', n_5') = \sum_{n'',n_5'';A''} \mathcal{M}_{A',n',n_5';A'',n'',n_5''}^{(M)} \omega^{A''}(n'', n_5''). \quad (\text{C.43})$$

To find these we first need to extract the gauge transformation rules on the links of our system. We recall that, generally, links transform as

$$U_{\mu}(n, n_5) \rightarrow \Omega(n, n_5) U_{\mu}(n, n_5) \Omega^{\dagger}(n + \hat{\mu}, n_5) \quad (\text{C.44})$$

$$U_5(n, n_5) \rightarrow \Omega(n, n_5) U_5(n, n_5) \Omega^{\dagger}(n, n_5 + 1) \quad (\text{C.45})$$

where  $\Omega(n, n_5)$  is a gauge transformation that can be parametrized as

$$\Omega(n, n_5) = e^{i\omega^A(n, n_5)\sigma^A} = 1 + i\omega^A(n, n_5)\sigma^A. \quad (\text{C.46})$$

Then we determine the rules as following

$$\begin{aligned}
 & \delta v_{\mu_0}(n, n_5) + i\delta v_{\mu_A}(n, n_5)\sigma^A \\
 &= \Omega(n, n_5)(v_{\mu_0}(n, n_5) + iv_{\mu_A}(n, n_5)\sigma^A)\Omega^\dagger(n + \hat{\mu}, n_5) - (v_{\mu_0}(n, n_5) + iv_{\mu_A}(n, n_5)\sigma^A) \\
 &= (1 + i\omega^B(n, n_5)\sigma^B)(v_{\mu_0}(n, n_5) + iv_{\mu_A}(n, n_5)\sigma^A)(1 - i\omega^C(n + \hat{\mu}, n_5)\sigma^C) \\
 &\quad - (v_{\mu_0}(n, n_5) + iv_{\mu_A}(n, n_5)\sigma^A) \\
 &= i\omega^B(n, n_5)\sigma^B v_{\mu_0}(n, n_5) - \omega^B(n, n_5)\sigma^B v_{\mu_A}(n, n_5)\sigma^A - iv_{\mu_0}(n, n_5)\omega^B(n + \hat{\mu}, n_5)\sigma^B \\
 &\quad + v_{\mu_A}\omega^B(n + \hat{\mu}, n_5)\sigma^A\sigma^B \\
 &= iv_{\mu_0}(n, n_5)\sigma^B(\omega^B(n, n_5) - \omega^B(n + \hat{\mu})) \\
 &\quad + v_{\mu_A}(n, n_5)(\omega^B(n + \hat{\mu}, n_5)\sigma^A\sigma^B - \omega^B(n, n_5)\sigma^B\sigma^A) \\
 &= -iv_{\mu_0}(n, n_5)(\omega^A(n + \hat{\mu}, n_5) - \omega^A(n, n_5))\sigma^A \\
 &\quad + v_{\mu_A}(n, n_5)\left[\omega^B(n + \hat{\mu}, n_5)(\delta^{AB}\mathbb{1} + i\epsilon^{ABC}\sigma^C) - \omega^B(n, n_5)(\delta^{BA}\mathbb{1} + i\epsilon^{BAC}\sigma^C)\right] \\
 &= -iv_{\mu_0}(n, n_5)(\omega^A(n + \hat{\mu}) - \omega^A(n, n_5))\sigma^A + v_{\mu_A}(n, n_5)(\omega^A(n + \hat{\mu}) - \omega^A(n, n_5)) \\
 &\quad + iv_{\mu_C}(n, n_5)\left[\omega^B(n + \hat{\mu})\epsilon^{CBA}\sigma^A - \omega^B(n, n_5)\epsilon^{BCA}\sigma^A\right] \\
 &= v_{\mu_A}(n, n_5)(\omega^A(n + \hat{\mu}, n_5) - \omega^A(n, n_5)) + i\left[-v_{\mu_0}(n, n_5)(\omega^A(n + \hat{\mu}, n_5) - \omega^A(n, n_5))\right. \\
 &\quad \left. - v_{\mu_C}(n, n_5)\epsilon^{ABC}(\omega^B(n + \hat{\mu}) + \omega^B(n, n_5))\right]\sigma^A. \tag{C.47}
 \end{aligned}$$

To sum up the gauge transformations of links along the usual four dimensions read as

$$\begin{aligned}
 \delta v_{\mu_0}(n, n_5) &= v_{\mu_A}(n, n_5)\left(\omega^A(n + \hat{\mu}, n_5) - \omega^A(n, n_5)\right) \\
 \delta v_{\mu_C}(n, n_5) &= -v_{\mu_0}(n, n_5)\left(\omega^C(n + \hat{\mu}, n_5) - \omega^C(n, n_5)\right) \\
 &\quad - \epsilon^{ABC}v_{\mu_B}(n, n_5)\left(\omega^A(n + \hat{\mu}, n_5) + \omega^A(n, n_5)\right) \tag{C.48}
 \end{aligned}$$

and along the extra dimension as

$$\begin{aligned}
 \delta v_{5_0}(n, n_5) &= v_{5_A}(n, n_5)\left(\omega^A(n, n_5 + 1) - \omega^A(n, n_5)\right) \\
 \delta v_{5_C}(n, n_5) &= -v_{5_0}(n, n_5)\left(\omega^C(n, n_5 + 1) - \omega^C(n, n_5)\right) \\
 &\quad - \epsilon^{ABC}v_{5_B}(n, n_5)\left(\omega^A(n, n_5 + 1) + \omega^A(n, n_5)\right). \tag{C.49}
 \end{aligned}$$

Now we apply the above transformations to Eq. (C.43) for directions along the four-dimensional space and the fifth direction. We omit the terms that vanish when they are evaluated at the mean-field background.

We start with links along a  $\mu$  direction

$$\begin{aligned}
 \delta f_{\mu_{A'}} &= \sum_{n'; n'_5; A'} \delta v_{\mu'_A}(n', n'_5) - \delta v_{\mu'_A}(n' - \hat{\mu}, n'_5) \\
 &= \sum_{n'; n'_5; A'} \left[ -v_{\mu_0}(n', n'_5) (\omega^{A'}(n' + \hat{\mu}, n'_5) - \omega^{A'}(n', n'_5)) \right. \\
 &\quad \left. + v_{\mu_0}(n' - \hat{\mu}, n'_5) (\omega^{A'}(n', n'_5) - \omega^{A'}(n' - \hat{\mu}, n'_5)) \right] \\
 &= \sum_{n'; n'_5; A'} \delta^{A', A''} \delta_{n'_5, n''_5} \left[ -v_{\mu_0}(n', n'_5) (\delta_{n'+\hat{\mu}, n''} - \delta_{n', n''}) \right. \\
 &\quad \left. + v_{\mu_0}(n' - \hat{\mu}, n'_5) (\delta_{n', n''} - \delta_{n'-\hat{\mu}, n''}) \right] \omega^{A''}(n'', n''_5) \\
 &= \sum_{n'; n'_5; A'} \delta^{A', A''} \delta_{n'_5, n''_5} \bar{v}_4(n'_5) \left( 2\delta_{n', n''} - \delta_{n'+\hat{\mu}, n''} - \delta_{n'-\hat{\mu}, n''} \right) \omega^{A''}(n'', n''_5)
 \end{aligned} \tag{C.50}$$

where in the last line we evaluated the expression in the mean-field background. In momentum space this is given by

$$\tilde{\delta} f_{\mu_{A'}} = \sum_{n'_5; A'} \delta^{A', A''} \delta_{n'_5, n''_5} \bar{v}_4(n'_5) \delta_{p', p''}^{(4)} \hat{p}'_{\mu}{}^2 \omega^{A''}(n'', n''_5). \tag{C.51}$$

Therefore,

$$\mathcal{M}_{A', p', n'_5; A'', p'', n''_5}^{(\mu)} = \sum_{n'_5; A'} \delta^{A', A''} \delta_{n'_5, n''_5} \bar{v}_4(n'_5) \delta_{p', p''}^{(4)} \hat{p}'_{\mu}{}^2. \tag{C.52}$$

The same is repeated for links along the extra dimension

$$\begin{aligned}
 \delta f_{5_{A'}} &= \sum_{n'; n'_5; A'} \delta v_{5'_A}(n', n'_5) - \delta v_{5'_A}(n', n'_5 - 1) \\
 &= \sum_{n'; n'_5; A'} \left[ -v_{5_0}(n', n'_5) (\omega^{A'}(n', n'_5 + 1) - \omega^{A'}(n', n'_5)) \right. \\
 &\quad \left. + v_{5_0}(n', n'_5 - 1) (\omega^{A'}(n', n'_5) - \omega^{A'}(n', n'_5 - 1)) \right]
 \end{aligned}$$

$$\begin{aligned}
 &= \sum_{n'; n'_5; A'} \delta^{A', A''} \delta_{n', n''} \left[ -v_{50}(n', n'_5) (\delta_{n'_5+1, n''_5} - \delta_{n'_5, n''_5}) \right. \\
 &\quad \left. + v_{50}(n', n'_5 - 1) (\delta_{n'_5, n''_5} - \delta_{n'_5-1, n''_5}) \right] \omega^{A''}(n'', n''_5) \\
 &= \sum_{n'; n'_5; A'} \delta^{A', A''} \delta_{n', n''} \left[ \delta_{n'_5, n''_5} (\bar{v}_5(n'_5) + \bar{v}_5(n'_5 - 1)) - \bar{v}_5(n'_5) \delta_{n'_5+1, n''_5} \right. \\
 &\quad \left. - \bar{v}_5(n'_5 - 1) \delta_{n'_5-1, n''_5} \right] \omega^{A''}(n'', n''_5). \tag{C.53}
 \end{aligned}$$

As before, in the last line we evaluated the expression at the mean-field values. In momentum space this is given by

$$\begin{aligned}
 \tilde{\delta} f_{5, A'} = \sum_{n'_5; A'} \delta^{A', A''} \delta_{p', p''}^{(4)} \left[ \delta_{n'_5, n''_5} (\bar{v}_5(n'_5) + \bar{v}_5(n'_5 - 1)) \right. \\
 \left. - \bar{v}_5(n'_5) \delta_{n'_5+1, n''_5} - \bar{v}_5(n'_5 - 1) \delta_{n'_5-1, n''_5} \right] \omega^{A''}(n'', n''_5). \tag{C.54}
 \end{aligned}$$

Therefore,

$$\begin{aligned}
 \mathcal{M}_{A', p', n'_5; A'', p'', n''_5}^{(5)} = \sum_{n'_5; A'} \delta^{A', A''} \delta_{p', p''}^{(4)} \left[ \delta_{n'_5, n''_5} (\bar{v}_{50}(n'_5) + \bar{v}_{50}(n'_5 - 1)) \right. \\
 \left. - \bar{v}_{50}(n'_5) \delta_{n'_5+1, n''_5} - \bar{v}_{50}(n'_5 - 1) \delta_{n'_5-1, n''_5} \right]. \tag{C.55}
 \end{aligned}$$

Finally, putting everything together, the Faddeev-Popov determinant that needs to be included in the first-order corrections to the free energy is given by

$$\tilde{D}_{FP} = \det \left[ \mathcal{M}_{A', p', n'_5; A'', p'', n''_5} \right] = \det \left[ \sum_{\mu} \mathcal{M}_{A', p', n'_5; A'', p'', n''_5}^{(\mu)} + \gamma \mathcal{M}_{A', p', n'_5; A'', p'', n''_5}^{(5)} \right]. \tag{C.56}$$

# Appendix D

## Derivations of expressions for observables in the Mean-Field Approach

Here, we fill in the gaps in the full derivation of the expressions stated in Section 4.2.

Before looking at each observable in detail we use a common feature for all of them which is the property that

$$\text{Tr}(O\Delta) = \text{Tr}(\tilde{O}\tilde{\Delta}) \quad (\text{D.1})$$

The argument goes as following:  $\Delta$  can be taken to be  $\tilde{\Delta}$  in Fourier space, by applying Parseval's theorem and using the property that the delta function is an even function.

We start with an expression that looks like

$$\sum_x f(x)g(x) \quad (\text{D.2})$$

and we go to momentum space

$$\sum_x f(x)g(x) = \sum_x \sum_{p',p''} \frac{1}{N} e^{ip'x} \tilde{f}(p') e^{ip''x} \tilde{g}(p'')$$



$$\begin{aligned}
 &= \sum_{p', p''} \frac{1}{N} \tilde{f}(p') \tilde{g}(p'') \sum_x e^{ix(p''+p')} \\
 &= \sum_{p', p''} \tilde{f}(p') \tilde{g}(p'') \delta_{p', -p''} \\
 &= \sum_{p'} \tilde{f}(p') \tilde{g}(-p'). \tag{D.3}
 \end{aligned}$$

According to this if  $\tilde{g}(-p')$  is an even function then we can say that  $\tilde{g}(-p') = \tilde{g}(p')$  and equivalently for our functions we can say that

$$\text{Tr}(O\Delta) = \text{Tr}(\tilde{O}\tilde{\Delta}) \tag{D.4}$$

as our observables  $O$  are delta functions that are even functions.

## D.1 Scalar Mass

In order to get Eq. (4.36) we first need to find the first derivative of the observable with respect to one link which is found to be

$$\begin{aligned}
 \frac{\delta \text{Tr}\{P_1(m_0, m_1, \vec{m}_{23}, m_5)\}}{\delta v_{M_\alpha}(n_0, n_1, \vec{n}_{23}, n_5)} &= 2\delta_{n_0, m_0} \delta_{\vec{n}_{23}, \vec{m}_{23}} \delta_{n_5, m_5} \delta_{M, 1} \delta_{\alpha, 0} \sum_{m_1=0}^{L-1} \delta_{n_1, m_1} (\bar{v}_5(m_5))^{L-1} \\
 &= 2 \frac{P_1^{(0)}}{\bar{v}_4(m_5)} D^{(L)}(n_1) \delta_{n_0, m_0} \delta_{\vec{n}_{23}, \vec{m}_{23}} \delta_{n_5, m_5} \delta_{M, 1} \delta_{\alpha, 0} \tag{D.5}
 \end{aligned}$$

where  $P_1^{(0)}$  and  $D^{(L)}(n_1)$  are the quantities defined in Eq. (4.37) and Eq. (4.38) respectively. The factor 2 comes from the trace of the identity matrix and the last delta function comes from the fact that for  $\alpha = A$  the trace vanishes.

From Eq. (4.33) it is clear that we need to evaluate the expression

$$A = \frac{\delta \text{Tr}\{P_1(t_0 + t, m'_1, \vec{m}'_{23}, m_5)\}}{\delta v_{M'_{\alpha'}}(n'_0, n'_1, \vec{n}'_{23}, n'_5)} \frac{\delta \text{Tr}\{P_1(t_0, m''_1, \vec{m}''_{23}, m_5)\}}{\delta v_{M''_{\alpha''}}(n''_0, n''_1, \vec{n}''_{23}, n''_5)} \tag{D.6}$$

which can be easily determined using Eq. (D.5) and it can be shown to be

$$A = \left( 2 \frac{P_1^{(0)}}{\bar{v}_4(m_5)} D^{(L)}(n'_1) \delta_{n'_0, t_0+t} \delta_{\vec{n}'_{23}, \vec{m}'_{23}} \delta_{n'_5, m_5} \delta_{M', 1} \delta_{\alpha', 0} \right)$$

$$\begin{aligned}
 & \left( 2 \frac{P_1^{(0)}}{\bar{v}_4(m_5)} D^{(L)}(n_1'') \delta_{n_0'', t_0} \delta_{\bar{n}_{23}'', \bar{m}_{23}''} \delta_{n_5'', m_5} \delta_{M'', 1} \delta_{\alpha'', 0} \right) \\
 & = 4 \frac{(P_1^{(0)})^2}{\bar{v}_4(m_5)^2} D^{(L)}(n_1') D^{(L)}(n_1'') \delta_{M', 1} \delta_{M'', 1} \delta_{\alpha', 0} \delta_{\alpha'', 0} \delta_{n_5', m_5} \delta_{n_5'', m_5} \delta_{n_0', t_0+t} \delta_{n_0'', t_0} \delta_{\bar{n}_{23}', \bar{m}_{23}'} \delta_{\bar{n}_{23}'', \bar{m}_{23}''}.
 \end{aligned} \tag{D.7}$$

Considering the full expression in Eq. (4.33) and by taking the averaged version of the observable as in Eq. (D.7) we find the two-point function at first order to be

$$\begin{aligned}
 C^{(1)}(t; m_5) & = \frac{1}{2} \text{Tr} \left\{ \frac{1}{T} \sum_{t_0} \frac{1}{L^4} \sum_{\bar{m}_{23}', \bar{m}_{23}''} 4 \frac{(P_1^{(0)})^2}{\bar{v}_4(m_5)^2} \left[ D^{(L)}(n_1') D^{(L)}(n_1'') \delta_{M', 1} \delta_{M'', 1} \delta_{\alpha', 0} \delta_{\alpha'', 0} \right. \right. \\
 & \quad \delta_{n_5', m_5} \delta_{n_5'', m_5} \delta_{n_0', t_0+t} \delta_{n_0'', t_0} \delta_{\bar{n}_{23}', \bar{m}_{23}'} \delta_{\bar{n}_{23}'', \bar{m}_{23}''} + D^{(L)}(n_1'') D^{(L)}(n_1') \delta_{M', 1} \delta_{M'', 1} \delta_{\alpha', 0} \delta_{\alpha'', 0} \\
 & \quad \left. \delta_{n_5', m_5} \delta_{n_5'', m_5} \delta_{n_0', t_0} \delta_{n_0'', t_0+t} \delta_{\bar{n}_{23}', \bar{m}_{23}'} \delta_{\bar{n}_{23}'', \bar{m}_{23}''} \right] \Delta^{-1} \left. \right\} \\
 & = \frac{1}{2} \text{Tr} \left\{ 4 \frac{(P_1^{(0)})^2}{\bar{v}_4(m_5)^2} D^{(L)}(n_1') D^{(L)}(n_1'') \delta_{M', 1} \delta_{M'', 1} \delta_{\alpha', 0} \delta_{\alpha'', 0} \delta_{n_5', m_5} \delta_{n_5'', m_5} \right. \\
 & \quad \left. \frac{1}{T} \sum_{t_0} \frac{1}{L^4} \sum_{\bar{m}_{23}', \bar{m}_{23}''} \left( \delta_{n_0', t_0+t} \delta_{n_0'', t_0} \delta_{\bar{n}_{23}', \bar{m}_{23}'} \delta_{\bar{n}_{23}'', \bar{m}_{23}''} + \delta_{n_0', t_0} \delta_{n_0'', t_0+t} \delta_{\bar{n}_{23}', \bar{m}_{23}'} \delta_{\bar{n}_{23}'', \bar{m}_{23}''} \right) \Delta^{-1} \right\}.
 \end{aligned} \tag{D.8}$$

This expression in momentum space is given by

$$\begin{aligned}
 C^{(1)}(t; m_5) & = \frac{1}{2} \text{Tr} \left\{ 4 \frac{(P_1^{(0)})^2}{\bar{v}_4(m_5)^2} \frac{1}{TL^3} \sum_{n', n''} e^{ip'_0 n'_0} e^{-ip''_0 n''_0} e^{ip'_1 n'_1} e^{-ip''_1 n''_1} e^{i\vec{p}'_{23} \vec{n}'_{23}} e^{-i\vec{p}''_{23} \vec{n}''_{23}} \right. \\
 & \quad D^{(L)}(n_1') D^{(L)}(n_1'') \delta_{M', 1} \delta_{M'', 1} \delta_{\alpha', 0} \delta_{\alpha'', 0} \delta_{n_5', m_5} \delta_{n_5'', m_5} \frac{1}{T} \sum_{t_0} \frac{1}{L^4} \sum_{\bar{m}_{23}', \bar{m}_{23}''} \\
 & \quad \left. \left( \delta_{n_0', t_0+t} \delta_{n_0'', t_0} \delta_{\bar{n}_{23}', \bar{m}_{23}'} \delta_{\bar{n}_{23}'', \bar{m}_{23}''} + \delta_{n_0', t_0} \delta_{n_0'', t_0+t} \delta_{\bar{n}_{23}', \bar{m}_{23}'} \delta_{\bar{n}_{23}'', \bar{m}_{23}''} \right) \tilde{\Delta}^{-1} \right\} \\
 & = \frac{1}{2} \text{Tr} \left\{ 4 \frac{1}{TL^3} \frac{(P_1^{(0)})^2}{\bar{v}_4(m_5)^2} \delta_{M', 1} \delta_{M'', 1} \delta_{\alpha', 0} \delta_{\alpha'', 0} \delta_{n_5', m_5} \delta_{n_5'', m_5} \sum_{n'_1, n''_1} e^{ip'_1 n'_1} e^{-ip''_1 n''_1} \right. \\
 & \quad D^{(L)}(n_1') D^{(L)}(n_1'') \left[ \frac{1}{T} \sum_{t_0} \frac{1}{L^4} \sum_{\bar{m}_{23}', \bar{m}_{23}''} \sum_{n'_0, n''_0} \sum_{\bar{n}'_{23}, \bar{n}''_{23}} e^{ip'_0 n'_0} e^{-ip''_0 n''_0} e^{i\vec{p}'_{23} \vec{n}'_{23}} e^{-i\vec{p}''_{23} \vec{n}''_{23}} \right. \\
 & \quad \left. \left. \left( \delta_{n_0', t_0+t} \delta_{n_0'', t_0} \delta_{\bar{n}_{23}', \bar{m}_{23}'} \delta_{\bar{n}_{23}'', \bar{m}_{23}''} + \delta_{n_0', t_0} \delta_{n_0'', t_0+t} \delta_{\bar{n}_{23}', \bar{m}_{23}'} \delta_{\bar{n}_{23}'', \bar{m}_{23}''} \right) \right] \tilde{\Delta}^{-1} \right\}
 \end{aligned}$$

$$\begin{aligned}
 &= \frac{1}{2} \text{Tr} \left\{ 4 \frac{1}{\mathcal{N}_{(4)} \bar{v}_4(m_5)^2} \frac{(P_1^{(0)})^2}{\bar{v}_4(m_5)^2} \delta_{M',1} \delta_{M'',1} \delta_{a',0} \delta_{a'',0} \delta_{n'_5,m_5} \delta_{n''_5,m_5} D^{(L)}(p'_1) D^{(L)}(-p''_1) \right. \\
 &\quad \frac{1}{T} \sum_{t_0} \frac{1}{L^4} \sum_{\vec{m}'_{23}, \vec{m}''_{23}} \left( e^{ip'_0(t_0+t)} e^{-ip''_0 t_0} e^{i\vec{p}'_{23} \vec{m}'_{23}} e^{-i\vec{p}''_{23} \vec{m}''_{23}} \right. \\
 &\quad \left. \left. + e^{ip'_0 t_0} e^{-ip''_0(t_0+t)} e^{i\vec{p}'_{23} \vec{m}'_{23}} e^{-i\vec{p}''_{23} \vec{m}''_{23}} \right) \tilde{\Delta}^{-1} \right\} \\
 &= \frac{1}{2} \text{Tr} \left\{ 4 \frac{1}{\mathcal{N}_{(4)} \bar{v}_4(m_5)^2} \frac{(P_1^{(0)})^2}{\bar{v}_4(m_5)^2} \delta_{M',1} \delta_{M'',1} \delta_{a',0} \delta_{a'',0} \delta_{n'_5,m_5} \delta_{n''_5,m_5} D^{(L)}(p'_1) D^{(L)}(-p''_1) \right. \\
 &\quad \frac{1}{T} \sum_{t_0} \frac{1}{L^4} \sum_{\vec{m}'_{23}, \vec{m}''_{23}} \left( e^{i(p'_0-p''_0)t_0} e^{ip'_0 t_0} e^{i\vec{p}'_{23} \vec{m}'_{23}} e^{-i\vec{p}''_{23} \vec{m}''_{23}} \right. \\
 &\quad \left. \left. + e^{i(p'_0-p''_0)t_0} e^{-ip''_0 t_0} e^{i\vec{p}'_{23} \vec{m}'_{23}} e^{-i\vec{p}''_{23} \vec{m}''_{23}} \right) \tilde{\Delta}^{-1} \right\} \\
 &= \frac{1}{2} \text{Tr} \left\{ 4 \frac{1}{\mathcal{N}_{(4)} \bar{v}_4(m_5)^2} \frac{(P_1^{(0)})^2}{\bar{v}_4(m_5)^2} \delta_{M',1} \delta_{M'',1} \delta_{a',0} \delta_{a'',0} \delta_{n'_5,m_5} \delta_{n''_5,m_5} D^{(L)}(p'_1) D^{(L)}(-p''_1) \right. \\
 &\quad \left. \left( \delta_{p'_0, p''_0} e^{ip'_0 t} \delta_{\vec{p}'_{23}, 0} \delta_{\vec{p}''_{23}, 0} + \delta_{p'_0, -p''_0} e^{-ip''_0 t} \delta_{\vec{p}'_{23}, 0} \delta_{\vec{p}''_{23}, 0} \right) \tilde{K}^{-1} \right\} \\
 &= \frac{4}{\mathcal{N}_{(4)} \bar{v}_4(m_5)^2} \sum_{p'_0} \cos(p'_0 t) \\
 &\quad \sum_{p'_1} |\tilde{D}^L(p'_1)|^2 \tilde{\Delta}^{-1}((p'_0, p'_1, \vec{0}_{23}, m_5), 1, 0; (p'_0, p'_1, \vec{0}_{23}, m_5), 1, 0) \quad (\text{D.9})
 \end{aligned}$$

where  $\tilde{D}^L(p'_1)$  is defined in Eq. (4.40).

## D.2 Static Potential

In order to find the first-order corrections to the Wilson loop as given in Eq. (4.46) and consequently to be able to measure the static quark-antiquark potential, we first need to calculate the first and second derivative of the temporal line defined in Eq. (4.42) with respect to the matrix  $V$ . Before showing the resultant derivatives, we define the functions  $\mathcal{G}(t')$  and  $\mathcal{G}'(t'; t'')$  to be

$$\mathcal{G}(t') = \prod_{m_0=t_0}^{t_0+t-1} (\bar{v}_4(m_5) \mathbb{1} + v_{0\alpha}(m_0, m_1, \vec{m}_{23}, m_5) \sigma^\alpha) (\bar{v}_4(m_5) \mathbb{1} + v_{0\alpha}(t', m_1, \vec{m}_{23}, m_5) \sigma^\alpha)^{-1} \quad (\text{D.10})$$

$$\mathcal{G}'(t'; t'') = \prod_{m_0=t_0}^{t_0+t-1} (\bar{v}_4(m_5)\mathbb{1} + v_{0\alpha}(m_0, m_1, \vec{m}_{23}, m_5)\sigma^\alpha) (\bar{v}_4(m_5)\mathbb{1} + v_{0\alpha}(t', m_1, \vec{m}_{23}, m_5)\sigma^\alpha)^{-1} (\bar{v}_4(m_5)\mathbb{1} + v_{0\alpha}(t'', m_1, \vec{m}_{23}, m_5)\sigma^\alpha)^{-1}. \quad (\text{D.11})$$

When they are evaluated at the mean-field values we get

$$\mathcal{G}(t')|_{\bar{v}} = \bar{v}_4(m_5)^{t-1} \quad (\text{D.12})$$

$$\mathcal{G}(t'; t'')|_{\bar{v}} = \bar{v}_4(m_5)^{t-2}. \quad (\text{D.13})$$

The first derivative is calculated to be

$$\begin{aligned} \frac{\delta l^{(t)}(t_0, r, \vec{m}_{23}, m_5)}{\delta v_{M_\alpha}(n)} &= \left( \frac{\delta v_{0_0}(t_0, r, \vec{m}_{23}, m_5)\mathbb{1}}{\delta v_{M_\alpha}(n)} + \frac{i\delta v_{0_A}(t_0, r, \vec{m}_{23}, m_5)\sigma^A}{\delta v_{M_\alpha}(n)} \right) \mathcal{G}(t_0) \\ &+ \left( \frac{\delta v_{0_0}(t_0+1, r, \vec{m}_{23}, m_5)\mathbb{1}}{\delta v_{M_\alpha}(n)} + \frac{i\delta v_{0_A}(t_0+1, r, \vec{m}_{23}, m_5)\sigma^A}{\delta v_{M_\alpha}(n)} \right) \mathcal{G}(t_0+1) + \dots \\ &+ \left( \frac{\delta v_{0_0}(t_0+t-1, r, \vec{m}_{23}, m_5)\mathbb{1}}{\delta v_{M_\alpha}(n)} + \frac{i\delta v_{0_A}(t_0+t-1, r, \vec{m}_{23}, m_5)\sigma^A}{\delta v_{M_\alpha}(n)} \right) \mathcal{G}(t_0+t-1) \\ &= \delta_{M,0}\delta_{n_1,r}\delta_{\vec{n}_{23},\vec{m}_{23}}\delta_{n_5,m_5} \left[ (\delta_{\alpha,0}\delta_{n_0,t_0} + i\sigma^A\delta_{\alpha,A}\delta_{n_0,t_0})\mathcal{G}(t_0) \right. \\ &+ (\delta_{\alpha,0}\delta_{n_0,t_0+1} + i\sigma^A\delta_{\alpha,A}\delta_{n_0,t_0+1})\mathcal{G}(t_0+1) + \dots \\ &+ \left. (\delta_{\alpha,0}\delta_{n_0,t_0+t-1} + i\sigma^A\delta_{\alpha,A}\delta_{n_0,t_0+t-1})\mathcal{G}(t_0+t-1) \right] \\ &= \delta_{M,0}\delta_{n_1,r}\delta_{\vec{n}_{23},\vec{m}_{23}}\delta_{n_5,m_5} (\delta_{\alpha,0} + i\delta_{\alpha,A}\sigma^A) \left[ \delta_{n_0,t_0}\mathcal{G}(t_0) + \delta_{n_0,t_0+1}\mathcal{G}(t_0+1) + \dots \right. \\ &+ \left. \delta_{n_0,t_0+t-1}\mathcal{G}(t_0+t-1) \right]. \quad (\text{D.14}) \end{aligned}$$

Similarly, the first derivative  $l^{(t)\dagger}(t_0, r, \vec{m}_{23}, m_5)$  is given by

$$\begin{aligned} \frac{\delta l^{(t)\dagger}(t_0, r, \vec{m}_{23}, m_5)}{\delta v_{M_\alpha}(n)} &= \delta_{M,0}\delta_{n_1,r}\delta_{\vec{n}_{23},\vec{m}_{23}}\delta_{n_5,m_5} (\delta_{\alpha,0} - i\delta_{\alpha,A}\sigma^A) \\ &\left[ \delta_{n_0,t_0}\mathcal{G}(t_0) + \delta_{n_0,t_0+1}\mathcal{G}(t_0+1) + \dots + \delta_{n_0,t_0+t-1}\mathcal{G}(t_0+t-1) \right]. \quad (\text{D.15}) \end{aligned}$$

The second derivative of the temporal line is found to be

$$\begin{aligned}
 \frac{\delta^2 l^{(t)}(t_0, r, \vec{m}_{23}, m_5)}{\delta v_{M''_{\alpha''}}(n'') \delta v_{M'_{\alpha'}}(n')} &= \delta_{M',0} \delta_{n'_1,r} \delta_{\vec{n}'_{23}, \vec{m}_{23}} \delta_{n'_5, m_5} (\delta_{\alpha',0} \mathbb{1} + i \delta_{\alpha',A} \sigma^A) \left[ \delta_{n'_0, t_0} \delta_{M'',0} \delta_{n''_1, r} \right. \\
 &\quad \delta_{\vec{n}''_{23}, \vec{m}_{23}} \delta_{n''_5, m_5} (\delta_{\alpha'',0} \mathbb{1} + i \delta_{\alpha'',B} \sigma^B) \left[ \delta_{n''_0, t_0+1} \mathcal{G}'(t_0; t_0+1) + \delta_{n''_0, t_0+2} \mathcal{G}'(t_0; t_0+2) + \dots \right. \\
 &\quad \left. \left. + \delta_{n''_0, t_0+t-1} \mathcal{G}'(t_0; t_0+t-1) \right] + \delta_{n'_0, t_0+1} \delta_{M'',0} \delta_{n''_1, r} \delta_{\vec{n}''_{23}, \vec{m}_{23}} \delta_{n''_5, m_5} (\delta_{\alpha'',0} \mathbb{1} + i \delta_{\alpha'',B} \sigma^B) \right. \\
 &\quad \left[ \delta_{n''_0, t_0} \mathcal{G}'(t_0+1; t_0) + \delta_{n''_0, t_0+2} \mathcal{G}'(t_0+1; t_0+2) + \dots + \delta_{n''_0, t_0+t-1} \mathcal{G}'(t_0+1; t_0+t-1) \right] \\
 &\quad \left. + \dots + \delta_{n'_0, t_0+t-1} \delta_{M'',0} \delta_{n''_1, r} \delta_{\vec{n}''_{23}, \vec{m}_{23}} \delta_{n''_5, m_5} (\delta_{\alpha'',0} \mathbb{1} + i \delta_{\alpha'',B} \sigma^B) \left[ \delta_{n''_0, t_0} \mathcal{G}'(t_0+t-1; t_0) \right. \right. \\
 &\quad \left. \left. + \delta_{n''_0, t_0+1} \mathcal{G}'(t_0+t-1; t_0+1) + \dots + \delta_{n''_0, t_0+t-2} \mathcal{G}'(t_0+t-1; t_0+t-2) \right] \right] \\
 &= \delta_{M',0} \delta_{M'',0} \delta_{n'_1, r} \delta_{n''_1, r} \delta_{\vec{n}'_{23}, \vec{m}_{23}} \delta_{\vec{n}''_{23}, \vec{m}_{23}} \delta_{n'_5, m_5} \delta_{n''_5, m_5} (\delta_{\alpha',0} \mathbb{1} + i \delta_{\alpha',A} \sigma^A) (\delta_{\alpha'',0} \mathbb{1} + i \delta_{\alpha'',B} \sigma^B) \\
 &\quad \left[ \delta_{n'_0, t_0} \left( \delta_{n''_0, t_0+1} \mathcal{G}'(t_0; t_0+1) + \delta_{n''_0, t_0+2} \mathcal{G}'(t_0; t_0+2) + \dots + \delta_{n''_0, t_0+t-1} \mathcal{G}'(t_0; t_0+t-1) \right) \right. \\
 &\quad \left. + \delta_{n'_0, t_0+1} \left( \delta_{n''_0, t_0} \mathcal{G}'(t_0+1; t_0) + \delta_{n''_0, t_0+2} \mathcal{G}'(t_0+1; t_0+2) + \dots \right. \right. \\
 &\quad \left. \left. + \delta_{n''_0, t_0+t-1} \mathcal{G}'(t_0+1; t_0+t-1) \right) + \dots + \delta_{n'_0, t_0+t-1} \left( \delta_{n''_0, t_0} \mathcal{G}'(t_0+t-1; t_0) \right. \right. \\
 &\quad \left. \left. + \delta_{n''_0, t_0+1} \mathcal{G}'(t_0+t-1; t_0+t) + \dots + \delta_{n''_0, t_0+t-2} \mathcal{G}'(t_0+t-1; t_0+t-2) \right) \right]. \tag{D.16}
 \end{aligned}$$

Using similar arguments we can say that

$$\begin{aligned}
 \frac{\delta^2 l^{(t)\dagger}(t_0, r, \vec{m}_{23}, m_5)}{\delta v_{M''_{\alpha''}}(n'') \delta v_{M'_{\alpha'}}(n')} &= \delta_{M',0} \delta_{M'',0} \delta_{n'_1, r} \delta_{n''_1, r} \delta_{\vec{n}'_{23}, \vec{m}_{23}} \delta_{\vec{n}''_{23}, \vec{m}_{23}} \delta_{n'_5, m_5} \delta_{n''_5, m_5} \\
 &\quad (\delta_{\alpha',0} \mathbb{1} - i \delta_{\alpha',A} \sigma^A) (\delta_{\alpha'',0} \mathbb{1} - i \delta_{\alpha'',B} \sigma^B) \left[ \delta_{n'_0, t_0} \left( \delta_{n''_0, t_0+1} \mathcal{G}'(t_0; t_0+1) \right. \right. \\
 &\quad \left. \left. + \delta_{n''_0, t_0+2} \mathcal{G}'(t_0; t_0+2) + \dots + \delta_{n''_0, t_0+t-1} \mathcal{G}'(t_0; t_0+t-1) \right) \right. \\
 &\quad \left. + \delta_{n'_0, t_0+1} \left( \delta_{n''_0, t_0} \mathcal{G}'(t_0+1; t_0) + \delta_{n''_0, t_0+2} \mathcal{G}'(t_0+1; t_0+2) + \dots \right. \right. \\
 &\quad \left. \left. + \delta_{n''_0, t_0+t-1} \mathcal{G}'(t_0+1; t_0+t-1) \right) + \dots + \delta_{n'_0, t_0+t-1} \left( \delta_{n''_0, t_0} \mathcal{G}'(t_0+t-1; t_0) \right. \right. \\
 &\quad \left. \left. + \delta_{n''_0, t_0+1} \mathcal{G}'(t_0+t-1; t_0+t) + \dots + \delta_{n''_0, t_0+t-2} \mathcal{G}'(t_0+t-1; t_0+t-2) \right) \right]. \tag{D.17}
 \end{aligned}$$

It is clear now that we have all the derivatives that appear in Eq.(4.46) so we can

evaluate the whole expression. In fact, for our convenience we evaluate lines one by one calling them  $L_1 - L_4$ . So we have

$$\begin{aligned}
 L_1 = & \text{Tr} \left\{ \delta_{M',0} \delta_{n'_1,0} \delta_{\vec{n}'_{23}, \vec{m}_{23}} \delta_{n'_5, m_5} (\delta_{\alpha',0} \mathbb{1} + i \delta_{\alpha',A} \sigma^A) \left( \delta_{n'_0, t_0} \mathcal{G}(t_0) + \delta_{n'_0, t_0+1} \mathcal{G}(t_0 + 1) \right. \right. \\
 & + \dots + \delta_{n'_0, t_0+t-1} \mathcal{G}(t_0 + t - 1) \left. \right) l^{(r)}(t_0 + t, \vec{m}_{23}, m_5) \\
 & \delta_{M'',0} \delta_{n''_1, r} \delta_{\vec{n}''_{23}, \vec{m}_{23}} \delta_{n''_5, m_5} (\delta_{\alpha'',0} \mathbb{1} - i \delta_{\alpha'',B} \sigma^B) \left( \delta_{n''_0, t_0} \mathcal{G}(t_0) + \delta_{n''_0, t_0+1} \mathcal{G}(t_0 + 1) \right. \\
 & + \dots + \delta_{n''_0, t_0+t-1} \mathcal{G}(t_0 + t - 1) \left. \right) l^{(r)\dagger}(t_0, \vec{m}_{23}, m_5) \left. \right\} \Big|_{\bar{V}} \\
 = & 2\bar{v}_4(m_5)^{2(t+r)-2} \delta_{M',0} \delta_{M'',0} \delta_{n'_1,0} \delta_{n''_1, r} \delta_{\vec{n}''_{23}, \vec{m}_{23}} \delta_{\vec{n}'_{23}, \vec{m}_{23}} \delta_{n'_5, m_5} \delta_{n''_5, m_5} \\
 & (\delta_{\alpha',0} \delta_{\alpha'',0} + \delta_{\alpha',A} \delta_{\alpha'',A}) (\delta_{n'_0, t_0} + \delta_{n'_0, t_0+1} + \dots + \delta_{n'_0, t_0+t-1}) \\
 & (\delta_{n''_0, t_0} + \delta_{n''_0, t_0+1} + \dots + \delta_{n''_0, t_0+t-1}). \tag{D.18}
 \end{aligned}$$

Similarly, the second line in Eq.(4.46) is given by

$$\begin{aligned}
 L_2 = & 2\bar{v}_4(m_5)^{2(t+r)-2} \delta_{M',0} \delta_{M'',0} \delta_{n'_1,0} \delta_{n''_1, r} \delta_{\vec{n}''_{23}, \vec{m}_{23}} \delta_{\vec{n}'_{23}, \vec{m}_{23}} \delta_{n'_5, m_5} \delta_{n''_5, m_5} \\
 & (\delta_{\alpha',0} \delta_{\alpha'',0} + \delta_{\alpha',A} \delta_{\alpha'',A}) (\delta_{n'_0, t_0} + \delta_{n''_0, t_0+1} + \dots + \delta_{n''_0, t_0+t-1}) \\
 & (\delta_{n'_0, t_0} + \delta_{n'_0, t_0+1} + \dots + \delta_{n'_0, t_0+t-1}). \tag{D.19}
 \end{aligned}$$

Using the second derivative in Eq. (D.16) the third line reads as

$$\begin{aligned}
 L_3 = & \text{Tr} \left\{ \delta_{M',0} \delta_{M'',0} \delta_{n'_1,0} \delta_{n''_1,0} \delta_{\vec{n}''_{23}, \vec{m}_{23}} \delta_{\vec{n}'_{23}, \vec{m}_{23}} \delta_{n'_5, m_5} \delta_{n''_5, m_5} (\delta_{\alpha',0} \mathbb{1} + i \delta_{\alpha',A} \sigma^A) \right. \\
 & (\delta_{\alpha',0} \mathbb{1} + i \delta_{\alpha',B} \sigma^B) \left[ \delta_{n'_0, t_0} \left( \delta_{n''_0, t_0+1} \mathcal{G}'(t_0; t_0 + 1) + \delta_{n''_0, t_0+2} \mathcal{G}'(t_0; t_0 + 2) + \dots \right. \right. \\
 & + \delta_{n''_0, t_0+t-1} \mathcal{G}'(t_0; t_0 + t - 1) \left. \right) + \delta_{n'_0, t_0+1} \left( \delta_{n''_0, t_0} \mathcal{G}'(t_0 + 1; t_0) \right. \\
 & + \delta_{n''_0, t_0+2} \mathcal{G}'(t_0 + 1; t_0 + 2) + \dots + \delta_{n''_0, t_0+t-1} \mathcal{G}'(t_0 + 1; t_0 + t - 1) \left. \right) + \dots \\
 & + \delta_{n'_0, t_0+t-1} \left( \delta_{n''_0, t_0} \mathcal{G}'(t_0 + t - 1; t_0) + \delta_{n''_0, t_0+1} \mathcal{G}'(t_0 + t - 1; t_0 + t) \right. \\
 & + \dots + \delta_{n''_0, t_0+t-2} \mathcal{G}'(t_0 + t - 1; t_0 + t - 2) \left. \right) \left. \right] l^{(r)}(t_0 + t, \vec{m}_{23}, m_5) \\
 & l^{(t)\dagger}(t_0, r, \vec{m}_{23}, m_5) l^{(r)\dagger}(t_0, \vec{m}_{23}, m_5) \left. \right\} \Big|_{\bar{V}} \\
 = & 2\bar{v}_4(m_5)^{2(t+r)-2} \delta_{M',0} \delta_{M'',0} \delta_{n'_1,0} \delta_{n''_1,0} \delta_{\vec{n}''_{23}, \vec{m}_{23}} \delta_{\vec{n}'_{23}, \vec{m}_{23}} \delta_{n'_5, m_5} \delta_{n''_5, m_5}
 \end{aligned}$$

$$\begin{aligned}
 & (\delta_{\alpha',0}\delta_{\alpha'',0} - \delta_{\alpha',A}\delta_{\alpha'',A}) \left( \delta_{n'_0,t_0} (\delta_{n''_0,t_0+1} + \delta_{n''_0,t_0+2} + \dots + \delta_{n''_0,t_0+t-1}) \right. \\
 & + \delta_{n'_0,t_0+1} (\delta_{n''_0,t_0} + \delta_{n''_0,t_0+2} + \dots + \delta_{n''_0,t_0+t-1}) + \dots \\
 & \left. + \delta_{n'_0,t_0+t-1} (\delta_{n''_0,t_0} + \delta_{n''_0,t_0+1} + \dots + \delta_{n''_0,t_0+t-2}) \right). \tag{D.20}
 \end{aligned}$$

Using similar arguments

$$\begin{aligned}
 L_4 = & 2\bar{v}_4(m_5)^{2(t+r)-2} \delta_{M',0} \delta_{M'',0} \delta_{n'_1,r} \delta_{n''_1,r} \delta_{\vec{n}'_{23},\vec{m}_{23}} \delta_{\vec{n}''_{23},\vec{m}_{23}} \delta_{n'_5,m_5} \delta_{n''_5,m_5} \\
 & (\delta_{\alpha',0}\delta_{\alpha'',0} - \delta_{\alpha',A}\delta_{\alpha'',A}) \left( \delta_{n'_0,t_0} (\delta_{n''_0,t_0+1} + \delta_{n''_0,t_0+2} + \dots + \delta_{n''_0,t_0+t-1}) \right. \\
 & + \delta_{n'_0,t_0+1} (\delta_{n''_0,t_0} + \delta_{n''_0,t_0+2} + \dots + \delta_{n''_0,t_0+t-1}) + \dots \\
 & \left. + \delta_{n'_0,t_0+t-1} (\delta_{n''_0,t_0} + \delta_{n''_0,t_0+1} + \dots + \delta_{n''_0,t_0+t-2}) \right). \tag{D.21}
 \end{aligned}$$

Putting everything together, according to Eq. (4.44) with the observable under consideration to be the averaged Wilson loop, the first-order corrections to the latter in coordinate space are given by

$$\begin{aligned}
 O_W^{(1)} = & \frac{1}{2} \frac{1}{T} \sum_{t_0} \frac{1}{L^2} \sum_{\vec{m}_{23}} \text{Tr} \left\{ 2\bar{v}_4(m_5)^{2(t+r)-2} \delta_{M',0} \delta_{M'',0} \delta_{\vec{n}'_{23},\vec{m}_{23}} \delta_{\vec{n}''_{23},\vec{m}_{23}} \delta_{n'_5,m_5} \delta_{n''_5,m_5} \right. \\
 & \left[ (\delta_{\alpha',0}\delta_{\alpha'',0} + \delta_{\alpha',A}\delta_{\alpha'',A}) (\delta_{n'_1,0}\delta_{n''_1,r} + \delta_{n'_1,r}\delta_{n''_1,0}) \right. \\
 & (\delta_{n'_0,t_0} + \delta_{n'_0,t_0+1} + \dots + \delta_{n'_0,t_0+t-1}) (\delta_{n''_0,t_0} + \delta_{n''_0,t_0+1} + \dots + \delta_{n''_0,t_0+t-1}) \\
 & + (\delta_{\alpha',0}\delta_{\alpha'',0} - \delta_{\alpha',A}\delta_{\alpha'',A}) (\delta_{n'_1,0}\delta_{n''_1,0} + \delta_{n'_1,r}\delta_{n''_1,r}) \\
 & (\delta_{n'_0,t_0} (\delta_{n''_0,t_0+1} + \delta_{n''_0,t_0+2} + \dots + \delta_{n''_0,t_0+t-1}) \\
 & + \delta_{n'_0,t_0+1} (\delta_{n''_0,t_0} + \delta_{n''_0,t_0+2} + \dots + \delta_{n''_0,t_0+t-1}) + \dots \\
 & \left. \left. + \delta_{n'_0,t_0+t-1} (\delta_{n''_0,t_0} + \delta_{n''_0,t_0+1} + \dots + \delta_{n''_0,t_0+t-2}) \right) \right] \Delta^{-1} \left. \right\}. \tag{D.22}
 \end{aligned}$$

In momentum space this is found to be

$$\begin{aligned}
 O_W^{(1)} = & \frac{1}{T} \sum_{t_0} \frac{1}{L^2} \sum_{\vec{m}_{23}} \text{Tr} \left\{ \bar{v}_4(m_5)^{2(t+r)-2} \delta_{M',0} \delta_{M'',0} \delta_{\vec{n}'_{23},\vec{m}_{23}} \delta_{\vec{n}''_{23},\vec{m}_{23}} \delta_{n'_5,m_5} \delta_{n''_5,m_5} \right. \\
 & \frac{1}{TL^3} \sum_{n'_0,n''_0} e^{ip'_0 n'_0} e^{-ip''_0 n''_0} \sum_{n'_1,n''_1} e^{ip'_1 n'_1} e^{-ip''_1 n''_1} \sum_{\vec{n}'_{23},\vec{n}''_{23}} e^{i\vec{p}'_{23} \vec{n}'_{23}} e^{-i\vec{p}''_{23} \vec{n}''_{23}}
 \end{aligned}$$

$$\begin{aligned}
 & \left[ (\delta_{\alpha',0}\delta_{\alpha'',0} + \delta_{\alpha',A}\delta_{\alpha'',A}) (\delta_{n'_1,0}\delta_{n''_1,r} + \delta_{n'_1,r}\delta_{n''_1,0}) \right. \\
 & (\delta_{n'_0,t_0} + \delta_{n'_0,t_0+1} + \dots + \delta_{n'_0,t_0+t-1}) (\delta_{n''_0,t_0} + \delta_{n''_0,t_0+1} + \dots + \delta_{n''_0,t_0+t-1}) \\
 & + (\delta_{\alpha',0}\delta_{\alpha'',0} - \delta_{\alpha',A}\delta_{\alpha'',A}) (\delta_{n'_1,0}\delta_{n''_1,0} + \delta_{n'_1,r}\delta_{n''_1,r}) \\
 & (\delta_{n'_0,t_0} (\delta_{n''_0,t_0+1} + \delta_{n''_0,t_0+2} + \dots + \delta_{n''_0,t_0+t-1}) \\
 & + \delta_{n'_0,t_0+1} (\delta_{n''_0,t_0} + \delta_{n''_0,t_0+2} + \dots + \delta_{n''_0,t_0+t-1}) + \dots \\
 & \left. + \delta_{n'_0,t_0+t-1} (\delta_{n''_0,t_0} + \delta_{n''_0,t_0+1} + \dots + \delta_{n''_0,t_0+t-2}) \right] \tilde{\Delta}^{-1} \Big\} \\
 = & \frac{\bar{v}_4(m_5)^{2(t+r)-2}}{\mathcal{N}_{(4)}} \text{Tr} \left\{ \delta_{M',0}\delta_{M'',0}\delta_{n'_5,m_5}\delta_{n''_5,m_5} \frac{1}{L^2} \sum_{\vec{m}_{23}} e^{i\vec{p}_{23}\vec{m}'_{23}} e^{-i\vec{p}'_{23}\vec{m}''_{23}} \right. \\
 & \frac{1}{T} \sum_{t_0} \left[ (\delta_{\alpha',0}\delta_{\alpha'',0} + \delta_{\alpha',A}\delta_{\alpha'',A}) (e^{ip'_1 0} e^{-ip''_1 r} + e^{ip'_1 r} e^{-ip''_1 0}) \right. \\
 & (e^{ip'_0 t_0} + e^{ip'_0(t_0+1)} + \dots + e^{ip'_0(t_0+t-1)}) (e^{-ip''_0 t_0} + e^{-ip''_0(t_0+1)} + \dots + e^{-ip''_0(t_0+t-1)}) \\
 & + (\delta_{\alpha',0}\delta_{\alpha'',0} - \delta_{\alpha',A}\delta_{\alpha'',A}) (e^{ip'_1 0} e^{-ip''_1 0} + e^{ip'_1 r} e^{-ip''_1 r}) \\
 & \left[ e^{ip'_0 t_0} (e^{-ip''_0(t_0+1)} + e^{-ip''_0(t_0+2)} + \dots + e^{-ip''_0(t_0+t-1)}) \right. \\
 & + e^{ip'_0(t_0+1)} (e^{-ip''_0 t_0} + e^{-ip''_0(t_0+2)} + \dots + e^{-ip''_0(t_0+t-1)}) + \dots \\
 & \left. \left. + e^{ip'_0(t_0+t-1)} (e^{-ip''_0 t_0} + e^{-ip''_0(t_0+1)} + \dots + e^{-ip''_0(t_0+t-2)}) \right] \right] \tilde{\Delta}^{-1} \Big\} \\
 = & \frac{\bar{v}_4(m_5)^{2(t+r)-2}}{\mathcal{N}_{(4)}} \text{Tr} \left\{ \delta_{M',0}\delta_{M'',0}\delta_{n'_5,m_5}\delta_{n''_5,m_5}\delta_{\vec{p}_{23},\vec{p}'_{23}} \left[ (\delta_{\alpha',0}\delta_{\alpha'',0} + \delta_{\alpha',A}\delta_{\alpha'',A}) \right. \right. \\
 & (e^{ip'_1 0} e^{-ip''_1 r} + e^{ip'_1 r} e^{-ip''_1 0}) \frac{1}{T} \sum_{t_0} \left( e^{i(p'_0-p''_0)t_0} (1 + e^{-ip''_0} + \dots + e^{-ip''_0(t-1)}) \right. \\
 & + e^{i(p'_0-p''_0)t_0} (e^{ip'_0} + e^{ip'_0} e^{-ip''_0} + \dots + e^{ip'_0} e^{-ip''_0(t-1)}) + \dots \\
 & \left. \left. + e^{i(p'_0-p''_0)t_0} (e^{ip'_0(t-1)} + e^{ip'_0(t-1)} e^{-ip''_0} + \dots + e^{ip'_0(t-1)} e^{-ip''_0(t-1)}) \right) \right. \\
 & + (\delta_{\alpha',0}\delta_{\alpha'',0} - \delta_{\alpha',A}\delta_{\alpha'',A}) (e^{ip'_1 0} e^{-ip''_1 0} + e^{ip'_1 r} e^{-ip''_1 r}) \\
 & \frac{1}{T} \sum_{t_0} \left( e^{i(p'_0-p''_0)t_0} (e^{-ip''_0} + e^{-i2p''_0} + \dots + e^{-ip''_0(t-1)}) \right. \\
 & + e^{i(p'_0-p''_0)t_0} (e^{ip'_0} + e^{ip'_0} e^{-i2p''_0} + \dots + e^{ip'_0} e^{-ip''_0(t-1)}) + \dots \\
 & \left. \left. + e^{i(p'_0-p''_0)t_0} (e^{ip'_0(t-1)} + e^{ip'_0(t-1)} e^{-ip''_0} + \dots + e^{ip'_0(t-1)} e^{-ip''_0(t-2)}) \right) \right] \tilde{\Delta}^{-1} \Big\} \\
 = & \frac{\bar{v}_4(m_5)^{2(t+r)-2}}{\mathcal{N}_{(4)}} \text{Tr} \left\{ \delta_{M',0}\delta_{M'',0}\delta_{n'_5,m_5}\delta_{n''_5,m_5}\delta_{\vec{p}_{23},\vec{p}'_{23}} \delta_{p'_0,p''_0} \delta_{p'_1,p''_1} \right.
 \end{aligned}$$



$$\begin{aligned}
 & \left[ 2 \cos(p_1 r) (\delta_{\alpha',0} \delta_{\alpha'',0} + \delta_{\alpha',A} \delta_{\alpha'',A}) (1 + e^{-ip'_0} + \dots + e^{-ip'_0(t-1)} + e^{ip'_0} + 1 + \dots \right. \\
 & + e^{-ip'_0(t-2)} + \dots + e^{ip'_0(t-1)} + e^{ip'_0(t-2)} + \dots + 1) \\
 & + 2 (\delta_{\alpha',0} \delta_{\alpha'',0} - \delta_{\alpha',A} \delta_{\alpha'',A}) (e^{-ip'_0} + e^{-i2p'_0} + \dots + e^{-ip'_0(t-1)} + e^{ip'_0} + e^{-ip'_0} + \dots \\
 & \left. + e^{-ip'_0(t-2)} + \dots + e^{ip'_0(t-1)} + e^{ip'_0(t-2)} + \dots + e^{ip'_0}) \right] \tilde{\Delta}^{-1} \Big\}. \quad (\text{D.23})
 \end{aligned}$$

The above equation has two main products that are added together, one in lines 2-3 and the other in lines 4-5. To find a neat expression for the Wilson loop as  $t \rightarrow \infty$ , we take a closer look at the temporal term of each product. By inspection, it is clear that the first temporal term,  $f_1(t)$  and the second temporal term  $f_2(t)$  can be written as

$$f_1(t) = t + 2 \sum_{n=1}^{t-1} (t-n) \cos(np'_0) \quad (\text{D.24})$$

$$f_2(t) = 2 \sum_{n=1}^{t-1} (t-n) \cos(np'_0). \quad (\text{D.25})$$

We recall two formulas from basic algebra as given below

$$\sum_{n=1}^N \cos(an) = \frac{\cos\left(\frac{a(N+1)}{2}\right) \sin\left(\frac{aN}{2}\right)}{\sin\frac{a}{2}} \quad (\text{D.26})$$

$$\sum_{n=1}^N \sin(an) = \frac{\cos\frac{a}{2} - \cos\left(\left(N + \frac{1}{2}\right)a\right)}{2 \sin\frac{a}{2}} \quad (\text{D.27})$$

and taking the derivative of Eq. (D.27) with respect to  $a$  we can find

$$\sum_{n=1}^N n \cos(an) = -\frac{1}{4} + \frac{\left(N + \frac{1}{2}\right) \sin\left(a\left(N + \frac{1}{2}\right)\right)}{2 \sin\frac{a}{2}} - \frac{\cos\frac{a}{2}}{4 \sin^2\frac{a}{2}} \left( \cos\frac{a}{2} - \cos\left(\left(N + \frac{1}{2}\right)a\right) \right). \quad (\text{D.28})$$

Using the above expressions the temporal terms can be written as

$$f_1(t) = \frac{(1 - \cos(tp'_0))}{2 \sin^2\frac{p'_0}{2}} \quad (\text{D.29})$$

and

$$f_2(t) = \frac{(1 - \cos(tp'_0))}{2 \sin^2\frac{p'_0}{2}} - t. \quad (\text{D.30})$$

In Chapter 4 we discussed that the static potential can be extracted from the Wilson loop when the limit  $t \rightarrow \infty$  is taken. Therefore, we are interested in the values of the temporal terms in this specific limit. The function  $f_1(t)$  is a periodic function with a period of  $2\pi$  and it shows a peak at the origin which is given by  $t^2$  in the large  $t$  limit. Hence, in this limit we can express both  $f_1(t)$  and  $f_2(t)$  as  $t^2\delta_{p0',0}$ .

Putting everything together, we can say that the first-order corrections of the Wilson loop in the limit  $t \rightarrow \infty$  can be written as

$$\begin{aligned}
 O_W^{(1)} &= \frac{\bar{v}_4(m_5)^{2(t+r)-2}}{\mathcal{N}_{(4)}} \text{Tr} \left\{ \delta_{M',0} \delta_{M'',0} \delta_{n'_5, m_5} \delta_{n''_5, m_5} \delta_{\vec{p}'_{23}, \vec{p}''_{23}} \delta_{p'_0, 0} \delta_{p'_0, p''_0} \delta_{p'_1, p''_1} \right. \\
 &\quad \left. \left[ 2 \cos(p_1 r) t^2 (\delta_{\alpha', 0} \delta_{\alpha'', 0} + \delta_{\alpha', A} \delta_{\alpha'', A}) + 2 t^2 (\delta_{\alpha', 0} \delta_{\alpha'', 0} - \delta_{\alpha', A} \delta_{\alpha'', A}) \right] \tilde{\Delta}^{-1} \right\} \\
 &= \frac{\bar{v}_4(m_5)^{2(t+r)-2}}{\mathcal{N}_{(4)}} t^2 \sum_{p'_1, p'_2, p'_3} \delta_{p'_0, 0} \\
 &\quad \left[ (2 \cos(p'_1 r) + 2) \tilde{\Delta}^{-1} \left( (0, p'_1, \vec{p}'_{23}, m_5), 0, 0; (0, p'_1, \vec{p}'_{23}, m_5), 0, 0 \right) \right. \\
 &\quad \left. + 3 (2 \cos(p'_1 r) - 2) \tilde{\Delta}^{-1} \left( (0, p'_1, \vec{p}'_{23}, m_5), 0, 1; (0, p'_1, \vec{p}'_{23}, m_5), 0, 1 \right) \right].
 \end{aligned} \tag{D.31}$$

# Appendix E

## Further results from the warped model

### E.1 Fits of the measured static potential to different functional forms

In the figures below we show the fits of the static potential for different layers for  $\beta = 2.50$ ,  $\gamma = 1.00$ ,  $k = 0.10$  and  $N_5 = 8$ .

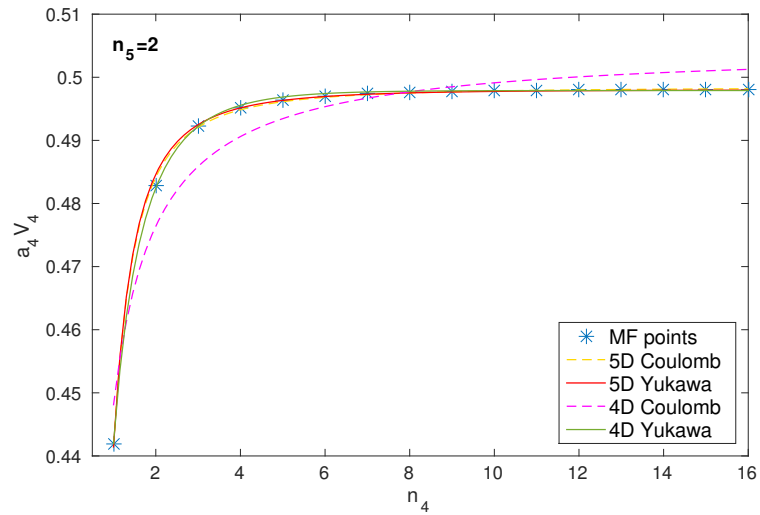


Figure E.1: Fits to the static potential for  $\beta = 2.50$ ,  $\gamma = 1.00$ ,  $k = 0.10$  and  $N_5 = 8$  using various potential forms for  $n_5 = 2$ .

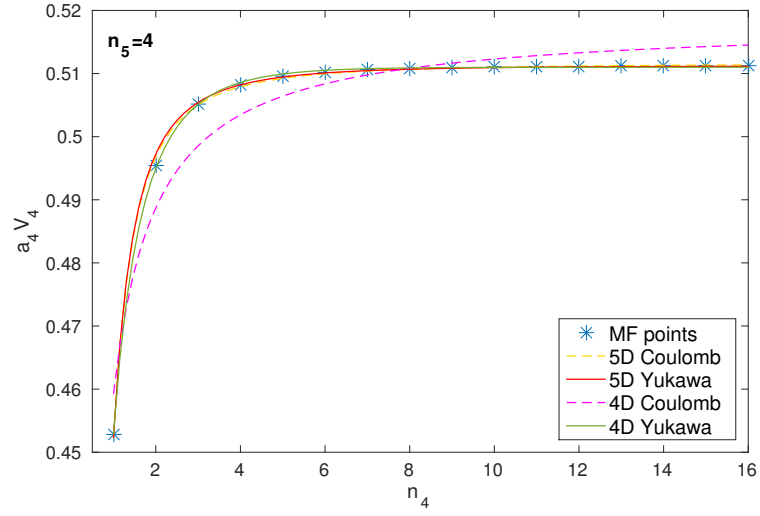


Figure E.2: Fits to the static potential for  $\beta = 2.50$ ,  $\gamma = 1.00$ ,  $k = 0.10$  and  $N_5 = 8$  using various potential forms for  $n_5 = 4$ .

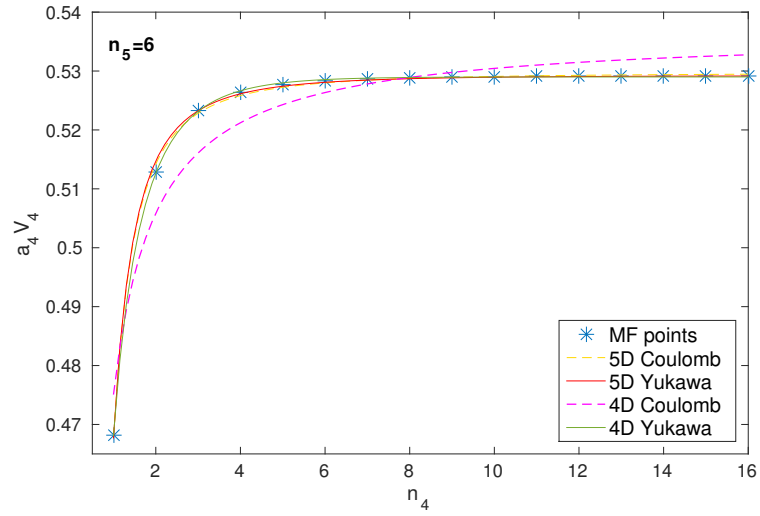


Figure E.3: Fits to the static potential for  $\beta = 2.50$ ,  $\gamma = 1.00$ ,  $k = 0.10$  and  $N_5 = 8$  using various potential forms for  $n_5 = 6$ .

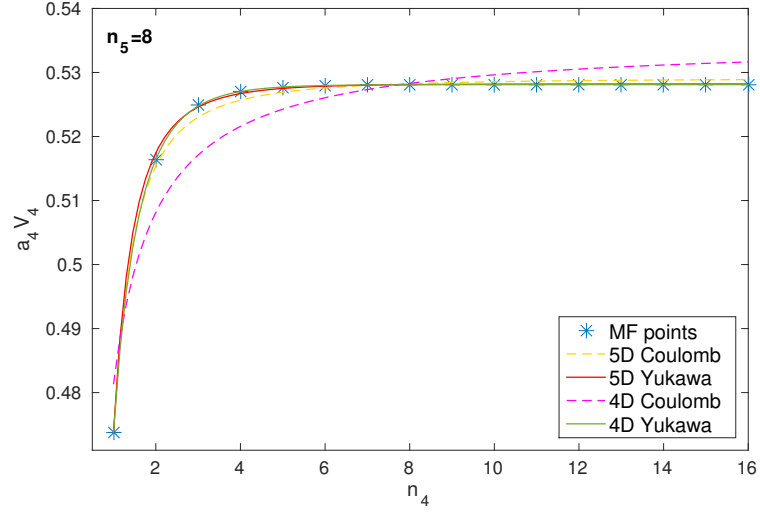


Figure E.4: Fits to the static potential for  $\beta = 2.50$ ,  $\gamma = 1.00$ ,  $k = 0.10$  and  $N_5 = 8$  using various potential forms for  $n_5 = 8$ .

## E.2 Fitting parameters of the potential

The values of the fitting parameters for different functional forms of the potential as given in Table 4.2 are shown here.  $R^2(\text{adj})$  is the adjusted to degrees of freedom determining the goodness of the fit.  $R^2$  is found by

$$R^2 = 1 - \frac{RSS}{SST} \quad (\text{E.1})$$

where RSS is called the residual sum of squares and it measures the deviation of the response values from the fit to the response values, i.e.

$$RSS = \sum_i (y_{\text{fit}_i} - y_i)^2 \quad (\text{E.2})$$

and SST is the sum of squares of the response values about their mean, i.e.

$$SST = \sum_i (y_i - \bar{y})^2. \quad (\text{E.3})$$

The adjusted  $R^2$  takes into account the number of fitting parameters,  $d$ , and the number of measurements,  $n$ , and gives a better estimation of the goodness of the

fit. In particular it multiplies the ratio  $RSS/SST$  by the factor  $(n-1)/(n-d-1)$ .

Layer	Type of potential	a	b	$m_Y$	$R^2(\text{adj})$
$n_5 = 1$	5D Coulombic	0.3041	0.04644	-	0.9902
	5D Yukawa	0.304	0.002648	0.0568	0.9889
	4D Coulombic	0.3094	0.04726	-	0.9622
	4D Yukawa	0.3042	0.06752	0.3943	0.999
$n_5 = 2$	5D Coulombic	0.3067	0.04745	-	0.9894
	5D Yukawa	0.3065	0.004111	0.0860	0.9874
	4D Coulombic	0.3122	0.04833	-	0.9636
	4D Yukawa	0.3069	0.06837	0.3854	0.999
$n_5 = 3$	5D Coulombic	0.3099	0.04879	-	0.9881
	5D Yukawa	0.3097	0.00399	0.0811	0.9861
	4D Coulombic	0.3156	0.04978	-	0.9658
	4D Yukawa	0.3102	0.06931	0.3712	0.9999
$n_5 = 4$	5D Coulombic	0.314	0.05005	-	0.9861
	5D Yukawa	0.3139	0.002075	0.04096	0.9847
	4D Coulombic	0.3199	0.05171	-	0.9689
	4D Yukawa	0.3143	0.07043	0.3516	0.9999
$n_5 = 5$	5D Coulombic	0.3191	0.05299	-	0.9829
	5D Yukawa	0.3191	0.002066	0.03898	0.9813
	4D Coulombic	0.3254	0.05439	-	0.9732
	4D Yukawa	0.3197	0.07182	0.3237	0.9999
$n_5 = 6$	5D Coulombic	0.3261	0.05661	-	0.9771
	5D Yukawa	0.3261	0.002005	0.03539	0.975
	4D Coulombic	0.3329	0.05845	-	0.9796
	4D Yukawa	0.327	0.07358	0.2806	0.9999
$n_5 = 7$	5D Coulombic	0.3364	0.06296	-	0.9625
	5D Yukawa	0.3364	0.001004	0.01594	0.9595
	4D Coulombic	0.3441	0.06579	-	0.9903
	4D Yukawa	0.3383	0.07587	0.1991	0.9999
$n_5 = 8$	5D Coulombic	0.3357	0.0621	-	0.9667
	5D Yukawa	0.3357	0.00161	0.02591	0.964
	4D Coulombic	0.3432	0.06467	-	0.9873
	4D Yukawa	0.3372	0.07649	0.2231	0.9999

Table E.1: Fitting parameters for  $\beta = 2.30, \gamma = 0.505, k = 0.10$  for  $T = L = 32, N_5 = 8$ .

Layer	Type of potential	a	b	$m_Y$	$R^2(\text{adj})$
$n_5 = 1$	5D Coulombic	0.3045	0.04707	-	0.9903
	5D Yukawa	0.3044	0.0041	0.08615	0.9884
	4D Coulombic	0.3067	0.04188	-	0.9281
	4D Yukawa	0.3045	0.06593	0.3648	0.9995
$n_5 = 2$	5D Coulombic	0.3071	0.04812	-	0.9895
	5D Yukawa	0.3071	0.00192	0.03984	0.9888
	4D Coulombic	0.3094	0.04287	-	0.9297
	4D Yukawa	0.3072	0.06669	0.3553	0.9995
$n_5 = 3$	5D Coulombic	0.3104	0.04954	-	0.9881
	5D Yukawa	0.3104	0.001831	0.03691	0.9874
	4D Coulombic	0.3128	0.04424	-	0.9327
	4D Yukawa	0.3105	0.06777	0.3431	0.9996
$n_5 = 4$	5D Coulombic	0.3146	0.05144	-	0.986
	5D Yukawa	0.3145	0.002669	0.05164	0.9848
	4D Coulombic	0.3171	0.04609	-	0.9371
	4D Yukawa	0.3147	0.0689	0.3239	0.9996
$n_5 = 5$	5D Coulombic	0.3199	0.03905	-	0.9815
	5D Yukawa	0.3199	0.002177	0.03898	0.9813
	4D Coulombic	0.3225	0.04871	-	0.9435
	4D Yukawa	0.3201	0.0702	0.2955	0.9996
$n_5 = 6$	5D Coulombic	0.3272	0.05811	-	0.9757
	5D Yukawa	0.3271	0.001402	0.0241	0.9749
	4D Coulombic	0.3306	0.05278	-	0.9535
	4D Yukawa	0.3274	0.07211	0.2546	0.9997
$n_5 = 7$	5D Coulombic	0.3382	0.06547	-	0.9581
	5D Yukawa	0.3382	0.001068	0.0163	0.9595
	4D Coulombic	0.3415	0.06056	-	0.9723
	4D Yukawa	0.3388	0.0748	0.1789	0.9998
$n_5 = 8$	5D Coulombic	0.3369	0.06379	-	0.9576
	5D Yukawa	0.3369	0.001886	0.02953	0.9657
	4D Coulombic	0.3401	0.05837	-	0.9793
	4D Yukawa	0.3373	0.07642	0.2214	0.9999

Table E.2: Fitting parameters for  $\beta = 2.30, \gamma = 0.505, k = 0.10$  for  $T = L = 100, N_5 = 8$ .

# Appendix F

## Mathematical Framework for fermions in a warped background

### F.1 Vielbeins

This section is based on [82]. From standard Differential Geometry, we know that a differential basis for a tangent space  $T_p$  is spanned by

$$\hat{e}_M = \partial_M \tag{F.1}$$

and we can write any vector in this basis as  $V = V^M \hat{e}_M$ . Similarly, for a cotangent space,  $T_p^*$  we have a differential basis that can be written as

$$\hat{e}^M = dx^M \tag{F.2}$$

and they are usually referred to as the coordinate basis as they depend on the position.

In a curved manifold, it is desired to define a basis which is independent of the coordinates. This basis is usually called local or non-coordinate basis and is spanned by basis vector  $\hat{e}_a$  such that they obey the signature of the manifold,



i.e.

$$\hat{e}_a \cdot \hat{e}_b = \eta_{ab}. \quad (\text{F.3})$$

With same arguments a similar non-coordinate basis can be defined for the cotangent space. Now, one can relate the coordinate and non-coordinate bases using

$$\hat{e}_M(x) = e_M^a(x)\hat{e}_a \quad (\text{F.4})$$

where the matrix  $e_M^a(x)$  is called the vielbein and it is an invertible matrix. We use capital Roman letters,  $M, N, P, \dots$ , to denote the components in the coordinate space and small latin,  $a, b, c, \dots$  for components in the local space. The vielbeins have the following orthonormality conditions

$$e^M_a(x)e_N^a(x) = \delta^M_N \quad e_M^a(x)e^M_b(x) = \delta^a_b \quad (\text{F.5})$$

and satisfy

$$g_{MN}(x) = e_M^a e_N^a \eta_{ab}. \quad (\text{F.6})$$

One uses vielbeins to transform components of vectors expressed in coordinate basis to the non-coordinate basis and vice versa. For example,

$$V^M = e^M_a V^a \quad \text{and} \quad V^a = e_M^a V^M. \quad (\text{F.7})$$

Finally, we can use the general coordinate-dependent metric,  $g_{MN}$  to raise or lower coordinate space indices ( $M, N, P, \dots$ ) and the Minkowski metric,  $\eta_{MN}$  to do this on non-coordinate space indices ( $a, b, c, \dots$ ).

## F.2 Spin Connections

In standard GR, we know that affine connections are introduced to absorb the effect of the curvature of a manifold when trying to look at a local point. The aforementioned are objects that depend on the coordinates. The equivalent in non-coordinate space is given by the spin connection,  $\Omega_M$ . In the case of fermions, which are spinors of the Lorentz group, the spin connection can be found using

$\Omega_M^{ab}\sigma_{ab}$  with  $\sigma_{ab} = \frac{1}{4}[\gamma_a, \gamma_b]$  and it is defined as

$$\Omega_M^{ab}\sigma_{ab} = \left( \frac{1}{2}e^{Na}(\partial_M e_N^b - \partial_N e_M^b) - \frac{1}{2}e^{Nb}(\partial_M e_N^a - \partial_N e_M^a) - \frac{1}{2}e^{Pa}e^{Qb}(\partial_P e_{Qc} - \partial_Q e_{Pc})e_\mu^c \right) \sigma_{ab} \quad (\text{F.8})$$

### F.2.1 Derivations of spin connections for the warped case

The full derivations for  $\Omega_\mu^{ab}\sigma_{ab}$  and  $\Omega_5^{ab}\sigma_{ab}$  are given here.

$$\begin{aligned} \Omega_\mu^{ab}\gamma_a\gamma_b &= \left( \frac{1}{2}e^{Na}(\partial_\mu e_N^b - \partial_N e_\mu^b) - \frac{1}{2}e^{Nb}(\partial_\mu e_N^a - \partial_N e_\mu^a) \right. \\ &\quad \left. - \frac{1}{2}e^{Pa}e^{Qb}(\partial_P e_{Qc} - \partial_Q e_{Pc})e_\mu^c \right) \gamma_a\gamma_b \\ &= \left( -\frac{1}{2}e^{5a}\partial_5 e_\mu^b + \frac{1}{2}e^{5b}\partial_5 e_\mu^a - \frac{1}{2}e^{5a}e^{\nu b}(\partial_5 e_{\nu c})e_\mu^c + \frac{1}{2}e^{\nu a}e^{5b}(\partial_5 e_{\nu c})e_\mu^c \right) \gamma_a\gamma_b \\ &= \left( \frac{1}{2} \frac{f(y)'}{2\sqrt{f(y)}} (e^{5b}\delta_\mu^a - e^{5a}\delta_\mu^b) \right. \\ &\quad \left. - \frac{1}{2}\eta^{ad}e_d^5\eta^{be}e_\nu^c(\partial_5\eta_{cf}e_\nu^f)e_\mu^c + \frac{1}{2}\eta^{ad}e_d^\nu\eta^{be}e_e^5(\partial_5\eta_{cf}e_\nu^f)e_\mu^c \right) \gamma_a\gamma_b \\ &= \left( \frac{f(y)'}{4\sqrt{f(y)}} (\eta^{bc}e_c^5\delta_\mu^a - \eta^{ac}e_c^5\delta_\mu^b) \right. \\ &\quad \left. - \frac{1}{2} \frac{f(y)'}{2\sqrt{f(y)}} \left( \eta^{ad}\delta_d^5\eta^{be} \frac{\delta_e^\nu}{\sqrt{f(y)}} \eta_{cf}\delta_\nu^f e_\mu^c - \eta^{ad} \frac{\delta_d^\nu}{\sqrt{f(y)}} \eta^{be}\delta_e^5\eta_{cf}\delta_\nu^f e_\mu^c \right) \right) \gamma_a\gamma_b \\ &= \frac{f(y)'}{4\sqrt{f(y)}} (\delta_\mu^a\gamma_a\gamma^c\delta_c^5 - \delta_\mu^b\gamma^c\gamma_b\delta_\mu^b) + \frac{f(y)'}{4\sqrt{f(y)}} \eta_{cf}\delta_\nu^f\delta_\mu^c (\gamma^d\delta_d^\nu\gamma^e\delta_e^5 - \gamma^d\delta_d^5\gamma^e\delta_e^\nu) \\ &= \frac{f(y)'}{2\sqrt{f(y)}} \gamma_\mu\gamma^5 + \frac{f(y)'}{2\sqrt{f(y)}} \gamma_\mu\gamma^5 \\ &= \frac{f(y)'}{\sqrt{f(y)}} \gamma_\mu\gamma^5. \end{aligned} \quad (\text{F.9})$$

The same term arises from evaluating  $\Omega_\mu^{ab}\gamma_b\gamma_a$  with the opposite sign, therefore we can conclude that

$$\Omega_\mu \equiv \frac{1}{2}\Omega_\mu^{ab}\sigma_{ab} = \frac{1}{4} \frac{f(y)'}{\sqrt{f(y)}} \gamma_\mu\gamma^5 \quad (\text{F.10})$$

where  $\gamma_\mu$  and  $\gamma^5$  are the usual gamma matrices in Minkowski spacetime.

$$\begin{aligned}
 \Omega_5^{ab}\gamma_a\gamma_b &= \left( \frac{1}{2}e^{Na}(\partial_5 e_N^b - \partial_N e_5^b) - \frac{1}{2}e^{Nb}(\partial_5 e_N^a - \partial_N e_5^a) \right. \\
 &\quad \left. - \frac{1}{2}\left( e^{5a}e^{\mu b}(\partial_5 e_{\mu c})e_5^c - e^{\mu a}e^{5b}(\partial_5 e_{\mu c})e_5^c \right) \right) \gamma_a\gamma_b \\
 &= \left( \frac{1}{2}(e^{\mu a}\partial_5 e_\mu^b - e^{\mu b}\partial_5 e_\mu^a) - \frac{1}{2}e^{5a}e^{\mu b}(\partial_5 e_{\mu c})e_5^c + \frac{1}{2}e^{\mu a}e^{5b}(\partial_5 e_{\mu c})e_5^c \right) \gamma_a\gamma_b \\
 &= \left( \frac{1}{2}e_c^\mu \eta^{ca} \frac{f(y)'}{2\sqrt{f(y)}} \delta_\mu^b - \frac{1}{2}e_c^\mu \eta^{bc} \frac{f(y)'}{2\sqrt{f(y)}} \delta_\mu^a \right. \\
 &\quad \left. - \frac{1}{2}\eta^{ad}e_d^5 \eta^{be}e_e^\mu (\partial_5 \eta_{cf}e_\mu^f)e_5^c + \frac{1}{2}\eta^{ad}e_d^\mu \eta^{be}e_e^5 (\partial_5 \eta_{cf}e_\mu^f)e_5^c \right) \gamma_a\gamma_b \\
 &= \frac{f(y)'}{4f(y)} (\delta_c^\mu \eta^{ca} \delta_\mu^b - \delta_c^\mu \eta^{bc} \delta_\mu^a) \gamma_a\gamma_b \\
 &\quad - \frac{1}{2} \frac{f(y)'}{2\sqrt{f(y)}} \left( \eta^{ad} \delta_d^5 \eta^{be} \frac{\delta_e^\mu}{\sqrt{f(y)}} \eta_{cf} \delta_\mu^f e_5^c + \eta^{ad} \frac{\delta_d^\mu}{\sqrt{f(y)}} \eta^{be} \delta_e^5 \eta_{cf} \delta_\mu^f e_5^c \right) \gamma_a\gamma_b \\
 &= \frac{f(y)'}{4f(y)} (\gamma^\mu \gamma_\mu - \gamma_\mu \gamma^\mu) - \frac{f(y)'}{4f(y)} (-\eta_{5\mu} \gamma^5 \gamma^\mu + \eta_{5\mu} \gamma^\mu \gamma^5) \\
 &= 0
 \end{aligned} \tag{F.11}$$

Therefore,  $\Omega_5^{ab}\sigma_{ab} = 0$ .

### F.3 Dirac operators in momentum space

Here, we show the procedure for going from coordinate space to Fourier space for the four different Wilson-Dirac operators, evaluated at the mean-field background, the inverse of which appears in the expressions of the currents in Eq.(4.79) and Eq(4.80). The Wilson-Dirac operator  $\mathcal{M}_{n,n_5;n+\hat{\mu},n_5}$  in momentum space is given by

$$\begin{aligned}
 \tilde{\mathcal{M}}_{p',n_5;p'',n_5}^{(1)} &= \sum_n e^{ip'n} e^{-ip''n} e^{-ip'_\mu n} f(n_5)^2 \left[ - \sum_\mu \frac{\gamma_\mu}{\sqrt{f(n_5)}} \frac{1}{2} \bar{v}_4(n_5) (e^{ip'_\mu} - e^{-ip'_\mu}) \delta_{n_5, n_5} \right. \\
 &\quad \left. - \frac{\gamma_5}{2} \left( \frac{\bar{v}_5(n_5)}{\sqrt{f(n_5)}} \delta_{n_5+1, n_5} - \frac{\bar{v}_5(n_5-1)}{\sqrt{f(n_5-1)}} \delta_{n_5-1, n_5} \right) \right. \\
 &\quad \left. + \left( \frac{f(n_5)'}{f(n_5)} \gamma_5 + m \right) \delta_{n_5, n_5} \right]
 \end{aligned}$$

$$\begin{aligned}
 & + \sum_{\mu} \frac{1}{2\sqrt{f(n_5)}} (\bar{v}_4(n_5)e^{ip'_\mu} - 2 + \bar{v}_4(n_5)e^{-ip'_\mu}) \delta_{n_5, n_5} \\
 & + \frac{1}{2} \left( \frac{\bar{v}_5(n_5)}{\sqrt{f(n_5)}} \delta_{n_5+1, n_5} - 2\delta_{n_5, n_5} + \frac{\bar{v}_5(n_5-1)}{\sqrt{f(n_5-1)}} \delta_{n_5-1, n_5} \right) \\
 & = \delta_{p', p''}^{(4)} e^{-ip'_\mu} \left[ - \sum_{\mu} i\gamma_{\mu} f(n_5)^{3/2} \bar{v}_4(n_5) \sin(p'_\mu) \delta_{n_5, n_5} \right. \\
 & - \frac{\gamma_5}{2} \left( \bar{v}_5(n_5) f(n_5)^{3/2} \delta_{n_5+1, n_5} - \frac{\bar{v}_5(n_5-1) f(n_5)^2}{\sqrt{f(n_5-1)}} \delta_{n_5-1, n_5} \right) \\
 & + \left( f(n_5)' f(n_5) \gamma_5 + m - 4f(n_5)^{3/2} \right) \delta_{n_5, n_5} \\
 & + f(n_5)^{3/2} \bar{v}_4(n_5) \sum_{\mu} \cos(p'_\mu) \delta_{n_5, n_5} \\
 & \left. + \frac{1}{2} \left( \bar{v}_5(n_5) f(n_5)^{3/2} \delta_{n_5+1, n_5} - 2f(n_5)^2 \delta_{n_5, n_5} + \frac{\bar{v}_5(n_5-1) f(n_5)^2}{\sqrt{f(n_5-1)}} \delta_{n_5-1, n_5} \right) \right] \\
 & = \delta_{p', p''}^{(4)} e^{-ip'_\mu} \left[ \bar{v}_4(n_5) f(n_5)^{3/2} \sum_{\mu} \left( -i\gamma_{\mu} \sin(p'_\mu) + \cos(p'_\mu) \right) \delta_{n_5, n_5} \right. \\
 & + \frac{\bar{v}_5(n_5) f(n_5)^{3/2}}{2} (-\gamma_5 + 1) \delta_{n_5+1, n_5} - \frac{\bar{v}_5(n_5-1) f(n_5)^2}{2\sqrt{f(n_5-1)}} (\gamma_5 + 1) \delta_{n_5-1, n_5} \\
 & \left. + \left( f(n_5)' f(n_5) \gamma_5 + m - 4f(n_5)^{3/2} - f(n_5)^2 \right) \delta_{n_5, n_5} \right] \quad (F.12)
 \end{aligned}$$

and similarly for  $\mathcal{M}_{n+\hat{\mu}, n_5; n, n_5}$  we find

$$\begin{aligned}
 \tilde{\mathcal{M}}_{p', n_5; p'', n_5}^{(2)} & = \delta_{p', p''}^{(4)} e^{ip'_\mu} \left[ \bar{v}_4(n_5) f(n_5)^{3/2} \sum_{\mu} \left( -i\gamma_{\mu} \sin(p'_\mu) + \cos(p'_\mu) \right) \delta_{n_5, n_5} \right. \\
 & + \frac{\bar{v}_5(n_5) f(n_5)^{3/2}}{2} (-\gamma_5 + 1) \delta_{n_5+1, n_5} - \frac{\bar{v}_5(n_5-1) f(n_5)^2}{2\sqrt{f(n_5-1)}} (\gamma_5 + 1) \delta_{n_5-1, n_5} \\
 & \left. + \left( f(n_5)' f(n_5) \gamma_5 - 4f(n_5)^{3/2} + (m-1) f(n_5)^2 \right) \delta_{n_5, n_5} \right] \quad (F.13)
 \end{aligned}$$

We also find  $\mathcal{M}_{n, n_5; n, n_5+1}$  in momentum space to be

$$\begin{aligned}
 \mathcal{M}_{p', n_5; p'', n_5+1} & = \sum_n e^{ip'n} e^{-ip''n} \left[ - \sum_{\mu} \gamma_{\mu} f(n_5)^{3/2} \frac{1}{2} \bar{v}_4(n_5) (e^{ip'_\mu} - e^{-ip'_\mu}) \delta_{n_5, n_5+1} \right. \\
 & - \frac{\gamma_5}{2} \left( \bar{v}_5(n_5) f(n_5)^{3/2} \delta_{n_5+1, n_5+1} - \frac{\bar{v}_5(n_5-1) f(n_5)^2}{\sqrt{f(n_5-1)}} \delta_{n_5-1, n_5+1} \right) \\
 & \left. + \left( f(n_5)' f(n_5) \gamma_5 + m f(n_5)^2 \right) \delta_{n_5, n_5+1} \right]
 \end{aligned}$$

$$\begin{aligned}
 & + \sum_{\mu} \frac{f(n_5)^{3/2}}{2} (\bar{v}_4(n_5)e^{ip'_\mu} - 2 + \bar{v}_4(n_5)e^{-ip'_\mu}) \delta_{n_5, n_5+1} \\
 & + \frac{f(n_5)^2}{2} \left( \frac{\bar{v}_5(n_5)}{\sqrt{f(n_5)}} \delta_{n_5+1, n_5+1} - 2\delta_{n_5, n_5+1} + \frac{\bar{v}_5(n_5-1)}{\sqrt{f(n_5-1)}} \delta_{n_5-1, n_5+1} \right) \Big] \\
 & = \delta_{p', p''}^{(4)} \left[ - \sum_{\mu} i\gamma_{\mu} f(n_5)^{3/2} \bar{v}_4(n_5) \sin(p'_\mu) \delta_{n_5, n_5+1} \right. \\
 & - \frac{\gamma_5}{2} \left( \bar{v}_5(n_5) f(n_5)^{3/2} \delta_{n_5+1, n_5+1} - \frac{\bar{v}_5(n_5-1) f(n_5)^2}{\sqrt{f(n_5-1)}} \delta_{n_5-1, n_5+1} \right) \\
 & + \left( f(n_5)' f(n_5) \gamma_5 + m f(n_5)^2 - 4f(n_5)^{3/2} \right) \delta_{n_5, n_5+1} \\
 & + f(n_5)^{3/2} \bar{v}_4(n_5) \sum_{\mu} \cos(p'_\mu) \delta_{n_5, n_5+1} \\
 & \left. + \frac{f(n_5)^2}{2} \left( \frac{\bar{v}_5(n_5)}{\sqrt{f(n_5)}} \delta_{n_5+1, n_5+1} - 2\delta_{n_5, n_5+1} + \frac{\bar{v}_5(n_5-1)}{2\sqrt{f(n_5-1)}} \delta_{n_5-1, n_5+1} \right) \right] \\
 & = \delta_{p', p''}^{(4)} \left[ \bar{v}_4(n_5) f(n_5)^{3/2} \sum_{\mu} \left( -i\gamma_{\mu} \sin(p'_\mu) + \cos(p'_\mu) \right) \delta_{n_5, n_5+1} \right. \\
 & + \frac{\bar{v}_5(n_5) f(n_5)^{3/2}}{2} (-\gamma_5 + 1) \delta_{n_5+1, n_5+1} - \frac{\bar{v}_5(n_5-1) f(n_5)^2}{2\sqrt{f(n_5-1)}} (\gamma_5 + 1) \delta_{n_5-1, n_5+1} \\
 & \left. + \left( f(n_5)' f(n_5) \gamma_5 - 4f(n_5)^{3/2} + (m-1) f(n_5)^2 \right) \delta_{n_5, n_5+1} \right] \quad (\text{F.14})
 \end{aligned}$$

and similarly,

$$\begin{aligned}
 \mathcal{M}_{p', n_5+1; p'', n_5} & = \delta_{p', p''}^{(4)} \left[ \bar{v}_4(n_5) f(n_5)^{3/2} \sum_{\mu} \left( -i\gamma_{\mu} \sin(p'_\mu) + \cos(p'_\mu) \right) \delta_{n_5+1, n_5} \right. \\
 & + \frac{\bar{v}_5(n_5) f(n_5)^{3/2}}{2} (-\gamma_5 + 1) \delta_{n_5+2, n_5} - \frac{\bar{v}_5(n_5-1) f(n_5)^2}{2\sqrt{f(n_5-1)}} (\gamma_5 + 1) \delta_{n_5, n_5} \\
 & \left. + \left( f(n_5)' f(n_5) \gamma_5 - 4f(n_5)^{3/2} + (m-1) f(n_5)^2 \right) \delta_{n_5+1, n_5} \right] \quad (\text{F.15})
 \end{aligned}$$

# Bibliography

- [1] T. Kaluza, *On the Problem of Unity in Physics*, *Sitzungsber.Preuss.Akad.Wiss.Berlin (Math.Phys.)* **1921** (1921) 966–972.
- [2] O. Klein, *Quantum Theory and Five-Dimensional Theory of Relativity. (In German and English)*, *Z.Phys.* **37** (1926) 895–906.
- [3] K. Akama, *An Early Proposal of 'Brane World'*, *Lect.Notes Phys.* **176** (1982) 267–271, [[hep-th/0001113](#)].
- [4] V. Rubakov and M. Shaposhnikov, *Do We Live Inside a Domain Wall?*, *Phys.Lett.* **B125** (1983) 136–138.
- [5] M. B. Green and J. H. Schwarz, *Anomaly Cancellation in Supersymmetric D=10 Gauge Theory and Superstring Theory*, *Phys.Lett.* **B149** (1984) 117–122.
- [6] I. Antoniadis, *A Possible new dimension at a few TeV*, *Phys.Lett.* **B246** (1990) 377–384.
- [7] J. Dai, R. Leigh, and J. Polchinski, *New Connections Between String Theories*, *Mod.Phys.Lett.* **A4** (1989) 2073–2083.
- [8] P. Horava and E. Witten, *Heterotic and type I string dynamics from eleven-dimensions*, *Nucl.Phys.* **B460** (1996) 506–524, [[hep-th/9510209](#)].
- [9] P. Horava and E. Witten, *Eleven-dimensional supergravity on a manifold with boundary*, *Nucl. Phys.* **B475** (1996) 94–114, [[hep-th/9603142](#)].
- [10] A. Lukas, B. A. Ovrut, K. S. Stelle, and D. Waldram, *The Universe as a domain wall*, *Phys. Rev.* **D59** (1999) 086001, [[hep-th/9803235](#)].
- [11] V. A. Rubakov, *Large and infinite extra dimensions: An Introduction*, *Phys. Usp.* **44** (2001) 871–893, [[hep-ph/0104152](#)]. [*Usp. Fiz. Nauk*171,913(2001)].
- [12] G. Dvali and M. A. Shifman, *Domain walls in strongly coupled theories*, *Phys.Lett.* **B396** (1997) 64–69, [[hep-th/9612128](#)].
- [13] Y. Hosotani, *Dynamical Mass Generation by Compact Extra Dimensions*, *Phys.Lett.* **B126** (1983) 309.
- [14] M. Kubo, C. Lim, and H. Yamashita, *The Hosotani mechanism in bulk gauge*

- theories with an orbifold extra space  $S^{*1} / Z(2)$ , *Mod.Phys.Lett.* **A17** (2002) 2249–2264, [hep-ph/0111327].*
- [15] N. Arkani-Hamed, S. Dimopoulos, and G. Dvali, *Phenomenology, astrophysics and cosmology of theories with submillimeter dimensions and TeV scale quantum gravity*, *Phys.Rev.* **D59** (1999) 086004, [hep-ph/9807344].
- [16] L. Randall and R. Sundrum, *A Large mass hierarchy from a small extra dimension*, *Phys.Rev.Lett.* **83** (1999) 3370–3373, [hep-ph/9905221].
- [17] L. Randall and R. Sundrum, *An Alternative to compactification*, *Phys.Rev.Lett.* **83** (1999) 4690–4693, [hep-th/9906064].
- [18] N. Manton, *A New Six-Dimensional Approach to the Weinberg-Salam Model*, *Nucl.Phys.* **B158** (1979) 141.
- [19] N. Irges and F. Knechtli, *Non-perturbative definition of five-dimensional gauge theories on the  $R^{*4} \times S^{*1}/Z(2)$  orbifold*, *Nucl. Phys.* **B719** (2005) 121–139, [hep-lat/0411018].
- [20] N. Irges and F. Knechtli, *Non-perturbative mass spectrum of an extra-dimensional orbifold*, hep-lat/0604006.
- [21] N. Irges and F. Knechtli, *Lattice gauge theory approach to spontaneous symmetry breaking from an extra dimension*, *Nucl. Phys.* **B775** (2007) 283–311, [hep-lat/0609045].
- [22] N. Irges, F. Knechtli, and K. Yoneyama, *Higgs mechanism near the 5d bulk phase transition*, *Phys. Lett.* **B722** (2013) 378–383, [arXiv:1212.5514].
- [23] N. Irges, F. Knechtli, and K. Yoneyama, *Mean-Field Gauge Interactions in Five Dimensions II. The Orbifold*, *Nucl. Phys.* **B865** (2012) 541–567, [arXiv:1206.4907].
- [24] M. Alberti, N. Irges, F. Knechtli, and G. Moir, *Five-Dimensional Gauge-Higgs Unification: A Standard Model-Like Spectrum*, *JHEP* **09** (2015) 159, [arXiv:1506.0603].
- [25] G. Cossu, H. Hatanaka, Y. Hosotani, and J.-I. Noaki, *Polyakov loops and the Hosotani mechanism on the lattice*, *Phys. Rev.* **D89** (2014), no. 9 094509, [arXiv:1309.4198].
- [26] J. E. Hetrick, *Lattice Investigations of the Hosotani Mechanism of Spontaneous Symmetry Breaking*, *PoS LATTICE2013* (2014) 102.
- [27] R. Sundrum, *Effective field theory for a three-brane universe*, *Phys.Rev.* **D59** (1999) 085009, [hep-ph/9805471].
- [28] I. Montvay and G. Munster, *Quantum fields on a lattice*, .
- [29] H. Rothe, *Lattice gauge theories: An Introduction*, *World Sci.Lect.Notes Phys.* **74** (2005) 1–605.

- 
- [30] C. Gattringer and C. B. Lang, *Quantum chromodynamics on the lattice*, *Lect.Notes Phys.* **788** (2010) 1–343.
- [31] M. Creutz, *QUARKS, GLUONS AND LATTICES*, .
- [32] K. G. Wilson, *Confinement of Quarks*, *Phys.Rev.* **D10** (1974) 2445–2459.
- [33] M. Luscher, K. Symanzik, and P. Weisz, *Anomalies of the Free Loop Wave Equation in the WKB Approximation*, *Nucl. Phys.* **B173** (1980) 365.
- [34] H. B. Nielsen and M. Ninomiya, *No Go Theorem for Regularizing Chiral Fermions*, *Phys. Lett.* **B105** (1981) 219.
- [35] H. B. Nielsen and M. Ninomiya, *Absence of Neutrinos on a Lattice. 1. Proof by Homotopy Theory*, *Nucl. Phys.* **B185** (1981) 20. [Erratum: Nucl. Phys.B195,541(1982)].
- [36] H. B. Nielsen and M. Ninomiya, *Absence of Neutrinos on a Lattice. 2. Intuitive Topological Proof*, *Nucl. Phys.* **B193** (1981) 173.
- [37] A. Hasenfratz and P. Hasenfratz, *The Scales of Euclidean and Hamiltonian Lattice QCD*, *Nucl. Phys.* **B193** (1981) 210.
- [38] F. Karsch, *SU(N) Gauge Theory Couplings on Asymmetric Lattices*, *Nucl. Phys.* **B205** (1982) 285–300.
- [39] Y. Fu and H. B. Nielsen, *A Layer Phase in a Nonisotropic U(1) Lattice Gauge theory: Dimensional Reduction a new way*, *Nucl.Phys.* **B236** (1984) 167.
- [40] A. Kennedy and B. Pendleton, *Improved heatbath method for Monte Carlo calculations in lattice gauge theories*, *Phys.Lett.* **B156** (1985) 393–399.
- [41] J.-M. Drouffe and J.-B. Zuber, *Strong Coupling and Mean Field Methods in Lattice Gauge Theories*, *Phys.Rept.* **102** (1983) 1.
- [42] C. Itzykson and J. M. Drouffe, *STATISTICAL FIELD THEORY. VOL. 1: FROM BROWNIAN MOTION TO RENORMALIZATION AND LATTICE GAUGE THEORY*. 1989.
- [43] M. Creutz, *Gauge Fixing, the Transfer Matrix, and Confinement on a Lattice*, *Phys. Rev.* **D15** (1977) 1128.
- [44] W. Ruhl, *The Mean Field Perturbation Theory of Lattice Gauge Models With Covariant Gauge Fixing*, *Z. Phys.* **C18** (1983) 207.
- [45] H. Flyvbjerg, P. Mansfield, and B. Soderberg, *HIGH PRECISION MEAN FIELD RESULTS FOR LATTICE GAUGE THEORIES*, *Nucl. Phys.* **B240** (1984) 171.
- [46] B. E. Lautrup and W. Ruhl, *HIGHER ORDER MEAN FIELD EXPANSIONS FOR LATTICE GAUGE THEORIES*, *Z. Phys.* **C23** (1984) 49.



- 
- [47] L. D. Faddeev and V. N. Popov, *Feynman Diagrams for the Yang-Mills Field*, *Phys. Lett.* **B25** (1967) 29–30.
- [48] L. Del Debbio, R. D. Kenway, E. Lambrou, and E. Rinaldi, *The transition to a layered phase in the anisotropic five-dimensional  $SU(2)$  Yang-Mills theory*, *Phys.Lett.* **B724** (2013), no. 1-3 133–137, [[arXiv:1305.0752](#)].
- [49] L. Del Debbio, R. D. Kenway, E. Lambrou, and E. Rinaldi, *Searching for a continuum 4D field theory arising from a 5D non-abelian gauge theory*, *PoS LATTICE2013* (2014) 107, [[arXiv:1309.6249](#)].
- [50] M. Creutz, *Confinement and the Critical Dimensionality of Space-Time*, *Phys.Rev.Lett.* **43** (1979) 553–556.
- [51] H. Kawai, M. Nio, and Y. Okamoto, *On existence of nonrenormalizable field theory: Pure  $SU(2)$  lattice gauge theory in five-dimensions*, *Prog. Theor. Phys.* **88** (1992) 341–350.
- [52] S. Ejiri, J. Kubo, and M. Murata, *A Study on the nonperturbative existence of Yang-Mills theories with large extra dimensions*, *Phys.Rev.* **D62** (2000) 105025, [[hep-ph/0006217](#)].
- [53] S. Chandrasekharan and U. J. Wiese, *Quantum link models: A Discrete approach to gauge theories*, *Nucl. Phys.* **B492** (1997) 455–474, [[hep-lat/9609042](#)].
- [54] R. Brower, S. Chandrasekharan, and U. J. Wiese, *QCD as a quantum link model*, *Phys. Rev.* **D60** (1999) 094502, [[hep-th/9704106](#)].
- [55] P. de Forcrand, A. Kurkela, and M. Panero, *The phase diagram of Yang-Mills theory with a compact extra dimension*, *JHEP* **1006** (2010) 050, [[arXiv:1003.4643](#)].
- [56] L. Del Debbio, A. Hart, and E. Rinaldi, *Light scalars in strongly-coupled extra-dimensional theories*, *JHEP* **1207** (2012) 178, [[arXiv:1203.2116](#)].
- [57] B. Svetitsky and L. G. Yaffe, *Critical Behavior at Finite Temperature Confinement Transitions*, *Nucl. Phys.* **B210** (1982) 423.
- [58] F. Knechtli, M. Luz, and A. Rago, *On the phase structure of five-dimensional  $SU(2)$  gauge theories with anisotropic couplings*, *Nucl.Phys.* **B856** (2012) 74–94, [[arXiv:1110.4210](#)].
- [59] Y. K. Fu and H. B. Nielsen, *Some Properties of the Layer Phase*, *Nucl. Phys.* **B254** (1985) 127.
- [60] D. B. Kaplan, *A Method for simulating chiral fermions on the lattice*, *Phys. Lett.* **B288** (1992) 342–347, [[hep-lat/9206013](#)].
- [61] C. P. Korthals-Altes, S. Nicolis, and J. Prades, *Chiral defect fermions and the layered phase*, *Phys. Lett.* **B316** (1993) 339–344, [[hep-lat/9306017](#)].

- 
- [62] A. Hulsebos, C. P. Korthals-Altes, and S. Nicolis, *Gauge theories with a layered phase*, *Nucl. Phys.* **B450** (1995) 437–451, [[hep-th/9406003](#)].
- [63] A. Hulsebos, *Anisotropic gauge theories: A Numerical study of the Fu-Nielsen model*, *Nucl. Phys. Proc. Suppl.* **42** (1995) 618–620, [[hep-lat/9412031](#)].
- [64] S. Nicolis, *Layered Phase Investigations*, *PoS LAT2007* (2007) 273, [[arXiv:0710.1714](#)].
- [65] P. Dimopoulos, K. Farakos, A. Kehagias, and G. Koutsoumbas, *Lattice evidence for gauge field localization on a brane*, *Nucl.Phys.* **B617** (2001) 237–252, [[hep-th/0007079](#)].
- [66] P. Dimopoulos, K. Farakos, and S. Vrentzos, *The 4-D Layer Phase as a Gauge Field Localization: Extensive Study of the 5-D Anisotropic U(1) Gauge Model on the Lattice*, *Phys.Rev.* **D74** (2006) 094506, [[hep-lat/0607033](#)].
- [67] K. Farakos and S. Vrentzos, *Establishment of the Coulomb law in the layer phase of a pure U(1) lattice gauge theory*, *Phys.Rev.* **D77** (2008) 094511, [[arXiv:0801.3722](#)].
- [68] N. Irges and F. Knechtli, *Mean-Field Gauge Interactions in Five Dimensions I. The Torus*, *Nucl.Phys.* **B822** (2009) 1–44, [[arXiv:0905.2757](#)].
- [69] D. Berman and E. Rabinovici, *Layer Phases in Unisotropic Lattice Gauge Theories*, *Phys. Lett.* **B157** (1985) 292.
- [70] M. Murata and H. So, *Five-dimensional lattice gauge theory as multilayer world*, [hep-lat/0306003](#).
- [71] K. Farakos and S. Vrentzos, *Exploration of the phase diagram of 5d anisotropic SU(2) gauge theory*, *Nucl.Phys.* **B862** (2012) 633–649, [[arXiv:1007.4442](#)].
- [72] M. Creutz, *Overrelaxation and Monte Carlo simulation*, *Phys.Rev.* **D36** (1987) 515.
- [73] **SciDAC Collaboration, LHPC Collaboration, UKQCD Collaboration** Collaboration, R. G. Edwards and B. Joo, *The Chroma software system for lattice QCD*, *Nucl.Phys.Proc.Suppl.* **140** (2005) 832, [[hep-lat/0409003](#)].
- [74] F. Winter, *Accelerating QDP++ using GPUs*, *PoS LATTICE2011* (2011) 050, [[arXiv:1105.2279](#)].
- [75] M. Laine, H. B. Meyer, K. Rummukainen, and M. Shaposhnikov, *Localization and mass generation for nonAbelian gauge fields*, *JHEP* **01** (2003) 068, [[hep-ph/0211149](#)].
- [76] A. Coste, A. Gonzalez-Arroyo, J. Jurkiewicz, and C. P. Korthals Altes, *Zero Momentum Contribution to Wilson Loops in Periodic Boxes*, *Nucl. Phys.* **B262** (1985) 67.

- [77] B. Petersson and T. Reisz, *Polyakov loop correlations at finite temperature*, *Nucl. Phys.* **B353** (1991) 757–784.
- [78] C. G. Broyden, *A Class of Methods for Solving Nonlinear Simultaneous Equations*, *Mathematics of Computation (American Mathematical Society)* **19 (92)** (1965) 577–593.
- [79] R. Sommer, *A New way to set the energy scale in lattice gauge theories and its applications to the static force and alpha-s in SU(2) Yang-Mills theory*, *Nucl. Phys.* **B411** (1994) 839–854, [[hep-lat/9310022](#)].
- [80] S. Elitzur, *Impossibility of Spontaneously Breaking Local Symmetries*, *Phys. Rev.* **D12** (1975) 3978–3982.
- [81] R. Narayanan and U. Wolff, *Two loop computation of a running coupling lattice Yang-Mills theory*, *Nucl. Phys.* **B444** (1995) 425–446, [[hep-lat/9502021](#)].
- [82] N. D. Birrell and P. C. W. Davies, *Quantum Fields in Curved Space*. Cambridge Monographs on Mathematical Physics. Cambridge Univ. Press, Cambridge, UK, 1984.

# Publications

L. Del Debbio, R. D. Kenway, E. Lambrou, and E. Rinaldi, “The transition to a layered phase in the anisotropic five-dimensional SU(2) Yang-Mills theory”, *Phys.Lett.*, vol. B724, no. 1-3, pp. 133-137, 2013.

L. Del Debbio, R. D. Kenway, E. Lambrou, and E. Rinaldi, “Searching for a continuum 4D field theory arising from a 5D non-abelian gauge theory”, *PoS*, vol. LATTICE2013, p. 107, 2014.

R. D. Kenway, E. Lambrou, “Five-dimensional gauge theories in a warped background”, *PoS*, vol. LATTICE2015, p. 232, 2016.